

DESIGN AND EVALUATION OF WELLBORE STRENGTHENING
MATERIALS FOR FRACTURED RESERVOIRS

A THESIS SUBMITTED TO
THE GRADUATE SCHOOL OF NATURAL AND APPLIED SCIENCES
OF
MIDDLE EAST TECHNICAL UNIVERSITY

BY

UĞUR GARGILI

IN PARTIAL FULFILLMENT OF THE REQUIREMENTS
FOR
THE DEGREE OF MASTER OF SCIENCE
IN
PETROLEUM AND NATURAL GAS ENGINEERING

AUGUST 2019

Approval of the thesis:

**DESIGN AND EVALUATION OF WELLBORE STRENGTHENING
MATERIALS FOR FRACTURED RESERVOIRS**

submitted by **UĞUR GARGILI** in partial fulfillment of the requirements for the degree of **Master of Science in Petroleum and Natural Gas Engineering Department, Middle East Technical University** by,

Prof. Dr. Halil Kalıpçılar
Dean, Graduate School of **Natural and Applied Sciences**

Assoc. Prof. Dr. Çağlar Sınayuç
Head of Department, **Petroleum and Natural Gas Eng.**

Assist. Prof. Dr. İsmail Durgut
Supervisor, **Petroleum and Natural Gas Eng., METU**

Examining Committee Members:

Prof. Dr. Serhat Akın
Petroleum and Natural Gas Engineering Dept., METU

Assist. Prof. Dr. İsmail Durgut
Petroleum and Natural Gas Eng., METU

Assoc. Prof. Dr. Gürşat Altun
Petroleum and Natural Gas Engineering Dept., ITU

Date: 28.08.2019

I hereby declare that all information in this document has been obtained and presented in accordance with academic rules and ethical conduct. I also declare that, as required by these rules and conduct, I have fully cited and referenced all material and results that are not original to this work.

Name, Surname: Uğur Gargılı

Signature:

ABSTRACT

DESIGN AND EVALUATION OF WELLBORE STRENGTHENING MATERIALS FOR FRACTURED RESERVOIRS

Gargılı, Uğur

Master of Science, Petroleum and Natural Gas Engineering

Supervisor: Assist. Prof. Dr. İsmail Durgut

August 2019, 195 pages

The lost circulation is a primary consideration while drilling through fractured carbonate formations. Uncontrolled lost circulation may result in high nonproductive drilling time and cost, stuck pipe, side-tracks, blowouts and occasionally, the abandonment of expensive wells depending upon the severity of the loss. Additionally, drill solids entering the reservoir as a result of lost circulation may plug the pore throats, leading to a significant decrease in production.

In the industry, there are two approaches to struggle with loss circulation; to treat (control and stop) losses after they occur, or alternatively strengthen the loss zones to prevent losses. Indeed, it has been proved that it is easier and more effective to prevent occurrence of losses than to attempt to control and stop them once they started.

Preventive method is also known as wellbore strengthening. The method aims to both alter stresses around wellbore and minimize fluid loss. They are effective not only on natural fractures but also induced fractures which occurs during drilling.

The objective of this study is to determine optimum concentration and particle size distribution for fractured reservoir zones. A polymer-based reservoir drill-in fluid supported by wellbore strengthening materials (WSM) was used in this study. Sized ground marble (GM) was chosen as a WSM because of its hydrochloric acid solubility and reservoir non-damaging nature. Sized GM was used as a WSM in different

concentration and in different particle size range. The experiments were conducted by using Permeability Plugging Apparatus (PPA). Fractured formations were simulated by using metal slotted disks with fracture width of 400, 800 and 1200 microns. Tests were conducted at room temperature (about 20 to 25 degrees Celcius). During the study, a total 269 tests are run to investigate the effect of different particle size distribution, concentration and fracture width. The results have been compared according to maximum sealing time required to reach assumed pressure and fluid loss values, therefore, optimum composition has been determined.

Keywords: Permeability Plugging Apparatus, Slotted Discs, Fractured Formations, Ground Marble, Wellbore Strengthening Materials

ÖZ

ÇATLAKLI REZERVUARLAR İÇİN KUYU CİDARI GÜÇLENDİRME MALZEMELERİNİN TASARIMI VE DEĞERLENDİRİLMESİ

Gargılı, Uğur
Yüksek Lisans, Petrol ve Doğal Gaz Mühendisliği
Tez Danışmanı: Dr. Öğr. Üyesi İsmail Durgut

Ağustos 2019, 195 sayfa

Sirkülasyon kaybı, yoğun çatlaklı karbonatlı formasyon sondajlarında öncelikli düşünülmeli gereken hususlardandır. Kontrol edilemeyen sirkülasyon kaybı; sondajda yüksek zaman kayıpları ve maliyetleriyle, sondaj dizisi sıkışmalarıyla, kuyuyu yeniden yönlendirmeye, kontrolsüz kuyu gelişleriyle ve kayıplarının şiddetine bağlı olarak kuyu terkedilmesi ile sonuçlanabilir. Bunların yanında, sirkülasyon kaybı sonucu formasyona katı madde girişi gözenekler arası geçitleri tıkayabilir ve üretimde gözle görünür bir düşüşe neden olabilir.

Endüstride sirkülasyon kaybı ile mücadele etmek için iki yaklaşım bulunmaktadır; sirkülasyon kaybı olduktan sonra kontrol altına almak ve durdurmak, ya da sirkülasyon kaybının gerçekleşebileceği formasyonları kayıpları önlemek amacıyla güçlendirmek. Nitekim, sirkülasyon kayıplarını gerçekleştirmeden engellemenin daha kolay ve etkili olduğu kanıtlanmıştır.

Sirkülasyon kayıplarını önlemek için kullanılan yöntem kuyu cidarı güçlendirme(KCG) olarak bilinir. Bu yöntem, hem kuyu cidarında meydana gelen stresleri değiştirmeyi hem de sıvı kaybını en aza indirmeyi amaçlamaktadır. KCG, hem doğal çatlaklarda hem de sondaj sırasında oluşan çatlaklarda etkili bir biçimde uygulanabilir.

Bu çalışma, çatlaklı rezervuar alanları için en uygun derişim ve parçacık boyut dağılımını belirlemeyi amaçlamaktadır. Bu çalışmada, kuyu cidarı güçlendirme malzemeleriyle (KCGM) desteklenmiş polimer bazlı rezervuar sondaj sıvıları kullanılmıştır. Hidroklorik asitteki çözünürlüğü ve rezervuara zarar vermeyen yapısı nedeniyle boyutlandırılmış doğal mermer KCGM olarak seçilmiştir. Farklı derişim ve parçacık boyutlarındaki mermerler kullanılmıştır. Deneyler, geçirgenlik tıkama aygıtında yapılmıştır. Çatlaklı formasyonlar 400, 800 ve 1200 mikron çatlak genişliğine sahip metal yarıklı diskler kullanılarak benzetimlenmiştir. Testler oda sıcaklığında (yaklaşık 20-25°C) yapılmıştır. Bu çalışmada parçacık boyut dağılımının, derişimin ve çatlak genişliğinin etkilerini gözlemlemek için 269 test yapıldı. Sonuçlar hedeflenen basınca ulaşma süreleri ve sıvı kayıpları değerlerine göre karşılaştırıldı. En uygun derişim ve parçacık boyut dağılımları belirlendi.

Anahtar Kelimeler: Geçirgenlik Tıkama Aygıtı, Yarıklı Diskler, Çatlaklı Formasyonlar, Mermer, Kuyu Cidarı Güçlendirme Malzemeleri

To My Beloved Family

ACKNOWLEDGEMENTS

I would like to thank Assoc. Prof. Dr. İsmail Hakkı Gücüyener. His great experience, enthusiasm, determination and the continuous support from determining the topic of thesis to the end of this research helped me throughout the study.

I wish to express my sincere gratitude to my supervisor Assist.Prof. Dr. İsmail Durgut, for his continuous guidance, support, patience and valuable advices.

Furthermore, I would like to thank Hüseyin Ali Doğan, Ahmet Ay and Ahmet Sönmez for technical support and contribution during experiments.

I owe special thanks to my colleague Özgür Fırat Akel for his support through the process of writing the thesis.

GEOS Energy Inc. is also acknowledged for supplying experimental setup and additives.

My beloved family deserves appreciation for their encouragement, endless support and patience.

TABLE OF CONTENTS

ABSTRACT	v
ÖZ.....	vii
ACKNOWLEDGEMENTS	x
TABLE OF CONTENTS	xi
LIST OF TABLES	xxi
LIST OF FIGURES	xxxii
CHAPTERS	
1. INTRODUCTION	1
2. LITERATURE REVIEW	5
3. STATEMENT OF PROBLEM.....	25
4. THEORY	27
5. EXPERIMENTAL SET-UP AND PROCEDURE.....	31
5.1. Determination of Particle Size Distribution	31
5.2. Composition of Drill-In Fluid	33
5.3. Additives Used in Drill-In Fluid Add.....	34
5.3.1. Modified Starch	34
5.3.2. XCD Polymer	34
5.3.3. Biocide	34
5.3.4. Ground Marble.....	34
5.4. Determination of Rheological Properties of Drill-In Fluid	35
5.5. Preparation of Drill-in Fluid.....	36
5.6. Sealing Capability Tests	36

5.6.1. Customization of Slots & Parts of Permeability Plugging Apparatus.....	37
5.6.2. Test Procedure	42
6. RESULTS AND DISCUSSION	47
6.1. Filtration Control.....	49
6.2. Fluid Rheology.....	50
6.3. Effect of Particle Size Distribution of Ground Marble on Sealing 400 microns fracture width	52
6.3.1. Results Obtained for Total Concentration of 30 ppb for 400- μ m Slot Size	53
6.3.2. Results Obtained for Total Concentration of 28 ppb for 400- μ m Slot Size	55
6.3.3. Results Obtained for Total Concentration of 26 ppb for 400- μ m Slot Size	55
6.3.4. Results Obtained for Total Concentration of 24 ppb for 400- μ m Slot Size	56
6.3.5. Results Obtained for Total Concentration of 22 ppb for 400- μ m Slot Size	57
6.3.6. Results Obtained for Total Concentration of 20 ppb for 400- μ m Slot Size	58
6.3.7. Results Obtained for Total Concentration of 16 ppb for 400- μ m Slot Size	61
6.3.8. Results Obtained for Total Concentration of 14 ppb for 400- μ m Slot Size	62
6.3.9. Results Obtained for Total Concentration of 12 ppb for 400- μ m Slot Size	62

6.3.10. Results Obtained for Total Concentration of 10 ppb for 400- μ m Slot Size	63
6.3.11. Results Obtained for Total Concentration of 8 ppb for 400- μ m Slot Size	63
6.3.12. Results Obtained for Total Concentration of 6 ppb for 400- μ m Slot Size	64
6.3.13. Results Obtained for Total Concentration of 4 ppb for 400- μ m Slot Size	66
6.4. Effect of Concentration of Ground Marble on Sealing 400 microns fracture width	68
6.5. Effect of Particle Size Distribution of Ground Marble on Sealing 800 microns fracture width	69
6.5.1. Results Obtained for Total Concentration of 30 ppb for 800- μ m Slot Size	69
6.5.2. Results Obtained for Total Concentration of 28 ppb for 800- μ m Slot Size	74
6.5.3. Results Obtained for Total Concentration of 26 ppb for 800- μ m Slot Size	75
6.5.4. Results Obtained for Total Concentration of 24 ppb for 800- μ m Slot Size	75
6.5.5. Results Obtained for Total Concentration of 22 ppb for 800- μ m Slot Size	76
6.5.6. Results Obtained for Total Concentration of 20 ppb for 800- μ m Slot Size	77
6.6. Effect of Concentration of Ground Marble on Sealing 800 microns fracture width	80

6.7. Effect of Particle Size Distribution of Ground Marble on Sealing 1200 microns fracture width	82
6.7.1. Results Obtained for Total Concentration of 30 ppb for 1200- μ m Slot Size	82
6.7.2. Results Obtained for Total Concentration of 60 ppb for 1200- μ m Slot Size	84
6.8. Effect of Concentration of Ground Marble on Sealing 1200 microns Fracture width.....	86
6.9. Effect of Fracture Width on Sealing	87
7. CONCLUSION.....	89
8. RECOMMENDATIONS.....	91
REFERENCES	93
APPENDICES	99
A. Technical Data Sheet of AMYLOTROL	99
B. Technical Data Sheet of REOZAN D	101
C. Technical Data Sheet of GEOCIDE T.....	103
D. Specifications of Grace Viscometer	104
E. Specifications of Permeability Plugging Apparatus	104
F. Effect of Particle Size Distribution of Ground Marble on Sealing 400- μ Fracture Width.....	105
F. I. Results Obtained for Total Concentration of 30 ppb for 400- μ m Slot	105
F. I. 1. FMC 30-0-0, FMC 0-30-0 & FMC 0-0-30	105
F. I. 2. FMC 10-10-10.....	106
F. II. Results Obtained for Total Concentration of 28 ppb for 400- μ m Slot....	107
F. II. 1. FMC 8-10-10	107

F. II. 2. FMC 10-8-10	108
F. II. 3. FMC 10-10-8	109
F. III. Results Obtained for Total Concentration of 26 ppb for 400- μ m Slot...	110
F. III. 1. FMC 6-10-10	110
F. III. 2. FMC 10-6-10	111
F. III. 3. FMC 10-10-6	112
F. IV. Results Obtained for Total Concentration of 24 ppb for 400- μ m Slot...	113
F. IV. 1. FMC 4-10-10	113
F. IV. 2. FMC 10-4-10	114
F. IV. 3. FMC 10-10-4	115
F. V. Results Obtained for Total Concentration of 22 ppb for 400- μ m Slot....	116
F. V. 1. FMC 2-10-10	116
F. V. 2. FMC 10-2-10	117
F. V. 3. FMC 10-10-2	118
F. VI. Results Obtained for Total Concentration of 20 ppb for 400- μ m Slot...	119
F. VI. 1. FMC 0-10-10	119
F. VI. 2. FMC 10-0-10	120
F. VI. 3. FMC 10-10-0	121
F. VII. Results Obtained for Total Concentration of 16 ppb for 400- μ m Slot .	122
F. VII. 1. FMC 8-6-2	122
F. VIII. Results Obtained for Total Concentration of 14 ppb for 400- μ m Slot	123
F. VIII. 1. FMC 6-6-2	123
F. IX. Results Obtained for Total Concentration of 12 ppb for 400- μ m Slot...	124
F. IX. 1. FMC 4-6-2	124

F. X. Results Obtained for Total Concentration of 10 ppb for 400- μ m Slot....	125
F. X. 1. FMC 2-6-2	125
F. X. 2. FMC 4-6-0	126
F. X. 3. FMC 4-4-2	127
F. XI. Results Obtained for Total Concentration of 8 ppb for 400- μ m Slot Size.....	128
F. XI. 1. FMC 4-2-2	128
F. XII. Results Obtained for Total Concentration of 6 ppb for 400- μ m Slot Size.....	129
F. XII. 1. FMC 4-0-2.....	129
F. XII. 2. FMC 4-2-0.....	130
F. XIII. Results Obtained for Total Concentration of 4 ppb for 400- μ m Slot..	131
F. XIII. 1. FMC 2-2-0	131
G. Effect of Concentration of Ground Marble on Sealing 400- μ Fracture Width	132
G. I. 1. FMC 4-3-1	132
G. I. 2. FMC 12-9-3	133
G. I. 3. FMC 16-12-4	134
H. Effect of Particle Size Distribution of Ground Marble on Sealing 800- μ fracture width.....	135
H. I. Results Obtained for Total Concentration of 30 ppb for 800- μ m Slot.....	135
H. I. 1. FMC 30-0-0, FMC 0-30-0 & FMC 0-0-30.....	135
H. I. 2. FMC 10-10-10	136
H. I. 3. FMC 10-6-14	137
H. I. 4. FMC 10-2-18	138
H. I. 5. FMC 10-18-2	139

H. I. 6. FMC 10-14-6.....	140
H. I. 7. FMC 2-10-18.....	141
H. I. 8. FMC 6-10-14.....	142
H. I. 9. FMC 14-10-6.....	143
H. I. 10. FMC 18-10-2.....	144
H. I. 11. FMC 18-2-10.....	145
H. I. 12. FMC 14-6-10.....	146
H. I. 13. FMC 6-14-10.....	147
H. I. 14. FMC 2-18-10.....	148
H. I. 15. FMC 18-6-6.....	149
H. I. 16. FMC 6-18-6.....	150
H. I. 17. FMC 6-6-18.....	151
H. II. Results Obtained for Total Concentration of 28 ppb for 800- μ m Slot....	152
H. II. 1. FMC 8-10-10	152
H. II. 2. FMC 10-8-10	153
H. II. 3. FMC 10-10-8	154
H. III. Results Obtained for Total Concentration of 26 ppb for 800- μ m Slot ..	155
H. III. 1. FMC 6-10-10.....	155
H. III. 2. FMC 10-6-10.....	156
H. III. 3. FMC 10-10-6.....	157
H. IV. Results Obtained for Total Concentration of 24 ppb for 800- μ m Slot ..	158
H. IV. 1. FMC 4-10-10.....	158
H. IV. 2. FMC 10-4-10.....	159
H. IV. 3. FMC 10-10-4.....	160

H. V. Results Obtained for Total Concentration of 22 ppb for 800- μ m Slot...	161
H. V. 1. FMC 2-10-10.....	161
H. V. 2. FMC 10-2-10.....	162
H. V. 3. FMC 10-10-2.....	163
H. VI. Results Obtained for Total Concentration of 20 ppb for 800- μ m Slot..	164
H. VI. 1. FMC 0-10-10	164
H. VI. 2. FMC 10-0-10	165
H. VI. 3. FMC 10-10-0	166
H. VI. 4. FMC 6-6-8	167
I. Effect of Concentration of Ground Marble on Sealing 800- μ fracture.....	168
I. I. 1. FMC 15-15-15.....	168
I. I. 2. FMC 20-20-20.....	169
I. I. 3. FMC 9-15-21.....	170
I. I. 4. FMC 12-20-28.....	171
J. Effect of Particle Size Distribution of Ground Marble on Sealing 1200- μ Fracture Width.....	172
J. I. Results Obtained for Total Concentration of 30 ppb for 1200- μ Slot.....	172
J. I. 1. FMC 30-0-0, FMC 0-30-0 & FMC 0-0-30	172
J. I. 2. FMC 10-10-10	173
J. I. 3. FMC 10-6-14	174
J. I. 4. FMC 10-2-18	175
J. I. 5. FMC 10-18-2	176
J. I. 6. FMC 10-14-6	177
J. I. 7. FMC 6-10-14	178

J. I. 8. FMC 2-10-18.....	179
J. I. 9. FMC 18-10-2.....	180
J. I. 10. FMC 14-10-6.....	181
J. I. 11. FMC 6-14-10.....	182
J. I. 12. FMC 2-18-10.....	183
J. I. 13. FMC 18-2-10.....	184
J. I. 14. FMC 14-6-10.....	185
J. II. Results Obtained for Total Concentration of 60 ppb for 1200- μ Slot.....	186
J. II. 1. FMC 20-4-36.....	186
J. II. 2. FMC 20-12-28.....	187
J. II. 3. FMC 15-15-30.....	188
J. II. 4. FMC 10-10-40.....	189
J. II. 5. FMC 25-5-30.....	190
J. III. Results Obtained for Total Concentration of 90 ppb for 1200- μ Slot.....	191
J. III. 1. FMC 15-30-45.....	191
J. IV. Results Obtained for Total Concentration of 120 ppb for 1200- μ Slot ..	192
J. IV. 1. FMC 20-40-60.....	192
J. V. Results Obtained for Total Concentration of 150 ppb for 1200- μ Slot....	193
J. V. 1. FMC 25-50-75.....	193
K. Effect of Concentration of Ground Marble on Sealing 1200- μ Fracture.....	194
K. I. 1. FMC 16-16-16.....	194
K. I. 2. FMC 20-20-20.....	195

|

LIST OF TABLES

TABLES

Table 2.1: Fundamental differences between wellbore strengthening mechanisms (Cock et al, 2012).....	13
Table 2.2: Shape Factor of Different Materials (Kumar et. al., 2010).....	14
Table 2.3: Composition of LCM used for comparing different slots (Kumar and Savari, 2011).....	18
Table 2.4: Fluid Loss Results for comparison of constant area slots and tapered slots (Kumar and Savari,2011).....	18
Table 2.5: Fluid Loss Testing Performed on Tapered Slot with different Particles..	19
Table 2.6: Individual LCM concentration and PSD tested in Low Pressure Testing Apparatus (Alsaba et al., 2014b).....	21
Table 2.7: Concentration and PSD of LCM Blends tested in Low Pressure Testing Apparatus (Alsaba et al., 2014b).....	22
Table 5.1: Sieves Standard No. Mesh Sizes and Standard Sieves Designation	31
Table 5.2: Particle Size Distribution of Ground Marble	32
Table 5.3: Composition of Drill-in Fluid.	33
Table 5.4: The properties of Tap Water	33
Table 5.5: Dimensions of Re-designed Slots	40
Table 5.6: Examples of Mud Loss and Total Sealing Time Tables	43
Table 6.1: Results of Fluid Loss Measurement during 30 minutes.....	50
Table 6.2: PV, YP, LSRYP and LSRV at 0.0636 sec ⁻¹ values of Base A, Base B and Base C fluid.....	51
Table 6.3: Mud Loss & Total Sealing Time Values for FMC 10-10-10 on 400-micron fracture	54
Table 6.4: Comparison of FMC 8-10-10, FMC 10-8-10 & FMC 10-10-8	55

Table 6.5: Comparison of FMC 6-10-10, FMC 10-6-10 & FMC 10-10-6.....	56
Table 6.6: Comparison of FMC 4-10-10, FMC 10-4-10 & FMC 10-10-4.....	57
Table 6.7: Comparison of FMC 2-10-10, FMC 10-2-10 & FMC 10-10-2.....	58
Table 6.8: Comparison of FMC 0-10-10, FMC 10-0-10 & FMC 10-10-0.....	59
Table 6.9: Mud Loss & Total Sealing Time Values for FMC 8-6-2 on 400-micron fracture width.....	62
Table 6.10: Comparison of FMC 2-6-2, FMC 4-4-2 & FMC 4-6-0.....	63
Table 6.11: Mud Loss & Total Sealing Time Values for FMC 4-0-2 on 400-micron fracture width.....	65
Table 6.12: Comparison of FMC 4-0-2 and FMC 4-2-0	66
Table 6.13: Mud Loss & Total Sealing Time Values for FMC 2-2-0 on 400 micron fracture width.....	67
Table 6.14: Comparison of Best Results for Sealing of 400 μm fracture width	67
Table 6.15: The effect of concentration on sealing 400-micron fracture width	68
Table 6.16: Mud Loss & Total Sealing Time Values for FMC 10-10-10 on 800-micron fracture width	70
Table 6.17: Comparison of importance of coarse and medium sized particles	71
Table 6.18: Comparison of importance of fine sized and coarse sized particles on 800-micron fracture width	72
Table 6.19: Comparison of the Importance of Fine and Medium Particle Ranges ...	73
Table 6.20: Comparison of FMC 18-6-6, FMC 6-18-6 and FMC 6-6-18	74
Table 6.21: Comparison of FMC 8-10-10, FMC 10-8-10 & FMC 10-10-8.....	74
Table 6.22: Comparison of FMC 6-10-10, FMC 10-6-10 & FMC 10-10-6.....	75
Table 6.23: Comparison of FMC 4-10-10, FMC 10-4-10 and FMC 10-10-4	75
Table 6.24: Comparison of FMC 2-10-10, FMC 10-2-10 and FMC 10-10-2	76
Table 6.25: Comparison of FMC 0-10-10, FMC 10-0-10 and FMC 10-10-0	77
Table 6.26: Mud Loss & Total Sealing Time Values for FMC 6-6-8 on 800-micron fracture width.....	78
Table 6.27: Comparison of Successful Results on Sealing of 800- μm Fracture Width	79

Table 6.28: Effect of Concentration on Sealing (1)	81
Table 6.29: Effect of Concentration on Sealing (2)	81
Table 6.30: Comparison of Maximum Sealing Pressures of Different Compositions on the 1200- μ m fracture width (1).....	83
Table 6.31: Comparison of Maximum Sealing Pressures of Different Compositions on the 1200- μ m fracture width (2).....	83
Table 6.32: Comparison of Maximum Sealing Pressures of Different Compositions on the 1200- μ m fracture width (3).....	84
Table 6.33: Effect of Concentration on Sealing 1200- μ m Fracture Width.....	86
Table 6.34: Total Sealing Time and Total Mud Loss Values for FMC 10-10-10 composition on different fracture width.....	87
Table F.1: Mud Loss & Total Sealing Time Values for each particle range individually.....	105
Table F.2: Mud Loss & Total Sealing Time Values for FMC 10-10-10 on 400-micron slot.....	106
Table F.3: Mud Loss & Total Sealing Time Values for FMC 8-10-10 on 400-micron slots.....	107
Table F.4: Mud Loss & Total Sealing Time Values for FMC 10-8-10 on 400-micron fracture width.....	108
Table F.5: Mud Loss&Total Sealing Time Values for FMC 10-10-8 on 400-micron fracture width... ..	109
Table F.6: Mud Loss & Total Sealing Time Values for FMC 6-10-10 on 400-micron fracture width... ..	110
Table F.7: Mud Loss & Total Sealing Time Values for FMC 10-6-10 on 400-micron fracture width... ..	111
Table F.8: Mud Loss & Total Sealing Time Values for FMC 10-10-6 on 400-micron fracture width... ..	112
Table F.9: Mud Loss & Total Sealing Time Values for FMC 4-10-10 on 400-micron fracture width... ..	113

Table F.10: Mud Loss & Total Sealing Time Values for FMC 10-4-10 on 400-micron fracture width.....	114
Table F.11: Mud Loss & Total Sealing Time Values for FMC 10-10-4 on 400-micron fracture width.....	115
Table F.12: Mud Loss & Total Sealing Time Values for FMC 2-10-10 on 400-micron fracture width.....	116
Table F.13: Mud Loss & Total Sealing Time Values for FMC 10-2-10 on 400-micron fracture width.....	117
Table F.14: Mud Loss & Total Sealing Time Values for FMC 10-10-2 on 400-micron fracture width.....	118
Table F.15: Mud Loss & Total Sealing Time Values for FMC 0-10-10 on 400-micron fracture width.....	119
Table F.16: Mud Loss & Total Sealing Time Values for FMC 10-0-10 on 400-micron fracture width.....	120
Table F.17: Mud Loss & Total Sealing Time Values for FMC 10-10-0 on 400-micron fracture width.....	121
Table F.18: Mud Loss & Total Sealing Time Values for FMC 8-6-2 on 400-micron fracture width.....	122
Table F.19: Mud Loss & Total Sealing Time Values for FMC 6-6-2 on 400-micron fracture width.....	123
Table F.20: Mud Loss & Total Sealing Time Values for FMC 4-6-2 on 400-micron fracture width.....	124
Table F.21: Mud Loss & Total Sealing Time Values for FMC 2-6-2 on 400-micron fracture width.....	125
Table F.22: Mud Loss & Total Sealing Time Values for FMC 4-6-0 on 400-micron fracture width.....	126
Table F.23: Mud Loss & Total Sealing Time Values for FMC 4-4-2 on 400-micron fracture width.....	127
Table F.24: Mud Loss & Total Sealing Time Values for FMC 4-2-2 on 400-micron fracture width.....	128

Table F.25: Mud Loss & Total Sealing Time Values for FMC 4-0-2 on 400-micron fracture width.....	129
Table F.26: Mud Loss & Total Sealing Time Values for FMC 4-2-0 on 400-micron fracture width.....	130
Table F.27: Mud Loss & Total Sealing Time Values for FMC 2-2-0 on 400-micron fracture width.....	131
Table G.1: Mud Loss & Total Sealing Time Values for FMC 4-3-1 on 400-micron fracture width.....	132
Table G.2: Mud Loss & Total Sealing Time Values for FMC 12-9-3 on 400-micron fracture width.....	133
Table G.3: Mud Loss & Total Sealing Time Values for FMC 16-12-4 on 400-micron fracture width.....	134
Table H.1: Mud Loss & Total Sealing Time Values for each particle range individually.....	135
Table H.2: Mud Loss&Total Sealing Time Values for FMC 10-10-10 on 800-micron fracture width.....	136
Table H.3: Mud Loss & Total Sealing Time Values for FMC 10-6-14 on 800-micron fracture width.....	137
Table H.4: Mud Loss &Total Sealing Time Values for FMC 10-2-18 on 800-micron fracture width.....	138
Table H.5: Mud Loss &Total Sealing Time Values for FMC 10-18-2 on 800-micron fracture width.....	139
Table H.6: Mud Loss&Total Sealing Time Values for FMC 10-14-06 on 800-micron fracture width.....	140
Table H.7: Mud Loss & Total Sealing Time Values for FMC 18-10-2 on 800-micron fracture width.....	141
Table H.8: Mud Loss & Total Sealing Time Values for FMC 6-10-14 on 800-micron fracture width.....	142
Table H.9: Mud Loss & Total Sealing Time Values for FMC 14-10-6 on 800-micron fracture width.....	143

Table H.10: Mud Loss & Total Sealing Time Values for FMC 18-10-2 on 800-micron fracture width..... 144

Table H.11: Mud Loss & Total Sealing Time Values for FMC 18-2-10 on 800-micron fracture width..... 145

Table H.12: Mud Loss & Total Sealing Time Values for FMC 14-6-10 on 800-micron fracture width..... 146

Table H.13: Mud Loss & Total Sealing Time Values for FMC 6-14-10 on 800-micron fracture width..... 147

Table H.14: Mud Loss & Total Sealing Time Values for FMC 2-18-10 on 800-micron fracture width..... 148

Table H.15: Mud Loss & Total Sealing Time Values for FMC 18-6-6 on 800-micron fracture width..... 149

Table H.16: Mud Loss & Total Sealing Time Values for FMC 6-18-6 on 800-micron fracture width..... 150

Table H.17: Mud Loss & Total Sealing Time Values for FMC 6-6-18 on 800-micron fracture width..... 151

Table H.18: Mud Loss & Total Sealing Time Values for FMC 8-10-10 on 800-micron fracture width..... 152

Table H.19: Mud Loss & Total Sealing Time Values for FMC 10-8-10 on 800-micron fracture width..... 153

Table H.20: Mud Loss & Total Sealing Time Values for FMC 10-10-8 on 800-micron fracture width..... 154

Table H.21: Mud Loss & Total Sealing Time Values for FMC 6-10-10 on 800 micron fracture width..... 155

Table H.22: Mud Loss & Total Sealing Time Values for FMC 10-6-10 on 800 micron fracture width..... 156

Table H.23: Mud Loss & Total Sealing Time Values for FMC 10-10-6 on 800-micron fracture width..... 157

Table H.24: Mud Loss & Total Sealing Time Values for FMC 4-10-10 on 800-micron fracture width..... 158

Table H.25: Mud Loss & Total Sealing Time Values for FMC 10-4-10 on 800-micron fracture width.....	159
Table H.26: Mud Loss & Total Sealing Time Values for FMC 10-10-4 on 800-micron fracture width.....	160
Table H.27: Mud Loss & Total Sealing Time Values for FMC 2-10-10 on 800-micron fracture width.....	161
Table H.28: Mud Loss & Total Sealing Time Values for FMC 10-2-10 on 800-micron fracture width.....	162
Table H.29: Mud Loss & Total Sealing Time Values for FMC 10-10-2 on 800-micron fracture width.....	163
Table H.30: Mud Loss & Total Sealing Time Values for FMC 0-10-10 on 800-micron fracture width.....	164
Table H.31: Mud Loss & Total Sealing Time Values for FMC 10-0-10 on 800-micron fracture width.....	165
Table H.32: Mud Loss & Total Sealing Time Values for FMC 4-10-10 on 800-micron fracture width.....	166
Table H.33: Mud Loss & Total Sealing Time Values for FMC 6-6-8 on 800-micron fracture width.....	167
Table I.1: Mud Loss & Total Sealing Time Values for FMC 15-15-15 on 800-micron fracture width.....	168
Table I.2: Mud Loss & Total Sealing Time Values for FMC 20-20-20 on 800-micron fracture width.....	169
Table I.3: Mud Loss & Total Sealing Time Values for FMC 9-15-21 on 800-micron fracture width.....	170
Table I. 4: Mud Loss & Total Sealing Time Values for FMC 12-20-28 on 800-micron fracture width.....	171
Table J.1: Mud Loss & Total Sealing Time Values for each particle range individually on 1200-micron fracture width.....	172
Table J.2: Mud Loss & Total Sealing Time Values for FMC 10-10-10 on 1200-micron fracture width.....	173

Table J.3: Mud Loss&Total Sealing Time Values for FMC 10-6-14 on 1200-micron fracture width.....	174
Table J.4: Mud Loss & Total Sealing Time Values for FMC 10-2-18 on 1200-micron fracture width.....	175
Table J.5: Mud Loss&Total Sealing Time Values for FMC 10-18-2 on 1200-micron fracture width.....	176
Table J.6: Mud Loss&Total Sealing Time Values for FMC 10-14-6 on 1200-micron fracture width.....	177
Table J.7: Mud Loss &Total Sealing Time Values for FMC 6-10-14 on 1200-micron fracture width.....	178
Table J.8: Mud Loss & Total Sealing Time Values for FMC 2-10-18 on 1200-micron fracture width.....	179
Table J.9: Mud Loss &Total Sealing Time Values for FMC 18-10-2 on 1200-micron fracture width.....	180
Table J.10: Mud Loss & Total Sealing Time Values for FMC 14-10-6 on 1200-micron fracture width.....	181
Table J.11: Mud Loss&Total Sealing Time Values for FMC 6-14-10 on 1200-micron fracture width.....	182
Table J.12: Mud Loss &Total Sealing Time Values for FMC 2-18-10 on 1200-micron fracture width.....	183
Table J.13: Mud Loss&Total Sealing Time Values for FMC 18-2-10 on 1200-micron fracture width.....	184
Table J.14: Mud Loss&Total Sealing Time Values for FMC 14-6-10 on 1200-micron fracture width.....	185
Table J.15: Mud Loss& Total Sealing Time Values for FMC 20-4-36 on 1200-micron fracture width.....	186
Table J.16: Mud Loss & Total Sealing Time Values for FMC 20-12-28 on 1200-micron fracture width	187
Table J.17: Mud Loss & Total Sealing Time Values for FMC 15-15-30 on 1200-micron fracture width	188

Table J.18: Mud Loss & Total Sealing Time Values for FMC 10-10-40 on 1200-micron fracture width.....189

Table J.19: Mud Loss & Total Sealing Time Values for FMC 25-5-30 on 1200-micron fracture width.....190

Table J.20: Mud Loss & Total Sealing Time Values for FMC 15-30-45 on 1200-micron fracture width.....191

Table J.21: Mud Loss & Total Sealing Time Values for FMC 20-40-60 on 1200-micron fracture width.....192

Table J.22: Mud Loss & Total Sealing Time Values for FMC 25-50-75 on 1200-micron fracture width.....193

Table K.1: Mud Loss & Total Sealing Time Values for FMC 16-16-16 on 1200-micron fracture width.....194

Table K.2: Mud Loss & Total Sealing Time Values for FMC 20-20-20 on 1200-micron fracture width.....195

LIST OF FIGURES

FIGURES

Figure 1.1: Density ranges for different drilling fluid systems (Lake & Mitchell, 2006)	3
Figure 2.1: Schematics of PPA (Mostafavi et al, 2011).....	7
Figure 2.2: Schematic of Permeable Fracture Test Device (Hetteema et al, 2007).....	9
Figure 2.3: Corrugated Aluminum Platens for Fracture Tester (Sanders et al, 2008)	10
Figure 2.4: Schematics of Impermeable Fracture Test Device.....	11
Figure 2.5: Alteration in Fracture Width with Changing Equivalent Circulating Density (ECD) (Kumar et al, 2010).....	15
Figure 2.6: Low Pressure LCM Test Apparatus (Alsaba et al.,2014b).....	20
Figure 2.7: High Pressure Test Apparatus (Alsaba et al. 2014).....	23
Figure 4.1: Stress Cage Concept (Cock et al., 2011).....	28
Figure 4.2: Fracture Closure Stress Concept (Growcock, 2011).....	29
Figure 4.3: Fracture Tip Isolation Concept in (a)(left figure) WBDFs (b)(right figure) OBDFs (Cock, 2012).....	30
Figure 5.1: Numbers of sieves and their mesh sizes in micron.....	32
Figure 5.2: GRACE M3600 Automatic Viscometer.....	35
Figure 5.3: Normal PPA Assembly.....	37
Figure 5.4: Illustration of bridge formed by particles in the needle valve.....	38
Figure 5.5: Front view (the left figure) and bottom view (the right figure) of redesigned top cap.....	38
Figure 5.6: Representation of accumulation of particles inside the fracture due to inappropriate flow channel.....	39

Figure 5.7: Front view (left figure) and Bottom view(right figure) of redesigned slots	39
Figure 5.8: Drawings of redesigned slots	40
Figure 5.9: Final Configuration of slots.....	41
Figure 5.10: PPA Assembly used in the test.....	41
Figure 5.11: Hand Pump Gauge	43
Figure 5.12: Representation of Pressure Sealing Test Graphs	45
Figure 6.1: Comparison of Filtration Values	49
Figure 6.2: Shear Stress vs Shear Rate Graph of Base A, Base B & Base C fluids. .51	
Figure 6.3: Viscosity vs Shear Rate Graph of Base A, Base B and Base C Fluids on log-log coordinates	52
Figure 6.4: Pressure vs Time curve for FMC 10-10-10 on sealing 400-micron fracture width	54
Figure 6.5: Illustration of Particle Breaking under pressure	57
Figure 6.6: Illustration of flow through the highly permeable sands (Petropedia, 2018)	59
Figure 6.7: Pressure vs Time curve for FMC 8-6-2 on 400-micron fracture width .61	
Figure 6.8: Pressure vs Time curve for FMC 4-0-2 on 400-micron fracture width .64	
Figure 6.9: Pressure vs Time curve for FMC 2-2-0 on 400 micron fracture width..66	
Figure 6.10: Pressure vs Time curve for FMC 10-10-10 on 800-micron fracture width	70
Figure 6.11: Pressure vs Time curve for FMC 6-6-8 on 800-micron fracture width78	
Figure F.1: Pressure vs Time curve for each particle range individually on sealing 400-micron fracture width.....	105
Figure F.2: Pressure vs Time curve for FMC 10-10-10 on sealing 400-micron fracture width.....	106
Figure F.3: Pressure vs Time curve for FMC 8-10-10 on 400-micron fracture width.....	107

Figure F.4: Pressure vs Time curve for FMC 10-8-10 on 400-micron fracture width.....	108
Figure F.5: Pressure vs Time curve for FMC 10-10-8 on 400-micron fracture width.....	109
Figure F.6: Pressure vs Time curve for FMC 6-10-10 on 400-micron fracture width.....	110
Figure F.7: Pressure vs Time curve for FMC 10-6-10 on 400-micron fracture width.....	111
Figure F.8: Pressure vs Time curve for FMC 10-10-6 on 400-micron fracture width.....	112
Figure F.9: Pressure vs Time curve for FMC 4-10-10 on 400-micron fracture width.....	113
Figure F.10: Pressure vs Time curve for FMC 10-4-10 on 400-micron fracture width.....	114
Figure F.11: Pressure vs Time curve for FMC 10-10-4 on 400-micron fracture width.....	115
Figure F.12: Pressure vs Time curve for FMC 2-10-10 on 400-micron fracture width.....	116
Figure F.13: Pressure vs Time curve for FMC 10-2-10 on 400-micron fracture width.....	117
Figure F.14: Pressure vs Time curve for FMC 10-10-2 on 400-micron fracture width.....	118
Figure F.15: Pressure vs Time curve for FMC 0-10-10 on 400-micron fracture width.....	119
Figure F.16: Pressure vs Time curve for FMC 10-0-10 on 400-micron fracture width.....	120
Figure F.17: Pressure vs Time curve for FMC 10-10-0 on 400-micron fracture width.....	121
Figure F.18: Pressure vs Time curve for FMC 8-6-2 on 400-micron fracture width.....	122

Figure F.19: Pressure vs Time curve for FMC 6-6-2 on 400-micron fracture width.....	123
Figure F.20: Pressure vs Time curve for FMC 4-6-2 on 400-micron fracture width.....	124
Figure F.21: Pressure vs Time curve for FMC 2-6-2 on 400-micron fracture width.....	125
Figure F.22: Pressure vs Time curve for FMC 4-6-0 on 400-micron fracture width.....	126
Figure F.23: Pressure vs Time curve for FMC 4-4-2 on 400-micron fracture width.....	127
Figure F.24: Pressure vs Time curve for FMC 4-2-2 on 400-micron fracture width.....	128
Figure F.25: Pressure vs Time curve for FMC 4-0-2 on 400-micron fracture width.....	129
Figure F.26: Pressure vs Time curve for FMC 4-2-0 on 400-micron fracture width.....	130
Figure F.27: Pressure vs Time curve for FMC 2-2-0 on 400-micron fracture width.....	131
Figure G.1: Pressure vs Time curve for FMC 4-3-1 on 400-micron fracture width.....	132
Figure G.2: Pressure vs Time curve for FMC 12-9-3 on 400-micron fracture width.....	133
Figure G.3: Pressure vs Time curve for FMC 12-9-3 on 400-micron fracture width.....	134
Figure H.1: Pressure vs Time curve for each particle range individually on sealing 800-micron fracture width.....	135
Figure H. 2: Pressure vs Time curve for FMC 10-10-10 on 800-micron fracture width.....	136
Figure H.3: Pressure vs Time curve for FMC 10-6-14 on 800-micron fracture width.....	137

Figure H.4: Pressure vs Time curve for FMC 10-2-18 on 800-micron fracture width.....	138
Figure H.5: Pressure vs Time curve for FMC 10-18-2 on 800-micron fracture width.....	139
Figure H.6: Pressure vs Time curve for FMC 10-14-6 on 800-micron fracture width.....	140
Figure H.7: Pressure vs Time curve for FMC 18-10-2 on 800-micron fracture width.....	141
Figure H.8: Pressure vs Time curve for FMC 6-10-14 on 800-micron fracture width.....	142
Figure H.9: Pressure vs Time curve for FMC 14-10-6 on 800-micron fracture width.....	143
Figure H.10: Pressure vs Time curve for FMC 18-10-2 on 800-micron fracture width.....	144
Figure H.11: Pressure vs Time curve for FMC 18-2-10 on 800-micron fracture width.....	145
Figure H.12: Pressure vs Time curve for FMC 14-6-10 on 800-micron fracture width.....	146
Figure H.13: Pressure vs Time curve for FMC 6-14-10 on 800-micron fracture width.....	147
Figure H.14: Pressure vs Time curve for FMC 2-18-10 on 800-micron fracture width.....	148
Figure H.15: Pressure vs Time curve for FMC 18-6-6 on 800-micron fracture width.....	149
Figure H.16: Pressure vs Time curve for FMC 6-18-6 on 800-micron fracture width.....	150
Figure H.17: Pressure vs Time curve for FMC 6-6-18 on 800-micron fracture width.....	151
Figure H.18: Pressure vs Time curve for FMC 8-10-10 on 800-micron fracture width.....	152

Figure H.19: Pressure vs Time curve for FMC 10-8-10 on 800-micron fracture width..... 153

Figure H.20: Pressure vs Time curve for FMC 10-10-8 on 800-micron fracture width..... 154

Figure H.21: Pressure vs Time curve for FMC 6-10-10 on 800-micron fracture width..... 155

Figure H.22: Pressure vs Time curve for FMC 10-6-10 on 800-micron fracture width..... 156

Figure H.23: Pressure vs Time curve for FMC 10-10-6 on 800-micron fracture width..... 157

Figure H.24: Pressure vs Time curve for FMC 4-10-10 on 800-micron fracture width..... 158

Figure H.25: Pressure vs Time curve for FMC 10-4-10 on 800-micron fracture width..... 159

Figure H.26: Pressure vs Time curve for FMC 10-10-4 on 800-micron fracture width..... 160

Figure H.27: Pressure vs Time curve for FMC 10-10-10 on 800-micron fracture width..... 161

Figure H.28: Pressure vs Time curve for FMC 10-2-10 on 800-micron fracture width..... 162

Figure H.29: Pressure vs Time curve for FMC 10-10-2 on 800-micron fracture width..... 163

Figure H.30: Pressure vs Time curve for FMC 0-10-10 on 800-micron fracture width..... 164

Figure H.31: Pressure vs Time curve for FMC 10-0-10 on 800-micron fracture width..... 165

Figure H.32: Pressure vs Time curve for FMC 10-10-0 on 800-micron fracture width..... 166

Figure H.33: Pressure vs Time curve for FMC 6-6-8 on 800-micron fracture width..... 167

Figure I.1: Pressure vs Time curve for FMC 15-15-15 on 800-micron fracture width.....	168
Figure I.2: Pressure vs Time curve for FMC 20-20-20 on 800-micron fracture width.....	169
Figure I.3: Pressure vs Time curve for FMC 9-15-21 on 800-micron fracture width.....	170
Figure I.4: Pressure vs Time curve for FMC 12-20-28 on 800-micron fracture width.....	171
Figure J.1: Pressure vs Time curve for FMC 10-10-10 on 1200-micron fracture width.....	173
Figure J.2: Pressure vs Time curve for FMC 10-6-14 on 1200-micron fracture width.....	174
Figure J.3: Pressure vs Time curve for FMC 10-2-18 on 1200-micron fracture width.....	175
Figure J.4: Pressure vs Time curve for FMC 10-14-6 on 1200-micron fracture width.....	177
Figure J.5: Pressure vs Time curve for FMC 6-10-14 on 1200-micron fracture width.....	178
Figure J.6: Pressure vs Time curve for FMC 2-10-18 on 1200-micron fracture width.....	179
Figure J.7: Pressure vs Time curve for FMC 14-10-6 on 1200-micron fracture width.....	181
Figure J.8: Pressure vs Time curve for FMC 6-14-10 on 1200-micron fracture width.....	182
Figure J.9: Pressure vs Time curve for FMC 2-18-10 on 1200-micron fracture width.....	183
Figure J.10: Pressure vs Time curve for FMC 18-2-10 on 1200-micron fracture width.....	184
Figure J.11: Pressure vs Time curve for FMC 14-6-10 on 1200-micron fracture width.....	185

Figure J.12: Pressure vs Time curve for FMC 20-4-36 on 1200-micron fracture width..... 186

Figure J.13: Pressure vs Time curve for FMC 20-12-28 on 1200-micron fracture width..... 187

Figure J.14: Pressure vs Time curve for FMC 15-15-30 on 1200-micron fracture width..... 188

Figure J.15: Pressure vs Time curve for FMC 10-10-40 on 1200-micron fracture width..... 189

Figure J.16: Pressure vs Time curve for FMC 25-5-30 on 1200-micron fracture width..... 190

Figure J.17: Pressure vs Time curve for FMC 15-30-45 on 800-micron fracture width..... 191

Figure J.18: Pressure vs Time curve for FMC 20-40-60 on 1200-micron fracture width..... 192

Figure J.19: Pressure vs Time curve for FMC 25-50-75 on 800-micron fracture width..... 193

Figure K.1: Pressure vs Time curve for FMC 16-16-16on 1200-micron fracture width..... 194

Figure K.2: Pressure vs Time curve for FMC 20-20-20 on 1200-micron fracture width..... 195

CHAPTER 1

INTRODUCTION

Over the past century, demand for oil and gas has significantly increased with growing economies. Drilling activities has shifted to explore deeper, harsher and more complex environments to meet this demand. While drilling these environments, operators face with many challenges where lost circulation is one of the main ones. Lost circulation can be defined as the loss of drilling fluids partially or totally into the formation. Due to the loss of the costly drilling fluid, drilling expenses increase and create non-productive time (NPT) which is spent for mitigating and regaining mud circulation. Apart from trouble cost for mud losses and non-productive operation time, it can also end up with lost of expensive downhole equipment or drilling problems such as differential stuck, blowout and abandonment of well. Moreover, since solids and liquid in the mud might invade into the target zone during drilling of reservoir section, it can result in unsatisfactory production rates due to formation damage.

In general, four types of formation have high potential for lost circulation;

- A. Natural or induced formation fractures
- B. Vugular and/or cavernous formations
- C. Highly permeable formations
- D. Unconsolidated formations.

Although, small fractures are found in almost all formations, highly conductive natural fractures are present mostly in chalks and limestone reservoirs where significant losses occur. In Turkey, highly fractured carbonate formations are encountered frequently and may lead to lost circulation while drilling. These natural fractures can be micro-fractured sized or large opening size with high interconnected channels.

While drilling, fluid pressure might exceed the formation fracture pressure. In impermeable and tight formations, induced fractures may occur and losses through these fractures can be encountered. Once these fractures are created, it may be difficult to remove it since the pressure required to lengthen a fracture is often lower than that required to initiate it. Therefore, it may never regain the original formation strength and lost circulation may never be stopped even though pressure over formation is reduced.

In general, circulation losses are classified in three groups based on the losses rate (bbl/hr):

- Seepage loss, (1-10 bbl/hr)
- Partial loss (10-500 bbl/hr)
- Total loss (over 500 bbl/hr).

This categorization is only valid for losses through permeable formations. In natural fractures, there is no barrier to stop the flow into the formation because of large opening size. Therefore, totally from hundreds to thousands of barrels of drilling fluid might be lost.

There are plenty of studies made for solving the lost circulation problem. All of these studies can be classified into two: Corrective (or Mitigating) Methods and Preventive Methods. Corrective methods include treating, i.e. controlling and stopping of losses after lost circulation occurs. On the other hand, Preventive Methods are applied prior to entering loss circulation zones and used to strength the wellbore and to prevent the occurrence of losses. This approach depends on propping and sealing the fractures using wellbore strengthening materials (WSMs) while drilling to enhance the fracture gradient and widen the operational window (Salehi and Nygaard, 2011). WSMs are drilling fluid additives which are specially sized and designed particulates. Resilient graphitic carbon, cellulosic fibre, ground nutshell and marble are examples of WSMs. They can be categorized also in Lost Circulation Materials. However, WSM's have proved effects on both to mitigate losses and for preventing them.

Ground Marble (GM) is often used to combat severe fluid losses. Its chemical composition is calcium carbonate (CaCO_3). GM is the most appropriate granular type of material that can be used for the design of Drill-in Fluids because of its mechanical and chemical properties. Also, it is resistant to high pressure differentials and also swap/surge and drill string impacts in the wellbore. It is chemically soluble in hydrochloric (HCl) acid which guarantees its removal from porous media and pore throats after invasion and allows using it even in production zones. In this study, ground marble will be tested as WSM with different range and concentration.

The range of particle size distribution (PSD) of ground marble used in this study will be based on the range of materials available in the market.

While drilling highly depleted fractured zones, drilling with conventional water-based and oil-based systems might be difficult and losses can be occurred due to high overbalance. In these environments, sometimes systems with lower densities which can be seen in Figure 1.1 may be used. As can be seen, these environments can be drilled with aerated mud, stable foam and mist or air. However, for drilling with these drilling fluids, it needs to set-up expensive surface equipment.

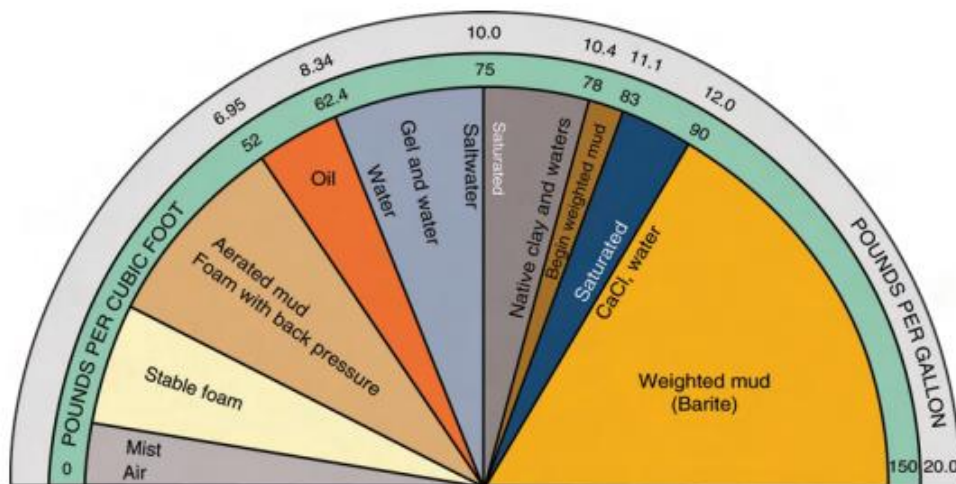


Figure 1.1: Density ranges for different drilling fluid systems (Lake & Mitchell, 2006)

By means of usage of wellbore strengthening materials in conventional oil or water-based systems, these highly depleted environments can be drilled without needed systems with lower densities.

Intention of the study is to conduct experimental investigation on determining optimum concentration and PSD, which enables to drill fractured reservoirs. To do this, firstly the wells in the Turkey is examined. According to the statistics which obtained from website of General Directorate of Mining and Petroleum Affairs, there is no well which is currently producing oil or gas deeper than 4200 metres. Also, the deepest geothermal well in Turkey is SY-23 located in Alaşehir, Manisa. The depth of this well is 4312 metres (Ülgen, Damcı & Gülmez, 2018). Since there is no deeper well than 4400 metres in Turkey, the fractured and depleted reservoirs at depth of 4400 metres had been chosen as target of this study. Conventional oil or water systems supported with wellbore strengthening materials that resist to 2000 psi overbalance should be preferred to eliminate the usage of systems with lower densities.

$$\text{Overbalance Pressure (psi)} = 0.052 * \text{Differential Mud Weight (ppg)} * \text{Depth (ft)}$$

$$2000 \text{ psi} = 0.052 * \Delta\rho * 4400\text{m} * 3.281 \text{ ft/m}$$

$$\Delta\rho = 2.66 \text{ lb/gal}$$

In general, the densities of conventional water-based drilling systems may change between 8.50 lb/gal and 9.34 lb/gal. By using of wellbore strengthening materials, environments with pore pressure ranging from 5.84 lb/gal to 6.65 lb/gal can be drilled. These densities can change according to the amount of used materials.

In this study, experiments conducted to find the effect of particle size distribution, concentration and the fracture size on sealing. Also, it is aimed to define optimum composition which seals the predetermined openings

CHAPTER 2

LITERATURE REVIEW

Wellbore Strengthening prevents occurrence of losses by strengthening the wellbore and enhancing the effective fracture pressure. Hoop Stress Enhancement (or Stress Cage Model), Fracture Closure Stress and Fracture Propagation Resistance (or Fracture Tip Isolation) are different mechanism of wellbore strengthening. Each mechanism uses different technique to prevent occurrence of losses. Detailed information about wellbore strengthening mechanisms can be found in Theory Chapter.

Many experimental studies have been conducted on lost circulation and wellbore strengthening. The DEA-13 experimental study conducted in the middle 1980s to early 1990s [Morita, Black and Fuh, (1996) , van Oort and Razavi, (2014), Fuh, Morita, Boyd and McGoffin, (1992)] is an early experimental investigation into lost circulation.

The aim of that study was to examine and understand why lost circulation occurs less frequently while drilling with water-based mud (WBM) than with oil based mud (OBM). A major observation of DEA-13 project was that fracture propagation pressure (FPP) is strongly related to mud type and significantly increased by the use of LCM additives.

This result was explained by a physical model called “tip screen-out” [Morita, Black and Fuh, (1996), Morita, Fuh and Black, (1996), Morita and Fuh (2012), Fuh, Morita, Boyd, McGoffin, (1992)], which indicates that the increase in FPP is due to isolation of the fracture tip and wellbore pressure by an LCM filtercake in the fracture.

Another major experimental effort, The GPRI 2000 project, was conducted in the late 1990s to early 2000s [van Oort, Friedheim, Pierce and Lee, (2011)]. The purpose of

the GPRI 2000 project was to evaluate the capabilities of different LCMs on increasing fracture gradient. The experimental results show that fracture reopening pressure (FRP) of a wellbore can be increased by using LCMs and this effect is more remarkable in WBM than in OBM or synthetic based muds (SBM).

A recent experimental study on lost circulation conducted from late 2000s to early 2010s is called the Lost Circulation and Wellbore Strengthening Research Cooperative Agreement (RCA) project [Guo, Cook, Way, Ji and Friedheim, (2014)]. The aim of this project was to investigate the wellbore strengthening mechanism and the effectiveness of different wellbore strengthening methods (preventive and remedial methods). The main results of this study include that (1) a preventive wellbore strengthening treatment is more effective than remedial treatment; (2) particle size distribution (PSD) and concentration of LCM are critical in wellbore strengthening; and (3) fracture pressure achieved with wellbore strengthening can be higher than the formation breakdown pressure (FBP).

Mostafavi et al. (2011) conducted experiments on not only PPA with a wide range of particles but also on core fracturing tests. Their aim was to develop a reliable model for wellbore strengthening by understanding the governing mechanism of particle sealing. PSD, concentration, fracture surface friction coefficient parameters were investigated and evaluated. Firstly, particles were selected in order to test all particle shapes. Resilient graphite, mica flakes, calcium carbonate, and two types of commercially used fibers were tested in different concentrations (8 lb/bbl, 17 lb/bbl, 35 lb/bbl) and mixtures after sieved and prepared to mix into water-based drilling fluid according to specific PSDs. The tests were conducted at atmospheric pressure. The known opening sizes used in this test 300 μm , 500 μm and 700 μm . Since the results of traditional PPA method of data analysis did not correlate with field experiences and core fracturing tests, new data analysis was designed and applied. Modified system can be seen in Figure 2.1. In this method, water was pumped with a constant flow rate of 0.067 ml/sec on the top of sample fluid of 350 ml to push the sample out of the vessel. Eventually, a bridge was formed by the particles on the fracture and prevented

the fluid exiting the vessel. Due to constant water injection, pressure increase was observed. The bridge collapsed at an elevated pressure and sealing rebuilt up. This situation repeated several times until the whole fluid (350 ml) exits the vessel. All pressures were recorded by using computer data acquisition system. Each test was repeated at least five times for reliability and average values of them were applied in the analysis. The test results were correlated by a core fracturing set-up.

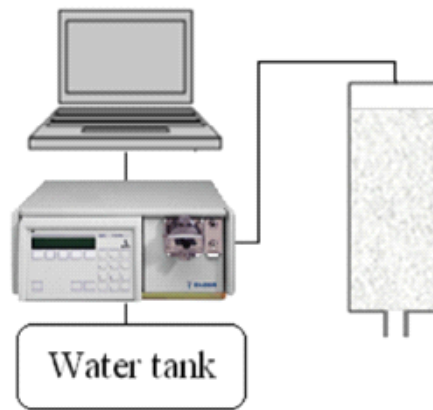


Figure 2.1: Schematics of PPA (Mostafavi et al, 2011)

Besides the effects of PSD and concentration, they also examined the impact of fracture surface coefficient. In order to investigate it, tests were conducted by using a smooth fracture surface and repeated it in wrinkled fracture surfaces.

Apart from the traditional data such as the maximum pressure observed in the cell (P_{max}) and the cumulative filtrate volume, they introduced terms like average pressure in the cell (P_{ave}), average peak pressure in the cell (P_{peak}), total number of bridges (N), total number of zero (Z), average number of bridges per minute (N_i), average number of zeros per minute (Z_i), average number of peaks per one zero (N_z). They eliminated the pressure related parameters due to differentiation with correlation tests on core fracturing, N_z , the number of bridges formed by particles with respect to the filtrate volume, was found the most important estimated parameters in order to evaluate the sealing properties of applied particles.

They developed two models according to the following results which were obtained from tests on PPA and core fracturing.

- ✓ Plugging is more important than sealing during bridge formation. If the large particles could not plug the opening first and smaller ones could not settle in the void between the large particles.
- ✓ Higher concentrations of particles reduced filtration and make it easier to form a bridge.
- ✓ If bridge is formed in a fracture with rough planes, higher pressure level is necessary to remove it.
- ✓ Size of the opening influences the stability of the sealing negatively. Larger particles are required to seal the openings.
- ✓ High resiliency of particles leads to build up stronger bridges over the fractures and higher pressures are required to reinitiate loss circulation.

Hettema et al. (2007) designed on unique high-pressure testing device for determining the sealing properties in fractured permeable formations as can be seen in the Figure 2.2. This device has the ability to measure two discrete fluid streams; (1) through the fracture tip and (2) through the formation matrix. Two parallel 175-micron soapstone plates were used in the cylindrical vessel of the device to simulate permeable medium. This apparatus consists of a cylindrical vessel, four high-pressure accumulators to handle both pore fluid and test fluid, four syringe pumps and a computer with data acquisition system. Permeable Fracture testing apparatus provides the capability of measurement of fluid losses at the tip and formation matrix, calculation of fracture width and estimation of seal location.

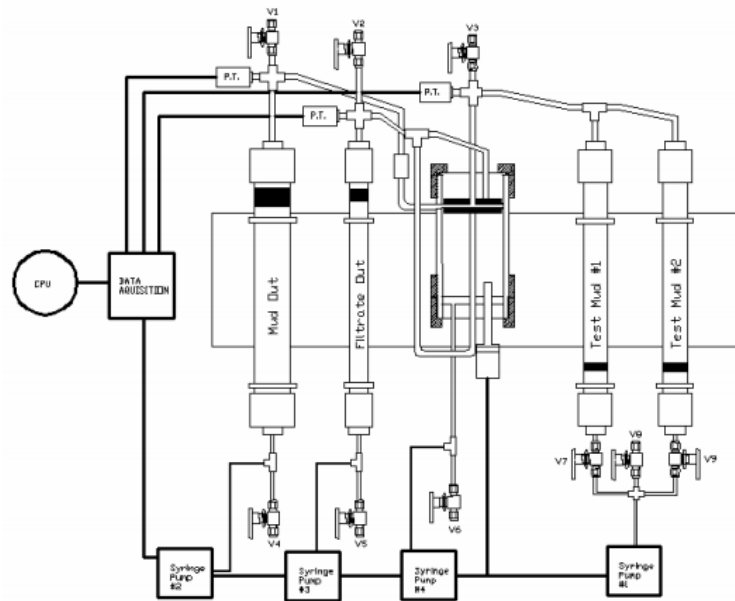


Figure 2.2: Schematic of Permeable Fracture Test Device (Hetteema et al, 2007)

Maximum sealing pressures, fracture size, leak-off rates through the tip and formation matrix, particle size and seal location data were gathered from this device. They were correlated with spurt loss values from PPA under similar condition with cut soapstone plates. The spurt loss values were strongly correlated for low loss volumes which also resulted in forming the most efficient seals whereas High-Temperature, High Pressure fluid loss values at 300 °F and 500 psi so different. Also Scanning Electron Microscope was used to see the physical nature of the fracture seals.

Results obtained from these tests,

- ✓ Fracture sealing in permeable media is highly dependent on both PSD and concentration. LCM materials should have a broad PSD for effective sealing.
- ✓ For highly permeable or highly porous medium, using of relatively coarse LCM blends is the most effective way to reduce spurt loss before formation of bridge.
- ✓ Effective sealing occurs at or near the mouth of the fracture. Higher mud losses are observed while sealing occurs further within the fracture (greater distance from mouth).

- ✓ Maximum sealing pressure increases with the increase in concentration of sized particles of LCM; not through total solids contribution of barite.
- ✓ Apart from spurt loss values, fluid loss is not a good parameter to measure the sealing efficiency.
- ✓ They proposed that the most effective LCM formulation should include blends of various grades of calcium carbonate (or ground marble), ground nut and graphite.

Another test apparatus has been developed by Sanders et al. (2008) to evaluate the sealing efficiency of LCM treatments in sealing impermeable fractured formations. Fracture faces were simulated by the two matched corrugated aluminum platens as in Figure 2.3. The fracture width is controlled by three set of screws. The most significant benefit of this apparatus is to measure changes in the fracture width with the increase in sealing pressure.



Figure 2.3: Corrugated Aluminum Platens for Fracture Tester (Sanders et al, 2008)

Impermeable Fracture Tester consists of three syringe pumps, in conjunction with two accumulators to control mud pressure and fracture tip pressure within in the fracture cell (FC). During the test, constant the fracture closure pressure and the fracture tip pressure was maintained. The volume of filtrate collected from the tip and the fracture closure volume were monitored by data acquisition system. Figure 2.4 shows all parts of test apparatus.

To achieve these functions, mud pressure, i.e. fluid pressure applied through the fracture and into the fracture tip by injecting the sample fluid at a constant flow rate, conduction loss, i.e. fluid lost into the fracture through the fracture tip, and change in fracture width is measured.

Dozens of materials including cellulosic, synthetic elastomers, rubber, polyethylene, polypropylene, mica, glass, graphite and petroleum coke-based materials, iron-based compounds and calcium carbonate were tested in this apparatus. The effect of shape, surface texture, material hardness, resilience, bulk density and size are also evaluated.

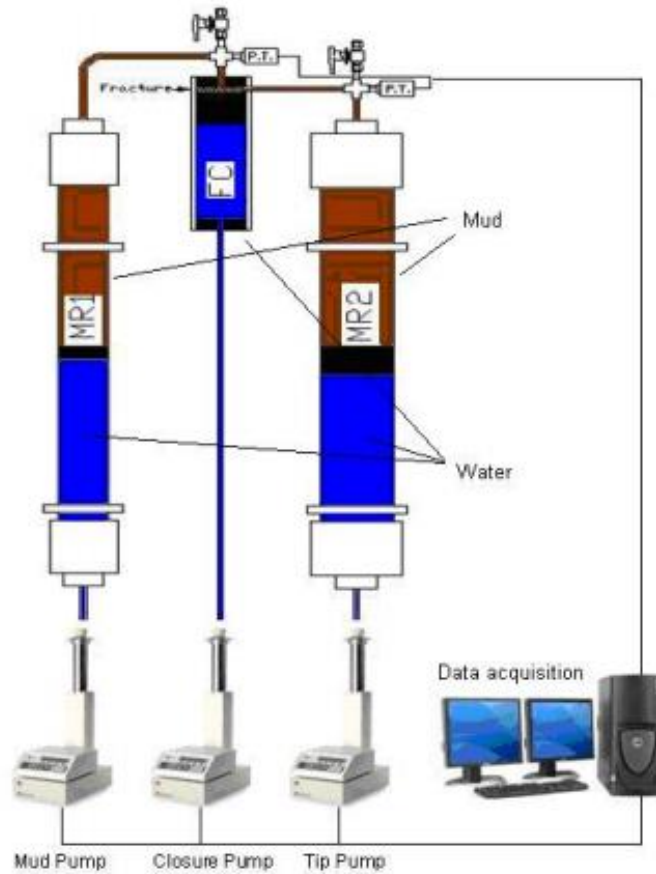


Figure 2.4: Schematics of Impermeable Fracture Test Device

According to test results, it was found that

- ✓ Proper size and distribution of sizes (particle-size range or PSD) are the most critical parameter for fracture sealing.
- ✓ Required maximum size will be determined by the anticipated fracture width. Efficient bridge can be achieved by good linear spread of particle below this upper size.
- ✓ Roughness particles have been shown to be more efficient in sealing whereas high aspect materials such as mica do not function well. In addition, if these two parameters are optimized successfully, increase in concentration leads to more rapid and efficient seal.
- ✓ Materials with a higher compressive strength will provide a more efficient seal. Besides, resiliency plays an important role in the overall performance of particles, however the importance of it is behind the other characteristics.
- ✓ The most effective LCM formulation should include blends of various grades of calcium carbonate (or ground marble), ground nut and graphite.

Mechanical strengthening of wellbore relies on particle size distribution (PSD), concentration and mechanical properties. (Mostafavi et al, 2011). Also, it is strongly believed that the increase in the fracture gradient is affected by the physical properties such as shape, strength, resiliency and the crushing resistance. The relation between these parameters and wellbore strengthening mechanism can be tabulated in Table 2.1.

Every WSM type has own characteristic physical properties. Their shape, strength and resiliency differ from each other somewhat. These physical properties were studied in many researches. As a result of many experiments, Sanders et al (2008) found that shape and texture are important parameters and spheroidal-shaped particles with rough surface and low aspect ratio are the optimum shape to maximize the sealing pressure. They also concluded that particles with high compressive strength shows a more efficient seal. In addition, high resilient materials play an important role in forming seal.

Table 2.1: *Fundamental differences between wellbore strengthening mechanisms (Cock et al, 2012)*

Category	Fracture Propagation Resistance	Stress Cage	Fracture Closure Stress
Application technique	Continuous in mud	Continuous in mud or pill squeeze	Continuous in mud or pill squeeze
Formation or closure stress applied?	No	No	Yes
Fracture tip isolation required?	Yes	No	Yes
High fluid loss required?	No	No	Yes
WSM particle strength	Unimportant	Somewhat Important	Unimportant
WSM particle size	Important	Important	Unimportant
WSM particle type	Important	Important	Unimportant

Alsaba et al. (2014c,2016) presented the effect of lost circulation material type, shape, concentration and particle size distribution (PSD) on sealing integrity with respect to differential pressure at different fracture widths. After sealing integrity tests, which will be explained later, materials and formed seals were examined under Optical Microscope and Scanning Electron Microscope to correlate performance of samples with the particle morphology. They found that particle shape, in terms of sphericity and roundness, exhibits significant effect on the overall seal integrity. The low sphericity and angularity of nutshells particles resulted in a better alignment of the particles within the fracture and maintaining higher seal integrities compared to graphite and calcium carbonate. In other words, thanks to irregular shape, nut shell particle perform better performance.

Kumar et al (2010) measured average shape factors like aspect ratio, sphericity and convexity for widely used particulates and it has been tabulated in Table 2.2 and the optical microscope imaging examination are also conducted to determine ideal shape. The widely used materials were found to have similar shape factors.

Table 2.2: Shape Factor of Different Materials (Kumar et. al., 2010)

Product	Generic Name	Nominal Diameter (µm)	Aspect Ratio	Sphericity	Convexity
GM 150	Ground Marble	150	1.42	0.54	0.96
GM 600	Ground Marble	600	1.57	0.51	0.96
RGC 400	Resilient Graphitic Carbon	400	1.57	0.48	0.90
RGC 1000	Resilient Graphitic Carbon	1000	1.42	0.53	0.91
Ground Nutshells M	Ground Nutshell	1450	1.50	0.50	0.91
Ground Nutshells F	Ground Nutshell	617	1.37	0.55	0.92
Ground Rubber	Ground Rubber	300	1.39	0.53	0.88
Cellulosic Fibre	Wood fibre	1063	1.63	0.44	0.92

According to Kumar and colleagues, the formed bridge in the fracture will be subjected to various wellbore stresses. One of them is Fracture Closure Stress. A cycle of fracture opening and closing occurs due to the changes in bottom hole pressures resulting from equivalent circulating density (ECD) which is shown in Figure 2.5. It leads to compression forces that stress the seal. It is expected to have bridge that should withstand these stresses and not undergo any significant change in its size. Then, particles with good crush strength or crush resistance has a great role in seal for endurance.

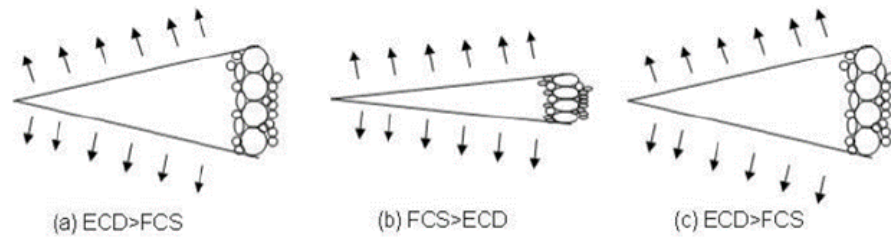


Figure 2.5: Alteration in Fracture Width with Changing Equivalent Circulating Density (ECD)
(Kumar et al, 2010)

Tinius Olsen Hydraulic Press Tester was used for crushing resistance determination and resiliency determination. They compare widely used materials such as Ground Marble (GM), Resilient Graphitic Carbon (RGC), Ground Nut Shells (GNS). Results can be shown as followings:

- ✓ GM acts like a brittle material since it was undergoing high compaction and its particle size reduced under load. Also, it shows ZERO resiliency in resiliency test.
- ✓ GNS acts like a ductile material. Although, it undergoes permanent deformation, there is no significant change in particle size and increase in particle size is observed. Also, during resiliency test it exhibits approximately 16% resiliency.
- ✓ RGC undergoes elastic deformation and it bears stresses without undergoing significant particle change and the resiliency of it is around 120% at 10000 psi.
- ✓ Blending just 20% by volume of RGC particles with other materials increase crushing resistance.

According to the crush test and resiliency tests, it is concluded that mechanical strength of material will play an important role for wellbore strengthening and Ground Marble or Ground Nut Shell may not be effective as WSM when used alone. Savari et al. (2014) supported this idea by indicating ground marble particles alone were not able to plug the tapered slot and plug breaking pressure, the maximum pressure which bridge withhold before further fluid loss was resumed, is zero for Ground Marble.

In this study, it was planned to design WSM for highly fractured carbonate reservoir that is why removal of particles after drilling or solubility of particles in acid were taken into consideration. Since Resilient Graphitic Carbon and Ground Nut Shells cannot be removed totally during acidizing operations, residual particles can plug hydraulic channels. They may not be recovered back from these hydraulic channels with backflow during production operations and that can lead to reduction in production. On the other hand, Ground Marble is chemically calcium carbonate and as it is known, calcium carbonate is the most widely used, granular type of bridging material. Its mechanical and chemical characteristics are the primary reasons to consider Ground Marble to be used in the production zones since it can be removed to recover the permeability of the rock by hydrochloric acidizing.

In this study, Ground Marble is also selected as WSM particles because of its solubility. Also, the results by Kumar et al (2010) showed that Ground Marble were not able to plug alone was also rechecked in this study.

There have been several studies for selection of material based on size to effectively plug the fracture or pore to keep the fluid loss at minimum.

Loeppke et al. (1990) studied high temperature and fracture dominated loss zones in geothermal fields instead of matrix loss zones. They developed models for single-particle bridging and multiple-particle bridging. These models indicate that size and shape have a great importance in determining the maximum allowable pressure differential across the plug. They stated that when dimension of particle is slightly larger than the fracture, higher maximum allowable pressure differentials are obtained for single particle bridging. They also emphasized that when concentration increases, the probability of forming a bridge increases whereas volume of spurt loss decreases.

Rojas et al. (1998) evaluated various fluid combinations which includes different particle sealing agents such as particulates (CaCO_3) and fibres in a standard API sand bed test, a purpose-built fracture crack cell and in the Permeability Plugging Apparatus (PPA). They found that the drilling fluid must contain a wide range of particles and

largest particles should be at least as large as the fracture width or the diameter of the largest pore throat. Also, sealing capability increases with increasing concentration.

Dick et al (2000) proposed ideal packing theory (IPT). This theory defines the total particle range required to seal all voids. The IPT is a graphical approach to determine optimum PSD of bridging material for given formation. The IPT uses either pore sizing from thin section analyses or permeability information, combined with PSD of bridging material. However, it is not valid for sealing of fractures since fractures have unlimited permeability.

Vickers et al (2006) tried to expand Ideal Packing Theory (IPT). IPT approach depends on an estimation of the median pore size estimated from permeability by taking the square root of the permeability. If the size distribution of pore throats in a reservoir were linear, IPT would be accurate. However, in a reservoir the most common pore throat will not be the middle of the size range. Therefore, according to this theory, bridging blend should meet the following standards:

$D(90) = \text{largest pore throat}$

$D(75) < 2/3 \text{ of largest pore throat}$

$D(50) \pm 1/3 \text{ mean pore throat}$

$D(25) = 1/7 \text{ of mean pore throat}$

$D(10) > \text{smallest pore throat}$

Whitfill (2008) proposed that the d50 of the particle size distribution should be equal to estimated fracture width. Therefore, Sufficient particles both larger and smaller than the estimated fracture width are present.

Alsaba et al (2016) found that to effectively seal fractures using granular LCM treatments, the D90 value should be equal or slightly larger than the anticipated fracture width.

Kumar and Savari (2011) used Permeability Plugging Apparatus to check relationship between resiliency and plugging capability. To analyze the performance of the fluid based on their plugging capability and fluid loss, test was carried out on 1016 μm , 1524 μm , 2032 μm , and 2540 μm constant area slots along with tapered slot where slot size tapers from 2500 μm to 1000 μm . Composition of the used LCM is given Table 2.3 and the fluid loss results are given in Table 2.4.

Table 2.3: *Composition of LCM used for comparing different slots (Kumar and Savari, 2011)*

Material	Ib/bbl
Nut Shell-1	7.5
Nut Shell-2	7.5
Ground Nut Shell- M	4
RGC 1000	5.5
RGC 400	8.25
RGC 100	8.25
Ground Marble 25	4.5
Ground Marble 5	4.5

Table 2.4: *Fluid Loss Results for comparison of constant area slots and tapered slots (Kumar and Savari,2011)*

	Fluid 1	Fluid 2	Fluid 3	Fluid 4	Fluid 5
Constant Area Slot (1016 micron)	18.67	37.18	25.85	4.48	10.35
Constant Area Slot (1524 micron)	24.51	47.88	8.85	6.87	13.27
Constant Area Slot (2032 micron)	19.05	47.35	7.24	7.53	9.11
Constant Area Slot (2540 micron)	71.65	86.55	73.6	68.97	66.16
Tapered Slot	41.85	38.2	81.11	48.53	14.92

They found that, the face of constant area slots is plugged and very minimal fluid invasion occurs into the inside the slot. However, plugging in tapered slot resembling wedge shape fracture took place inside the slot and higher fluid loss values measured. They concluded that using a tapered slot for plugging fracture is more realistic for wellbore strengthening.

Several more tests are done to establish the effectiveness of a tapered slot by using compositions which are from crush test results. The results can be seen in Table 2.5.

Table 2.5: Fluid Loss Testing Performed on Tapered Slot with different Particles

S1 No	Combination	Conc.	D(10) μm	D(50) μm	D(90) μm	Fluid Loss (ml)
1	GM 600/RGC 400	80/20	479	677	1230	20
2	GM 600/RGC 400	50/50	329	629	1159	70
3	GM 1200	100	8	943	1489	No control over fluid loss
4	RGC 100	100	604	1156	1539	20-30
5	GM 1200/RGC 400	80/20	11	847	1434	12
6	GM 1200/RGC 400	50/50	43	618	1307	5
7	GNS	100	243	1408	1935	5-7
8	GNS/RGC 50	80/20	49	1278	1879	18-20
9	GNS/RGC 400	80/20	250	1295	1888	10
10	GNS/RGC 1000	80/20	274	1339	1887	10

In the test, it was observed that;

- GM 1200 particles were able to plug the slot but did not control the fluid loss because the interstitial void in the plug was too large and continuous fluid loss occurs. By this way, pressure transmission from wellbore to the fracture tip cannot be stopped and fracture propagation occurs. They concluded that improper PSD could worsen the situation.
- The blend of Ground Marble(GM) and Resilient Graphitic Carbon(RGC) is the one of the most effective LCM combination. By this way, they proved the results obtained from resiliency and crushing test. They concluded that resilient particles decrease the crushing of the particles and lead to have good wellbore strengthening results.

- Crushing resistance is an important parameter for wellbore strengthening. If particles inside the fracture had a significant crush, it may lead to loss of stresses developed because of wellbore strengthening.

However, in these tests conducted on Permeability Plugging Apparatus, testing pressure and temperature is unspecified. The procedure was not explained detailly.

Alsaba et al. (2014b) studied the effect of LCM type, shape, concentration, PSD and temperature on the seal integrity with respect to differential pressure at different fracture widths using Low and High Pressure LCM Testing Apparatus. The low pressure apparatus is a simply modified version of standard API filter press as shown in Figure 2.6. A constant pressure of 100 psi implemented the fluid in the cell to force the fluid flow through the tapered discs until no more fluid is coming out. Fluid loss volume and the shut-off time is important here. According to these parameters, further investigation at high pressure testing apparatus are done.



Figure 2.6: Low Pressure LCM Test Apparatus (Alsaba et al.,2014b)

20 blends of four different LCMs at 15 and 50 ppb concentrations are screen out by using Low Pressure Apparatus. The formulation of these blends is tabulated below in Table 2.6-2.7. From these blends, Graphite and Sized calcium carbonate blends at 30 ppb and 80 ppb are used to follow the recommendations by Aston et al (2004). Graphite and Nut Shells at the concentration of 20 and 40 ppb is recommended by

Hettema et al. (2007). A 55- ppb graphite, calcium carbonate and cellulosic fiber were also recommended by Kumar et al (2011).

Table 2.6: Individual LCM concentration and PSD tested in Low Pressure Testing Apparatus
(Alsaba et al., 2014b)

LCM Type	D(50) microns	% of Total Concentration if used Individually			
		Case#1	Case#2	Case#3	Case#4
Graphite (G)	50	20	14	0	0
	100	20	20	20	0
	400	30	26	40	50
	1000	30	40	40	50
Sized CaCO ₃ (SCC)	5	16	6	0	0
	25	16	6	0	0
	50	16	13	0	0
	400	16	21	33	20
	600	18	27	33	27
	1200	18	27	34	53
Nut Shells (NS)	620	33.3	0	0	0
	1450	33.3	50	100	0
	2300	33.3	50	0	100
Cellulosic Fiber	312	50	100	0	-
	1060	50	0	100	-

Table 2.7: Concentration and PSD of LCM Blends tested in Low Pressure Testing Apparatus (Alsaba et al., 2014b)

LCM Type	D(50) microns	% of Total Concentration if used in combinations					
		G & SCC		G, SCC & CF		G & NS	
		Case#1	Case#2	Case#1	Case#2	Case#1	Case#2
Graphite (G)	50	10	6.7	3.6	2.4	10	6.5
	100	10	10	3.6	3.6	10	10
	400	15	13.3	5.5	4.8	15	13.5
	1000	15	20	5.5	7.3	15	20
Sized CaCO₃ (SCC)	5	3	0	4.4	0	-	-
	25	3	0	4.4	0	-	-
	50	7	0	9.5	0	-	-
	400	11	16.5	15.3	24	-	-
	600	14	16.5	19.6	24	-	-
	1200	14	17	19.6	24.7	-	-
Nut Shells (NS)	620	-	-	-	-	16.5	16.5
	1450	-	-	-	-	16.5	16.5
	2300	-	-	-	-	17	17
Cellulosic Fiber	312	-	-	4.5	4.5	-	-
	1060	-	-	4.5	4.5	-	-

A total of 160 tests were conducted with 4 different tapered slots. 100 ml fluid loss has been determined as cut-off value. If fluid loss goes over 100 ml, it is said to be non-controlled. In this test 26 blends were successful. Then, sealing efficiency of these blends are evaluated in High Pressure Test Apparatus shown in Figure 2.7.

This setup consists of four main components;

1. a plastic accumulator used to transfer the drilling fluids to the metal accumulator,
2. a metal accumulator used to inject the drilling fluids into the cell,
3. testing cell which is capable of holding pressures up to 10000 psi, and
4. syringe pump used for fluid injection and is connected to a computer for data logging.

The test is run by pumping LCM-laden drilling fluid with a constant rate of 25 ml/min until a rapid increase in injection pressure is observed. This increase shows that seal is formed. Once the seal has formed, a fluid which does not contain LCM particles is injected continuously until a significant pressure drop is observed. This indicates the seal efficiency. Here, seal efficiency is defined as the seal/bridge maximum breakdown pressure. This cycle repeated until no further seal can be formed. The reason of these repeating cycles is to check whether sealing efficiency or the seal integrity is repeatable.

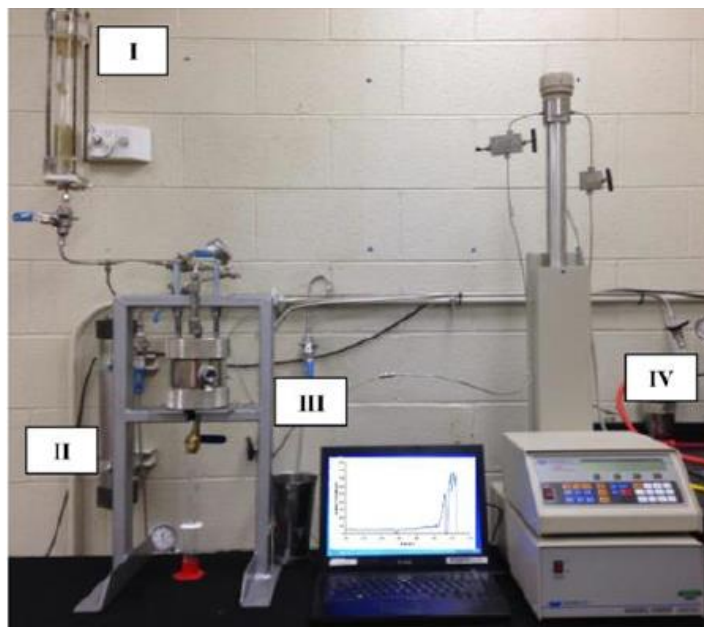


Figure 2.7: High Pressure Test Apparatus (Alsaba et al. 2014)

According to these tests, the following results are found:

- ✓ LCM can seal effectively if the D90 value is equal or slightly larger than the anticipated fracture width. However, when determining maximum size of conventional LCM particles, the risk of plugging downhole tools is taken into consideration.
- ✓ The broad range of PSD is necessary for a good sealing performance.
- ✓ Higher concentration was found to improve sealing efficiency.
- ✓ The irregular shape and the ability to deform under pressure improves seal integrity.
- ✓ A strong relationship between sealing efficiency and fluid loss values is observed.
- ✓ There is no significant effect of temperature on fluid loss.
- ✓ While granular particles (Ground Marble, Resilient Graphitic Carbon) have lower seal integrity, Fibrous material showed superior performance.

Due to swelling ability at higher temperatures, the sealing efficiency of Ground Nut Shells has improved

CHAPTER 3

STATEMENT OF PROBLEM

Lost circulation is one of the primary problems in drilling industry. There are several ways for treatment of lost circulation. Using wellbore strengthening materials is the most popular way for preventing lost circulation because of simplicity of usage and economic reasons. It is important to determine the type, composition, particle size, and the rheology of the fluid successfully.

Intention of the study is to conduct experimental investigation on determining optimum concentration and particle size distribution for sealing fractured reservoirs. By doing this, the effect of particle size distribution, concentration and fracture width on sealing are also examined.

CHAPTER 4

THEORY

The wellbore strengthening techniques have been extensively used in the drilling industry to prevent or mitigate drilling fluid loss. Wellbore strengthening can be defined as methods to artificially increase the maximum pressure a wellbore can withstand without intolerable mud losses. Wellbore strengthening aims to enhance the effective fracture pressure and widen the mud weight window, rather than increasing the strength of the wellbore rock [Ito, Zoback & Peska (2001), Abé, Keer, Mura (1976), Geertsma, De Klerk (1969), Feng & Gray (2016)]. By preventing and/or mitigating fluid loss, wellbore strengthening also reduces lost circulation associated NPT events, e.g. wellbore instability, pipe sticking, underground blowouts, and kicks.

Wellbore strengthening attempts to bridge, plug, or seal wellbore fractures with lost circulation materials (LCMs) to arrest the propagation of lost circulation in fracture(s). The pressure-bearing capacity of the wellbore can be enhanced by one or a combination of the following mechanisms in wellbore strengthening treatments.

- ✓ Bridge a fracture near its mouth to increase the local compressive hoop stress around the wellbore and enhance fracture opening resistance.
- ✓ Widen and prop a fracture to enhance the fracture closure stress that acts on closing the fracture.
- ✓ Form a filter cake in the fracture to isolate the fracture tip from wellbore pressure and enhance resistance to fracture propagation.

Hoop Stress Enhancement or Stress Cage Model

In this model, Alberty and McLean,(2004) proposed that with the addition of suitable WSM to the drilling fluid, the hoop stresses around the wellbore may be increased thanks to setting of WSM at the fracture mouth and forming a seal.

In this wellbore strengthening strategy, shallow fractures are induced and quickly sealed by WSMs that bridge and seal the fracture mouth. This seal creates stress cage in the adjacent rock, which also increase strength of the wellbore.[Aston, Alberty, McLean, de Jong & Armagost (2004), Song& Rojas (2006)]

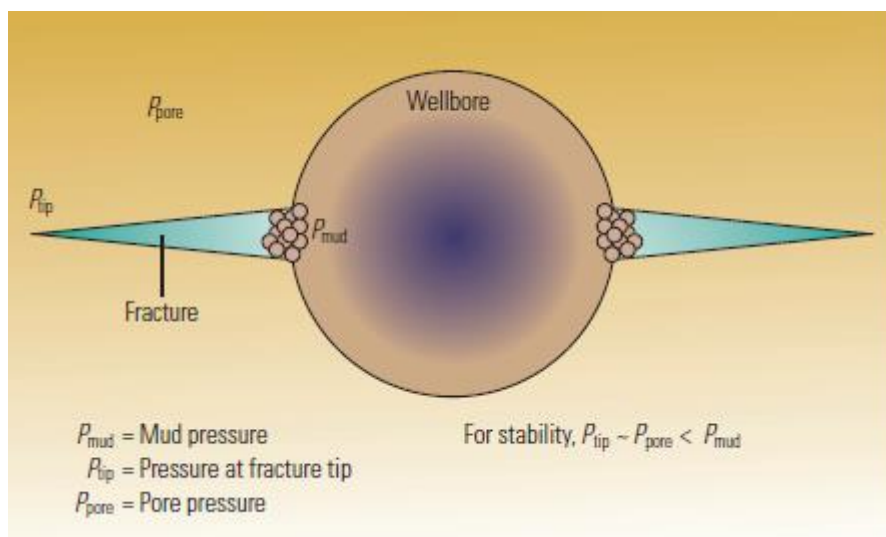


Figure 4.1: Stress Cage Concept (Cock et al., 2011)

Cock et al. (2011) stated that “for this mechanism to be successful, high concentration of bridging additives is required; they must strong enough to resist closure stress and they have to be appropriately sized to bridge near fracture mouth instead of deeper into the fracture.” They suggest that materials such as graphitic blends, ground petroleum coke, nut husks (like nut shells) and marbles work well in this mechanism.

Fracture Closure Stress (FCS)

Dupriest (2005) introduced this model to explain how WSMs could increase fracture gradient. In other way, Alsaba et al (2014a) explained FCS as the normal stress on the fracture plane keeping the fractures faces in contact. FCS is high-fluid-loss treatment for existing fractures. Although it can be applied as whole mud treatment, it is commonly applied via high-fluid-loss pills. These pills may be water-based in a non-aqueous system. After this operation is done, cross-linked polymer plugs or cement operation may be done.

In this method, WSM laden drilling fluid enters into the existing fractures. As fracture is widened, carrier fluid leaks from the drilling fluids mixture through the fracture walls or tip. The particles in this slurry consolidate and agglomerate during squeeze phase. Then, the communication between the wellbore and fracture tip are cut off. Therefore, sealing of the fracture tip is achieved. By isolating fracture tip, adjacent rock is compressed and it leads to changing near wellbore hoop stresses.

In this theory, plug can form anywhere in the fracture, unlike in stress caging theory.

According to Cock et al (2011), the ideal WSM which is suitable for this theory must be capable of relatively large particles of similar size and considerable roughness that do not pack well. They show diatomaceous earth or barite as an example.

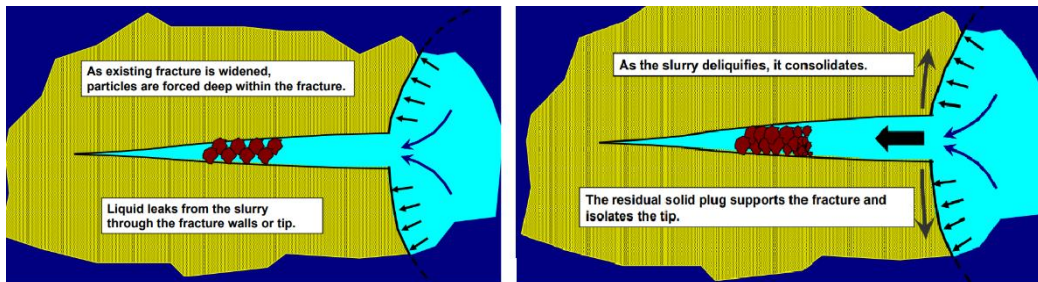


Figure 4.2: Fracture Closure Stress Concept (Growcock, 2011)

Fracture Propagation Resistance (Fracture Tip Isolation)

In this strategy, the tip of existing fractures is isolated from wellbore, the fracture propagation is stopped and fracture reopening pressure increases mechanically.

Actually, this strategy is a result of joint industry project known as the Drilling Engineering association (DEA)-13, which was conducted in the mid 1980s to determine why oil-base drilling fluids (OBDF) seemed to yield a lower fracture gradient than water-base drilling fluids (WBDF). They found that there is no difference in fracture initiation pressures for different fluid types and formulations, however fracture propagation behavior influenced by fluid type and composition is significantly different.

This difference explained by van Oort et al (2011) with a fracture tip screenout phenomenon. According to van Oort et al (2011), when fracture growth initiates, some amount of drilling fluid is lost into the new void space of the fracture. WSM laden drilling fluid enters into the fracture and starts to isolate or screen the fracture tip from the wellbore. Occurrence of this isolation varies according to fluid type.

In Water-Based Drilling Fluid (WBDF) systems, the fracture tip is isolated by an external filter cake. This prevent effective pressure communication between fracture tip and the drilling fluid. Therefore, fracture extension is blocked until drilling fluid pressure is high enough to puncture this barrier. (See Figure 4.3a)

In Oil-Based Drilling Fluids (OBDF), an ultrathin internal filter cake cannot block the communication between wellbore and fracture tip. This leads to fracture extension at lower propagation pressures than with a WBDF. (See Figure 4.3b)

Cock et al (2012) states that synthetic graphite, ground nut hulls, and oil dispersible cellulose particles are most effective in sealing a fracture and minimizing leakoff through the fracture tip.

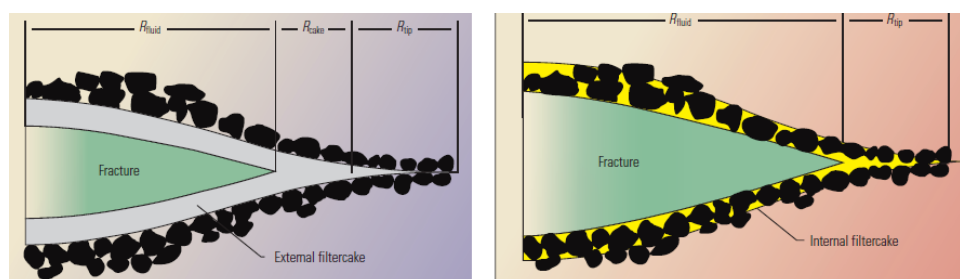


Figure 4.3: Fracture Tip Isolation Concept in (a)(left figure) WBDFs (b)(right figure) OBDFs (Cock, 2012)

Regardless of the strategy for solution, the ability to cure severe losses which occurs in fractures using WSM laden drilling fluids is of a great benefit in terms of reducing the costs and time. In this study, our intention is to expand usage of WSM in sealing fractures. Since fracture depth, shape and apertures may be highly variable, our aim to seal the fracture mouth by WSMs and increase the wellbore strength

CHAPTER 5

EXPERIMENTAL SET-UP AND PROCEDURE

5.1. Determination of Particle Size Distribution

The first step of this study is to determine the size distribution of ground marble. Dry sieve analysis was used to determine particle size distribution (PSD). During determination of sieve sizes used, available manufacturer's product range are taken into consideration. Therefore, production of specially designed ground marble for this study by manufacturer and availability of materials were ensured.

Samples of ground marble was obtained and separated according to sizes by sieving through a series of stacked sieves with different sizes respectively as shown as Figure 5.1. Size of sieves can be seen in Table 5.1.

Table 5.1: *Sieves Standard No. Mesh Sizes and Standard Sieves Designation*

(Dhanlal De Lloyd, 2000)

Mesh Size (μm)	TYLER (Mesh)	ASTM-E11 (No)	BS410 (Mesh)	DIN-4188 (mm)
50	60	60	60	0.250
850	20	20	20	0.850
1180	16	16	16	1.180



Figure 5.1: Numbers of sieves and their mesh sizes in micron

Particle size distribution of ground marble used in this study is presented in Table 5.2. According to it, a particle size under the size of 250 μm represent a fine sample, particles between 250 μm - 850 μm sizes indicate medium size and particle size includes between 850 μm - 1180 μm named coarse sample.

Table 5.2: Particle Size Distribution of Ground Marble

	Particle Size
Coarse	850 μm – 1180 μm
Medium	250 μm – 850 μm
Fine	< 250 μm

The ground marble samples were screened by using sieves and collected. Then, base fluid which will be described in the following sections were prepared and different amount of ground marble added to study the effect of particle size distribution and concentration on seal integrity.

5.2. Composition of Drill-In Fluid

The polymer-based drill-in fluid used in this study. This system is a specially designed for drilling through the reservoir section of a wellbore. Only additives essential for filtration control and cuttings carrying are present in a drill-in fluid. The drill-in fluid used in this study was formulated using modified starch, XCD, biocide and ground marble. The features of used additives will be explained detailly in Section 5.3. Goal-oriented tests were done to determine the concentration of used polymers. For instance, standard fluid loss tests were done to determine the concentration of Modified Starch, whereas rheology tests were done to determine the concentration of XCD polymer. Detailed information will be found in Results and Discussion Part. According to test results, the concentration of polymers used were shown in Table 5.3. In this study, triazine based biocide was also used with concentration of 0.5%.

Table 5.3: *Composition of Drill-in Fluid.*

Additive	Function	Concentration
M.Starch	Fluid loss reducer	7 lb/bbl
XCD	Suspending agent	2 lb/bbl
Biocide	Bactericide	0.5%

In this study, these additives were added to tap water. The chemical properties of tap water are shown in Table 5.4.

Table 5.4: *The properties of Tap Water*

Properties	Results
Alkalinity – P _f (ml)	0.00
Alkalinity – M _f (ml)	0.03
Sulfate (SO ₄ ⁻²) (mg/l)	120.00
Calcium (Ca ⁺²) (mg/l)	68.00
Total Hardness (mg/l)	88.00
Chloride (Cl ⁻) (mg/l)	350
Temperature (°F)	77

5.3. Additives Used in Drill-In Fluid Add

5.3.1. Modified Starch

Modified Starch, which is an anionic polymer, is a drilling mud additive which is used to control fluid loss in water base muds. In this study technical grade modified starch, which has brand name as AMYLOTROL by GEOS ENERGY INC is used with concentration of 7 lb/bbl. Detailed information is given in Appendix A.1.

5.3.2. XCD Polymer

XCD polymer is anionic, finely powdered, high molecular weight Xantham Gum biopolymer. It is used to achieve desirable rheology required for efficient cutting lifting in water-based muds. In this study, technical grade XCD polymer, which has brand name as REOZAN D by GEOS ENERGY INC was used in concentration of 2 lb/bbl. Detailed information can be reached in Appendix A.2.

5.3.3. Biocide

Triazine based biocide was used to protect modified starch and XCD polymer from the bacterial attack. In this study, technical grade Triazine based biocide, which has brand name as GEOCID T by GEOS ENERGY INC was used in concentration of 0.5%. Detailed information can be found in Appendix A.3.

5.3.4. Ground Marble

Its chemical composition is basically CaCO_3 with S.G of 2.7 g/cm^3 . GM is preferred to use in drill-in fluid because of the solubility in HCl acid. Different sizes of ground marble are used during the experiments. Samples are named regarding to their micron sizes after being sieved such as fine, medium and coarse.

5.4. Determination of Rheological Properties of Drill-In Fluid

GRACE M3600 Automatic Viscometer was used to determine the rheological properties of the drill-in fluid. It is a true coaxial cylinder, rotational viscometer. Specifications of the viscometer and measurement configurations are given in Appendix-A.4. Rheological measurements were performed according to API-13B.

Rheological properties used to characterize the drill-in fluid are plastic viscosity (PV), yield point (YP), low-shear rate yield point (LSRYP) and low-shear rate viscosity (LSRV). These parameters were calculated as below:

$$PV \text{ (cP)} = \Theta_{600} - \Theta_{300}$$

$$YP \text{ (lb/ft}^2\text{)} = \Theta_{300} - PV$$

$$LSRYP = \tau_y \text{ (lb/ft}^2\text{)} = 2 \Theta_3 - \Theta_6$$

LSRV at 0.0636 sec^{-1} is calculated by interpolating viscosity values measured at 0.0681 sec^{-1} and 0.0511 sec^{-1} .



Figure 5.2: GRACE M3600 Automatic Viscometer
(Grace Instrument Company, M3600 Viscometer Manual)

5.5. Preparation of Drill-in Fluid

1. 7 ppb Modified starch in 350 cc tap water is aged dynamically during overnight to become totally soluble and homogenized.
2. Added 2 ppb XCD polymer and mixed in mixer (Hamilton Beach brand) at 19770 rpm for 15 minutes to become totally soluble and homogenized.
3. Reduced the volume of drill-in fluid according to calculated volume increase of Wellbore Strengthening Material (WSM) sample to get 350 cm³ drill-in fluid embedded with WSM
4. Added WSM particles and mixed only one (1) more minute. It needs to mix only one (1) minute to avoid from gridding effect.
5. Samples are taken for the sealing capability tests.

5.6. Sealing Capability Tests

Sealing capability tests are done on Permeability Plugging Apparatus (PPA) which is shown in Figure 5.3. Specifications of the device are given in Appendix-A.5.

In this study, slotted steel discs are used to simulate highly fractured formations. During test, hydraulic pressure applied from bottom of test cell by a hand pump. The fluid in the cell try to flow through the aperture of slot. Steel slots are used to simulate fractured formations. If slot becomes plugged, the pressure on the gauge of hand pump starts to increase. By continuing pumping, pressure in the cell is increased. Once desired pressure reached, tests will be completed.



Figure 5.3: Normal PPA Assembly

5.6.1. Customization of Slots & Parts of Permeability Plugging Apparatus

Due to selected working pressure and wellbore strengthening material, the standard permeability plugging apparatus was customized and some changes were done on the apparatus.

During trial tests, firstly straight slots which are made of Grade 303 Stainless Steel were used. The reasons of use of steel are to simulate fracture width, avoid of bending of filtration medium during tests and reuse it. However, it is observed that although wellbore strengthening particles passed through the slots it could plug needle valve on the top cap as shown in Figure 5.4 and pressure increase due to this can lead to false results. In other words, used wellbore strengthening particles can plug space around

needle valve instead of slot and it can be interpreted incorrectly as that used particles sealed this fracture width.

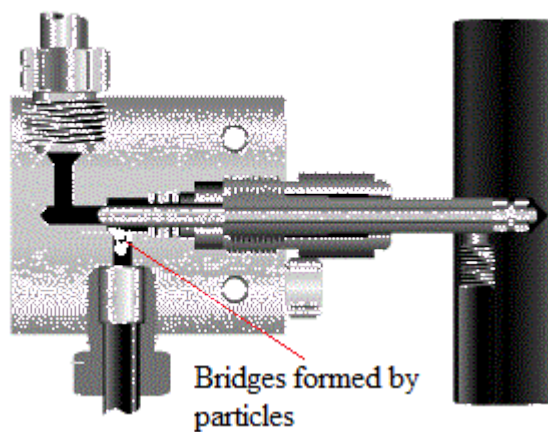


Figure 5.4: Illustration of bridge formed by particles in the needle valve

Furthermore, top cap was redesigned as shown in Figure 5.5 and removed needle valve since tests will have conducted at ambient temperature and there is no need back pressure to prevent boiling of sample fluid.

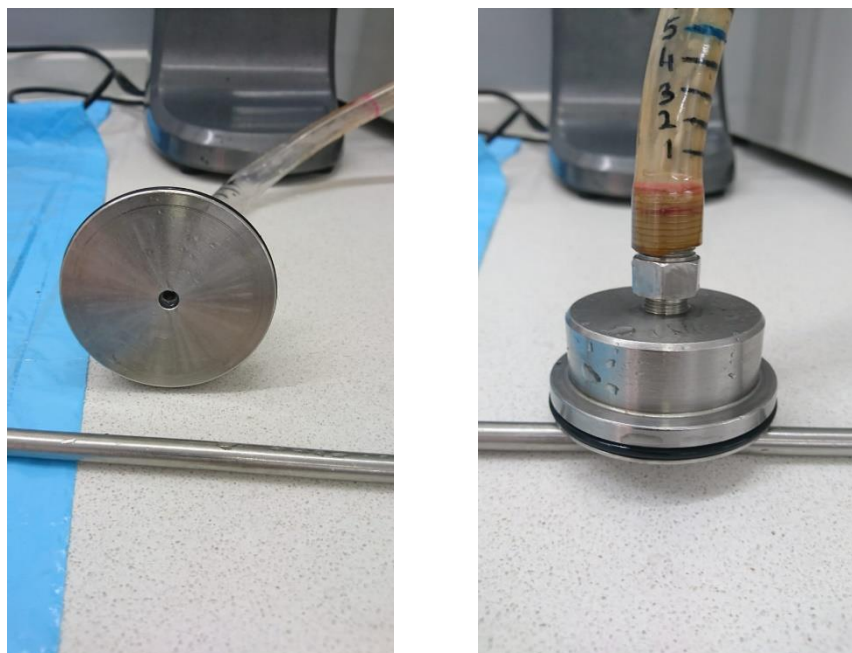


Figure 5.5: Front view (the left figure) and bottom view (the right figure) of redesigned top cap

During trial tests, it had been also realized that flow was not appropriate between slot and top cap. Since the slot is straight and some part of it faces the wall of top cap, the wellbore strengthening particles which passed through the fracture edge face with bulk structure of top cap. Then, these particles had lost their motion and started to accumulate at the fracture from edge to center and eventually they plugged the whole aperture as it is illustrated in Figure 5.6. Since this is not correct simulation of sealing, it was decided to change the structure of slots and created a void between slot and top cap.

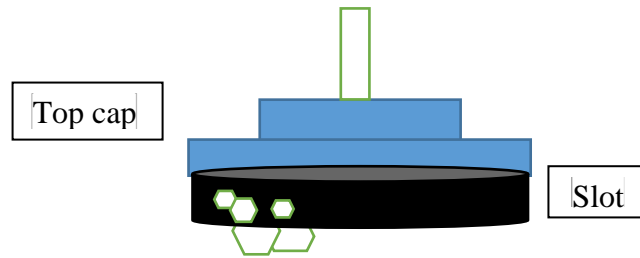


Figure 5.6: Representation of accumulation of particles inside the fracture due to inappropriate flow channel

Then, the slots which have void spaces as shown in Figure 5. were designed with Grade 303 Stainless Steel. However, they could not withstand high differential pressures and bended. Bending led to false results because it led to narrow fracture face and could be easily plugged. It was decided to produce slots from Grade 316 Stainless Steel and we faced with the same results.



Figure 5.7: Front view (left figure) and Bottom view(right figure) of redesigned slots

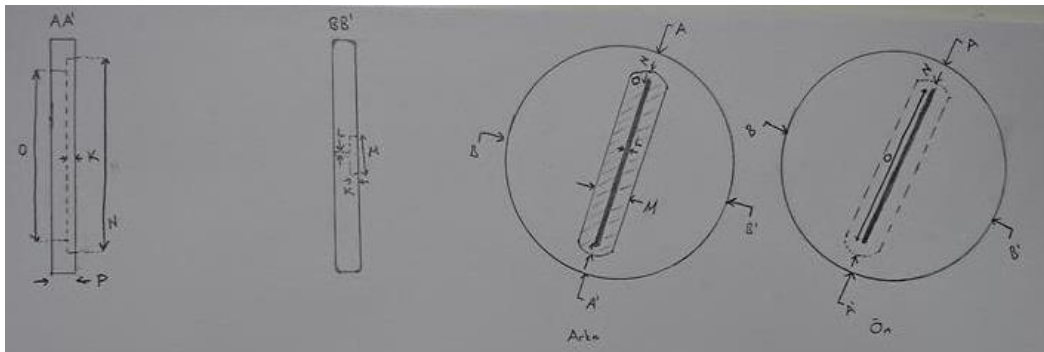


Figure 5.8: Drawings of redesigned slots

It has been decided to change structure of slots to increase its strength and to prevent bending. Slots were designed as shown in Figure 5.7 and Table 5.4. It has been decided to be manufactured by using Grade 316 Stainless Steel. After production, it was tested and it had observed that there was no bending. Final configuration of slots can be seen in Figure 5.8. In Figure 5.8, left hand side shows fracture face and right hand side shows void space behind the fracture.

Table 5.5: Dimensions of Re-designed Slots

K	L	M	N	O	P
2 mm	400 μ m	10 mm	54 mm	49 mm	6 mm
2 mm	800 μ m	10 mm	54 mm	49 mm	6 mm
2 mm	1200 μ m	10 mm	54 mm	49 mm	6 mm

- K represents depth of void space behind the fracture. It is necessary for appropriate flow after passing through the slot into the top cap.
- L represents fracture width.
- M shows width of void space behind the fracture. It is located on the back face of slot.
- N is used for length of void space behind the fracture.
- O represents fracture length.
- P indicates thickness of slots.

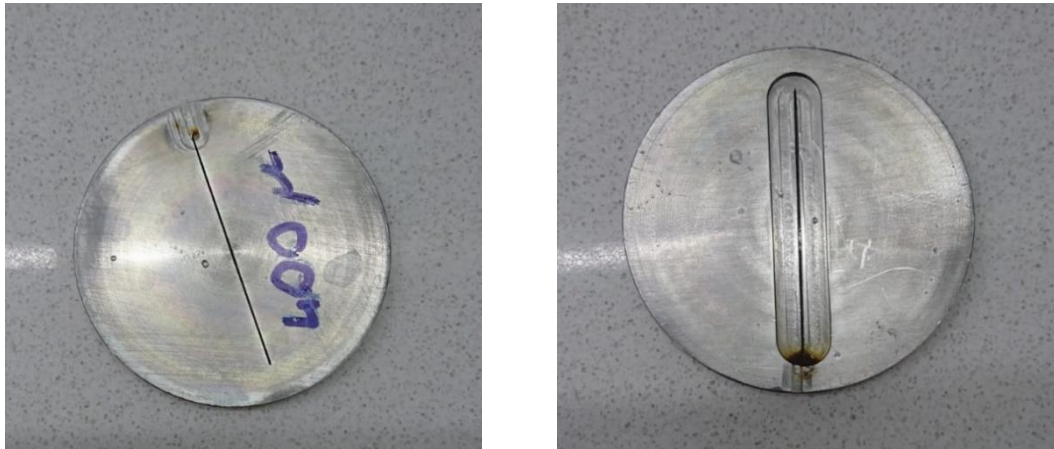


Figure 5.9: Final Configuration of slots

The test set up was redesigned after many experiences from trial tests and final shape is shown in Figure 5.10:



Figure 5.10: PPA Assembly used in the test

5.6.2. Test Procedure

Procedure for seal capability tests is given below step by step:

1. Collect WSM-laden mixture.
2. Drop defoamer into it to eliminate gas trapped in the mud.
3. Pour 350 ml of sample into the cell.
4. Place slot into the cell.
5. Start pumping of hydraulic oil. (STAGE-I is initiated)
6. When bridge starts to form, pressure on the gauge starts to increase. When it reaches lowest recordable pressure (100 psi) (see Figure 5.11), record the initial mud loss which indicates mud loss prior to sealing, i.e. mud loss up to 100 psi. (STAGE-I is finalized)
7. Continue to increase pumping with the rate of 10 psi/sec until pressure reaches 2000 psi. During this process whole pressure falls are recorded. (STAGE-II is initiated)
8. When pressure reaches 2000 psi, make sure that seal can withstand under 2000 psi without pressure falling.
 - If sudden pressure fall is observed, continue to recording pressure falls and pumping with the rate of 10 psi/sec increment.
 - If there is no sudden pressure fall, record mud loss values as mud loss in Stage II. (STAGE-II is finalized)Mud loss in Stage II indicates mud loss volume between 100 psi and 2000 psi. It shows that whole mud loss which occurs during all pressure increments and falls.
9. To see whether the seal can hold 2000 psi without break, wait 5 minutes and continue to record pressure and volume change (STAGE-III is initiated). Mud loss in Stage III shows mud loss during 5 minutes.
10. After 5 min, test is finished (STAGE-III is finished). Disassemble the cell and remove the slot.

11. Total mud loss volume is calculated by summation of mud loss in Stage I, Stage II and Stage III.

NOTE: Although the aim of this study is to determine optimum composition which seals the fracture quickly with lower mud loss, it is also necessary to define failing point. If mud loss value exceeds 125 ml, the test is stopped and recorded as “failed”. According to producer of the test set-up, if most of the sample is removed from the cell, pressuring piston could damage the top of the cell and may cause a pressure release.



Figure 5.11: Hand Pump Gauge

To understand graphs and tables in the following chapters, please look at Figure 5.12 and Table 5.6.

Table 5.6: Examples of Mud Loss and Total Sealing Time Tables

Code	Mud Loss (ml)				Total Sealing Time (sec)
	Stage I	Stage II	Stage III	Total	
FMC 6-14-10 D-800 μ	9.8	29.8	1.4	41	1526

Each test was named according to including wellbore strengthening material (WSM) concentration and fracture width of tested slot. Code of FMC 6-14-10 indicates

concentration of used each WSM concentration. The first number indicates that the concentration of fine size particles. In this example, FMC 6-14-10 includes 6 lb/bbl fine sized ground marble. Second number is used for the concentration of medium sized particles. FMC 6-14-10 has 14 lb/bbl medium sized ground marble. Third number presents the concentration of coarse size particles. FMC 6-14-10 composition includes 10 lb/bbl coarse sized particles. D-800 μ indicates that test was done on the fracture which has the width of 800 μ . For better understanding, the following examples can be examined.

FMC 08-06-12 D-400 μ indicates that WSM sample includes 8 ppb Fine, 6 ppb Medium and 12 ppb Coarse particles. Also, it indicates that test was done on slot which has 400- μ m fracture width. On the other hand, FMC 10-00-02-D1200 μ is used for test of the sample with 10 ppb Fine and 2 ppb Coarse GM particles on slot having 1200- μ m fracture width.

Test steps can be explained detailly in the following:

Stage I:

- When seal forms on the fracture face, the bridge shows resistance to the flow.
- If hydraulic oil pumping is continued, pressure in the cell increases.
- When it reaches the lowest recordable pressure (100 psi) on gauge, pressure vs time recording starts after mud loss value in Stage I had recorded.
- t_0 in the x axis of graph indicates the time which pressure reach 100 psi and it is accepted as 0.
- In stage I, it is recorded only the amount of fluid lost until bridge is formed.

Stage II: By the increment with rate of 10 psi/sec, whole pressure falls are recorded in Stage II. Since Pressure increment rate is constant, the time is easily calculated according to pressure data.

- If pressure reaches assumed maximum pressure sealing pressure (2000 psi), seal efficiency is tested under 2000 psi about 20 sec.

- If there is no sudden pressure fall, it means that Stage II finished and Mud Loss in Stage II is recorded. Since some amount of fluid passes through the bridge during all pressure falls, mud loss may be higher in this stage.

Stage III: After Stage II has ended, Stage III starts. Endurance of bridge under 2000 psi overbalance is tested during 5 min. As can be seen, pressure slightly reduces in 5 minutes, the reason of this filtration occurs in seal pack in 5 minutes

- Some amount of fluid releases the seal therefore, pressure inside the cell reduces.
- After 5 minutes, the mud loss in Stage III and total sealing time are recorded.

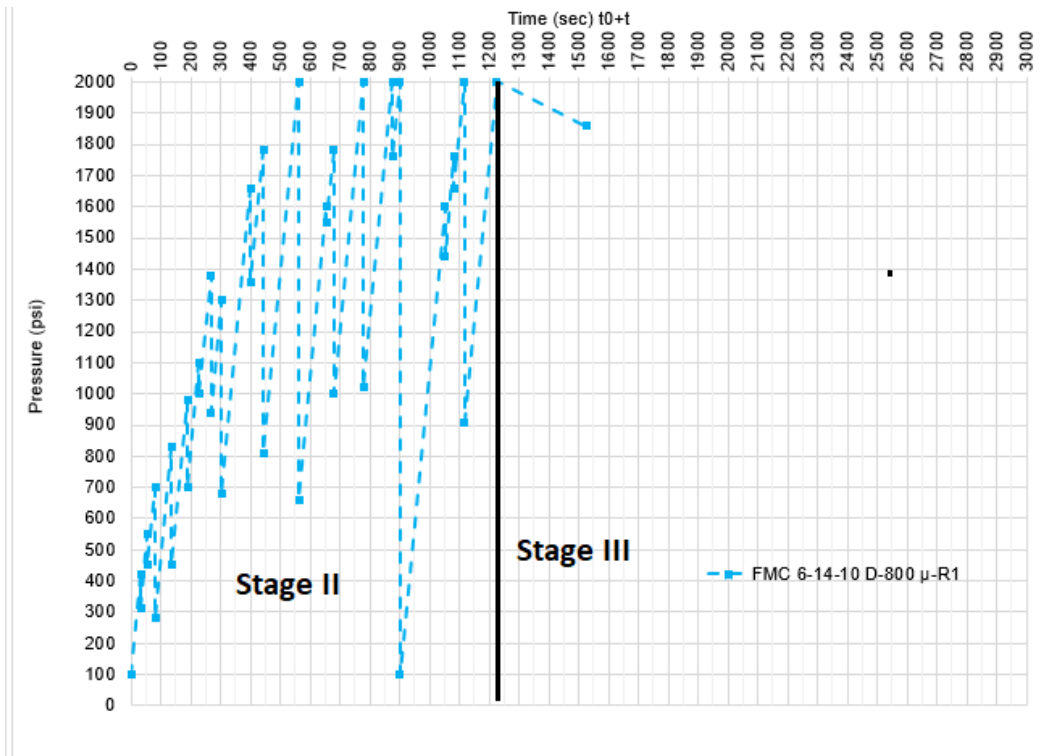


Figure 5.12: Representation of Pressure Sealing Test Graphs

CHAPTER 6

RESULTS AND DISCUSSION

In the first parts of this section, tests were done to determine suitable composition for drill-in fluid. The ideal concentration of modified starch and XCD polymers used in this study as filtration control and cuttings carrying additives of drill-in fluids respectively were determined according to these tests. The concentration of modified starch was determined by a result of standard API fluid loss test. Rheology tests were done to determine the amount of XCD polymer to avoid settling of Wellbore Strengthening Materials.

Based on the data obtained from several sealing capability tests of drill-in fluids with different sized ground marble samples with different concentrations, both particle size distribution and concentration effect on both sealing time and seal integrity are evaluated in other parts. Sealing pressure vs time curves at ambient temperature are presented for each sample of drill-in fluids in Appendix Part detailly. Total sealing time and mud loss volume in each stage for the same composition are given in the tables.

These tests results will be categorized firstly according to fracture width tests conducted on. Then, the effect of particle size distribution (PSD) on sealing will be evaluated for each fracture width separately and the optimum composition will be also determined in these sections. After that, the effect of concentration on sealing will be examined for each fracture width. Finally, the effect of fracture width on sealing will be evaluated.

All results of total sealing time have been evaluated according to following success criteria.

Success Criteria

The following criteria should be satisfied to define results as successful. In addition, the needs in the field applications are taken into consideration.

- **Rheological properties.** To suspend and keep uniform distribution of WSMs, low-shear rate viscosity values has gained importance. In this study, it is accepted that Low Shear Rate Viscosity (LSRV) must be above 60,000 cP as a rule of thumb. Their good suspension in the fluid can be ensured with this.
- **Seal Point:** Compositions must seal the fracture and resist to 2000 psi overbalance. Thanks to this, formations, which leads to lost circulation problems due to high pressure differentials even water-polymer drilling fluids used, can be drilled.

All results should meet the success conditions above. If the result of one test for the same sample did not meet these conditions, it could be said that this composition is not appropriate to use.

Recommended Range

Although the results meet the success criteria, the repeatability of tests is also important. To provide this, recommended range for each sample is presented. Since in use of standard deviation which is commonly used in statistics can cause that close data stay out from deviation range whereas the results diverge highly from each other can be taken place in deviation range, in this study $\pm 10\%$ of mean is accepted as recommended range. During the determination of this range, after the mean of three tests determined for each sample, 10% of it is calculated. By subtracting this value from mean, lower limit of recommended range is defined. By summing 10% of mean up to mean, upper limit is determined. If total sealing time of these three tests are not in this recommended range, the repeatability of tests can be seen as questionable.

Although mud losses are not primary indicator in comparison of samples, it can be used as secondary parameter to determine the optimum composition.

6.1. Filtration Control

Standard API fluid loss tests conducted to determine the concentration of modified starch which is commonly used for filtration control. During these tests the same amount of fine-sized ground marble is used as bridging agent. The effect of concentration of modified starch examined on low pressure (100 psi) filter press. Results during the tests can be seen in Figure 6.1 and detailed results tabulated in Table 6.1.

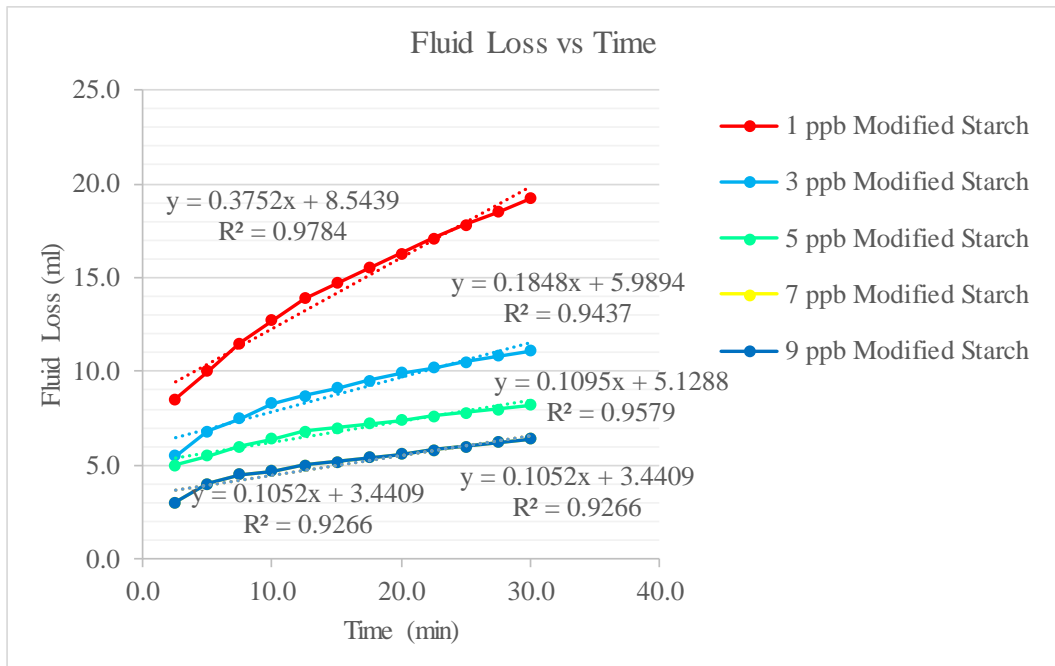


Figure 6.1: Comparison of Filtration Values

According to the results obtained from filtration tests, fluid loss decreased with increasing concentration of modified starch. However, the same values were obtained from tests with samples includes 7 lb/bbl and 9 lb/bbl modified starch. Therefore, 7 lb/bbl modified starch selected as the optimum concentration of fluid loss control agent since the same filtration loss data were obtained by less amount of additive.

Table 6.1: Results of Fluid Loss Measurement during 30 minutes

Chemicals	Concentration (lb/bbl)				
	Calcium Carbonate (Fine)	30	30	30	30
Modified Starch	1	3	5	7	9
Minutes	Fluid Loss (ml)				
2.5	8.5	5.5	5.0	3.0	3.0
5.0	10.0	6.8	5.5	4.0	4.0
7.5	11.5	7.5	6.0	4.5	4.5
10.0	12.7	8.3	6.4	4.7	4.7
12.5	13.9	8.7	6.8	5.0	5.0
15.0	14.7	9.1	7.0	5.2	5.2
17.5	15.5	9.5	7.2	5.4	5.4
20.0	16.3	9.9	7.4	5.6	5.6
22.5	17.1	10.2	7.6	5.8	5.8
25.0	17.8	10.5	7.8	6.0	6.0
27.5	18.5	10.8	8.0	6.2	6.2
30.0	19.2	11.1	8.2	6.4	6.4

6.2. Fluid Rheology

Rheological properties of different compositions which were mentioned in previous section were measured and listed in Table 6.2. The comparison of composition is also shown according to Shear Stress vs Shear Rate and Viscosity and Shear Rate in the Figure 6.1 and Figure 6.2, respectively.

Focusing on LSRV at 0.0636 sec^{-1} , Base B fluid was chosen as base fluid since the LSRV value of it bigger than 60,000 cp which is enough to suspend LCM samples. Although Base C shows better rheological properties, Base B is chosen to provide sufficient rheology with less XCD polymer concentration.

Since base fluid composition is the same for all composition, all wellbore strengthening material laden samples meet the rheological success criteria.

Table 6.2: PV, YP, LSRYP and LSRV at 0.0636 sec⁻¹ values of Base A, Base B and Base C fluid

Fluid	Base A	Base B	Base C
Ingredients	Concentration		
M.Starch	7 ppb	7 ppb	7 ppb
XCD	1 ppb	2 ppb	3 ppb
Parameters			
PV (cp)	4.893	8.806	12.328
YP (lb/100 ft²)	9.588	22.701	38.553
LSYP (lb/ 100 ft²)	4.11	14.481	20.352
LSRV @ 0.0636 sec⁻¹ (cp)	9586.41	67152.5	108177



Figure 6.2: Shear Stress vs Shear Rate Graph of Base A, Base B & Base C fluids

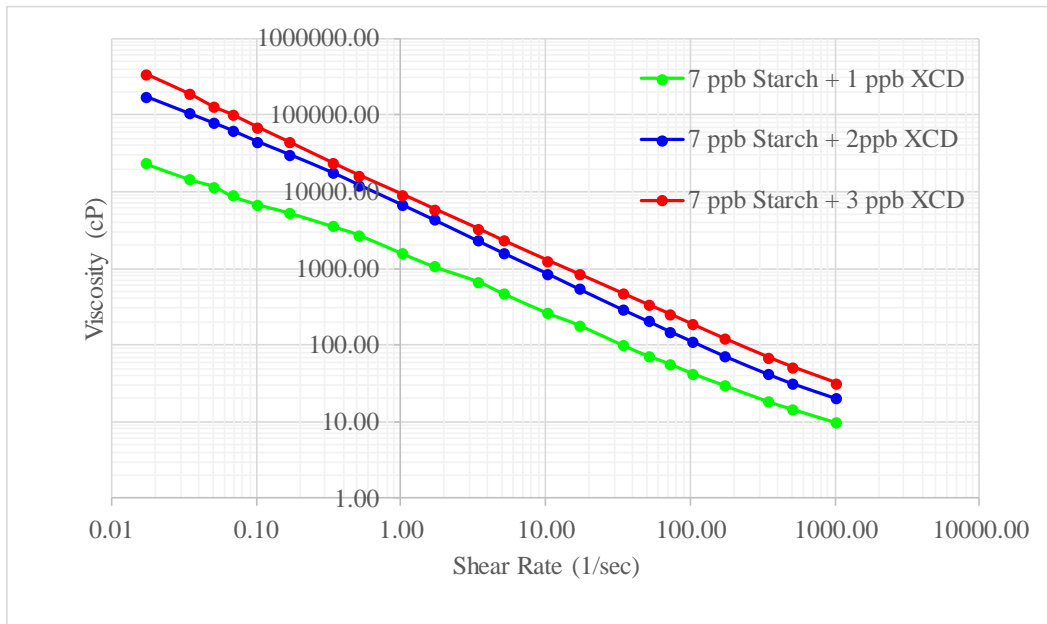


Figure 6.3: Viscosity vs Shear Rate Graph of Base A, Base B and Base C Fluids on log-log coordinates

6.3. Effect of Particle Size Distribution of Ground Marble on Sealing 400 microns fracture width

Firstly, FMC 10-10-10 was tested on 400- μ m slot size, since this composition seal the fracture during slot bending trial tests. Then, each particle size range was individually tested on the slot at the same concentration to see the effect of particle size distribution (PSD) on sealing.

Since aim of this study is to determine optimum wellbore Strengthening material composition which seal the fracture in this study, it was decided to check the importance of each particle range in sealing efficiency on 400-micron fracture width at lower concentrations.

After that, sealing efficiency of lower concentrations with different particle size distributions were tested. According to the results, comparison was carried out among the successful composition to determine optimum composition.

6.3.1. Results Obtained for Total Concentration of 30 ppb for 400- μ m Slot Size

Each particle size range was tested individually on the 400- μ m fracture width. 30 lb/bbl from each particle size range was taken and tested. Detailed results can be seen in Appendix F.I.1. According to the results obtained, fine-sized particles (FMC 30-0-0) and medium-sized particles (FMC 0-30-0) could not form a bridge on this slot when they were used alone. Although coarse-sized particle (FMC 0-0-30) could seal the fracture, it could not withstand higher pressure differentials when it was used individually. Once mud loss value went over 125 ml, the tests were finished and recorded as “failed” as mentioned before. However, the fracture sealed and withstand 2000 psi overbalance when it was used from each particle size range equally. Once 10 lb/bbl fine-sized, 10 lb/bbl medium-sized and 10 lb/bbl coarse-sized particles (FMC 10-10-10) were used, the bridge could be formed and aimed pressure was reached quickly as can be seen in Figure 6.4. After bridge was formed, pressure value reached to 2000 psi in 527.3 ± 3.5 sec according to Table 6.3. Observed total mud loss value was 4.2 ± 0.5 ml and all tests are in recommended range. Even these results can be used to show the importance of use of different particle size ranges.

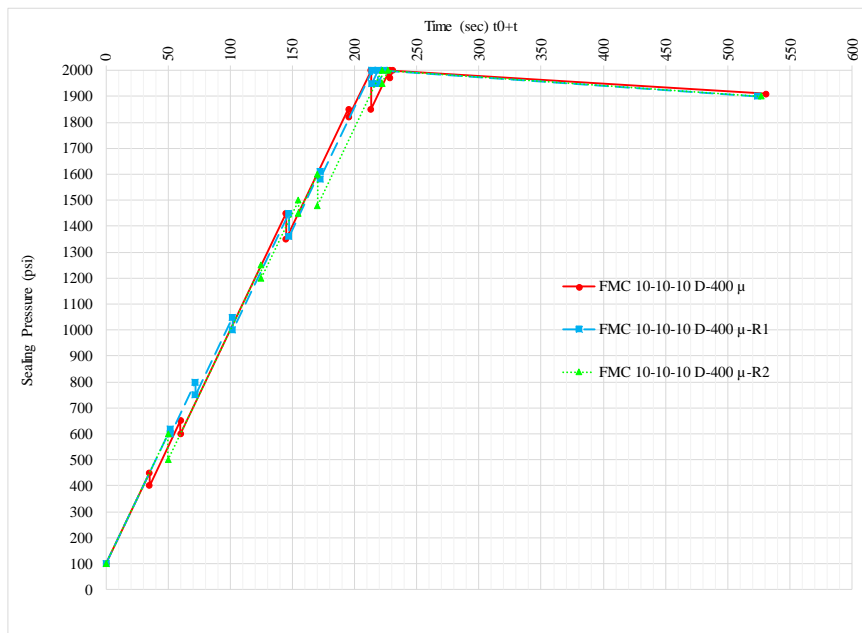


Figure 6.4: Pressure vs Time curve for FMC 10-10-10 on sealing 400-micron fracture width

Table 6.3: Mud Loss & Total Sealing Time Values for FMC 10-10-10 on 400-micron fracture width

Code	Mud Loss (ml)				Total Sealing Time (sec)
	Stage I	Stage II	Stage III	Total	
FMC 10-10-10 D-400μ	1.2	2.6	0.1	3.9	531.0
FMC 10-10-10 D-400μ-R1	1.6	2.2	0.2	4.0	524.0
FMC 10-10-10 D-400μ-R2	1.5	3.1	0.2	4.8	527.0
Mean	-	-	-	4.2	527.3
Std Dev	-	-	-	0.5	3.5
Deviation range, min	-	-	-	3.7	523.8
Deviation range, max	-	-	-	4.7	530.8
Recommended Range, min	-	-	-	-	474.6
Recommended Range, max	-	-	-	-	580.1

6.3.2. Results Obtained for Total Concentration of 28 ppb for 400- μ m Slot Size

Then, total concentration decreased to 28 lb/bbl and the effect of particle size distribution was examined. FMC 8-10-10, FMC 10-8-10 and FMC 10-10-8 compositions were tested on 400- μ m fracture width. Total sealing time and mud loss values of each composition was recorded. The mean of total sealing time and total mud loss values presented in Table 6.4. Detailed information can be found in Appendix F.II. According to these test results, FMC 10-8-10 & FMC 10-10-8 shows similar performance in terms of total sealing time whereas higher total sealing time was observed in FMC 8-10-10. However, mud loss value of FMC 8-10-10 was slightly higher than FMC 10-8-10 and FMC 10-10-8. Decrease in the concentration of fine-sized particles led to increase in total sealing time and total mud loss values. In other words, the aimed pressure can be reached later in FMC 8-10-10 than FMC 10-8-10 and FMC 10-10-8.

Table 6.4: Comparison of FMC 8-10-10, FMC 10-8-10 & FMC 10-10-8

Composition	Total Sealing Time (sec)			Total Mud Loss (ml)		
	Mean	Std Dev	Worst Case	Mean	Std Dev	Worst Case
FMC 8-10-10	570.7	42.3	617	6.2	0.9	7
FMC 10-8-10	526.7	13.5	540	5.1	1.5	6.6
FMC 10-10-8	517.7	19.1	538	4.7	1	5.8

6.3.3. Results Obtained for Total Concentration of 26 ppb for 400- μ m Slot Size

When total concentration of WSM decreased to 26 ppb, the performance of FMC 6-10-10, FMC 10-6-10 and FMC 10-10-6 were compared. Decrease in the concentration of fine-sized particles continued to increase total sealing time and mud loss values. Although this situation was the same for FMC 10-6-10, the increase in those values were not large as in FMC 6-10-10. However, FMC 10-10-6 composition sealed the fracture more quickly than others with lowest mud loss values. Besides all of these, one test result of FMC 6-10-10 composition stayed out from recommended range since pressure falls leads to increase in the difference between the total sealing times of the

same composition. Mean values of total sealing time and total mud loss can be seen in Table 6.5. Detailed results can be found in Appendix F.III.

Table 6.5: Comparison of FMC 6-10-10, FMC 10-6-10 & FMC 10-10-6

Composition	Total Sealing Time (sec)			Total Mud Loss (ml)		
	Mean	Std Dev	Worst Case	Mean	Std Dev	Worst Case
FMC 6-10-10*	589.7	72.7	673	7.4	1.7	9.3
FMC 10-6-10	552	40.7	599	5.9	0.4	6.3
FMC 10-10-6	527.7	10.4	536	4.5	0.5	5

*The results of FMC 6-10-10 composition is not in recommended range.

6.3.4. Results Obtained for Total Concentration of 24 ppb for 400- μ m Slot Size

While comparing the effect of the different particle size ranges at 24 ppb concentration, FMC 10-10-4 shows superior performance according to total sealing time and total mud loss values as shown in Table 6.6. As can be seen in Appendix F.IV.1, although, all tests with FMC 4-10-10 composition faced with major pressure falls, all tests met the success criteria and reached aimed pressure. However, third test of this composition (FMC 4-10-10 D-400 μ -R2) spent more time than others to reach aimed pressure. Therefore, total sealing time of it was largest and it led to staying out FMC 4-10-10 composition from the recommended range. In addition to suspicion about the repeatability of tests with FMC 4-10-10 composition, its sealing time and mud loss values were the highest among samples which includes 24 lb/bbl wellbore strengthening materials totally. On the other hand, the decrease in the concentration of medium-sized particles did not cause slight changes in total sealing time and mud loss values. FMC 10-4-10 showed nearly same time with FMC 10-6-10 composition. Again, decrease in the concentration of coarse-sized particles did not change in total sealing time and total mud loss values.

Table 6.6: Comparison of FMC 4-10-10, FMC 10-4-10 & FMC 10-10-4

Composition	Total Sealing Time (sec)			Total Mud Loss (ml)		
	Mean	Std Dev	Worst Case	Mean	Std Dev	Worst Case
FMC 4-10-10*	674	66.8	747	12.6	0.6	13.2
FMC 10-4-10	545.3	16	561	6.2	1.1	7.3
FMC 10-10-4	517	14	531	4.3	0.3	4.5

*The results of FMC 4-10-10 composition is not recommended range.

6.3.5. Results Obtained for Total Concentration of 22 ppb for 400- μ m Slot Size

At the total concentration of WSMs is 22 ppb, FMC 2-10-10 requires more time to reach the predetermined pressure and more fluid loss occurs during this process according to others. As can be seen in Appendix F.V.1, although all tests met the success criteria, in the third test, pressure in the cell which applied on the bridge was lost suddenly. That was strongly originated from breaking of particle on the mouth of the fracture under 2000 psi as it is illustrated in Figure 6.5. Endurance of bridge was damaged by this breaking and seal breaking occurred. Pressure in the cell fell since there was no barrier to resist. This led to bigger differentiation between total sealing time values. Therefore, this composition stayed out from recommended range. The repeat test with this composition might give different results.

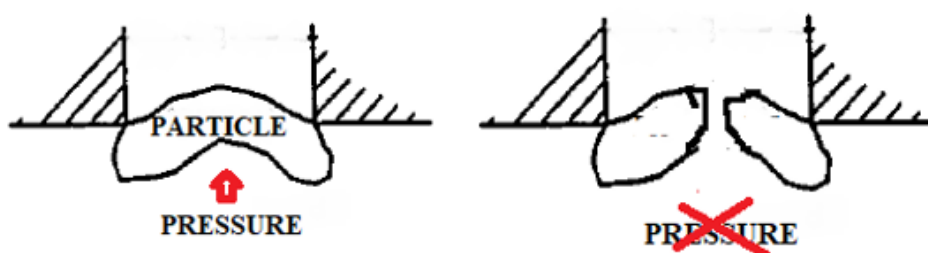


Figure 6.5: Illustration of Particle Breaking under pressure

The values in terms of total sealing time and total mud loss of FMC 10-2-10 are slightly bigger than FMC 10-10-2 as can be seen in Table 6.7. Decrease in the concentration of FMC 10-10-2 leads to slight increase in total sealing time whereas total mud loss can be seen the same with higher concentrations.

Table 6.7: Comparison of FMC 2-10-10, FMC 10-2-10 & FMC 10-10-2

Composition	Total Sealing Time (sec)			Total Mud Loss (ml)		
	Mean	Std Dev	Worst Case	Mean	Std Dev	Worst Case
FMC 2-10-10*	846	272.9	1161	22.7	9.7	33.8
FMC 10-2-10	583	39	623	8.8	0.9	9.4
FMC 10-10-2	558.3	20	578	4.6	5	5.1

*The results of FMC 2-10-10 composition is not recommended range.

6.3.6. Results Obtained for Total Concentration of 20 ppb for 400- μ m Slot Size

Then, total concentration decreased to 20 lb/bbl and the effect of the absence of one particle size ranges were also examined by this way. FMC 0-10-10, FMC 10-0-10 and FMC 10-10-0 were tested on 400- μ m fracture width.

Firstly, the effect of the absence of fine sized particles were examined. As can be seen in Appendix F.VI.1, none of these tests with FMC 0-10-10 composition could met the success criteria. Although plugging occurred at 100 psi, then bridge damaged and mud continued through the aperture. Once mud loss went over 125 ml, tests were finished. This situation resembles like highly permeable sands as illustrated in Figure 6.6. In the absence of fine-sized particles, medium and coarse sized particles accumulated at the mouth of the fracture. Since the voids between the particles could not filled, the mud flow through the bridge and fracture could not be prevented.



Figure 6.6: Illustration of flow through the highly permeable sands (Petropedia, 2018)

Although, absence of medium particles led to larger pressure drops, the bridge dealt with higher pressure differentials and met the success criteria whereas the absence of fine sized particles resulted in failure of tests. That means, the bridge is affected by the absence of fine sized range particles more significantly than the absence of medium sized range particles. On the other hand, the repeatability of FMC 10-0-10 is questionable since two tests were not in recommended range.

On the other hand, FMC 10-10-0 composition showed superior performance. Although there are no coarse-sized particles in the tested fluid, medium and fine sized particles formed a good pack and quickly sealed the fracture with lower mud loss values as can be seen in Table 6.8.

Table 6.8: Comparison of FMC 0-10-10, FMC 10-0-10 & FMC 10-10-0

Composition	Total Sealing Time (sec)			Total Mud Loss (ml)		
	Mean	Std Dev	Worst Case	Mean	Std Dev	Worst Case
FMC 0-10-10	-	-	-	>125	-	-
FMC 10-0-10*	597.3	120	735	12.3	2.2	14.6
FMC 10-10-0	541.7	9.3	548	4.6	0.5	5

*The results of FMC 10-0-10 composition is not in recommended range.

According to previous tests, the dependency of sealing integrity on particle size ranges can be summarized as follows:

- As the concentration of coarse sized particles decreased, total sealing time and mud loss values were not affected from it in comparison with medium sized and fine sized particles. The reason might be formation of good pack by medium and fine sized particles. Since medium size particles range includes larger particles than fracture width, it can plug the fracture width. When the fine sized particles filled the gaps between the medium sized particles, the fracture sealed. On the other hand, decrease in the concentration of fine sized particles resulted in higher total sealing time and mud loss. Also, in the absence of this range, bridge could not withstand higher pressures. That may be because coarse and medium sized particles plugged the opening, however interstitial voids could not be filled. It seems like if highly permeable formations are sealed, after a while the seal is broken and some amount of fluid passed through the slot until it is sealed again. However, the decrease in medium sized particles leads to slight increase in total sealing time and mud loss. In this case, fined sized particles and formed new sized particles after crushes filled the voids between the larger particles which requires slightly more time.
- As can be seen from the table, the concentration of fine sized particles is the most important parameter. In the absence of it, higher pressures cannot be reached. It is followed by medium sized particles since the lower concentration of it causes the more time and more fluid loss. The importance of coarse sized particles took place in the end of the line. Even the lack of these size, the total sealing and mud loss values are close to values in higher concentration of it.

To determine the optimum composition, the following tests were done.

6.3.7. Results Obtained for Total Concentration of 16 ppb for 400- μ m Slot Size

FMC 8-6-2 composition were tested on 400- μ m fracture width. It was observed that all tests met the success criteria and the fracture sealed quickly with lower mud loss values as can be seen in Figure 6.7. Although, in the second test (FMC 8-6-2 D-400 μ -R1), the aimed pressure was reached more quickly than in the third tests (FMC 8-6-2 D-400 μ -R2) with higher mud losses. The reason of this was the mud loss in Stage I and Stage III was larger in the second test as can be seen detailly in Table 6.9. It means that more fluid passed through the fracture until bridge has formed in Stage I. Also, the particle alignment in the second test might be worse according to other since higher mud loss was observed in Stage III. Beside all of these, tests were inside the recommended range. This composition might be applied in the field.

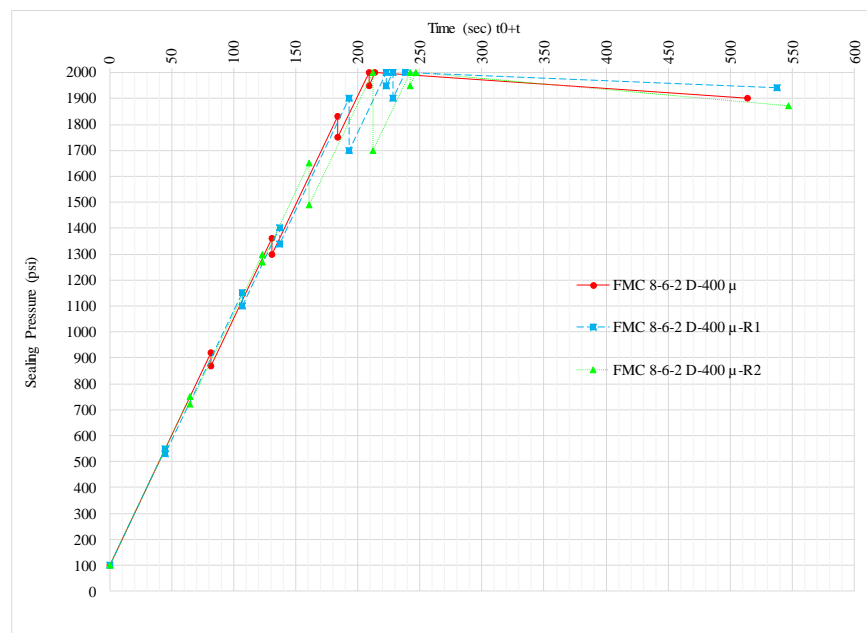


Figure 6.7: Pressure vs Time curve for FMC 8-6-2 on 400-micron fracture width

Table 6.9: Mud Loss & Total Sealing Time Values for FMC 8-6-2 on 400-micron fracture width

Code	Mud Loss (ml)				Total Sealing Time (sec)
	Stage I	Stage II	Stage III	Total	
FMC 8-6-2 D-400 μ	3.1	2	0.1	5.2	514
FMC 8-6-2 D-400 μ -R1	3.4	3	0.3	6.7	538
FMC 8-6-2 D-400 μ -R2	3	3.1	0.1	6.2	547
Mean	-	-	-	6.0	533.0
Std Dev	-	-	-	0.8	17.1
Deviation range, min	-	-	-	5.3	515.9
Deviation range, max	-	-	-	6.8	550.1
Recommended Range, min	-	-	-	-	479.7
Recommended Range, max	-	-	-	-	586.3

6.3.8. Results Obtained for Total Concentration of 14 ppb for 400- μ m Slot Size

Once satisfied results were obtained with FMC 8-6-2 composition, the concentration of fine-sized particles decreased to 6 lb/bbl and FMC 6-6-2 composition were tested on 400- μ m fracture width. The fracture sealed and aimed pressure was reached as can be seen in Appendix F.VIII.1. After bridge was formed, pressure value reached to 2000 psi in 615.7 ± 20.6 sec and observed total mud loss value was 9.7 ± 0.8 ml. All three tests with the same composition were inside the recommended range.

6.3.9. Results Obtained for Total Concentration of 12 ppb for 400- μ m Slot Size

Then, FMC 4-6-2 composition were tested. The bridge could be formed and it resist to 2000 psi overbalance as can be seen in Appendix F.IX.1. Aimed pressure reached in 576.7 ± 27.8 sec. Observed total mud loss value was 9.9 ± 0.6 ml. In the second test, (FMC 4-6-2 D-400 μ -R1) composition reached to aimed pressure more quickly than the first test. However, mud loss in the second test was larger because the mud loss value in Stage I was higher than in the first test. Beside these, all three tests were in recommended range.

6.3.10. Results Obtained for Total Concentration of 10 ppb for 400- μ m Slot Size

After that, the concentration of fine-sized particles decreased, FMC 2-6-2 composition tested on 400- μ m fracture width. The fracture sealed in 843.0 ± 145.0 sec. Total mud loss was observed 19.3 ± 6.7 ml. Also, two tests with the same composition stayed out from recommended range. Since sealing time and mud loss increased significantly according to previous tests, FMC 4-6-0 composition were tested. As can be seen in Appendix F.X.2, in the second test with this composition (FMC 4-6-0 D-400 μ -R1) the good pack of the particles was formed and aimed pressure was reached more quickly than others. This led to stay out this composition from the recommended range. Then, FMC 4-4-2 composition was tested. It was observed that FMC 4-4-2 and FMC 4-6-0 compositions showed really close performance in terms of total sealing time and total mud loss. However, not only the worst case of FMC 4-4-2 composition was better performance but also FMC 4-6-0 composition was not in recommended range due to deviations between the results from repeat tests with the same composition.

Table 6.10: Comparison of FMC 2-6-2, FMC 4-4-2 & FMC 4-6-0

Composition	Total Sealing Time (sec)			Total Mud Loss (ml)		
	Mean	Std Dev	Worst Case	Mean	Std Dev	Worst Case
FMC 2-6-2*	843	145	1010	19.3	6.7	27
FMC 4-4-2	613	4.4	618	11.5	0.8	12.1
FMC 4-6-0*	618.3	83.1	675	11.5	2	12.9

*The results of these compositions were not in recommended range.

6.3.11. Results Obtained for Total Concentration of 8 ppb for 400- μ m Slot Size

FMC 4-2-2 composition were tested on 400- μ m fracture width. As can be seen in Appendix F.XI.1, all tests met the success criteria. The fracture sealed in 685.0 ± 66.6 sec. Observed total mud loss value was 15.5 ± 1.9 ml. One of the tests with this composition was not in recommended range.

6.3.12. Results Obtained for Total Concentration of 6 ppb for 400- μ m Slot Size

FMC 4-0-2 composition was tested on 400- μ m fracture width. As can be seen in Figure 6.8, although many high pressure drops occurred, all three tests were able to reach 2000 psi eventually and met the success criteria. According to Table 6.8, total sealing time and total mud loss values were 1060.3 ± 148.3 sec and 44.4 ± 9.4 ml, respectively. As can be seen both these tests and previous tests, even the same composition on the same slots, the repeat tests could result in different sealing time and mud loss values due to pressure falls and their different damage on the bridge. Because of these pressure falls originated from seal breaks, high deviations in total sealing time was observed. These deviations led to staying out two of these tests from recommended range.

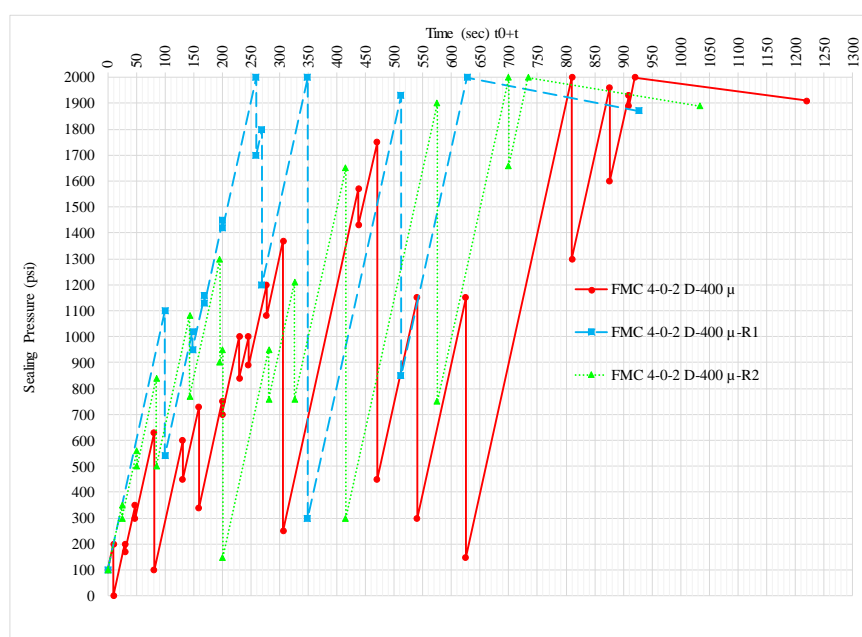


Figure 6.8: Pressure vs Time curve for FMC 4-0-2 on 400-micron fracture width

Table 6.11: Mud Loss & Total Sealing Time Values for FMC 4-0-2 on 400-micron fracture width

Code	Mud Loss (ml)				Total Sealing Time (sec)
	Stage I	Stage II	Stage III	Total	
FMC 4-0-2 D-400μ	27	27.4	0.6	55	1220
FMC 4-0-2 D-400μ-R1	24	13	0.1	37.1	927
FMC 4-0-2 D-400 μ -R2	25	16	0.2	41.2	1034
Mean	-	-	-	44.4	1060.3
Std Dev	-	-	-	9.4	148.3
Deviation range, min	-	-	-	35.1	912.1
Deviation range, max	-	-	-	53.8	1208.6
Recommended Range, min	-	-	-	-	954.3
Recommended Range, max	-	-	-	-	1166.4

Then 4-2-0 composition was tested on the same slot. As can be seen in Appendix F.XII.2, all tests satisfied the predetermined success criteria. However, the results of this composition were not in recommended range. The fracture sealed and observed total sealing time was 851.3 ± 110.8 sec. Recorded total mud loss value was 9.7 ± 2.1 ml.

As mentioned before, the importance of particle size distribution (PSD) on sealing the fracture is important. At the same concentration, the less total sealing time and mud loss values can be obtained with different particle size distribution design. For example, comparison of FMC 4-0-2 and FMC 4-2-0 shows that when medium sized particles used instead of coarse sized particles, aimed pressure can be reached quickly and less amount of fluid is lost through the bridge.

Table 6.12: Comparison of FMC 4-0-2 and FMC 4-2-0

Composition	Total Sealing Time (sec)			Total Mud Loss (ml)		
	Mean	Std Dev	Worst Case	Mean	Std Dev	Worst Case
FMC 4-0-2*	1060.3	148.3	1220	44.4	9.4	55
FMC 4-2-0*	851.3	110.8	976	19.7	2.1	22

*The results of these compositions were not in recommended range.

6.3.13. Results Obtained for Total Concentration of 4 ppb for 400- μ m Slot Size

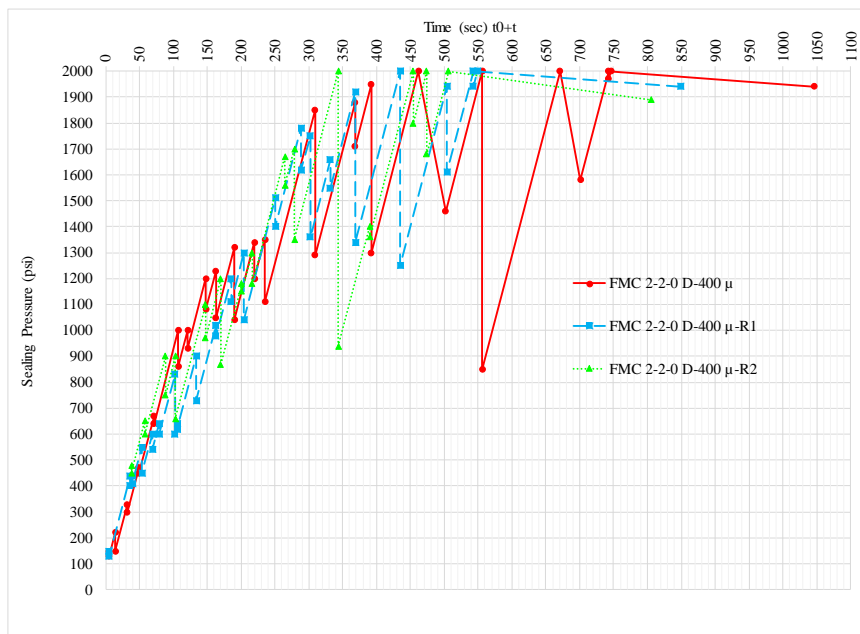


Figure 6.9: Pressure vs Time curve for FMC 2-2-0 on 400 micron fracture width

Although many pressure drops occurred in Figure 6.9, tests eventually met predetermined success criteria. However, it showed that by means of proper selection of particle size distribution, by using total concentration of 4-lb/bbl wellbore strengthening materials, 400- μ m fracture could be sealed. However, repeat tests with this composition might give different results since two of these tests stayed out from recommended range as can be seen in Table 6.13.

Table 6.13: Mud Loss & Total Sealing Time Values for FMC 2-2-0 on 400 micron fracture width

Code	Mud Loss (ml)				Total Sealing Time (sec)
	Stage I	Stage II	Stage III	Total	
FMC 2-2-0 D-400μ	14	12.4	0.4	26.8	1046
FMC 2-2-0 D-400 μ -R1	13	9.8	0.4	23.2	849
FMC 2-2-0 D-400μ-R2	11.8	7.2	0.4	19.4	806
Mean	-	-	-	23.1	900.3
Std Dev	-	-	-	3.7	128.0
Deviation range, min	-	-	-	19.4	772.4
Deviation range, max	-	-	-	26.8	1028.3
Recommended Range, min	-	-	-	-	810.3
Recommended Range, max	-	-	-	-	990.4

Although most of the tests examined before could seal the fracture and resist to aimed pressure, the lower total sealing time can be shown as in the Table 6.14.

Table 6.14: Comparison of Best Results for Sealing of 400 μ m fracture width

Composition	Total Sealing Time (sec)			Total Mud Loss (ml)		
	Mean	Std Dev	Worst Case	Mean	Std Dev	Worst Case
FMC 10-10-10	527.3	3.5	531	4.2	0.4	4.8
FMC 10-8-10	526.7	13.5	540	5.1	1.5	6.6
FMC 10-10-8	517.7	19.1	538	4.7	1	5.8
FMC 10-10-6	527.7	10.4	536	4.5	0.5	5
FMC 10-10-4	517	14	531	4.3	0.3	4.5
FMC 8-6-2	533	17.1	547	6	0.8	6.7

These all compositions met the predetermined success criteria and the results of them are repeatable. All of these compositions can be seen as successful and application of them can give good results.

In this study, although the mud loss in the test was slightly higher than other options, FMC 8-6-2 composition can be selected as optimum composition since the fracture was sealed by this composition at the same time with the others. Also, this composition includes less amount of coarse particles and total concentration of it is less than other alternatives.

6.4. Effect of Concentration of Ground Marble on Sealing 400 microns fracture width

To show the effect of concentration, FMC 8-6-2 is selected since it was selected as optimum concentration. By keeping the ratio between the particle size ranges, the effect of concentration on sealing 400- μ fracture width discussed in this section.

FMC 4-3-1, FMC 8-6-2, FMC 12-9-3 and FMC 16-12-4 compositions were compared according to total sealing time and mud loss values in Table 6.15. Detailed information about sealing pressure vs. time graph and total sealing time with mud loss values tables presented in Appendix G.

Table 6.15: The effect of concentration on sealing 400-micron fracture width

Composition	Success / Fail	Total Sealing Time (sec)		Total Mud Loss (ml)		Recommended or not
		Mean	Std Dev	Mean	Std Dev	
FMC 4-3-1	S	646.3	28.9	15.6	6.3	R
FMC 8-6-2	S	533	17.1	6	0.8	R
FMC 12-9-3	S	506.7	4.2	4.4	0.4	R
FMC 16-12-4	S	500.7	10.5	3	0.5	R

As it is expected, increasing concentration leads to more efficient seal. The number and severity of pressure falls decreased with increasing concentration. Therefore, total sealing time decreased. Fracture can be sealed quickly. Since the number of pressure falls decreased, less mud loss into the fracture occurred with increasing concentration.

6.5. Effect of Particle Size Distribution of Ground Marble on Sealing 800 microns fracture width

6.5.1. Results Obtained for Total Concentration of 30 ppb for 800- μ m Slot Size

Each particle size range was firstly tested individually on the 800- μ m fracture width. 30 lb/bbl from each particle size range was taken and tested. Detailed results can be seen in Appendix H.I.1. The same results were obtained also on this fracture width. While fine-sized particles (FMC 30-0-0) and medium-sized particles (FMC 0-30-0) could not form a bridge on this slot when they were used alone, coarse-sized particle (FMC 0-0-30) could succeed to form a bridge on the aperture. However, the bridge could not withstand higher pressure differentials when it was used individually and once mud loss value went over 125 ml, the tests were finished and recorded as “failed”. Therefore, it was concluded that each particle size range were not able to seal the fracture when they were used alone. In other words, one size range was not enough to plugged and sealed the fracture.

Then, FMC 10-10-10 were used, the bridge could be formed and aimed pressure was reached. According to data in Table 6.16, observed total sealing time and total mud loss value was 1130.3 ± 56.3 sec and 25.7 ± 1.5 ml. Although, all tests were in recommended range more severe pressure falls observed as can be seen in Figure 6.10. Therefore, other compositions with different particle size distribution at the same concentration were tested.

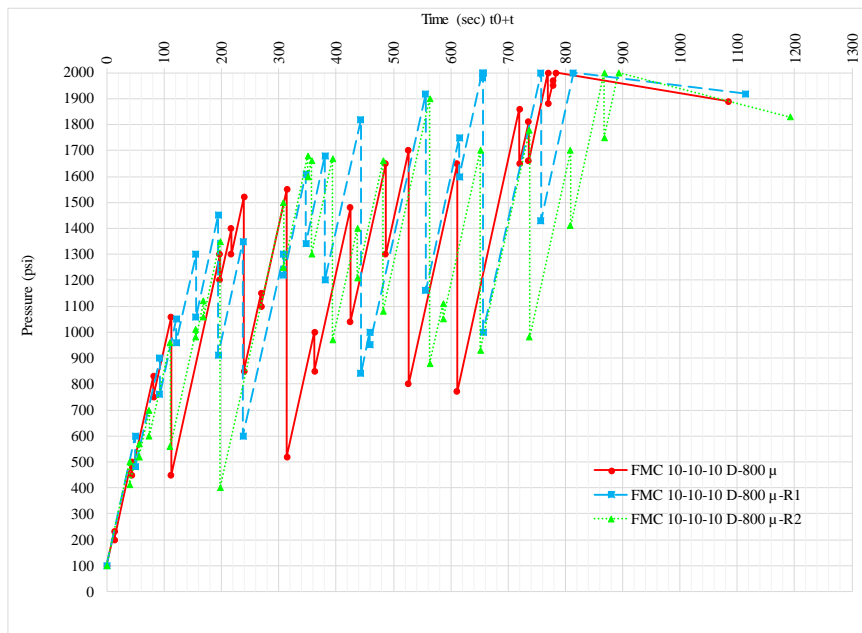


Figure 6.10: Pressure vs Time curve for FMC 10-10-10 on 800-micron fracture width

Table 6.16: Mud Loss & Total Sealing Time Values for FMC 10-10-10 on 800-micron fracture width

Code	Mud Loss (ml)				Total Sealing Time (sec)
	Stage I	Stage II	Stage III	Total	
FMC 10-10-10 D-800 μ	7.0	16.6	0.4	24.0	1084.0
FMC 10-10-10 D-800 μ -R1	7.0	18.4	0.8	26.2	1114.0
FMC 10-10-10 D-800 μ -R2	6.7	19.9	0.2	26.8	1193.0
Mean	-	-	-	25.7	1130.3
Std Dev	-	-	-	1.5	56.3
Deviation range, min	-	-	-	24.2	1074.0
Deviation range, max	-	-	-	27.1	1186.6
Recommended Range, min	-	-	-	-	1017.3
Recommended Range, max	-	-	-	-	1243.4

Firstly, the concentration of fine-sized particles was kept the same, the concentration of coarse and medium sized particles were changed and the effect of particle size distribution were examined. To do this, FMC 10-6-14, FMC 10-2-18, FMC 10,18-2 and FMC 10-14-6 compositions were tested on 800- μ fracture width. Comparison of these compositions according to total sealing time and total mud loss values can be found in Table 6.17. For detailed graph and tables, Appendix H.II can be checked out.

Table 6.17: Comparison of importance of coarse and medium sized particles

Composition	Total Sealing Time (sec)			Total Mud Loss (ml)		
	Mean	Std Dev	Worst Case	Mean	Std Dev	Worst Case
FMC 10-10-10	1130.3	56.3	1193	25.7	1.5	26.8
FMC 10-6-14*	928	177.4	1112	21.6	4.9	27
FMC 10-2-18*	1703.7	409.8	2155	46.1	11.5	57
FMC 10-18-2*	FAIL	FAIL	FAIL	>125	-	-
FMC 10-14-6*	1455	636.4	2140	35.5	16.7	53.6

*The repeatability of these tests are questionable.

According to these tests, it was observed that once the concentration of coarse particles and medium sized particles were close to each other more durable bridge could be formed as larger particles plug the fracture face, the voids filled with smaller particles and the bridge was formed. Besides all of these, size of coarse particles was slightly larger than fracture width although size of medium size particles was near to it. As the concentration of coarser particles decreases, the probability of forming plug decreases. In the absence of coarser particles, the bridge might not be sealed whereas coarse sized and fined sized particles could plug and resist higher pressure differentials in lack of medium sized particles. Therefore, the importance of coarse sized particles is more than of medium sized to seal the 800- μ fracture width and to reach aimed pressure.

Although the repeatability of FMC 10-6-14 composition was questionable, it showed better performance than FMC 10-10-10. Its both total sealing time and mud loss value

was smaller than FMC 10-10-10. While comparing worst values which were observed during test, mud loss values were almost the same, whereas total sealing time of FMC 10-6-14 was shorter than FMC 10-10-10. Therefore, it could be said that FMC 10-6-14 can show better performance.

After that, the concentration of medium sized particles was kept the same and the concentration of fine size and coarse size particles were changed to see the effect of changing fine-sized and coarse-sized particles inversely on sealing. FMC 2-10-18, FMC 6-10-14, FMC 14-10-6 and FMC 18-10-2 compositions were tested and compared in terms of total sealing time and mud loss values tabulated in Table 6.18.

Table 6.18: Comparison of importance of fine sized and coarse sized particles on 800-micron fracture width

Composition	Total Sealing Time (sec)			Total Mud Loss (ml)		
	Mean	Std Dev	Worst Case	Mean	Std Dev	Worst Case
FMC 10-10-10	1130.3	56.3	1193	25.7	1.5	26.8
FMC 2-10-18	FAIL	FAIL	FAIL	>125	-	-
FMC 6-10-14	890.3	53.4	947	23.6	2.2	25.2
FMC 14-10-6*	2605.7	473.6	2952	70.4	12.9	79.1
FMC 18-10-2	FAIL	FAIL	FAIL	>125	-	-

*The repeatability of this test is questionable.

As can be seen above results, decrease in the concentration of coarse sized particles affected sealing performance negatively. Total sealing time and mud loss values increased significantly. Also, in the absence of coarse-sized particles, the fracture could be sealed with cooperation of medium and fine-sized particles. However, aimed pressure could not be reached. On the other hand, the presence of fine-sized particles was also important. Although concentrations of coarse sized and medium sized particles were high, the bridge formed by these particles resembles like highly permeable sands. Fluid continued to flow through the bridge and fracture unless void

between the larger particles filled with fine particles. Also, if the difference between concentration of coarse sized and fined particles was too small, it has been observed good performance. FMC 6-10-14 showed the really good parameters in terms of total sealing time and mud loss. On the other hand, FMC 14-10-6 did not show good performance. The reason of this may be that the concentration of coarse sized particles is not enough to resist higher pressure values.

Then, the concentration of coarse-sized particles was kept and the effect of changing fine-sized and medium-sized particles were examined. In these tests, when concentration of fine-sized particles decreased, the concentration of medium-sized particles increased, or vice versa. The results are tabulated in Table 6.19. According to the results obtained from these tests, in the absence of fine-sized particles, although the bridge formed at low pressures, it could not withstand to higher pressure differentials. In addition, to get good performance, the concentration of particle-sized should close to each other like in FMC 6-14-10.

Table 6.19: Comparison of the Importance of Fine and Medium Particle Ranges

Composition	Total Sealing Time (sec)			Total Mud Loss (ml)		
	Mean	Std Dev	Worst Case	Mean	Std Dev	Worst Case
FMC 10-10-10	1130.3	56.3	1193	25.7	1.5	26.8
FMC 18-2-10*	1460.7	544.6	1899	37.8	17	53.6
FMC 14-6-10*	1618.3	695.5	2407	45.1	20.7	67
FMC 6-14-10*	1119.3	352.5	1523	29.2	10.2	41
FMC 2-18-10	FAIL	FAIL	FAIL	>125	-	-

*The repeatability of these tests are questionable.

Then FMC 18-6-6, FMC 6-18-6 and FMC 6-6-18 compositions were compared. According to the results shown in Table 6.20, FMC 18-6-6 showed the worse performance than the others. Total sealing time and total mud loss value were higher

than the others. In terms of total mud loss values, the second and the third ones were really close. Although FMC 6-18-6 composition was not recommended, mean of total sealing time and worst value of total sealing time was better than FMC 6-6-18.

Table 6.20: Comparison of FMC 18-6-6, FMC 6-18-6 and FMC 6-6-18

Composition	Total Sealing Time (sec)			Total Mud Loss (ml)		
	Mean	Std Dev	Worst Case	Mean	Std Dev	Worst Case
FMC 18-6-6*	2283	254.9	2574	67.4	7.2	74.2
FMC 6-18-6*	1241.3	230.3	1399	35	5	39.2
FMC 6-6-18	1362.3	115	1463	35.2	4.9	38.6

*The repeatability of these tests are questionable.

After all these tests, the effect of particles size distributions at lower concentrations were examined.

6.5.2. Results Obtained for Total Concentration of 28 ppb for 800- μ m Slot Size

When total concentration of wellbore strengthening materials decreased to 28 lb/bbl, FMC 8-10-10 shows better performance than FMC 10-8-10 and FMC 10-10-8. According to the results showed in Table 6.21, FMC 8-10-10 composition sealed the fracture quicker with lower mud losses. On the other hand, FMC 10-10-8 had good parameters than FMC 10-8-10. Although the results of tests are questionable, the worst pressure and mud loss values of FMC 10-10-8 are still better than FMC 10-8-10. Detailed graphs and tables can be found in Appendix H.II.2.

Table 6.21: Comparison of FMC 8-10-10, FMC 10-8-10 & FMC 10-10-8

Composition	Total Sealing Time (sec)			Total Mud Loss (ml)		
	Mean	Std Dev	Worst Case	Mean	Std Dev	Worst Case
FMC 8-10-10*	1051.7	247.1	1327	26.3	5.8	33
FMC 10-8-10*	1603.7	422.7	1963	38.9	11.2	49.6
FMC 10-10-8*	1209	171.2	1322	28.8	5.2	32

*The repeatability of these tests are questionable.

6.5.3. Results Obtained for Total Concentration of 26 ppb for 800- μ m Slot Size

Then, FMC 6-10-10, FMC 10-6-10 and FMC 10-10-6 were compared according to the results shown in Table 6.22. All these compositions were able to meet predetermined success criteria somehow. However, results of all compositions were not in the recommended ranges. Therefore, the repeatability of these tests are questionable. On the other, decrease in the concentration of coarse sized particles led to higher differentiations between the results.

Table 6.22: Comparison of FMC 6-10-10, FMC 10-6-10 & FMC 10-10-6

Composition	Total Sealing Time (sec)			Total Mud Loss (ml)		
	Mean	Std Dev	Worst Case	Mean	Std Dev	Worst Case
FMC 6-10-10*	1201	184.6	1361	29.3	4	33.4
FMC 10-6-10*	1171	246.5	1429	25.1	3.6	28
FMC 10-10-6*	1650.7	620.4	2211	42.6	15	54.2

*The repeatability of these tests are questionable.

6.5.4. Results Obtained for Total Concentration of 24 ppb for 800- μ m Slot Size

Although FMC 10-10-4 composition failed to keep its endurance under 2000 psi overbalance, FMC 4-10-10 and FMC 10-4-10 compositions were able to meet the success criteria. According to the results shown in Table 6.23, FMC 4-10-10 composition showed better performance than FMC 10-4-10 composition in terms of sealing time. Their mud loss values are close to each other.

Table 6.23: Comparison of FMC 4-10-10, FMC 10-4-10 and FMC 10-10-4

Composition	Total Sealing Time (sec)			Total Mud Loss (ml)		
	Mean	Std Dev	Worst Case	Mean	Std Dev	Worst Case
FMC 4-10-10*	1248	220.5	1492	34.2	6.9	42.1
FMC 10-4-10	1459.3	255	1662	34.9	4.6	38
FMC 10-10-4	FAIL	FAIL	FAIL	>125	-	-

The repeatability of these tests are questionable.

6.5.5. Results Obtained for Total Concentration of 22 ppb for 800- μ m Slot Size

When total concentration of wellbore strengthening materials decreased to 22 lb/bbl, FMC 2-10-10, FMC 10-2-10 and FMC 10-10-2 compositions were compared according to total sealing time and total mud loss values. FMC 2-10-10 and FMC 10-10-2 compositions sealed the fracture, they could not succeed to withstand under 2000 psi overbalance. Many pressure falls were observed. Once mud loss values went over 125 ml, the tests were finished. On the other hand, tests with FMC 10-2-10 composition were able to seal the fracture and met the success criteria as shown in Table 6.24. However, the big difference between the results of each test led to stayed out this composition from the recommended range.

Table 6.24: Comparison of FMC 2-10-10, FMC 10-2-10 and FMC 10-10-2

Composition	Total Sealing Time (sec)			Total Mud Loss (ml)		
	Mean	Std Dev	Worst Case	Mean	Std Dev	Worst Case
FMC 2-10-10	FAIL	FAIL	FAIL	>125	-	-
FMC 10-2-10*	1562.3	612.4	2269	36	15.5	53.8
FMC 10-10-2	FAIL	FAIL	FAIL	>125	-	-

*The repeatability of these tests are questionable.

The results obtained from test done with 22-lb/bbl wellbore strengthening materials showed that coarse sized particles are required to plug and seal the 800-micron fracture width. Also, fine sized particles are also required to fill the interstitial voids. The reason of being successful of FMC 10-2-10 is that fine sized particles plugged the openings voids filled by fine particles. However, it took time to enable seal integrity since all stresses were on the coarse sized particles and they crushed under these. This led to pressure falls and time loss. The presence of medium sized particles is not important as other two particle ranges, but, it is required to be present in the sample to distribute the stresses on the coarser particles and to support them.

6.5.6. Results Obtained for Total Concentration of 20 ppb for 800- μ m Slot Size

FMC 0-10-10, FMC 10-0-10 and FMC 10-10-0 compositions were tested on 800- μ m fracture width and the effect of absence of one particle size range were examined also by this way. In the absence of fine sized particles (FMC 0-10-10), the fracture could not be plugged. Although coarser sized particles might form a bridge on the mouth of the fracture, the gap between the particles could not filled. Fluid continued to flow through the bridge and once mud loss went over 125 ml, the tests were finished and recorded as “failed”. In the absence of medium sized particles, fine sized and coarse sized particles were able to plug and seal the fracture. Predetermined success criteria were met. Although, many and severe pressure falls observed, total sealing time values of all tests were in the recommended range. As can be seen in Appendix H..VI.2, total sealing time was 2039.3 ± 131.8 sec while total mud loss was 66.7 ± 3.3 ml. When coarse sized particles did not exist in the sample, the bridge could be formed on the fracture and this bridge could withstand lower pressure differentials. However, higher pressure differentials could not be reached by this composition.

Table 6.25: Comparison of FMC 0-10-10, FMC 10-0-10 and FMC 10-10-0

Composition	Total Sealing Time (sec)			Total Mud Loss (ml)		
	Mean	Std Dev	Worst Case	Mean	Std Dev	Worst Case
FMC 0-10-10	FAIL	FAIL	FAIL	>125	-	-
FMC 10-0-10	2039.3	131.8	2166	66.7	3.3	70.4
FMC 10-10-0	FAIL	FAIL	FAIL	>125	-	-

Then FMC 6-6-8 composition was tested. All tests sealed the fracture and reached to aimed pressure somehow as shown in the Figure 6.11. As can be seen in Table 6.26, the first test with this composition reached to 2000 psi quickly. Good alignment of particles on the bridge might lead to this. However, this situation cause that none of the tests with this composition take place in the recommended range.

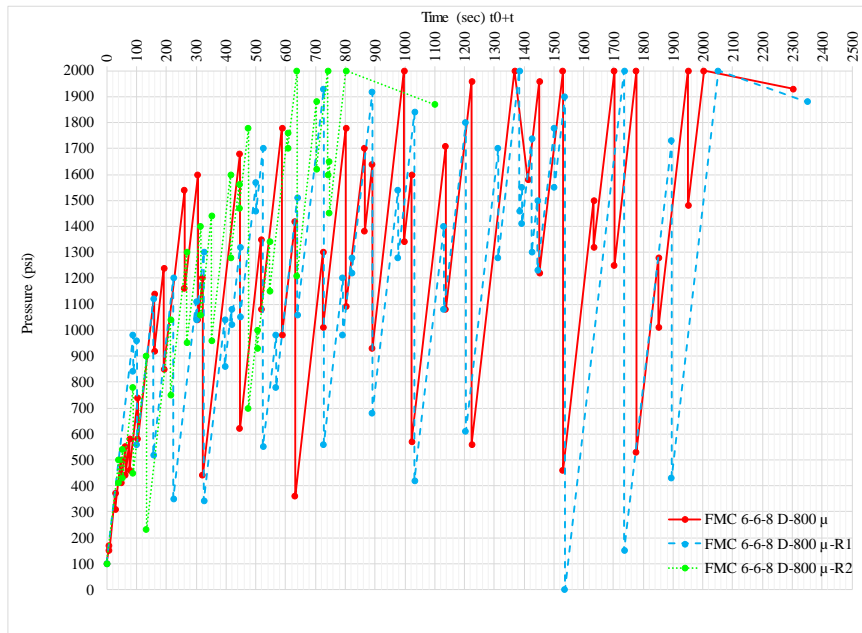


Figure 6.11: Pressure vs Time curve for FMC 6-6-8 on 800-micron fracture width

Table 6.26: Mud Loss & Total Sealing Time Values for FMC 6-6-8 on 800-micron fracture width

Code	Mud Loss (ml)				Total Sealing Time (sec)
	Stage I	Stage II	Stage III	Total	
FMC 6-6-8 D-800μ	14	52	1	67	2303
FMC 6-6-8 D-800μ-R1	9.8	55.6	0.7	66.1	2351
FMC 6-6-8 D-800μ-R2	9.2	20.8	1	31	1102
Mean	-	-	-	54.7	1918.7
Std Dev	-	-	-	20.5	707.7
Deviation range, min	-	-	-	34.2	1211.0
Deviation range, max	-	-	-	75.2	2626.3
Recommended Range, min	-	-	-	-	1726.8
Recommended Range, max	-	-	-	-	2110.5

As can be seen even in Table 6.26, even with this composition used, higher mud loss and higher sealing times were observed. It has been decided not to lessen concentrations.

Although, most of the tests examined before could seal the fracture and resist to aimed pressure, compositions with the lowest total sealing time values can be shown as in the Table 6.27.

Table 6.27: Comparison of Successful Results on Sealing of 800- μ m Fracture Width

Composition	Total Sealing Time (sec)			Total Mud Loss (ml)		
	Mean	Std Dev	Worst Case	Mean	Std Dev	Worst Case
FMC 10-10-10	1130.3	56.3	1193	25.7	1.5	26.8
FMC 8-10-10	1051.7	247.1	1327	26.3	5.8	33
FMC 10-6-14*	928	177.4	1112	21.6	4.9	27
FMC 6-10-14	890.3	53.4	947	23.6	2.2	25.2
FMC 6-14-10*	1119.3	352.5	1523	29.2	10.2	41

*The repeatability of these tests are questionable.

Although, mean of total sealing time for FMC 8-10-10 and FMC 6-14-10 compositions were less than FMC 10-10-10, their total mud loss and worst value of total sealing time were higher than FMC 10-10-10. That is why, FMC 10-10-10 composition selected instead.

Although the repeatability of FMC 10-6-14 was questionable, the results was pretty good. When looking at the worst value of total sealing time, it was better than most of the tests. Therefore, FMC 10-6-14*, FMC 10-10-10 and FMC 6-10-14 compositions can be applied to seal 800-micron fracture width. FMC 6-10-14 can be seen the best composition among these compositions since the worst mud loss volume was observed with this composition, besides lower total sealing time. Although in this

composition, concentration of coarse particles is high, since the maximum particle size is 1180 μ , it can be applied during drilling with downhole tools.

In general, it can be said that coarse and fine sized particles are important to seal 800-micron fracture width. The coarse sized range is important because the size of it is larger than fracture width. The coarse sized particles plugged fracture width and placed on the fracture mouth after some amount of fluid passed. The fine particles are also important since the voids between larger particles was filled by these. After coarser particles plugged the fractures, with the participation of fine sized particles, the perfect seal is formed. Although the importance of medium sized particles falls behind the others, the presence of it is also important. In high differential pressures, coarser particles have to resist the pressure behind. The force on them is higher. Some of them couldn't withstand these forces and crushing occurs. Crushed particles deform the stability of the bridge. Sometimes, voids open in the bridge and fluid loss resumes till the other particles healed the damaged parts. The medium size particles enable to distribute these forces and to heal these damaged parts quickly and endurance of the bridge might be strengthened.

6.6. Effect of Concentration of Ground Marble on Sealing 800 microns fracture width

The effect of concentration was examined by using FMC 10-10-10 and FMC 6-10-14 compositions on the 800- μ fracture width. Concentration of these particles increased by keeping the ratio between the particles size ranges the same.

Firstly, the concentration of FMC 10-10-10 composition increased. As can be seen in Table 6.28, mean of total sealing time and total mud loss decreased with increasing concentration as it was expected due that higher concentration led to decrease in the number and severity of pressure falls.

Table 6.28: Effect of Concentration on Sealing (1)

Composition	Total Sealing Time (sec)			Total Mud Loss (ml)		
	Mean	Std Dev	Worst Case	Mean	Std Dev	Worst Case
FMC 10-10-10	1130.3	56.3	1193	25.7	1.5	26.8
FMC 15-15-15*	1051.7	151.8	1184	19.7	1.7	21.1
FMC 20-20-20*	858.7	225.1	1116	14.3	6	21.1

*The repeatability of these tests are questionable.

Then, the concentration of FMC 6-10-14 composition increased by keeping the ratio between particle size ranges the same.

Table 6.29: Effect of Concentration on Sealing (2)

Composition	Total Sealing Time (sec)			Total Mud Loss (ml)		
	Mean	Std Dev	Worst Case	Mean	Std Dev	Worst Case
FMC 6-10-14	890.3	53.4	947	23.6	2.2	25.2
FMC 9-15-21*	1064	236.2	1064	22.2	6.5	29.4
FMC 12-20-28*	973.7	135.4	1103	18.8	3.9	21.6

*The repeatability of these tests are questionable.

It was expected that increase in the concentration of wellbore strengthening materials led to decrease in the total sealing time and decrease in mud losses. However, in these tests, due to seal breaks and pressure falls, total sealing times increased with increasing concentration. This exception showed that particle alignment and distribution in the bridge is also important. Sometimes increase in concentration might not be end up with decreasing total sealing time due to this. On the other hand, the mean of mud loss values decreased with increasing concentration. However, the worst values indicated different results. Especially in second test (FMC9-15-21), mud loss values increased significantly. This might be due to particles alignment on the face of the fracture.

6.7. Effect of Particle Size Distribution of Ground Marble on Sealing 1200 microns fracture width

Tests on the 1200- μm fracture width had started with each particle size range individually as it had done before. Then, FMC 10-10-10 was tested on 1200- μm slot size. After it was failed, other compositions with different particle size distributions at the same concentrations were tested. Then, total concentration of best results increased to 60 ppb.

6.7.1. Results Obtained for Total Concentration of 30 ppb for 1200- μm Slot Size

30 lb/bbl particle from each particles size range were tested on 1200- μm fracture width. None of these particles could not form a bridge on the fracture alone even at 100 psi. Once mud loss went over 125 ml, tests were finished and recorded as “failed”.

Then, FMC 10-10-10 composition was tested on the same fracture width. Although, the fracture was plugged by this composition at lower pressures. However, many seal breaks observed at higher pressure differentials. After upper limit passed over, the tests were finished and recorded as “failed”. During these tests, recorded maximum sealing pressures were 1340 psi, 1100 psi and 1240 psi in each test, respectively. After this composition was failed, different particle size distributions were tested on the same slot.

Firstly, the concentration of fine sized particles was kept the same and the concentration of coarse and medium sized particles changed. Then, FMC 10-6-14, FMC 10-2-18, FMC 10-18-2 and FMC 10-14-6 compositions were tested and detailed results can be found in Appendix J.I.

As can be seen from table 6.30, FMC 10-18-2 could not plug the fracture. Therefore, it can be concluded that in the absence of coarse sized particles, the fracture might not be sealed. On the other hand, other compositions sealed the fracture at lower pressure differentials. However, none of these compositions could reached the aimed pressure. Therefore, all of these were recorded as “failed”. FMC 10-14-6 sealed the fracture and

resisted to lower pressures than others as can be seen in Table 6.30. FMC 10-2-18 was the composition which reached highest pressure differentials. Also, each test of these compositions showed different results. During these tests, it was observed that increasing concentration of coarse sized particles leads to higher pressure differentials.

Table 6.30: Comparison of Maximum Sealing Pressures of Different Compositions on the 1200- μ m fracture width (1)

Composition	Maximum Sealing Pressures (psi)		
	Test #1	Test #2	Test #3
FMC 10-10-10	1340	1100	1240
FMC 10-18-2	0	0	0
FMC 10-14-6	340	440	900
FMC 10-6-14	1280	1450	1480
FMC 10-2-18	1960	1530	1600

Then, the concentration of medium sized particles was kept the same, the effect of change in the concentration of fine-sized and coarse-sized particles were examined. Then, FMC 6-10-14, FMC 2-10-18, FMC 14-10-6 and FMC 18-10-2 compositions were tested. Among these, FMC 18-10-2 composition could not form a bridge. Therefore, the same results were obtained. In the absence of coarse-sized particles, the bridge might not be sealed. Although other compositions could seal the fracture, none of them met predetermined success criteria. Recorded maximum sealing pressures were tabulated in Table 6.31. According to data on this table, FMC 6-10-14 showed the best performance among these compositions.

Table 6.31: Comparison of Maximum Sealing Pressures of Different Compositions on the 1200- μ m fracture width (2)

Composition	Maximum Sealing Pressures (psi)		
	Test #1	Test #2	Test #3
FMC 10-10-10	1340	1100	1240
FMC 2-10-18	900	800	330
FMC 6-10-14	1480	1180	1680
FMC 14-10-6	610	780	460
FMC 18-10-2	0	0	0

After that, the concentration of coarse-sized particles the same and the concentration of fine-sized and medium-sized particles changed. FMC 2-18-10, FMC 6-14-10, FMC 14-6-10 and FMC 18-2-10 compositions were tested to determine the effect of particle size distribution on sealing. All compositions plugged and sealed the fracture. However, aimed pressure could not be reached since they could not withstand higher pressure differentials. Recorded maximum sealing pressures during these tests tabulated in Table 6.32.

Table 6.32: Comparison of Maximum Sealing Pressures of Different Compositions on the 1200- μm fracture width (3)

Composition	Maximum Sealing Pressures (psi)		
	Test #1	Test #2	Test #3
FMC 10-10-10	1340	1100	1240
FMC 2-18-10	390	520	530
FMC 6-14-10	1100	1120	1210
FMC 14-6-10	1110	1220	1150
FMC 18-2-10	1260	1400	1100

While comparison all of tests done on 1200 μm , FMC 10-6-14 and FMC 10-2-18 showed good results in terms of observed maximum sealing pressures.

After failure of these tests, it was decided to increase concentration of particle size ranges to 60 lb/bbl to determine the optimum composition to seal 1200- μm fracture width.

6.7.2. Results Obtained for Total Concentration of 60 ppb for 1200- μm Slot Size

The concentration of FMC 10-6-14 and FMC 10-2-18 compositions were increased to 60 lb/bbl by keeping the ratio between the particle size ranges. Then, FMC 20-12-28 and FMC 20-4-36 compositions were tested. In addition to these compositions, FMC 15-15-30, FMC 10-10-40 and FMC 25-5-30 compositions were also tested.

In FMC 20-4-36 compositions, by means of increase in the concentration of coarse-sized particles, higher pressure values (1840 psi, 2000 psi and 1880 psi) could be

reached according to compositions with lower concentrations. In one test with this composition reached the aimed pressure. However, the bridges could not withstand under 2000 psi. In other two tests, aimed pressure could not be reached. Tests with these compositions recorded as “failed”.

Then, FMC 20-12-28 composition was tested on 1200- μ m fracture width. Although the first test with this composition reached to 2000 psi many times, the bridge were not withstand under this pressure. The second test reached to maximum 1880 psi. The third test reached aimed pressure once, then it had a seal break. All tests had seal breaks and pressure falls. Once mud losses passed over 125 ml, the tests were finished and recorded as “failed”.

After failure of these compositions, FMC 15-15-30, FMC 10-10-40 and FMC 25-5-30 compositions were tested on 1200- μ m fracture width. As can be seen in Appendix J.II, during testing of FMC 15-15-30 composition, many pressure falls occurred. Once mud loss passed the upper limit for mud loss, tests were finished. Recorded maximum sealing pressure for this test was 1800 psi. Since this composition already failed, other tests have not been done.

FMC 10-10-40 composition was tested. Although the test reached to 2000 psi two times, it could not resist to it. Once measured mud loss exceeded, the test was finished. Once this composition failed, repeat tests have not been done.

Then, FMC 25-5-30 composition was tested on 1200- μ m fracture width. After many pressure falls occurred, fluid loss passed the upper limit for mud loss and tests were finished. Recorded maximum sealing pressure was 1880 psi.

After these tests, it was observed that GM may not be effective to plug 1200- μ m fracture width and withstand under 2000 psi overbalance when it is used alone.

After these tests, higher concentrations were tested on the same fracture width to see whether 1200- μ m fracture width could be plugged with these particle size ranges or not. It was observed that FMC 15-30-45 (total WSM concentration of 90 lb/bbl),

FMC 20-40-60 (total WSM concentration of 120 lb/bbl) and FMC 25-50-75 (total concentration of 150 lb/bbl) compositions sealed the fracture. However, these concentrations are too high for continuous application in mud. Therefore, it was not suitable for wellbore strengthening mechanisms. However, 1200- μ m fracture width might be sealed with Lost Circulation Pill application by using higher concentrations of these particle size ranges.

6.8. Effect of Concentration of Ground Marble on Sealing 1200 microns Fracture width

Besides tests were done before, the concentration of FMC 10-10-10 composition increased to show the effect of concentration on sealing. As can be seen in 6.33, increasing concentration increased recorded maximum sealing pressures. Also, the bridge could be formed more easily and the bridges could become more durable with increasing concentration since the number of pressure fluctuations increased during these tests as shown in graphs and tables in Appendix K.

Table 6.33: Effect of Concentration on Sealing 1200- μ m Fracture Width

Composition	Maximum Sealing Pressures (psi)		
	Test #1	Test #2	Test #3
FMC 10-10-10	1340	1100	1240
FMC 16-16-16	1540	1400	1800
FMC 20-20-20	1780	1940	1980

6.9. Effect of Fracture Width on Sealing

The same composition tested on different fracture widths to see the effect of fracture width. FMC 10-10-10 composition has been chosen. As can be seen in Table 6.34, increasing fracture width size affected seal integrity negatively. As the fracture width increases, it gets difficult to form a bridge and resist to higher pressure differentials.

Table 6.34: Total Sealing Time and Total Mud Loss Values for FMC 10-10-10 composition on different fracture width

Fracture Width Size (µm)	Total Sealing Time (sec)			Total Mud Loss (ml)		
	Mean	Std Dev	Worst Case	Mean	Std Dev	Worst Case
400	527.3	3.5	531	4.2	0.5	4.8
800	1130.3	56.3	1193	25.7	1.5	26.8
1200	FAIL	FAIL	FAIL	>125	-	-

Results obtained in this study can be summarized as followings:

- Optimum wellbore strengthening concentration and particle size distribution of Ground Marble for 400-µm and 800-µm fracture width were determined.
- Sealing 1200-µm fracture width with particle size range used in this study is possible thanks to lost circulation pills applications.
- Particle crushing and seal breaks dominated the test results. Damage on the seal could be different for each sample. Even the composition was the same, the repeat tests could result in different sealing time and mud loss volumes in reaction to damage of pressure falls.
- PSD and concentration of WSM are critical parameters to seal the fracture.
- As stated by Sanders (2008), the required maximum size might be determined according to anticipated fracture width. Particle range can be determined at lower concentrations according to this. Particles which are larger than aperture plug the fracture face, then smaller particles filled the voids between larger

particles and sealing occurred. However, if maximum particle size was less than fracture width, sealing might be achieved at higher concentrations.

- As stated by Mostafavi et al (2011), increasing fracture width affects the seal integrity negatively. Larger particles and/or higher concentrations are required to seal larger apertures.
- Higher concentration reduces the number of pressure falls and amount of mud loss as the possibility of forming a bridge increases at higher concentrations.
- Contrary to statements done by Kumar et al. (2010), GM particles can be used as WSM alone depending on fracture width, particle size range, concentration and anticipated test pressure.
- Especially in Stage II, generally strong relationship observed between sealing efficiency and mud loss values. However, pressure falls and its damage on the seal can affect this relationship.

CHAPTER 7

CONCLUSION

This study was done to investigate the effect of Particle Size Distribution range, concentration and fracture width on sealing performance in Ground Marble laden drill-in fluids. Following conclusions are drawn as a result of experimental work:

1. Ground Marble particles can be used as wellbore strengthening materials to seal 400- μm and 800- μm fracture width and formed bridges resisted to 2000 psi.
2. Used particle size range of ground marble in this study may not be effective to plug the 1200- μm when used alone in wellbore strengthening applications under 2000 psi overbalance.
3. Particle Size Distribution has a major effect to seal the fracture regardless of the aperture.
4. The required maximum particle size might be determined according to anticipated fracture width.
5. In general, concentration influences total sealing time and mud loss values inversely proportional.
6. Pressure falls and damage on the bridge caused by them are highly effective on the results. Even the same composition is tested repeatedly, different sealing time and mud loss values observed depending on the severity of pressure falls.
7. Fracture size affects the stability of the seal inversely proportional. As the fracture width grows larger, sealing the fracture is getting harder.

CHAPTER 8

RECOMMENDATIONS

This study is an important step to understand the effect of particle size distribution, concentration of wellbore strengthening materials used to prevent lost circulation and the effect of fracture width on sealing. On the other hand, further studies are recommended for better understanding of wellbore strengthening material character and wellbore strengthening mechanism;

- Different particle size ranges might be chosen.
- Higher and lower fracture aperture might be considered.
- Although ground marble is the most commonly used type of granular wellbore strengthening material, different wellbore strengthening material types might be used for non-productive formations.
- Shape and number of slots can be reevaluated in the further studies.

REFERENCES

Abé, H., Keer, L. M. and Mura, T.1976. Growth rate of a penny-shaped crack in hydraulic fracturing of rocks, 2 J Geophys Res 81(35).6292–6298

Alberty, M.W. and McLean, M. R.2004. A physical model for stress cages. In: SPE Annual Technical Conference and Exhibition, 26–29 Sept, Houston, Texas. <https://doi.org/10.2118/90493-MS>

Alsaba, M., Nygaard, R., Saasen, A. and Nes, O. (2014). Lost Circulation Materials Capability of Sealing Wide Fractures. SPE Deepwater Drilling and Completions Conference.

Alsaba, M., Nygaard, R., Saasen, A., Nes, O.-M. (2014) Laboratory Evaluation of Sealing Wide Fractures Using Conventional Lost Circulation Materials. In: SPE Annual Technical Conference and Exhibition, Amsterdam, The Netherlands, 27-29 Oct. <https://doi.org/10.2118/170576-MS>

Alsaba, M., Nygaard, R., Saasen, A., Nes, O.-M. (2016) Experimental Investigation of Fracture Width Limitations of Granular Lost Circulation Treatments. Journal of Petroleum Exploration and Production Technology. <https://doi.org/10.1007/s13202-015-0225-3>

Aston, M.S., Alberty, M.W., McLean, M. R., de Jong, H. J. and Armagost, K. 2004. Drilling fluids for wellbore strengthening. Presented at the IADC/SPE Drilling Conference, 2–4 March, Dallas, Texas. <https://doi.org/10.2118/87130-MS>

Cook, J., Growcock, F., Guo, Q., Hodder, M. and Van Oort, E. 2011. Stabilizing the wellbore to prevent lost circulation. *Oilfield Rev* 23(4)

De Lloyd, D. 2000. Chemistry Department, the University of The West Indies, St. Augustine campus, The Republic of Trinidad and Tobago.

Dick, M. A., Heinz, T. J., Svoboda, C. F., & Aston, M. 2000, January 1. Optimizing the Selection of Bridging Particles for Reservoir Drilling Fluids. Society of Petroleum Engineers. <https://doi.org/10.2118/58793-MS>

Dupriest, F. E. 2005 Fracture closure stress (FCS) and lost returns practices. In: SPE/IADC Drilling Conference, 23–25 Feb, Amsterdam, Netherlands. <https://doi.org/10.2118/92192-MS>

Feng, Y., Gray, K. E. 2016. A parametric study for wellbore strengthening. *J Nat Gas Sci Eng.* 30:350–363

Fuh, G. F., Morita, N., Boyd, P. A. and McGoffin, S. J. (1992) A new approach to preventing lost circulation while drilling. In: SPE Annual Technical Conference and Exhibition, 4–7 Oct, Washington, D.C. <https://doi.org/10.2118/24599-MS>

Geertsma, J. and De Klerk, F. 1969. A rapid method of predicting width and extent of hydraulically induced fractures. *J Petrol Technol* 21(12):1571–1581

Guo, Q., Cook, J., Way, P., Ji, L. and Friedheim, J. E. 2014. A comprehensive experimental study on wellbore strengthening. In: IADC/SPE Drilling Conference and Exhibition, 4–6 March, Fort Worth, Texas, USA. <https://doi.org/10.2118/167957-MS>

Hettema, M., Horsrud, P., Taugbol, K., Friedheim, J., Huynh, H., Sanders, M.W. and Young, S. 2007. Development of an Innovative High-Pressure Testing Device for the Evaluation of Drilling Fluid Systems and Drilling Fluid Additives within Fractured Permeable Zones. OMC-2007-082, Offshore Mediterranean Conference and Exhibition, 28-30 March, Ravenna, Italy.

Ito, T., Zoback, M.D., Peska, P. 2001. Utilization of mud weights in excess of the least principal stress to stabilize wellbores: theory and practical examples. *SPE Drilling Completion* 16(4):221–229

Kumar, A., Savari, S. 2011, April. Lost Circulation Control and Wellbore Strengthening: Looking Beyond Particle Size Distribution. AADE National Technical Conference and Exhibition, Houston.

Kumar, A., Savari, S., Whitfill, D.L. and Jamison, D.E. 2010. Wellbore Strengthening: The Less-Studied Properties of Lost Circulation Materials. In: SPE Annual Technical Conference and Exhibition, Florence, Italy, 19-22 Sept. <http://dx.doi.org/10.2118/133484-MS>.

Lake, Larry W., and Robert F. Mitchell. Petroleum Engineering Handbook. Society of Petroleum Engineers, 2006.

Loeppke, G. E., Glowka, D. A., & Wright, E. K. 1990, March. Design and Evaluation of Lost Circulation Materials for Severe Environments. Journal of Petroleum Technology, 42(3). <https://doi.org/10.2118/18022-PA>

Morita, N., Black, A.D., Fuh, G.F. 1996. Borehole breakdown pressure with drilling fluids—I. Empirical results. Int J Rock Mech Min Sci Geomech Abstr 33(1):39–51

Morita, N., Fuh, G.-F. 2012 Parametric analysis of wellbore-strengthening methods from basic rock mechanics. SPE Drilling Completion 27(02):315–327

Morita, N., Fuh, G.F., Black, A.D. 1996. Borehole breakdown pressure with drilling fluids—II. Semi-analytical solution to predict borehole breakdown pressure. Int J Rock Mech Min Sci Geomech Abstr 33(1):53–69

Mostafavi, V., Hareland, G., Belayneh, M. and Aadnoy, B.S. 2011. Experimental and Mechanistic Modelling of Fracture Sealing Resistance with Respect to Fluid and Fracture Properties. In: 45th US Rock Mechanics / Geomechanics Symposium, 26-29 June, San Francisco, CA, USA.

Rojas, J. C., Bern, P. A., Fitzgerald, B. L., Modi, S., & Bezant, P. N. 1998, January 1. Minimising Down Hole Mud Losses. Society of Petroleum Engineers. <https://doi.org/10.2118/39398-MS>

Salehi, S. and Nygaard, R. 2011, 27-29 March. Evaluation of New Drilling Approach for Widening Operational Window: Implications for Wellbore Strengthening. SPE 140753. SPE Production and Operations Symposium. Oklahoma City, USA.

Sanders, M.V., Young, S. and Friedheim, J. 2008. Development and Testing of Novel Additives for Improved Wellbore Stability and Reduced Losses. AADE Fluids Conference and Exhibition, Houston, USA.

Savari, S., Whitfill, D.L., Jamison, D.E. and Kumar, A. 2014 A Method to Evaluate Lost Circulation Materials – Investigation of Effective Wellbore Strengthening Applications. In IADC/SPE Drilling Conference and Exhibition, Fort Worth, Texas, USA, 4-6 March. <https://doi.org/10.2118/167977-MS>

Song, J. and Rojas, J.C. 2006. Preventing mud losses by wellbore strengthening. In: SPE Russian Oil and Gas Technical Conference and Exhibition, 3–6 October, Moscow, Russia. <https://doi.org/10.2118/101593-MS>

Ülgen, U. B., Damcı, E., Gülmez, F. 2018. a New Insight of the Geothermal Systems in Turkey: First Geothermal Power Plant in Mountainous Area, “Özmen-1 GEPP”. 71st Geological Congress of Turkey.

van Oort, E., Friedheim, J.E., Pierce, T. and Lee, J. 2011. Avoiding losses in depleted and weak zones by constantly strengthening wellbores. SPE Drilling Completion 26(4):519–530

van Oort, E. and Razavi, O. S. 2014. Wellbore strengthening and casing smear: the common underlying mechanism. In: IADC/SPE Drilling Conference and Exhibition, 4–6 March, FortWorth, Texas, USA. <https://doi.org/10.2118/168041-MS>

Van Oort, E., Friedheim, J. E., Pierce, T., & Lee, J. 2011, December 1. Avoiding Losses in Depleted and Weak Zones by Constantly Strengthening Wellbores. Society of Petroleum Engineers. <https://doi.org/10.2118/125093-PA>

Vickers, S., Cowie, M., Jones, T., & Twynam, A. J. 2006. a New Methodology That Surpasses Current Bridging Theories to Efficiently Seal a Varied Pore Throat Distribution as Found in Natural Reservoir Formations. *Wiertnictwo Nafta Gaz*, 23(1), 501-515.

Whitfill, D. and Miller, M. 2008 Developing and Testing Lost Circulation Materials. AADE Fluids Conference and Exhibition, Houston, Texas, USA. 8–9 April.

APPENDICES

A. Technical Data Sheet of AMYLOTROL

DESCRIPTION

AMYLOTROL is a non-fermenting modified starch used as primary low viscosity fluid loss control agent in all water-base drilling fluids. It meets and surpasses ISO 13500, API Specification 13A – 16.

TYPICAL PROPERTIES

Appearance	: White powder
pH (1% solution)	: 7-9
Bulk Density	: 500 - 800 kg/m ³

FEATURES AND BENEFITS

AMYLOTROL is effective in all types of water-base drilling, workover and completion fluids.

AMYLOTROL imparts superior fluid loss control properties to the drilling fluids with minimum viscosity build-up.

AMYLOTROL reduces disintegration of cuttings and thus enhances solids removal process.

AMYLOTROL is non-ionic and thus has a good tolerance to monovalent and multivalent cations and is effective over a wide pH range.

AMYLOTROL is not susceptible to bacterial attack.

APPLICATION

AMYLOTROL can be used as fluid loss control agent in all types of the water-base drilling, workover and completion fluids.

LIMITATIONS

AMYLOTROL becomes less effective under the combined effect of high hardness and high pH as well as in saturated salt systems dictating greater additive consumption.

AMYLOTROL is thermally stable up to 132 °C (270 °F). The temperature stability can be increased by 20 °C using POLYTS P or POLYTS L temperature stabilizer.

AMYLOTROL may cause excess viscosity when added to drilling fluids with high solids content.

B. Technical Data Sheet of REOZAN D

DESCRIPTION

REOZAN D is an easily dispersible, high molecular weight biopolymer (xanthan gum) used as viscosifier in water-base fluid systems. It meets and surpasses ISO 13500, API Specifications 13A-19.

TYPICAL PROPERTIES

Appearance	: Cream colored powder
pH (1% solution)	:6-8
Bulk Density	: 650 - 900 kg/m ³

FEATURES AND BENEFITS

REOZAN D produces highly shear-thinning and thixotropic fluids with excellent hole cleaning and suspension capacity.

REOZAN D is effective in all types of fresh and sea water-base drilling fluids as well saturated monovalent salt systems.

REOZAN D is effective over a wide pH range and also provides some degree of fluid loss control.

REOZAN D causes minimum formation damage and is completely removed by acids and oxidizing agents.

REOZAN D disperses easily in fresh water or brine with minimum risk of “fish eyes” and lumping.

APPLICATION

REOZAN D is used to enhance hole cleaning and suspension capacity of fresh water and monovalent brine-base drilling and completion fluids.

LIMITATIONS

Soluble iron ion content greater than 40 mg/l causes rapid and severe cross-linking of REOZAN D. Citric acid is used to sequester the iron.

Since REOZAN D becomes less effective in fluids containing high calcium and high pH, the fluid must be pretreated with citric acid and/or sodium bicarbonate before drilling cement.

REOZAN D is thermally stable up to 150 °C (300 °F). The temperature stability can be increased by 20 °C using POLYTS L or POLYTS P temperature stabilizer.

REOZAN D is subject to bacterial degradation so a preservative such as GEOCID T or GEOCID G is recommended.

C. Technical Data Sheet of GEOCID T

DESCRIPTION

GEOCID T is a triazine based biocide used to control bacteria growth in water-base drilling, completion, workover and packer fluids.

TYPICAL PROPERTIES

Appearance	: Clear amber liquid
pH	:10–11
Specific Gravity	: 1.10 – 1.15

FEATURES AND BENEFITS

GEOCID T is compatible with all water-base drilling fluids.

GEOCID T is biodegradable and has low toxicity to marine life.

GEOCID T in small concentrations effectively controls aerobic and anaerobic bacteria.

GEOCID T is compatible with most oxygen and hydrogen sulfide scavengers.

GEOCID T also provides effective control on slime and corrosion caused by microorganisms in drilling, completion, workover and packer fluids.

APPLICATION

GEOCID T is used to protect bio-polymers (REOZAN D and REOZAN DS) and cellulosic LCM (FIBROCEL F, FIBROCEL M and FIBROCEL C) against to bacterial degradation.

GEOCID T is used for the prevention of slime and corrosion caused by sulfate reducing bacteria.

LIMITATIONS

GEOCID T is incompatible with oxygen scavengers (DRILSCAV OXA and DRILSCAV OXN) and some amine based shale inhibitors (CLAHIB N).

D. Specifications of Grace Viscometer

Temperature Range	Ambient (20 °F with chiller) to 212 °F
Pressure	Atmospheric Pressure
Sample Size	35-190 mL (depending on bob size & cup sleeve type)
Resolution	1 dyne/cm ²
Speed Range	0.01 to 600 rpm continuous
Shear Rate Range	0.0038 to 1020 sec ⁻¹
Shear Stress Range	2 to 3,600 dyne/cm ²
Viscosity Range	0.5 to 27,000,000 cP
Torque	7 μN.m to 14 mN.m
Accuracy	±0.5% of torque span or better

E. Specifications of Permeability Plugging Apparatus

Test pressure Range	0 to 5000 psi (34,474 kPa)
Temperature Range	50°F to 500 °F (10°C to 260 °C)
The maximum pressure for back receiver	750 psi (5,171 kPa)

F. Effect of Particle Size Distribution of Ground Marble on Sealing 400- μ Fracture Width

F. I. Results Obtained for Total Concentration of 30 ppb for 400- μ Slot

F. I. 1. FMC 30-0-0, FMC 0-30-0 & FMC 0-0-30

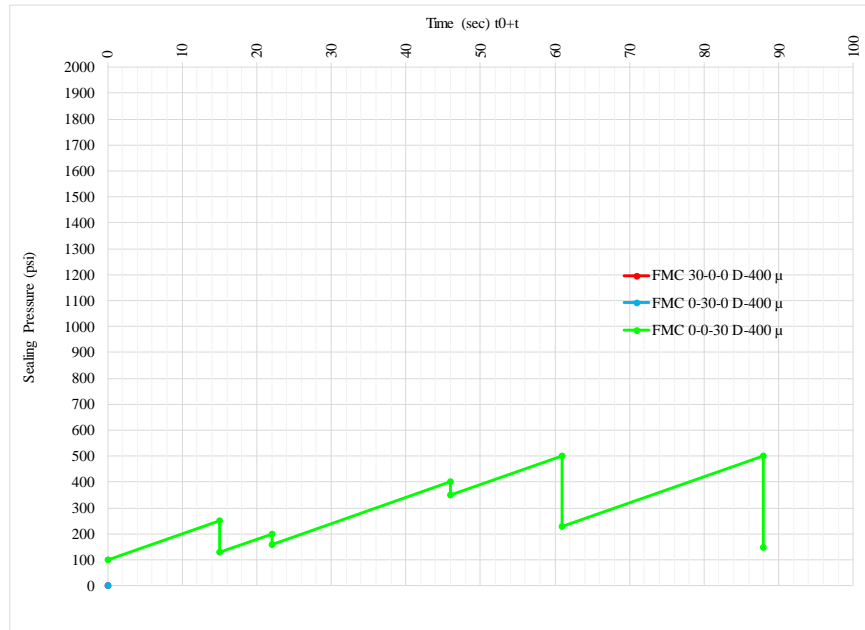


Figure F. 1: Pressure vs Time curve for each particle range individually on sealing 400-micron fracture width

Table F. 1: Mud Loss & Total Sealing Time Values for each particle range individually

Code	Mud Loss (ml)				Total Sealing Time (sec)
	Stage I	Stage II	Stage III	Total	
FMC 30-0-0 D-400 μ	*	*	*	>125	FAIL
FMC 0-30-0 D-400 μ	*	*	*	>125	FAIL
FMC 0-0-30 D-400 μ	32	*	*	>125	FAIL

F. I. 2. FMC 10-10-10

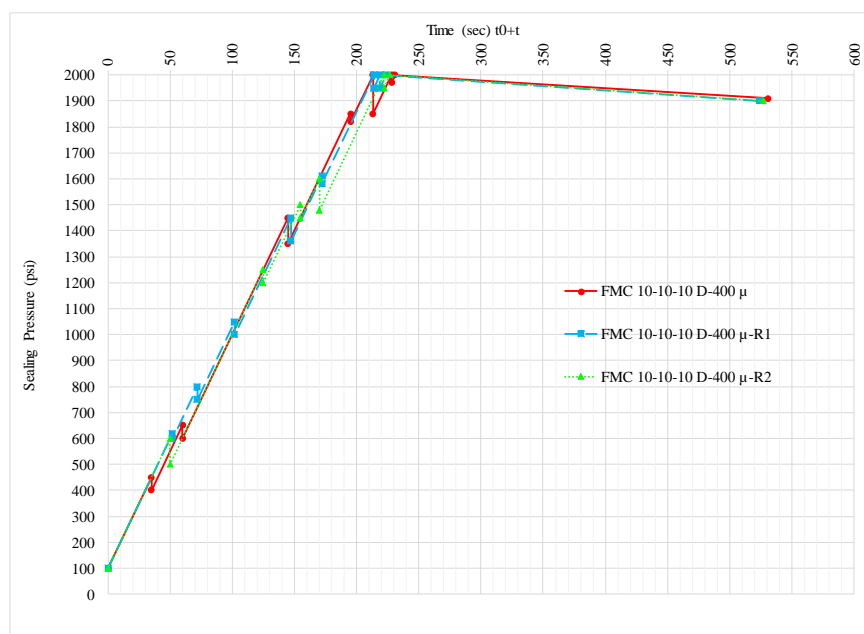


Figure F. 2: Pressure vs Time curve for FMC 10-10-10 on sealing 400-micron fracture width

Table F. 2: Mud Loss & Total Sealing Time Values for FMC 10-10-10 on 400-micron slot

Code	Mud Loss (ml)				Total Sealing Time (sec)
	Stage I	Stage II	Stage III	Total	
FMC 10-10-10 D-400μ	1.2	2.6	0.1	3.9	531.0
FMC 10-10-10 D-400μ-R1	1.6	2.2	0.2	4.0	524.0
FMC 10-10-10 D-400μ-R2	1.5	3.1	0.2	4.8	527.0
Mean	-	-	-	4.2	527.3
Std Dev	-	-	-	0.5	3.5
Deviation range, min	-	-	-	3.7	523.8
Deviation range, max	-	-	-	4.7	530.8
Recommended Range, min	-	-	-	-	474.6
Recommended Range, max	-	-	-	-	580.1

F. II. Results Obtained for Total Concentration of 28 ppb for 400- μ m Slot

F. II. 1. FMC 8-10-10

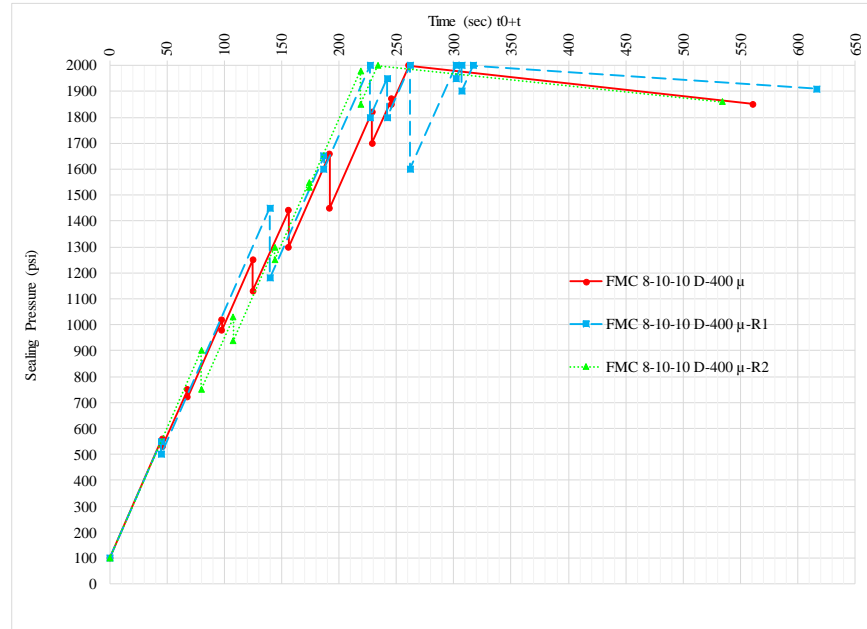


Figure F. 3: Pressure vs Time curve for FMC 8-10-10 on 400-micron fracture width

Table F. 3: Mud Loss & Total Sealing Time Values for FMC 8-10-10 on 400-micron slots

Code	Mud Loss (ml)				Total Sealing Time (sec)
	Stage I	Stage II	Stage III	Total	
FMC 8-10-10 D-400 μ	1.8	4.4	0.3	6.5	561
FMC 8-10-10 D-400 μ -R1	1.8	5	0.2	7	617
FMC 8-10-10 D-400 μ -R2	1	4	0.2	5.2	534
Mean	-	-	-	6.2	570.7
Std Dev	-	-	-	0.9	42.3
Deviation range, min	-	-	-	5.3	528.3
Deviation range, max	-	-	-	7.2	613.0
Recommended Range, min	-	-	-	-	513.6
Recommended Range, max	-	-	-	-	627.7

F. II. 2. FMC 10-8-10

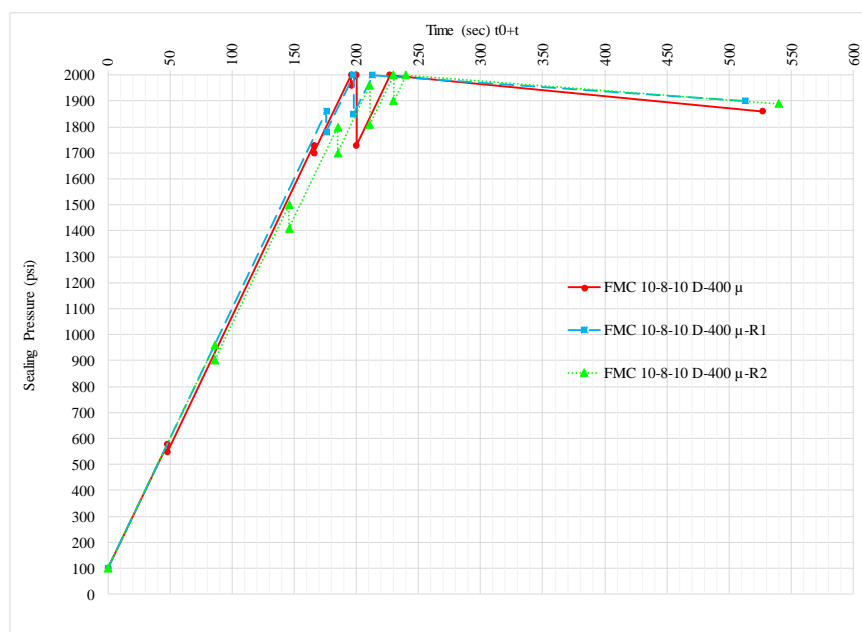


Figure F. 4: Pressure vs Time curve for FMC 10-8-10 on 400-micron fracture width

Table F. 4: Mud Loss & Total Sealing Time Values for FMC 10-8-10 on 400-micron fracture width

Code	Mud Loss (ml)				Total Sealing Time (sec)
	Stage I	Stage II	Stage III	Total	
FMC 10-8-10 D-400μ	1.4	2.2	0.1	3.7	527
FMC 10-8-10 D-400μ-R1	2.2	2.6	0.2	5	513
FMC 10-8-10 D-400μ-R2	3	3.4	0.2	6.6	540
Mean	-	-	-	5.1	526.7
Std Dev	-	-	-	1.5	13.5
Deviation range, min	-	-	-	3.6	513.2
Deviation range, max	-	-	-	6.6	540.2
Recommended Range, min	-	-	-	-	474.0
Recommended Range, max	-	-	-	-	579.3

F. II. 3. FMC 10-10-8

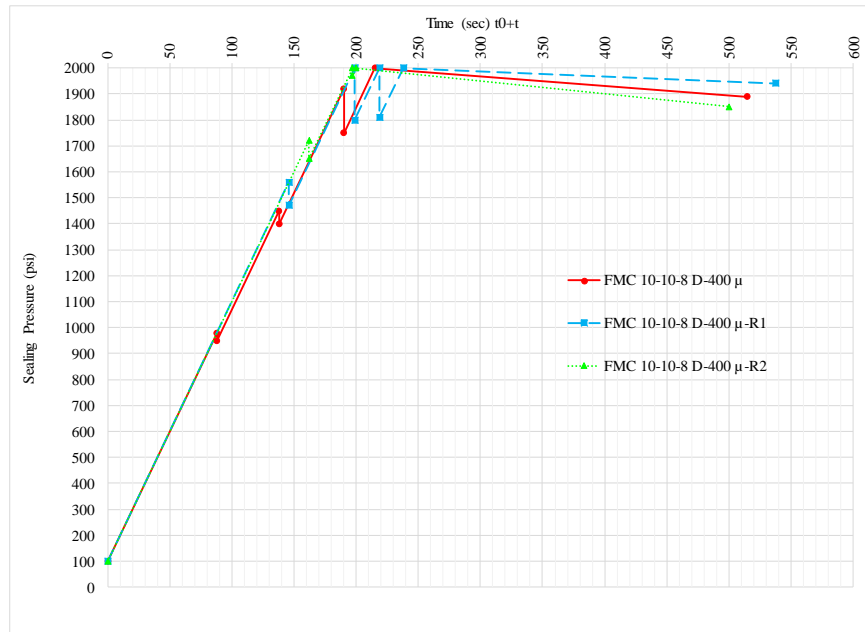


Figure F. 5: Pressure vs Time curve for FMC 10-10-8 on 400-micron fracture width

Table F. 5: Mud Loss & Total Sealing Time Values for FMC 10-10-8 on 400-micron fracture width

Code	Mud Loss (ml)				Total Sealing Time (sec)
	Stage I	Stage II	Stage III	Total	
FMC 10-10-8 D-400μ	1.2	2.8	0.1	4.1	515
FMC 10-10-8 D-400μ-R1	1.2	4.4	0.2	5.8	538
FMC 10-10-8 D-400μ-R2	1.6	2.4	0.1	4.1	500
Mean	-	-	-	4.7	517.7
Std Dev	-	-	-	1.0	19.1
Deviation range, min	-	-	-	3.7	498.5
Deviation range, max	-	-	-	5.6	536.8
Recommended Range, min	-	-	-	-	465.9
Recommended Range, max	-	-	-	-	569.4

F. III. Results Obtained for Total Concentration of 26 ppb for 400- μ m Slot

F. III. 1. FMC 6-10-10

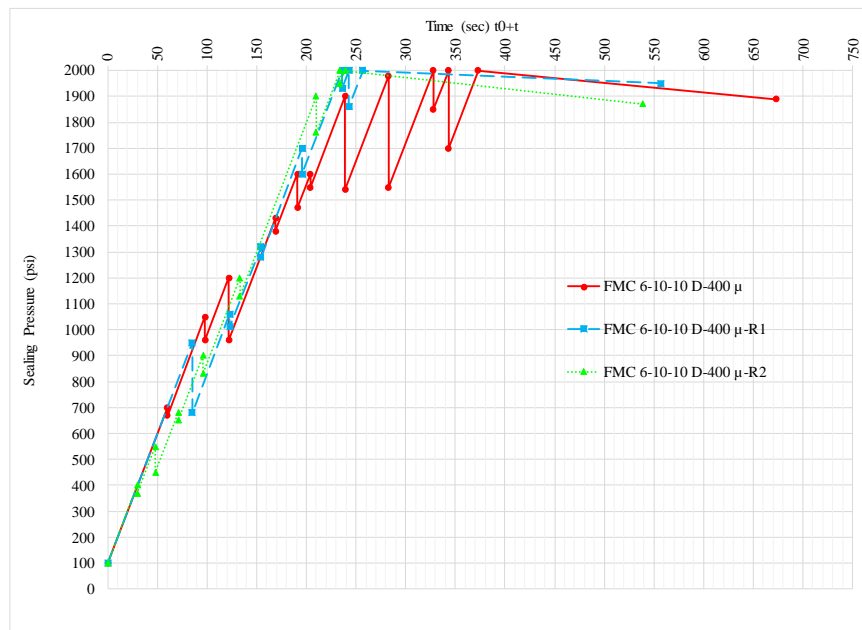


Figure F. 6: Pressure vs Time curve for FMC 6-10-10 on 400-micron fracture width

Table F. 6: Mud Loss & Total Sealing Time Values for FMC 6-10-10 on 400-micron fracture width

Code	Mud Loss (ml)				Total Sealing Time (sec)
	Stage I	Stage II	Stage III	Total	
FMC 6-10-10 D-400μ	2	7.2	0.1	9.3	673
FMC 6-10-10 D-400 μ -R1	2.2	4.3	0.1	6.6	557
FMC 6-10-10 D-400 μ -R2	2	4	0.2	6.2	539
Mean	-	-	-	7.4	589.7
Std Dev	-	-	-	1.7	72.7
Deviation range, min	-	-	-	5.7	516.9
Deviation range, max	-	-	-	9.1	662.4
Recommended Range, min	-	-	-	-	530.7
Recommended Range, max	-	-	-	-	648.6

F. III. 2. FMC 10-6-10

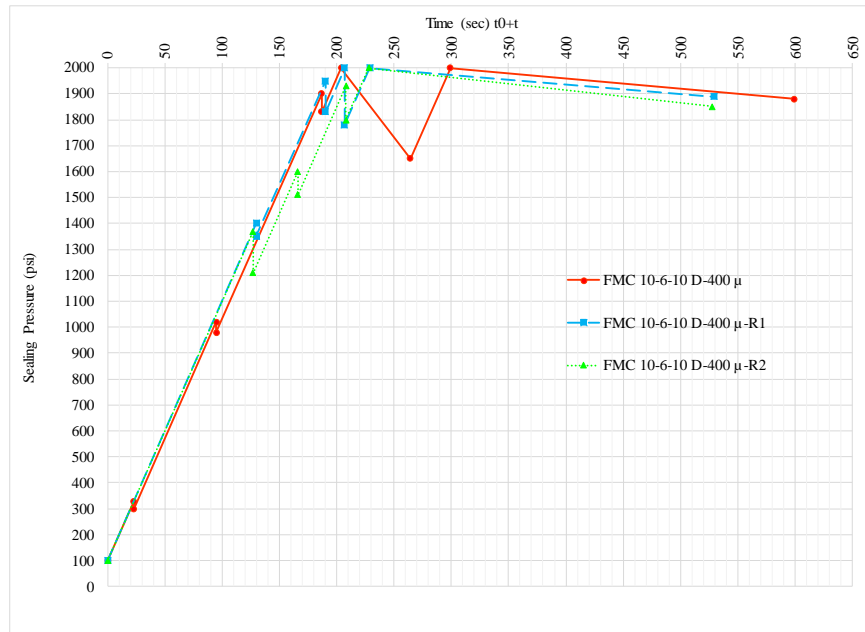


Figure F. 7: Pressure vs Time curve for FMC 10-6-10 on 400-micron fracture width

Table F. 7: Mud Loss & Total Sealing Time Values for FMC 10-6-10 on 400-micron fracture width

Code	Mud Loss (ml)				Total Sealing Time (sec)
	Stage I	Stage II	Stage III	Total	
FMC 10-6-10 D-400μ	3	2.9	0.1	6	599
FMC 10-6-10 D-400μ-R1	2.8	2.4	0.3	5.5	529
FMC 10-6-10 D-400μ-R2	3	3	0.3	6.3	528
Mean	-	-	-	5.9	552.0
Std Dev	-	-	-	0.4	40.7
Deviation range, min	-	-	-	5.5	511.3
Deviation range, max	-	-	-	6.3	592.7
Recommended Range, min	-	-	-	-	496.8
Recommended Range, max	-	-	-	-	607.2

F. III. 3. FMC 10-10-6

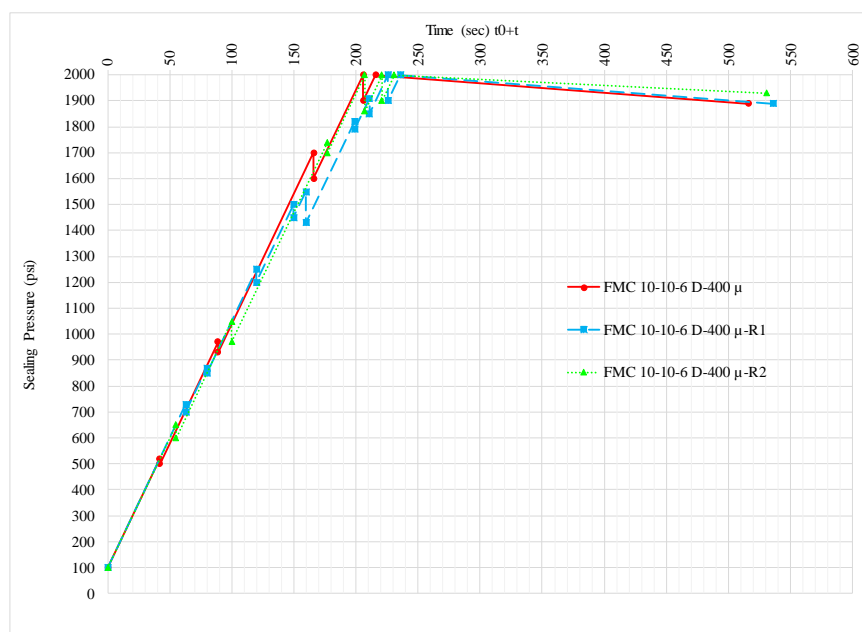


Figure F. 8: Pressure vs Time curve for FMC 10-10-6 on 400-micron fracture width

Table F. 8: Mud Loss & Total Sealing Time Values for FMC 10-10-6 on 400-micron fracture width

Code	Mud Loss (ml)				Total Sealing Time (sec)
	Stage I	Stage II	Stage III	Total	
FMC 10-10-6 D-400μ	1.4	2.6	0	4	516
FMC 10-10-6 D-400μ-R1	1	3.4	0.2	4.6	536
FMC 10-10-6 D-400μ-R2	1.6	3.2	0.2	5	531
Mean	-	-	-	4.5	527.7
Std Dev	-	-	-	0.5	10.4
Deviation range, min	-	-	-	4.0	517.3
Deviation range, max	-	-	-	5.0	538.1
Recommended Range, min	-	-	-	-	474.9
Recommended Range, max	-	-	-	-	580.4

F. IV. Results Obtained for Total Concentration of 24 ppb for 400- μ m Slot

F. IV. 1. FMC 4-10-10

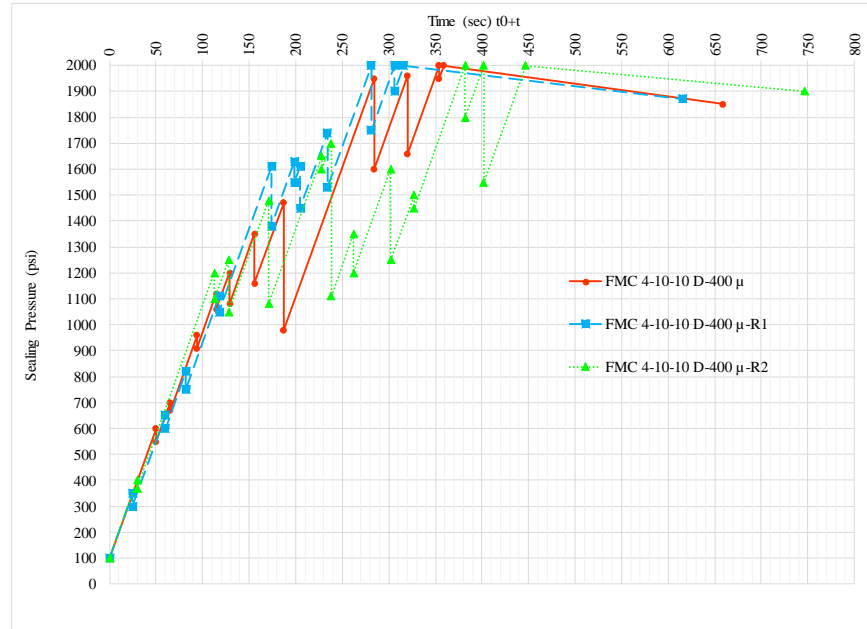


Figure F. 9: Pressure vs Time curve for FMC 4-10-10 on 400-micron fracture width

Table F. 9: Mud Loss & Total Sealing Time Values for FMC 4-10-10 on 400-micron fracture width

Code	Mud Loss (ml)				Total Sealing Time (sec)
	Stage I	Stage II	Stage III	Total	
FMC 4-10-10 D-400 μ	4.6	7.4	0.1	12.1	659
FMC 4-10-10 D-400 μ -R1	5.8	6.4	0.2	12.4	616
FMC 4-10-10 D-400μ-R2	4.8	8.2	0.2	13.2	747
Mean	-	-	-	12.6	674.0
Std Dev	-	-	-	0.6	66.8
Deviation range, min	-	-	-	12.0	607.2
Deviation range, max	-	-	-	13.1	740.8
Recommended Range, min	-	-	-	-	606.6
Recommended Range, max	-	-	-	-	741.4

F. IV. 2. FMC 10-4-10

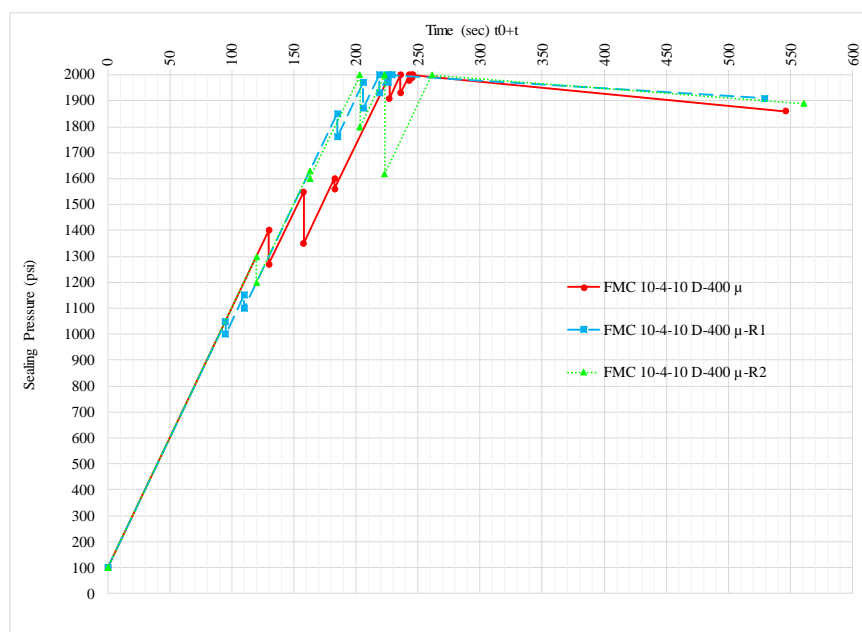


Figure F. 10: Pressure vs Time curve for FMC 10-4-10 on 400-micron fracture width

Table F. 10: Mud Loss & Total Sealing Time Values for FMC 10-4-10 on 400-micron fracture width

Code	Mud Loss (ml)				Total Sealing Time (sec)
	Stage I	Stage II	Stage III	Total	
FMC 10-4-10 D-400μ	3	3.1	0.1	6.2	546
FMC 10-4-10 D-400μ-R1	3.1	2.1	0	5.2	529
FMC 10-4-10 D-400μ-R2	3.4	3.8	0.1	7.3	561
Mean	-	-	-	6.2	545.3
Std Dev	-	-	-	1.1	16.0
Deviation range, min	-	-	-	5.2	529.3
Deviation range, max	-	-	-	7.3	561.3
Recommended Range, min	-	-	-	-	490.8
Recommended Range, max	-	-	-	-	599.9

F. IV. 3. FMC 10-10-4

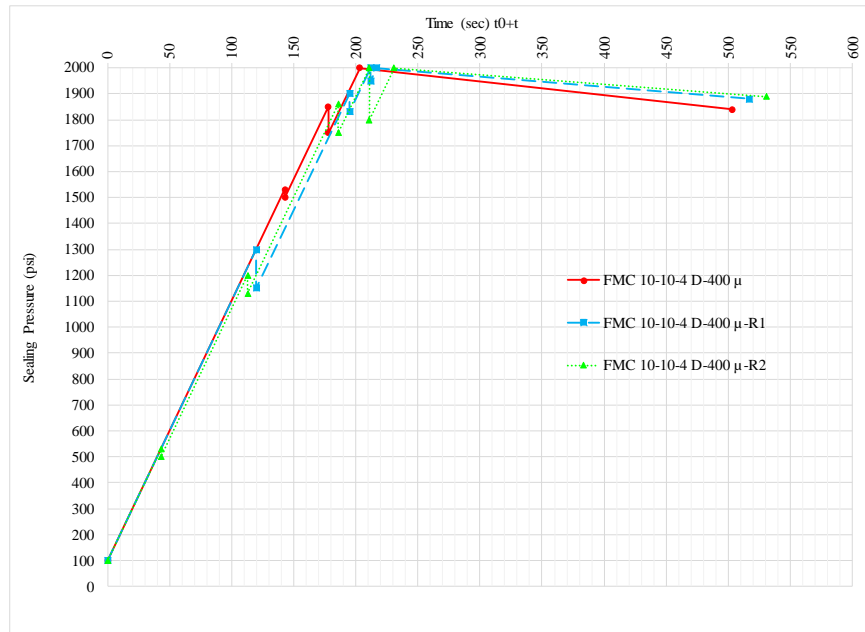


Figure F. 11: Pressure vs Time curve for FMC 10-10-4 on 400-micron fracture width

Table F. 11: Mud Loss & Total Sealing Time Values for FMC 10-10-4 on 400-micron fracture width

Code	Mud Loss (ml)				Total Sealing Time (sec)
	Stage I	Stage II	Stage III	Total	
FMC 10-10-4 D-400μ	1.8	2.4	0.3	4.5	503
FMC 10-10-4 D-400μ-R1	1.4	2.6	0	4	517
FMC 10-10-4 D-400μ-R2	1.2	3	0.3	4.5	531
Mean	-	-	-	4.3	517.0
Std Dev	-	-	-	0.3	14.0
Deviation range, min	-	-	-	4.0	503.0
Deviation range, max	-	-	-	4.6	531.0
Recommended Range, min	-	-	-	-	465.3
Recommended Range, max	-	-	-	-	568.7

F. V. Results Obtained for Total Concentration of 22 ppb for 400- μ m Slot

F. V. 1. FMC 2-10-10

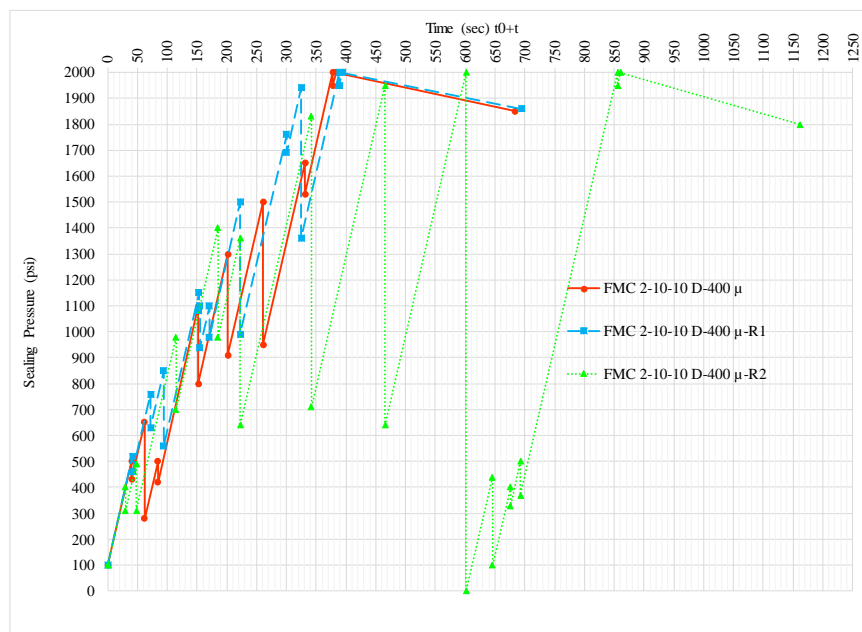


Figure F. 12: Pressure vs Time curve for FMC 2-10-10 on 400-micron fracture width

Table F. 12: Mud Loss & Total Sealing Time Values for FMC 2-10-10 on 400-micron fracture width

Code	Mud Loss (ml)				Total Sealing Time (sec)
	Stage I	Stage II	Stage III	Total	
FMC 2-10-10 D-400μ	9.6	8.4	1	19	683
FMC 2-10-10 D-400μ-R1	7	8	0.6	15.6	694
FMC 2-10-10 D-400μ-R2	8	24	1.8	33.8	1161
Mean	-	-	-	22.8	846.0
Std Dev	-	-	-	9.7	272.9
Deviation range, min	-	-	-	13.1	573.1
Deviation range, max	-	-	-	32.5	1118.9
Recommended Range, min	-	-	-	-	761.4
Recommended Range, max	-	-	-	-	930.6

F. V. 2. FMC 10-2-10

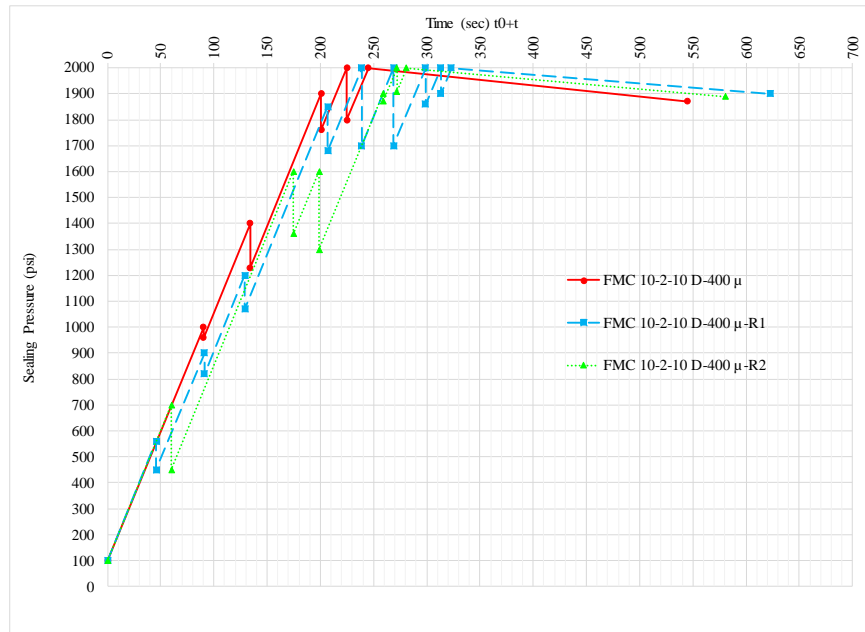


Figure F. 13: Pressure vs Time curve for FMC 10-2-10 on 400-micron fracture width

Table F. 13: Mud Loss & Total Sealing Time Values for FMC 10-2-10 on 400-micron fracture width

Code	Mud Loss (ml)				Total Sealing Time (sec)
	Stage I	Stage II	Stage III	Total	
FMC 10-2-10 D-400μ	4.8	2.6	0.3	7.7	545
FMC 10-2-10 D-400μ-R1	4	5.2	0.2	9.4	623
FMC 10-2-10 D-400μ-R2	5	4.2	0	9.2	581
Mean	-	-	-	8.8	583.0
Std Dev	-	-	-	0.9	39.0
Deviation range, min	-	-	-	7.8	544.0
Deviation range, max	-	-	-	9.7	622.0
Recommended Range, min	-	-	-	-	524.7
Recommended Range, max	-	-	-	-	641.3

F. V. 3. FMC 10-10-2

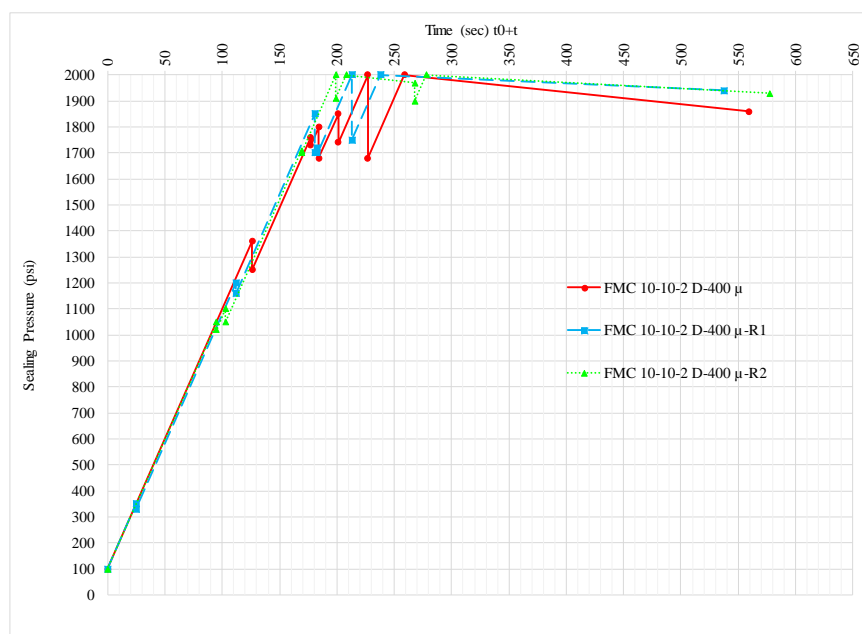


Figure F. 14: Pressure vs Time curve for FMC 10-10-2 on 400-micron fracture width

Table F. 14: Mud Loss & Total Sealing Time Values for FMC 10-10-2 on 400-micron fracture width

Code	Mud Loss (ml)				Total Sealing Time (sec)
	Stage I	Stage II	Stage III	Total	
FMC 10-10-2 D-400μ	1.4	3.6	0.1	5.1	559
FMC 10-10-2 D-400μ-R1	2	2.4	0.1	4.5	538
FMC 10-10-2 D-400μ-R2	1.8	2.2	0.1	4.1	578
Mean	-	-	-	4.6	558.3
Std Dev	-	-	-	0.5	20.0
Deviation range, min	-	-	-	4.1	538.3
Deviation range, max	-	-	-	5.1	578.3
Recommended Range, min	-	-	-	-	502.5
Recommended Range, max	-	-	-	-	614.2

F. VI. Results Obtained for Total Concentration of 20 ppb for 400- μ m Slot

F. VI. 1. FMC 0-10-10



Figure F. 15: Pressure vs Time curve for FMC 0-10-10 on 400-micron fracture width

Table F. 15: Mud Loss & Total Sealing Time Values for FMC 0-10-10 on 400-micron fracture width

Code	Mud Loss (ml)				Total Sealing Time (sec)
	Stage I	Stage II	Stage III	Total	
FMC 0-10-10 D-400 μ	57	*	*	>125	FAIL
FMC 0-10-10 D-400 μ -R1	73	*	*	>125	FAIL
FMC 0-10-10 D-400 μ -R2	64	*	*	>125	FAIL

F. VI. 2. FMC 10-0-10

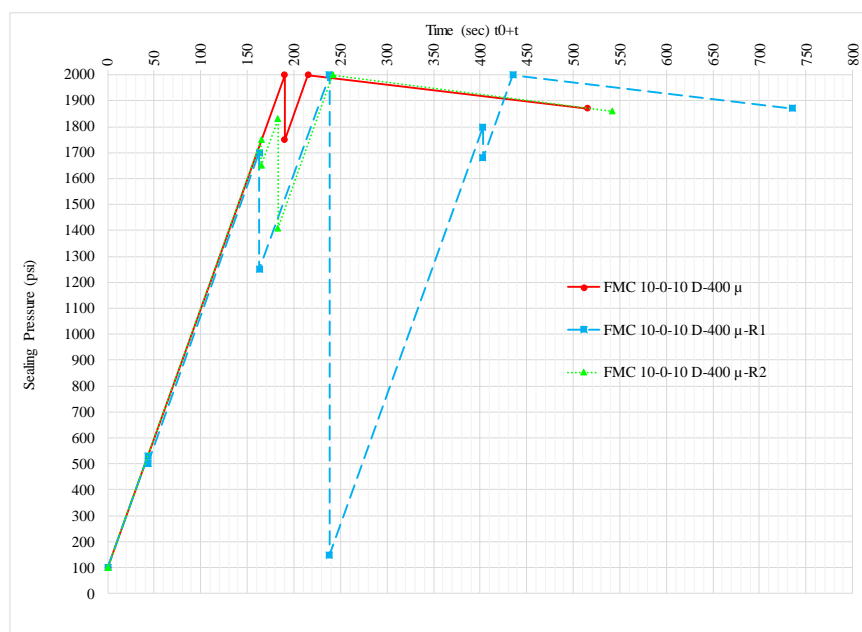


Figure F. 16: Pressure vs Time curve for FMC 10-0-10 on 400-micron fracture width

Table F. 16: Mud Loss & Total Sealing Time Values for FMC 10-0-10 on 400-micron fracture width

Code	Mud Loss (ml)				Total Sealing Time (sec)
	Stage I	Stage II	Stage III	Total	
FMC 10-0-10 D-400μ	8	2.1	0.2	10.3	515
FMC 10-0-10 D-400μ-R1	8.4	5.6	0.6	14.6	735
FMC 10-0-10 D-400μ-R2	8.4	3.6	0	12	542
Mean	-	-	-	12.3	597.3
Std Dev	-	-	-	2.2	120.0
Deviation range, min	-	-	-	10.1	477.3
Deviation range, max	-	-	-	14.5	717.3
Recommended Range, min	-	-	-	-	537.6
Recommended Range, max	-	-	-	-	657.1

F. VI. 3. FMC 10-10-0

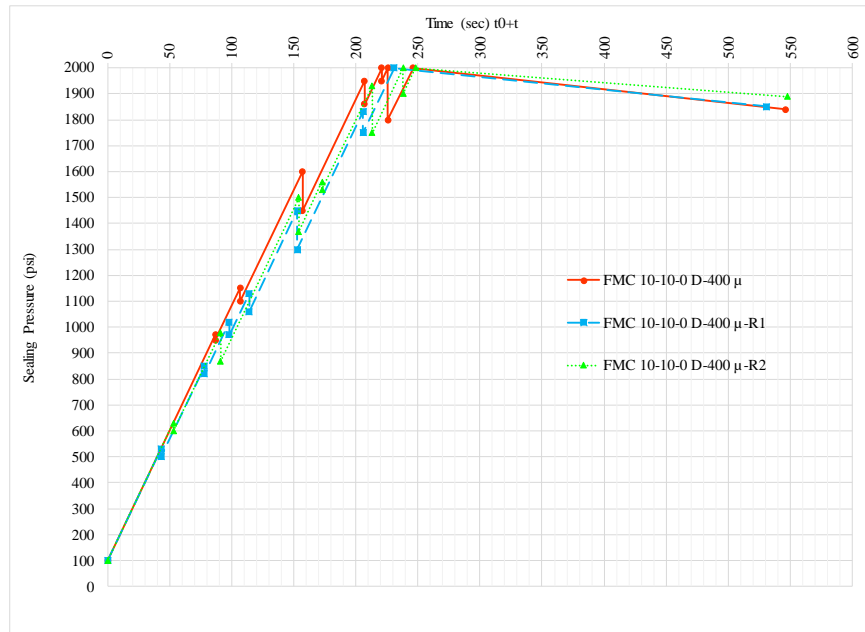


Figure F. 17: Pressure vs Time curve for FMC 10-10-0 on 400-micron fracture width

Table F. 17: Mud Loss & Total Sealing Time Values for FMC 10-10-0 on 400-micron fracture width

Code	Mud Loss (ml)				Total Sealing Time (sec)
	Stage I	Stage II	Stage III	Total	
FMC 10-10-0 D-400μ	1	3.4	0.3	4.7	546
FMC 10-10-0 D-400μ-R1	2	2.8	0.2	5	531
FMC 10-10-0 D-400μ-R2	0.8	3.2	0.1	4.1	548
Mean	-	-	-	4.6	541.7
Std Dev	-	-	-	0.5	9.3
Deviation range, min	-	-	-	4.1	532.4
Deviation range, max	-	-	-	5.1	551.0
Recommended Range, min	-	-	-	-	487.5
Recommended Range, max	-	-	-	-	595.8

F. VII. Results Obtained for Total Concentration of 16 ppb for 400- μ m Slot

F. VII. 1. FMC 8-6-2

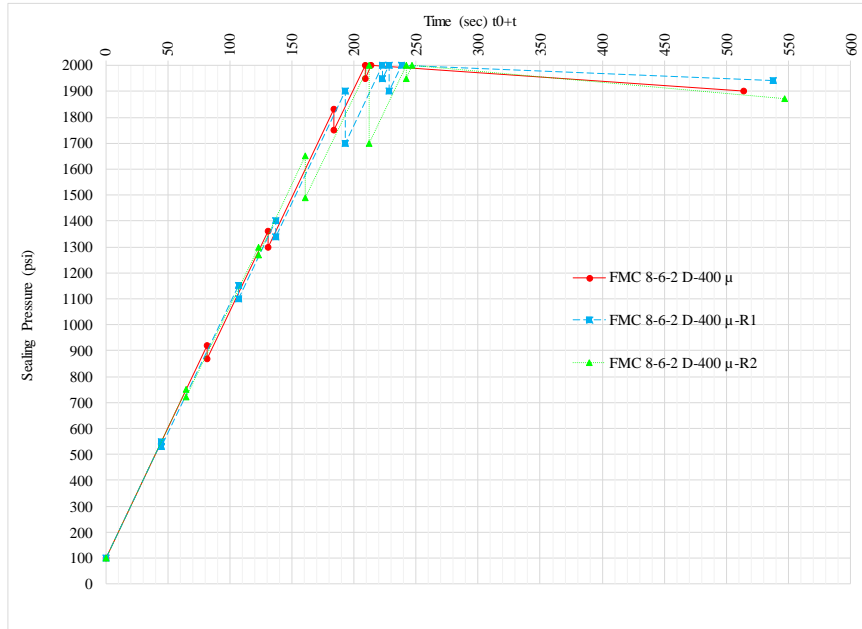


Figure F. 18: Pressure vs Time curve for FMC 8-6-2 on 400-micron fracture width

Table F. 18: Mud Loss & Total Sealing Time Values for FMC 8-6-2 on 400-micron fracture width

Code	Mud Loss (ml)				Total Sealing Time (sec)
	Stage I	Stage II	Stage III	Total	
FMC 8-6-2 D-400 μ	3.1	2	0.1	5.2	514
FMC 8-6-2 D-400 μ -R1	3.4	3	0.3	6.7	538
FMC 8-6-2 D-400 μ -R2	3	3.1	0.1	6.2	547
Mean	-	-	-	6.0	533.0
Std Dev	-	-	-	0.8	17.1
Deviation range, min	-	-	-	5.3	515.9
Deviation range, max	-	-	-	6.8	550.1
Recommended Range, min	-	-	-	-	479.7
Recommended Range, max	-	-	-	-	586.3

F. VIII. Results Obtained for Total Concentration of 14 ppb for 400- μ m Slot

F. VIII. 1. FMC 6-6-2

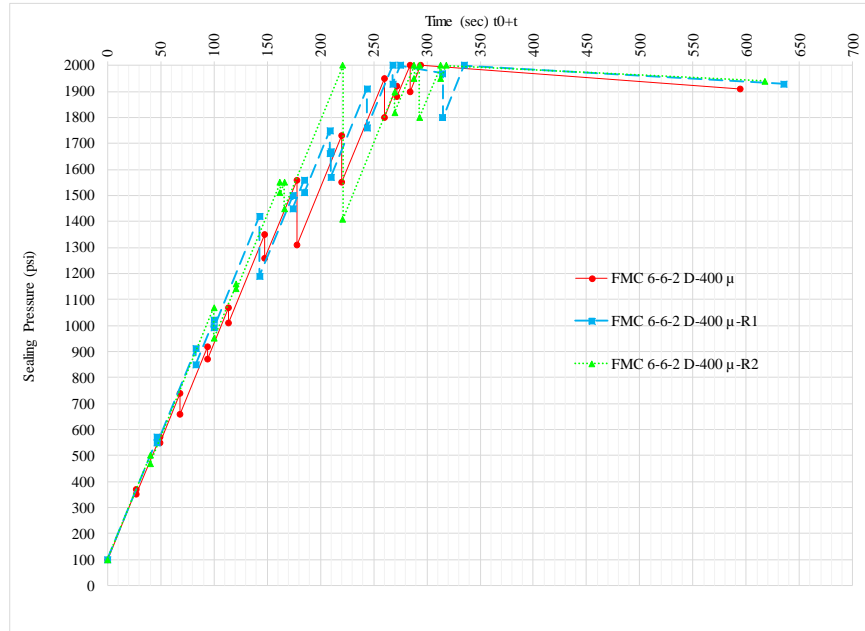


Figure F. 19: Pressure vs Time curve for FMC 6-6-2 on 400-micron fracture width

Table F. 19: Mud Loss & Total Sealing Time Values for FMC 6-6-2 on 400-micron fracture width

Code	Mud Loss (ml)				Total Sealing Time (sec)
	Stage I	Stage II	Stage III	Total	
FMC 6-6-2 D-400 μ	4.1	4.9	0.2	9.2	594
FMC 6-6-2 D-400 μ -R1	4.8	4.4	0.2	9.4	635
FMC 6-6-2 D-400 μ -R2	4.8	5.6	0.2	10.6	618
Mean	-	-	-	9.7	615.7
Std Dev	-	-	-	0.8	20.6
Deviation range, min	-	-	-	9.0	595.1
Deviation range, max	-	-	-	10.5	636.3
Recommended Range, min	-	-	-	-	554.1
Recommended Range, max	-	-	-	-	677.2

F. IX. Results Obtained for Total Concentration of 12 ppb for 400- μ m Slot

F. IX. 1. FMC 4-6-2

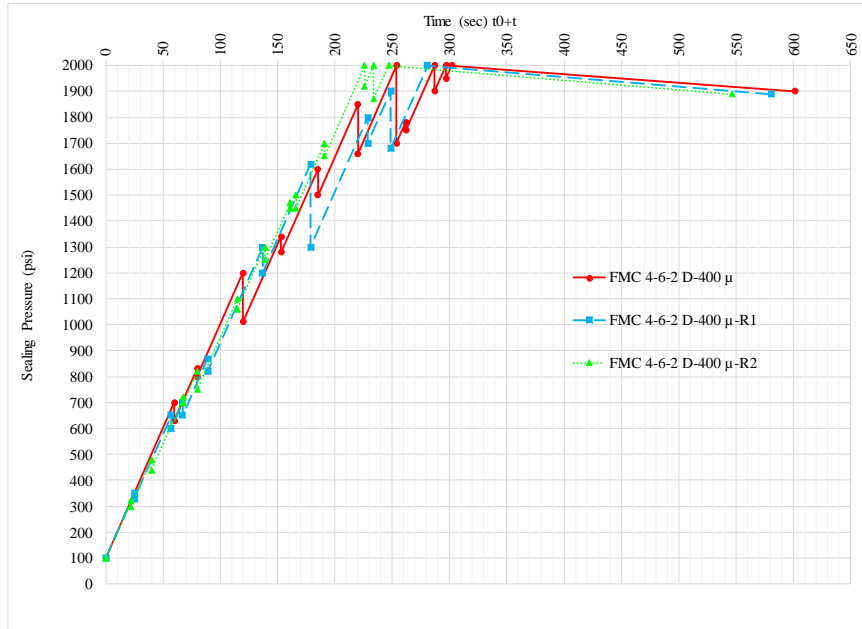


Figure F. 20: Pressure vs Time curve for FMC 4-6-2 on 400-micron fracture width

Table F. 20: Mud Loss & Total Sealing Time Values for FMC 4-6-2 on 400-micron fracture width

Code	Mud Loss (ml)				Total Sealing Time (sec)
	Stage I	Stage II	Stage III	Total	
FMC 4-6-2 D-400 μ	5	5	0.1	10.1	602
FMC 4-6-2 D-400 μ -R1	5.6	4.5	0.2	10.3	581
FMC 4-6-2 D-400 μ -R2	5.2	3.8	0.2	9.2	547
Mean	-	-	-	9.9	576.7
Std Dev	-	-	-	0.6	27.8
Deviation range, min	-	-	-	9.3	548.9
Deviation range, max	-	-	-	10.5	604.4
Recommended Range, min	-	-	-	-	519.0
Recommended Range, max	-	-	-	-	634.3

F. X. Results Obtained for Total Concentration of 10 ppb for 400- μ m Slot

F. X. 1. FMC 2-6-2

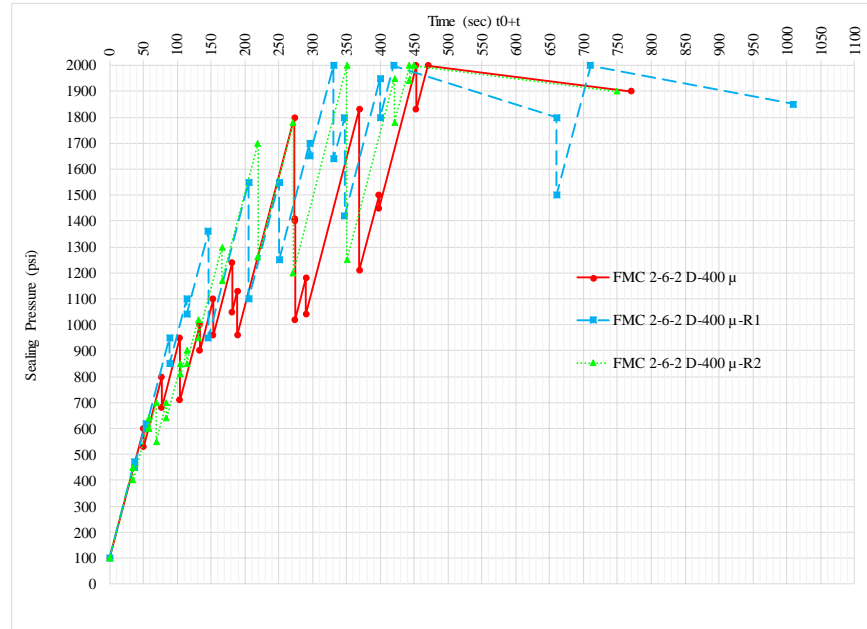


Figure F. 21: Pressure vs Time curve for FMC 2-6-2 on 400-micron fracture width

Table F. 21: Mud Loss & Total Sealing Time Values for FMC 2-6-2 on 400-micron fracture width

Code	Mud Loss (ml)				Total Sealing Time (sec)
	Stage I	Stage II	Stage III	Total	
FMC 2-6-2 D-400 μ	14	12.4	0.6	27	770
FMC 2-6-2 D-400μ-R1	8	7.8	0.6	16.4	1010
FMC 2-6-2 D-400μ-R2	7.8	6.4	0.4	14.6	749
Mean	-	-	-	19.3	843.0
Std Dev	-	-	-	6.7	145.0
Deviation range, min	-	-	-	12.6	698.0
Deviation range, max	-	-	-	26.0	988.0
Recommended Range, min	-	-	-	-	758.7
Recommended Range, max	-	-	-	-	927.3

F. X. 2. FMC 4-6-0

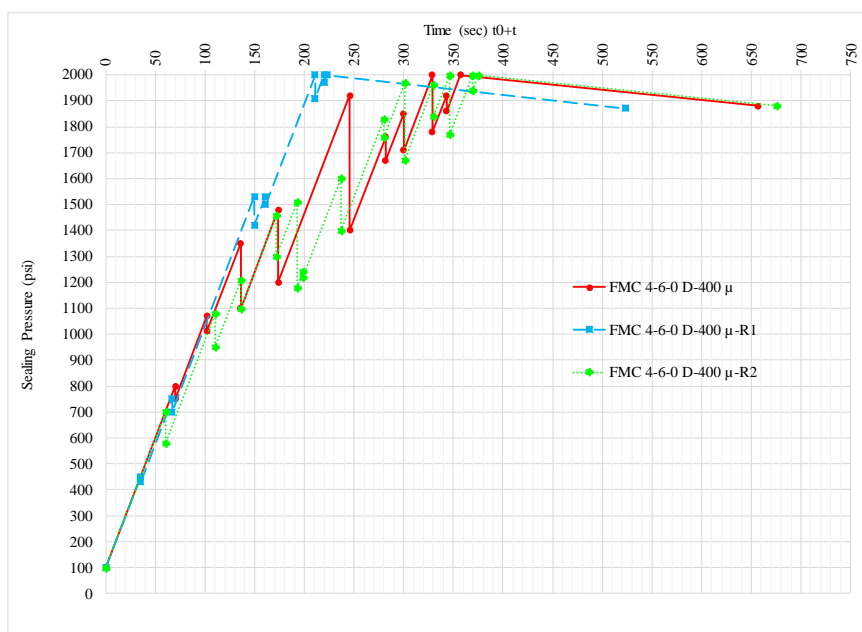


Figure F. 22: Pressure vs Time curve for FMC 4-6-0 on 400-micron fracture width

Table F. 22: Mud Loss & Total Sealing Time Values for FMC 4-6-0 on 400-micron fracture width

Code	Mud Loss (ml)				Total Sealing Time (sec)
	Stage I	Stage II	Stage III	Total	
FMC 4-6-0 D-400μ	6.2	6.6	0.1	12.9	657
FMC 4-6-0 D-400μ-R1	6	3	0.2	9.2	523
FMC 4-6-0 D-400μ-R2	5	7.2	0.2	12.4	675
Mean	-	-	-	11.5	618.3
Std Dev	-	-	-	2.0	83.1
Deviation range, min	-	-	-	9.5	535.3
Deviation range, max	-	-	-	13.5	701.4
Recommended Range, min	-	-	-	-	556.5
Recommended Range, max	-	-	-	-	680.2

F. X. 3. FMC 4-4-2

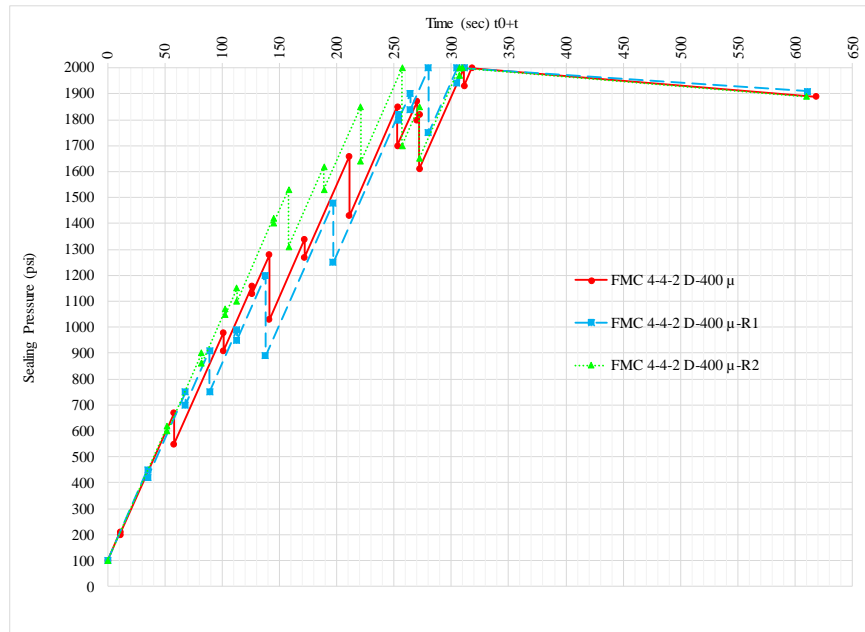


Figure F. 23: Pressure vs Time curve for FMC 4-4-2 on 400-micron fracture width

Table F. 23: Mud Loss & Total Sealing Time Values for FMC 4-4-2 on 400-micron fracture width

Code	Mud Loss (ml)				Total Sealing Time (sec)
	Stage I	Stage II	Stage III	Total	
FMC 4-4-2 D-400μ	6	6	0.1	12.1	618
FMC 4-4-2 D-400μ-R1	6.5	5.3	0.1	11.9	611
FMC 4-4-2 D-400μ-R2	5.5	4.9	0.2	10.6	610
Mean	-	-	-	11.5	613.0
Std Dev	-	-	-	0.8	4.4
Deviation range, min	-	-	-	10.7	608.6
Deviation range, max	-	-	-	12.3	617.4
Recommended Range, min	-	-	-	-	551.7
Recommended Range, max	-	-	-	-	674.3
Recommended Range, max	-	-	-	-	680.2

F. XI. Results Obtained for Total Concentration of 8 ppb for 400- μ m Slot Size

F. XI. 1. FMC 4-2-2

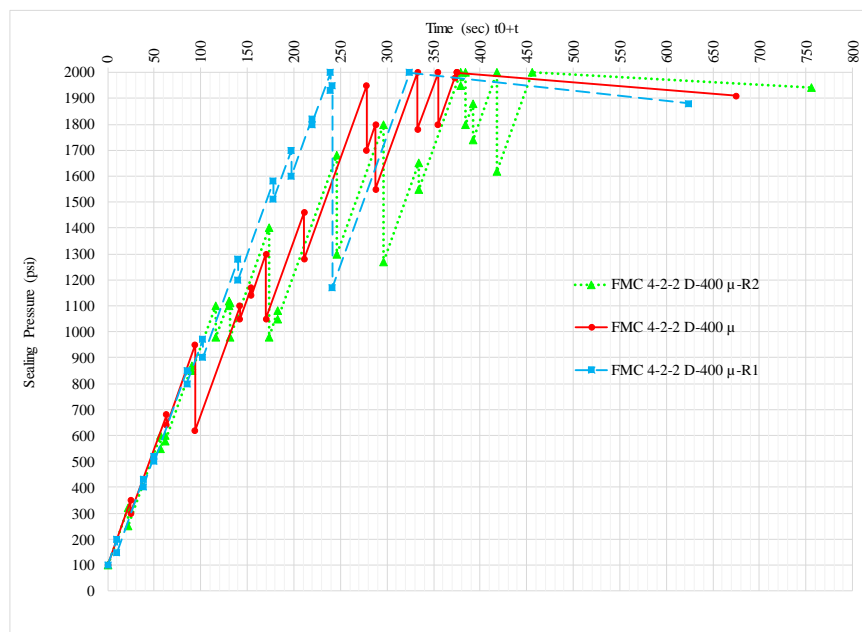


Figure F. 24: Pressure vs Time curve for FMC 4-2-2 on 400-micron fracture width

Table F. 24: Mud Loss & Total Sealing Time Values for FMC 4-2-2 on 400-micron fracture width

Code	Mud Loss (ml)				Total Sealing Time (sec)
	Stage I	Stage II	Stage III	Total	
FMC 4-2-2 D-400 μ	2	15	0.4	17.4	675
FMC 4-2-2 D-400 μ -R1	9.8	3.7	0.1	13.6	624
FMC 4-2-2 D-400μ-R2	9	6.4	0.2	15.6	756
Mean	-	-	-	15.5	685.0
Std Dev	-	-	-	1.9	66.6
Deviation range, min	-	-	-	13.6	618.4
Deviation range, max	-	-	-	17.4	751.6
Recommended Range, min	-	-	-	-	616.5
Recommended Range, max	-	-	-	-	753.5

F. XII. Results Obtained for Total Concentration of 6 ppb for 400- μ m Slot Size

F. XII. 1. FMC 4-0-2

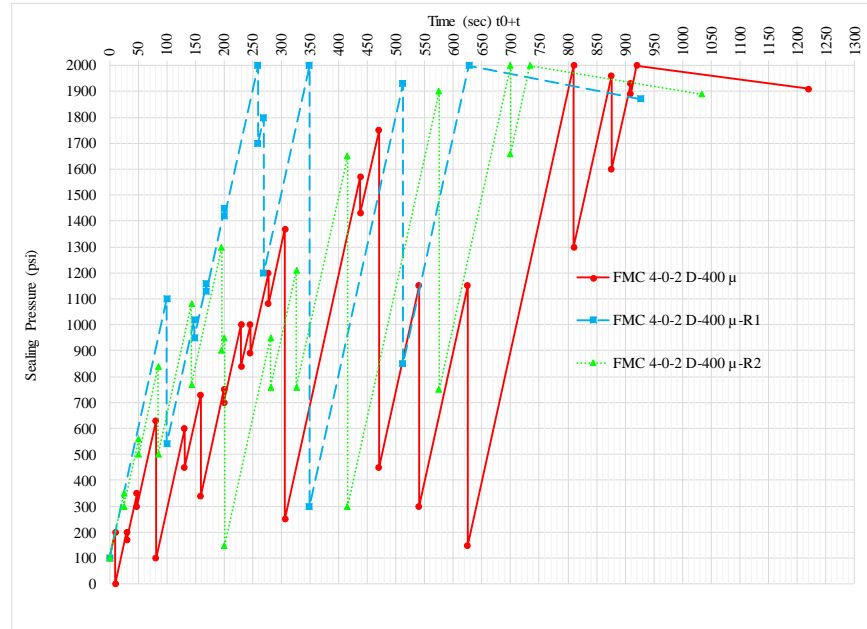


Figure F. 25: Pressure vs Time curve for FMC 4-0-2 on 400-micron fracture width

Table F. 25: Mud Loss & Total Sealing Time Values for FMC 4-0-2 on 400-micron fracture width

Code	Mud Loss (ml)				Total Sealing Time (sec)
	Stage I	Stage II	Stage III	Total	
FMC 4-0-2 D-400μ	27	27.4	0.6	55	1220
FMC 4-0-2 D-400μ-R1	24	13	0.1	37.1	927
FMC 4-0-2 D-400 μ -R2	25	16	0.2	41.2	1034
Mean	-	-	-	44.4	1060.3
Std Dev	-	-	-	9.4	148.3
Deviation range, min	-	-	-	35.1	912.1
Deviation range, max	-	-	-	53.8	1208.6
Recommended Range, min	-	-	-	-	954.3
Recommended Range, max	-	-	-	-	1166.4

F. XII. 2. FMC 4-2-0

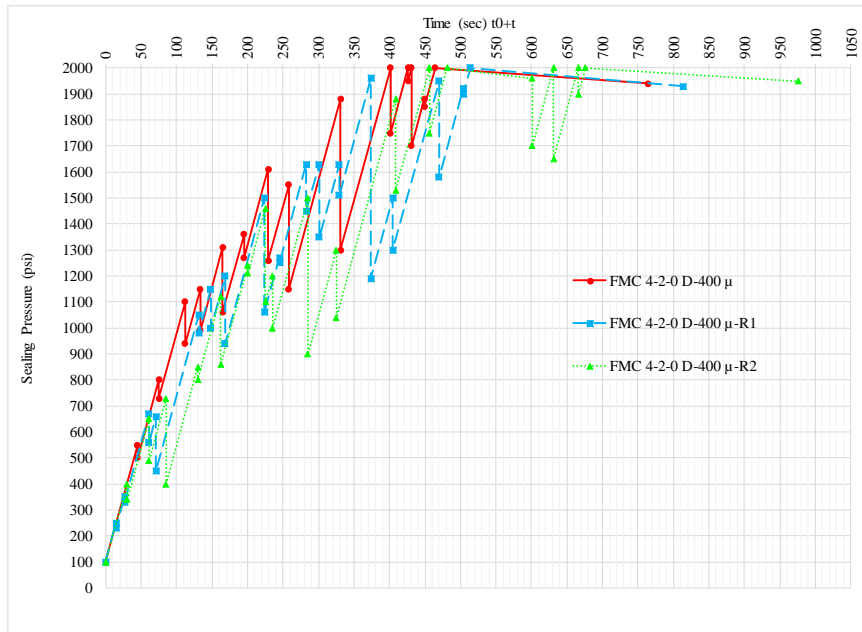


Figure F. 26: Pressure vs Time curve for FMC 4-2-0 on 400-micron fracture width

Table F. 26: Mud Loss & Total Sealing Time Values for FMC 4-2-0 on 400-micron fracture width

Code	Mud Loss (ml)				Total Sealing Time (sec)
	Stage I	Stage II	Stage III	Total	
FMC 4-2-0 D-400μ	11	6	0.8	17.8	764
FMC 4-2-0 D-400μ-R1	13	8.8	0.2	22	814
FMC 4-2-0 D-400μ-R2	10.4	8.8	0.2	19.4	976
Mean	-	-	-	19.7	851.3
Std Dev	-	-	-	2.1	110.8
Deviation range, min	-	-	-	17.6	740.5
Deviation range, max	-	-	-	21.9	962.2
Recommended Range, min	-	-	-	-	766.2
Recommended Range, max	-	-	-	-	936.5

F. XIII. Results Obtained for Total Concentration of 4 ppb for 400- μ m Slot

F. XIII. 1. FMC 2-2-0

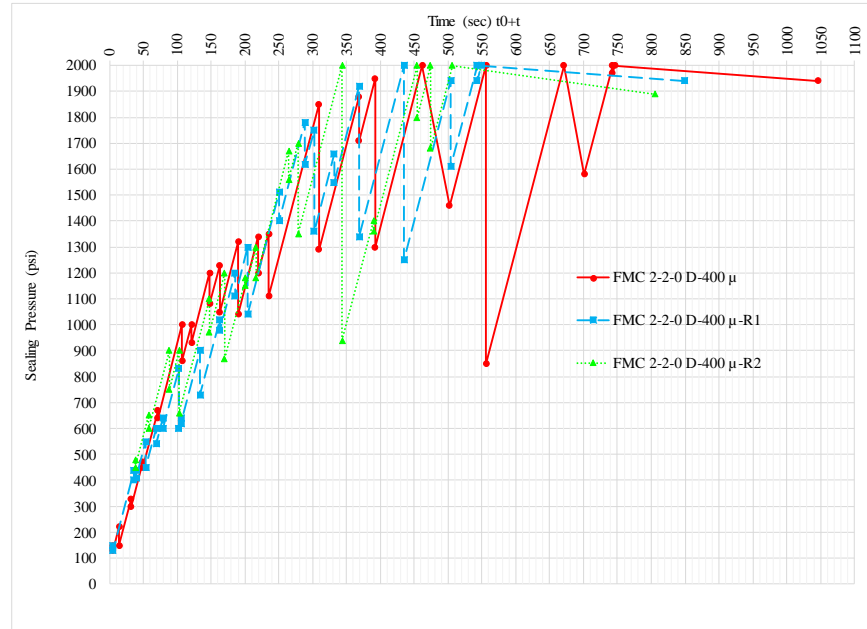


Figure F. 27: Pressure vs Time curve for FMC 2-2-0 on 400-micron fracture width

Table F. 27: Mud Loss & Total Sealing Time Values for FMC 2-2-0 on 400-micron fracture width

Code	Mud Loss (ml)				Total Sealing Time (sec)
	Stage I	Stage II	Stage III	Total	
FMC 2-2-0 D-400μ	14	12.4	0.4	26.8	1046
FMC 2-2-0 D-400 μ -R1	13	9.8	0.4	23.2	849
FMC 2-2-0 D-400μ-R2	11.8	7.2	0.4	19.4	806
Mean	-	-	-	23.1	900.3
Std Dev	-	-	-	3.7	128.0
Deviation range, min	-	-	-	19.4	772.4
Deviation range, max	-	-	-	26.8	1028.3
Recommended Range, min	-	-	-	-	810.3
Recommended Range, max	-	-	-	-	990.4

G. Effect of Concentration of Ground Marble on Sealing 400- μ Fracture Width

G. I. 1. FMC 4-3-1

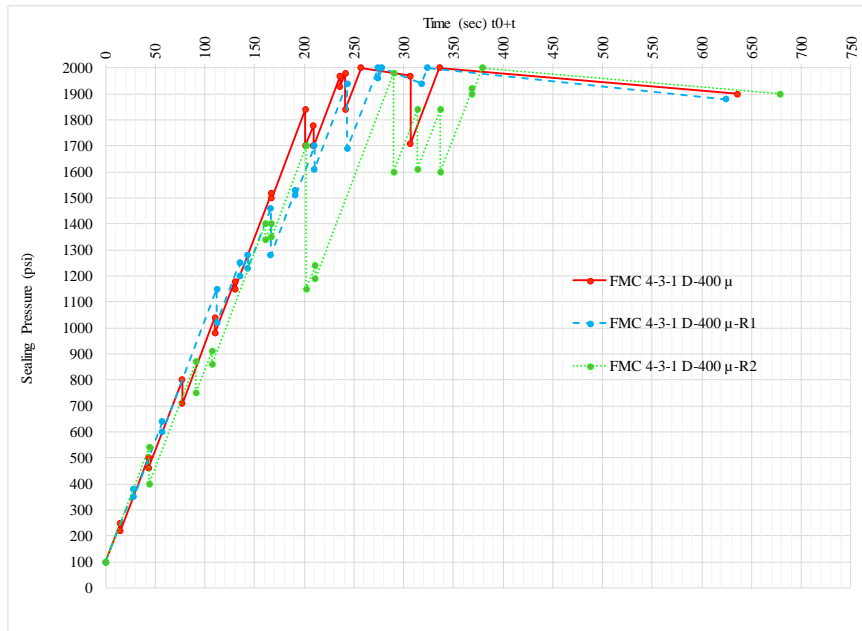


Figure G. 1: Pressure vs Time curve for FMC 4-3-1 on 400-micron fracture width

Table G. 1: Mud Loss & Total Sealing Time Values for FMC 4-3-1 on 400-micron fracture width

Code	Mud Loss (ml)				Total Sealing Time (sec)
	Stage I	Stage II	Stage III	Total	
FMC 4-3-1 D-400 μ	7.1	4.5	0.3	11.9	636
FMC 4-3-1 D-400 μ -R1	8.1	3.9	0.1	12.1	624
FMC 4-3-1 D-400 μ -R2	14.2	7.8	0.9	22.9	679
Mean	-	-	-	15.6	646.3
Std Dev	-	-	-	6.3	28.9
Deviation range, min	-	-	-	9.3	617.4
Deviation range, max	-	-	-	21.9	675.3
Recommended Range, min	-	-	-	-	581.7
Recommended Range, max	-	-	-	-	711.0

G. I. 2. FMC 12-9-3

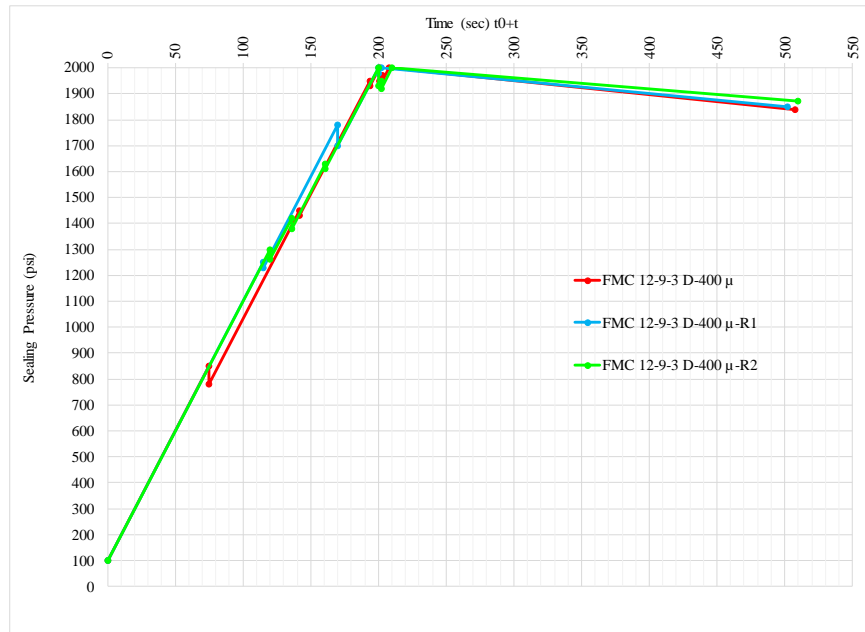


Figure G. 2: Pressure vs Time curve for FMC 12-9-3 on 400-micron fracture width

Table G. 2: Mud Loss & Total Sealing Time Values for FMC 12-9-3 on 400-micron fracture width

Code	Mud Loss (ml)				Total Sealing Time (sec)
	Stage I	Stage II	Stage III	Total	
FMC 12-9-3 D-400μ	1.5	2.3	0.1	3.9	508
FMC 12-9-3 D-400μ-R1	2.4	2	0.2	4.6	502
FMC 12-9-3 D-400μ-R2	2	2.4	0.2	4.6	510
Mean	-	-	-	4.4	506.7
Std Dev	-	-	-	0.4	4.2
Deviation range, min	-	-	-	4.0	502.5
Deviation range, max	-	-	-	4.8	510.8
Recommended Range, min	-	-	-	-	456.0
Recommended Range, max	-	-	-	-	557.3

G. I. 3. FMC 16-12-4

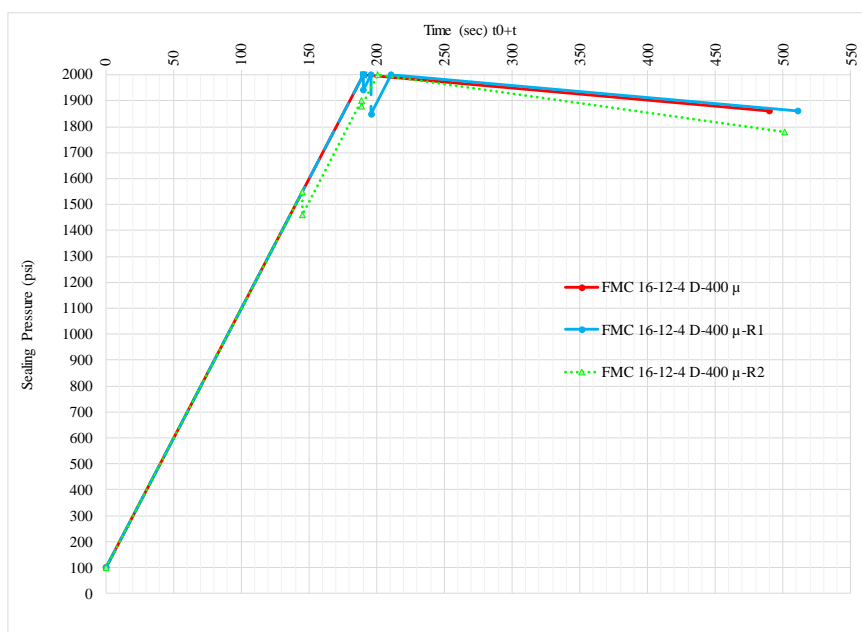


Figure G. 3: Pressure vs Time curve for FMC 12-9-3 on 400-micron fracture width

Table G. 3: Mud Loss & Total Sealing Time Values for FMC 16-12-4 on 400-micron fracture width

Code	Mud Loss (ml)				Total Sealing Time (sec)
	Stage I	Stage II	Stage III	Total	
FMC 16-12-4 D-400μ	0.6	1.8	0.3	2.7	490
FMC 16-12-4 D-400μ-R1	0.6	1.8	0.4	2.8	511
FMC 16-12-4 D-400μ-R2	1.1	2.4	0.1	3.6	501
Mean	-	-	-	3.0	500.7
Std Dev	-	-	-	0.5	10.5
Deviation range, min	-	-	-	2.5	490.2
Deviation range, max	-	-	-	3.5	511.2
Recommended Range, min	-	-	-	-	450.6
Recommended Range, max	-	-	-	-	550.7

H. Effect of Particle Size Distribution of Ground Marble on Sealing 800- μ fracture width

H. I. Results Obtained for Total Concentration of 30 ppb for 800- μ Slot

H. I. 1. FMC 30-0-0, FMC 0-30-0 & FMC 0-0-30

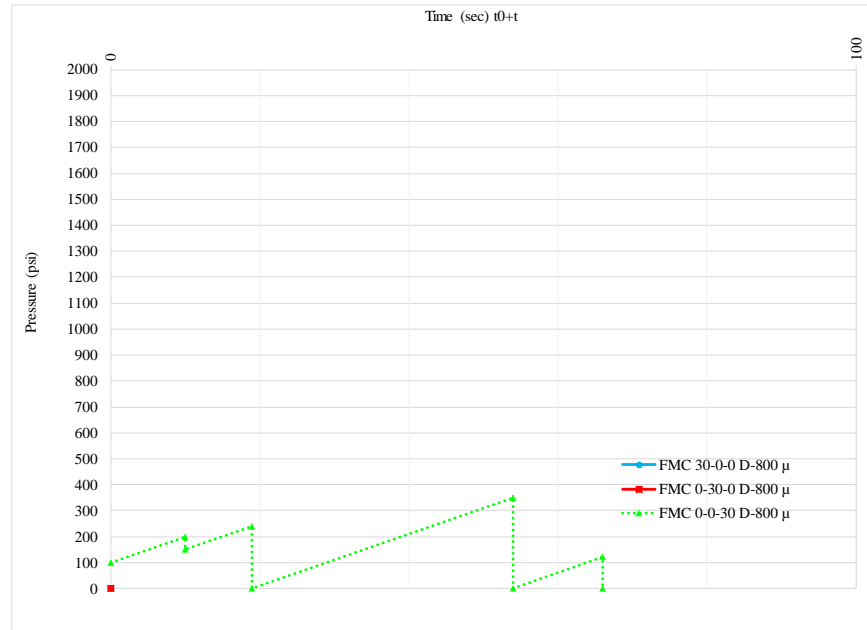


Figure H. 1: Pressure vs Time curve for each particle range individually on sealing 800-micron fracture width

Table H. 1: Mud Loss & Total Sealing Time Values for each particle range individually

Code	Mud Loss (ml)				Total Sealing Time (sec)
	Stage I	Stage II	Stage III	Total	
FMC 30-0-0 D-800 μ	*	*	*	>125	FAIL
FMC 0-30-0 D-800 μ	*	*	*	>125	FAIL
FMC 0-0-30 D-800 μ	50	*	*	>125	FAIL

H. I. 2. FMC 10-10-10

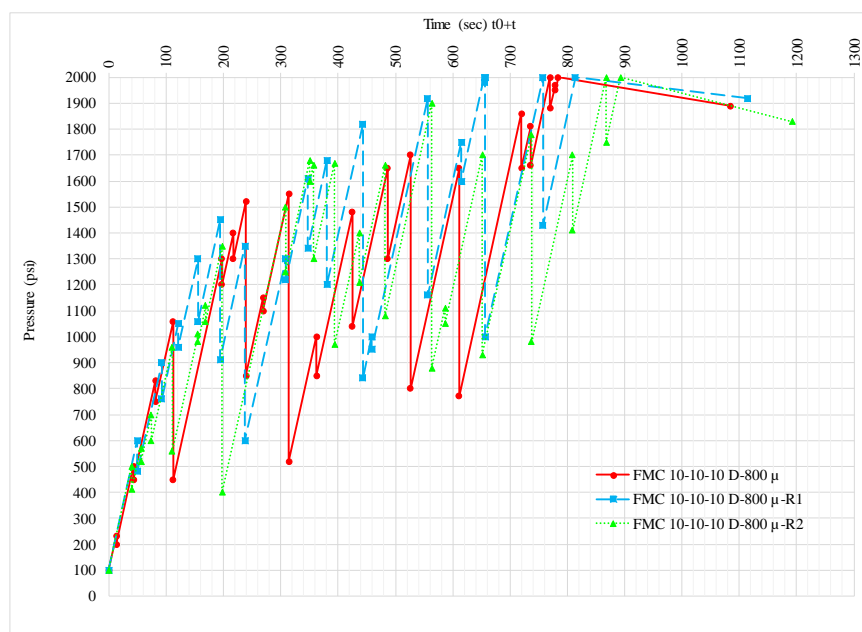


Figure H. 2: Pressure vs Time curve for FMC 10-10-10 on 800-micron fracture width

Table H. 2: Mud Loss&Total Sealing Time Values for FMC 10-10-10 on 800-micron fracture width

Code	Mud Loss (ml)				Total Sealing Time (sec)
	Stage I	Stage II	Stage III	Total	
FMC 10-10-10 D-800 μ	7.0	16.6	0.4	24.0	1084.0
FMC 10-10-10 D-800 μ -R1	7.0	18.4	0.8	26.2	1114.0
FMC 10-10-10 D-800 μ -R2	6.7	19.9	0.2	26.8	1193.0
Mean	-	-	-	25.7	1130.3
Std Dev	-	-	-	1.5	56.3
Deviation range, min	-	-	-	24.2	1074.0
Deviation range, max	-	-	-	27.1	1186.6
Recommended Range, min	-	-	-	-	1017.3
Recommended Range, max	-	-	-	-	1243.4

H. I. 3. FMC 10-6-14

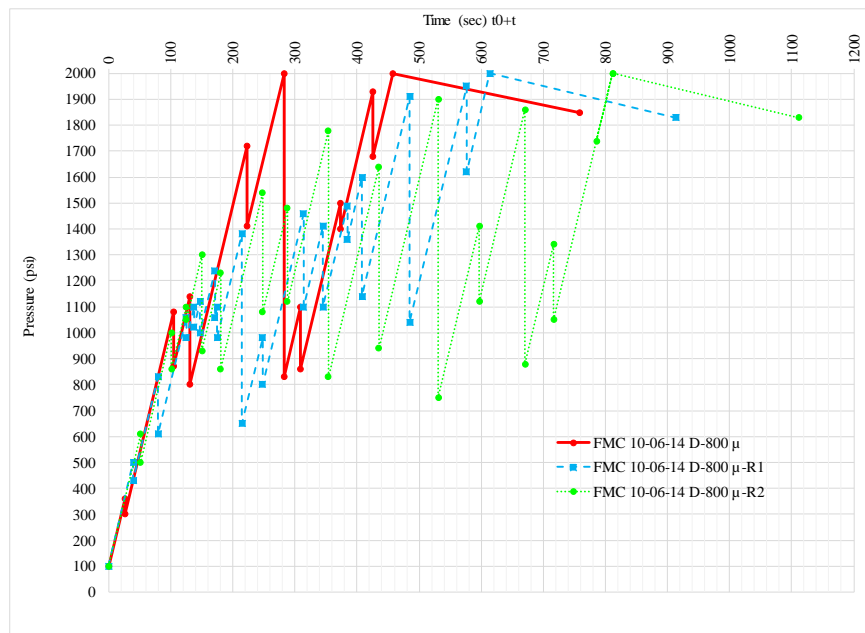


Figure H. 3: Pressure vs Time curve for FMC 10-6-14 on 800-micron fracture width

Table H. 3: Mud Loss & Total Sealing Time Values for FMC 10-6-14 on 800-micron fracture width

Code	Mud Loss (ml)				Total Sealing Time (sec)
	Stage I	Stage II	Stage III	Total	
FMC 10-06-14 D-800µ	8.6	8.6	0.4	17.6	758
FMC 10-06-14 D-800µ-R1	9	11	0.2	20.2	914
FMC 10-06-14 D-800µ-R2	9	17.1	0.9	27	1112
Mean	-	-	-	21.6	928.0
Std Dev	-	-	-	4.9	177.4
Deviation range, min	-	-	-	16.7	750.6
Deviation range, max	-	-	-	26.5	1105.4
Recommended Range, min	-	-	-	-	835.2
Recommended Range, max	-	-	-	-	1020.8

H. I. 4. FMC 10-2-18

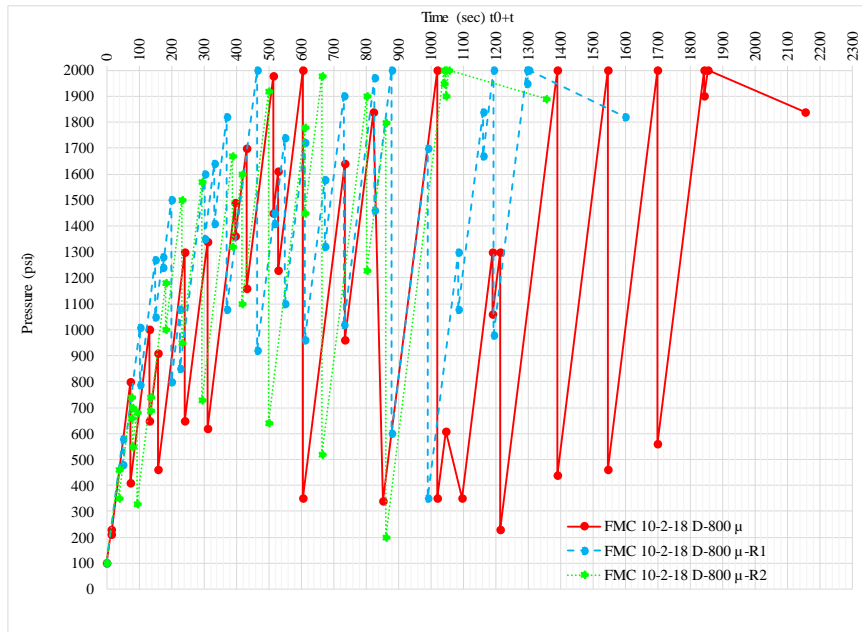


Figure H. 4: Pressure vs Time curve for FMC 10-2-18 on 800-micron fracture width

Table H. 4: Mud Loss & Total Sealing Time Values for FMC 10-2-18 on 800-micron fracture width

Code	Mud Loss (ml)				Total Sealing Time (sec)
	Stage I	Stage II	Stage III	Total	
FMC 10-02-18 D-800μ	10	46	1	57	2155
FMC 10-02-18 D-800μ-R1	12	34	1.2	47.2	1601
FMC 10-02-18 D-800μ-R2	8.2	25	0.9	34.1	1355
Mean	-	-	-	46.1	1703.7
Std Dev	-	-	-	11.5	409.8
Deviation range, min	-	-	-	34.6	1293.9
Deviation range, max	-	-	-	57.6	2113.4
Recommended Range, min	-	-	-	-	1533.3
Recommended Range, max	-	-	-	-	1874.0

H. I. 5. FMC 10-18-2

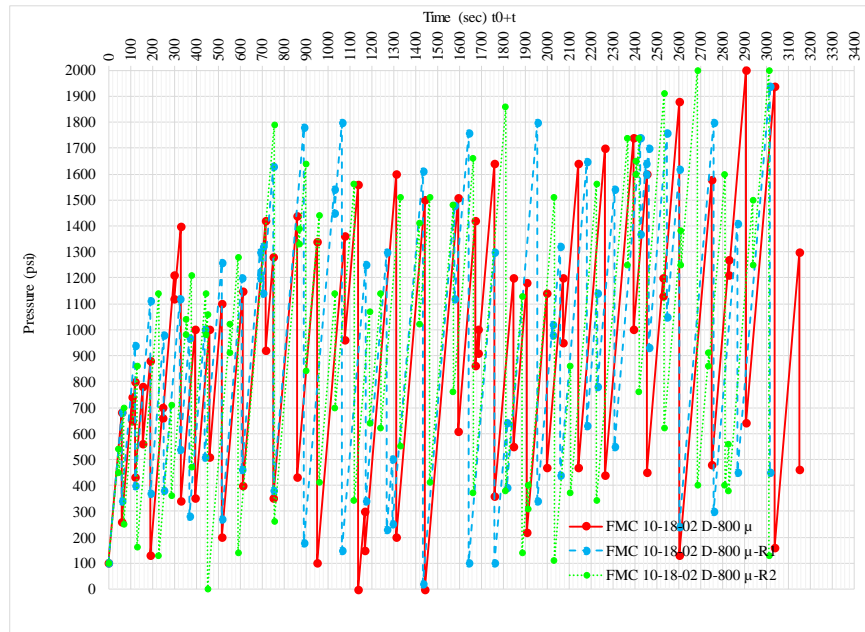


Figure H. 5: Pressure vs Time curve for FMC 10-18-2 on 800-micron fracture width

Table H. 5: Mud Loss & Total Sealing Time Values for FMC 10-18-2 on 800-micron fracture width

Code	Mud Loss (ml)				Total Sealing Time (sec)
	Stage I	Stage II	Stage III	Total	
FMC 10-18-02 D-800μ	14.4	*	*	>125	FAIL
FMC 10-18-02 D-800μ-R1	12.4	*	*	>125	FAIL
FMC 10-18-02 D-800μ-R2	14.2	*	*	>125	FAIL

H. I. 6. FMC 10-14-6

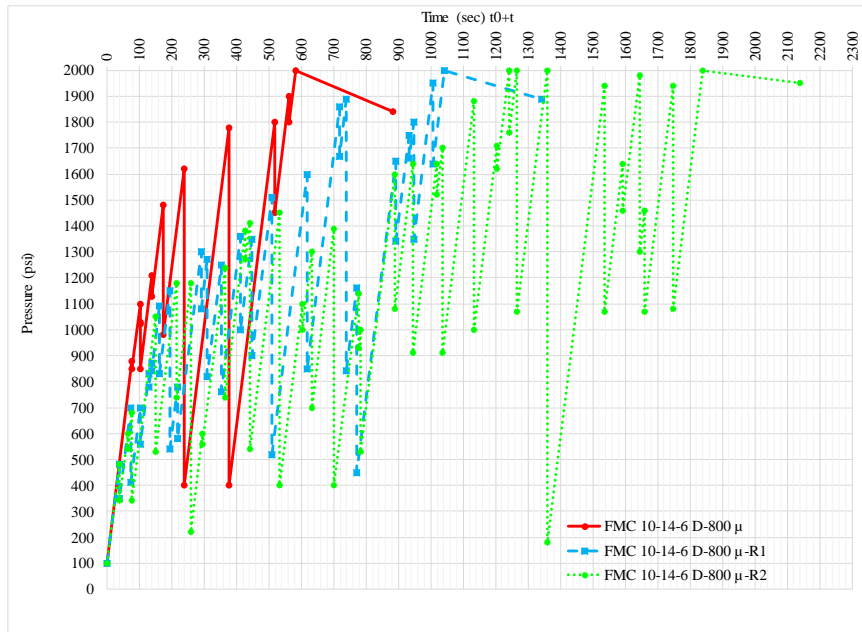


Figure H. 6: Pressure vs Time curve for FMC 10-14-6 on 800-micron fracture width

Table H. 6: Mud Loss&Total Sealing Time Values for FMC 10-14-06 on 800-micron fracture width

Code	Mud Loss (ml)				Total Sealing Time (sec)
	Stage I	Stage II	Stage III	Total	
FMC 10-14-06 D-800μ	8.9	11.3	0.4	20.6	882
FMC 10-14-06 D-800μ-R1	9.4	21.8	1	32.2	1343
FMC 10-14-06 D-800μ-R2	10.1	43.2	0.3	53.6	2140
Mean	-	-	-	35.5	1455.0
Std Dev	-	-	-	16.7	636.4
Deviation range, min	-	-	-	18.7	818.6
Deviation range, max	-	-	-	52.2	2091.4
Recommended Range, min	-	-	-	-	1309.5
Recommended Range, max	-	-	-	-	1600.5

H. I. 7. FMC 2-10-18

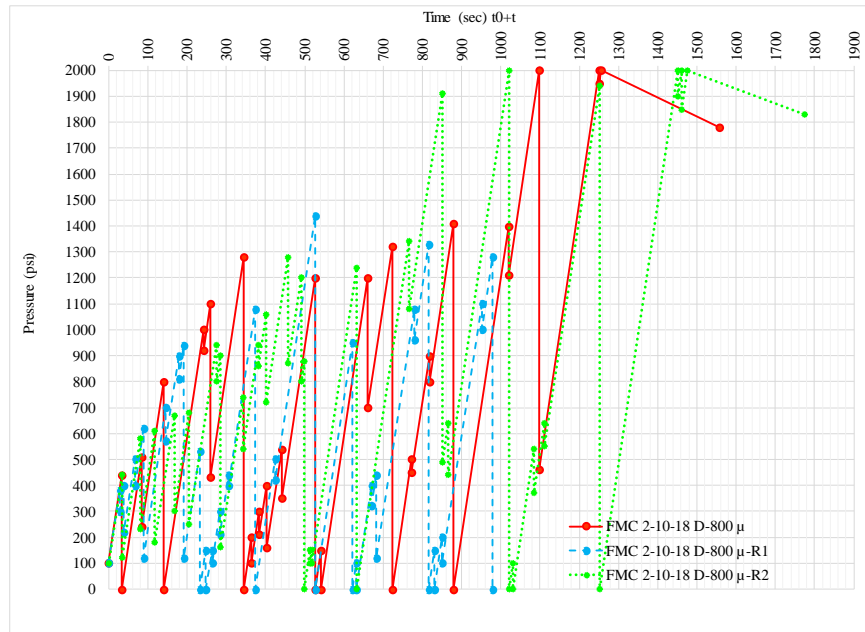


Figure H. 7: Pressure vs Time curve for FMC 18-10-2 on 800-micron fracture width

Table H. 7: Mud Loss & Total Sealing Time Values for FMC 18-10-2 on 800-micron fracture width

Code	Mud Loss (ml)				Total Sealing Time (sec)
	Stage I	Stage II	Stage III	Total	
FMC 02-10-18 D-800μ	12.8	96.2	1.3	110.3	1557
FMC 02-10-18 D-800μ-R1	14	*	*	>125	FAIL
FMC 02-10-18 D-800μ-R2	14	97	1	112	1776

H. I. 8. FMC 6-10-14

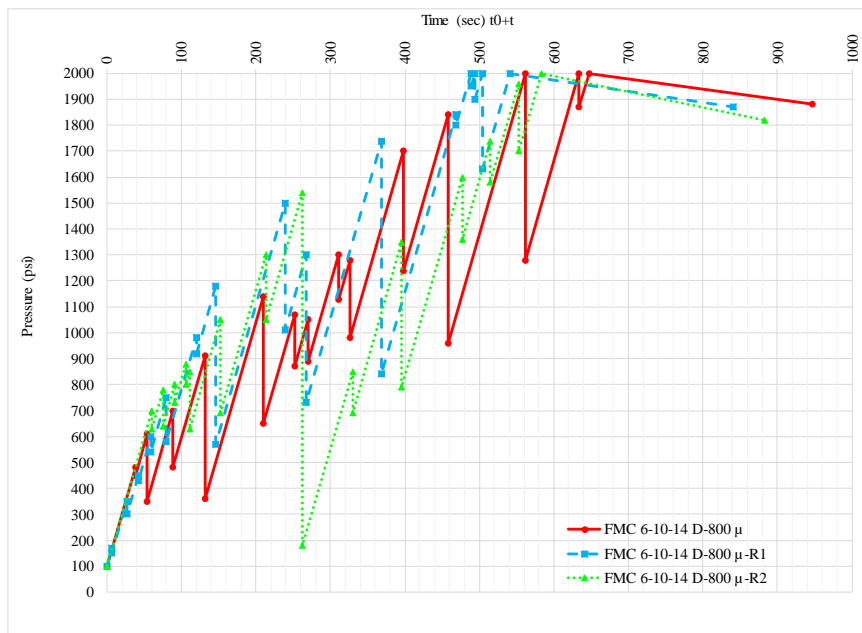


Figure H. 8: Pressure vs Time curve for FMC 6-10-14 on 800-micron fracture width

Table H. 8: Mud Loss & Total Sealing Time Values for FMC 6-10-14 on 800-micron fracture width

Code	Mud Loss (ml)				Total Sealing Time (sec)
	Stage I	Stage II	Stage III	Total	
FMC 06-10-14 D-800μ	10.1	14.1	1	25.2	947
FMC 06-10-14 D-800μ-R1	8.2	12.6	0.3	21.1	841
FMC 06-10-14 D-800μ-R2	11.3	12.5	0.7	24.5	883
Mean	-	-	-	23.6	890.3
Std Dev	-	-	-	2.2	53.4
Deviation range, min	-	-	-	21.4	837.0
Deviation range, max	-	-	-	25.8	943.7
Recommended Range, min	-	-	-	-	801.3
Recommended Range, max	-	-	-	-	979.4

H. I. 9. FMC 14-10-6

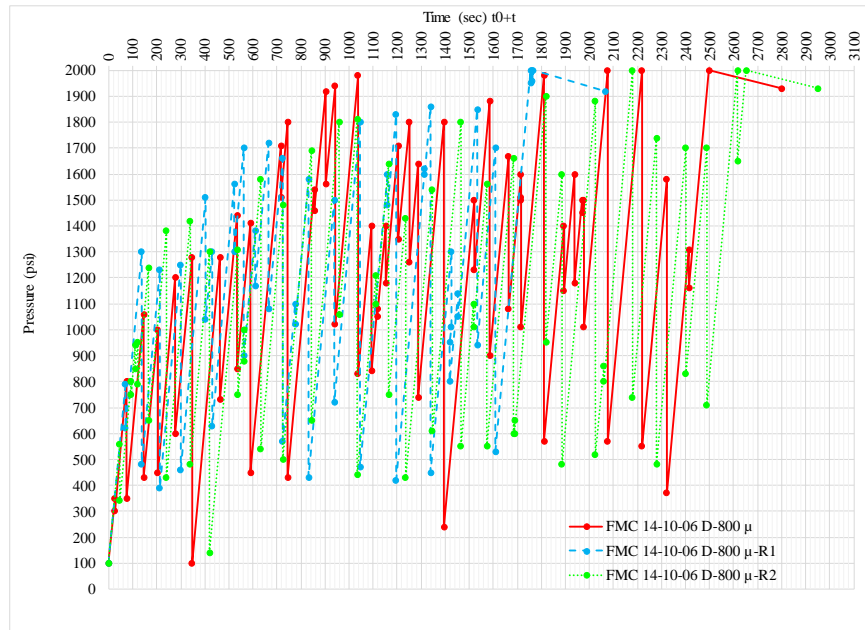


Figure H. 9: Pressure vs Time curve for FMC 14-10-6 on 800-micron fracture width

Table H. 9: Mud Loss & Total Sealing Time Values for FMC 14-10-6 on 800-micron fracture width

Code	Mud Loss (ml)				Total Sealing Time (sec)
	Stage I	Stage II	Stage III	Total	
FMC 14-10-06 D-800μ	8.2	67.7	0.7	76.6	2799
FMC 14-10-06 D-800μ-R1	12.1	43.3	0.2	55.6	2066
FMC 14-10-06 D-800μ-R2	11.2	67	0.9	79.1	2952
Mean	-	-	-	70.4	2605.7
Std Dev	-	-	-	12.9	473.6
Deviation range, min	-	-	-	57.5	2132.1
Deviation range, max	-	-	-	83.3	3079.3
Recommended Range, min	-	-	-	-	2345.1
Recommended Range, max	-	-	-	-	2866.2

H. I. 10. FMC 18-10-2

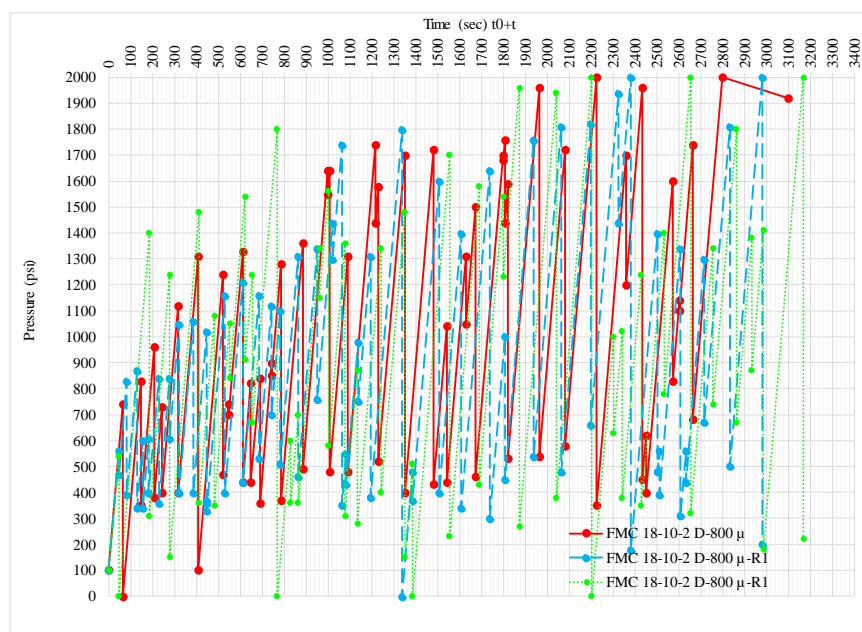


Figure H. 10: Pressure vs Time curve for FMC 18-10-2 on 800-micron fracture width

Table H. 10: Mud Loss & Total Sealing Time Values for FMC 18-10-2 on 800-micron fracture width

Code	Mud Loss (ml)				Total Sealing Time (sec)
	Stage I	Stage II	Stage III	Total	
FMC 18-10-02 D-800μ	22.4	92	0.2	114.6	3099
FMC 18-10-02 D-800μ-R1	19	*	*	>125	FAIL
FMC 18-10-02 D-800μ-R2	16	*	*	>125	FAIL

H. I. 11. FMC 18-2-10

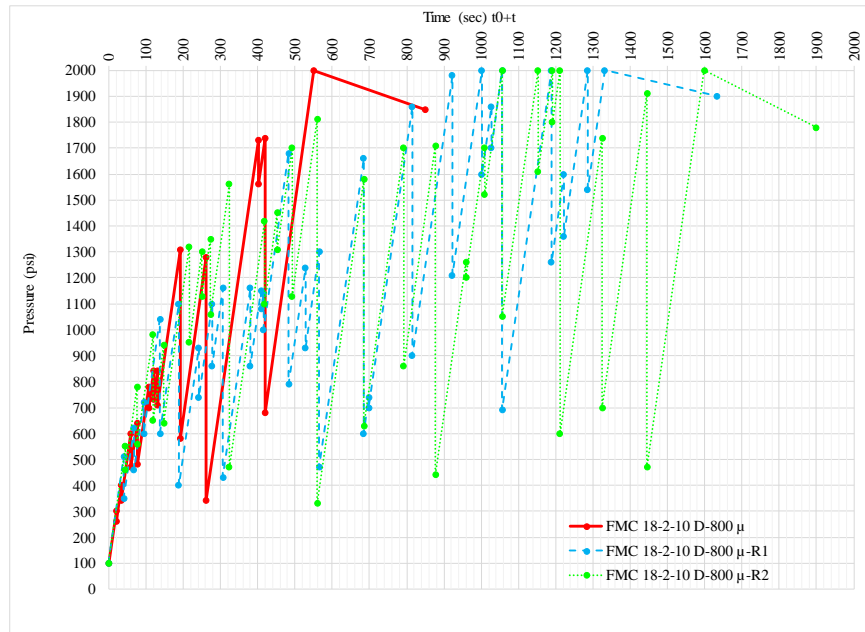


Figure H. 11: Pressure vs Time curve for FMC 18-2-10 on 800-micron fracture width

Table H. 11: Mud Loss & Total Sealing Time Values for FMC 18-2-10 on 800-micron fracture width

Code	Mud Loss (ml)				Total Sealing Time (sec)
	Stage I	Stage II	Stage III	Total	
FMC 18-02-10 D-800μ	9.8	9.6	0.4	19.8	851
FMC 18-02-10 D-800μ-R1	10	29	1	40	1632
FMC 18-02-10 D-800μ-R2	9.8	41.3	2.5	53.6	1899
Mean	-	-	-	37.8	1460.7
Std Dev	-	-	-	17.0	544.6
Deviation range, min	-	-	-	20.8	916.1
Deviation range, max	-	-	-	54.8	2005.3
Recommended Range, min	-	-	-	-	1314.6
Recommended Range, max	-	-	-	-	1606.7

H. I. 12. FMC 14-6-10

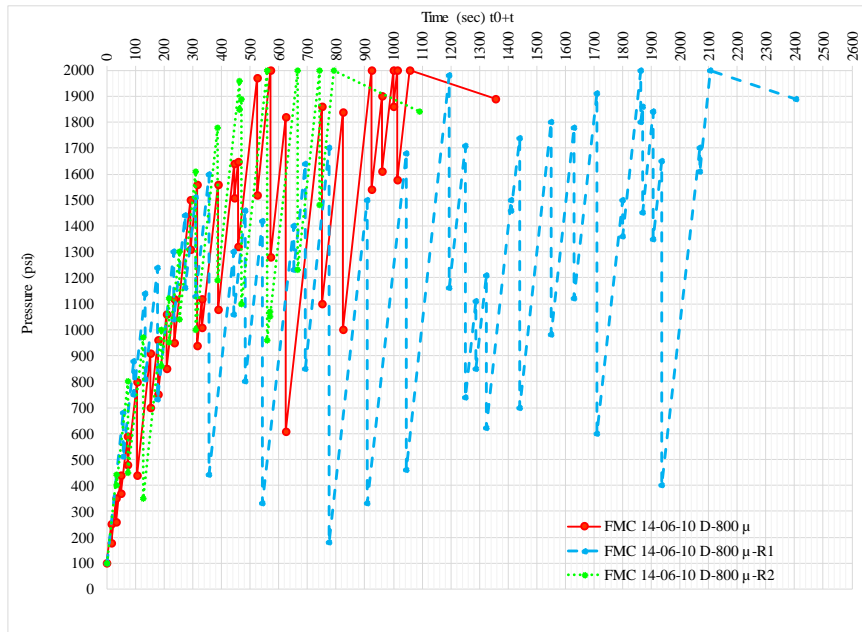


Figure H. 12: Pressure vs Time curve for FMC 14-6-10 on 800-micron fracture width

Table H. 12: Mud Loss & Total Sealing Time Values for FMC 14-6-10 on 800-micron fracture width

Code	Mud Loss (ml)				Total Sealing Time (sec)
	Stage I	Stage II	Stage III	Total	
FMC 14-06-10 D-800μ	13.6	28.6	0.2	42.4	1355
FMC 14-06-10 D-800μ-R1	13	54	0	67	2407
FMC 14-06-10 D-800μ-R2	8.4	17	0.4	25.8	1093
Mean	-	-	-	45.1	1618.3
Std Dev	-	-	-	20.7	695.5
Deviation range, min	-	-	-	24.3	922.9
Deviation range, max	-	-	-	65.8	2313.8
Recommended Range, min	-	-	-	-	1456.5
Recommended Range, max	-	-	-	-	1780.2

H. I. 13. FMC 6-14-10

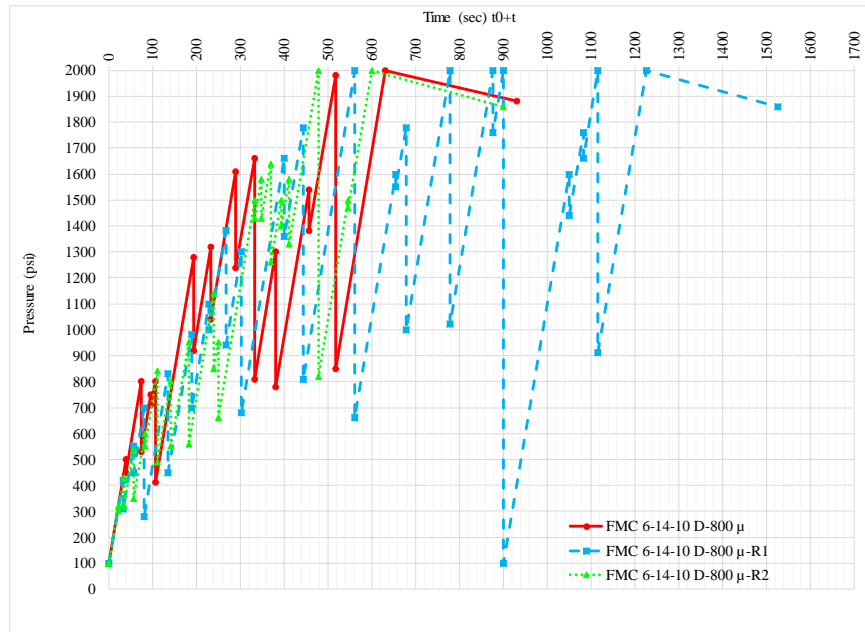


Figure H. 13: Pressure vs Time curve for FMC 6-14-10 on 800-micron fracture width

Table H. 13: Mud Loss & Total Sealing Time Values for FMC 6-14-10 on 800-micron fracture width

Code	Mud Loss (ml)				Total Sealing Time (sec)
	Stage I	Stage II	Stage III	Total	
FMC 06-14-10 D-800μ	9.2	12.8	1.2	23.2	932
FMC 06-14-10 D-800μ-R1	9.8	29.8	1.4	41	1526
FMC 06-14-10 D-800μ-R2	9.8	12.2	1.4	23.4	900
Mean	-	-	-	29.2	1119.3
Std Dev	-	-	-	10.2	352.5
Deviation range, min	-	-	-	19.0	766.8
Deviation range, max	-	-	-	39.4	1471.9
Recommended Range, min	-	-	-	-	1007.4
Recommended Range, max	-	-	-	-	1231.3

H. I. 14. FMC 2-18-10

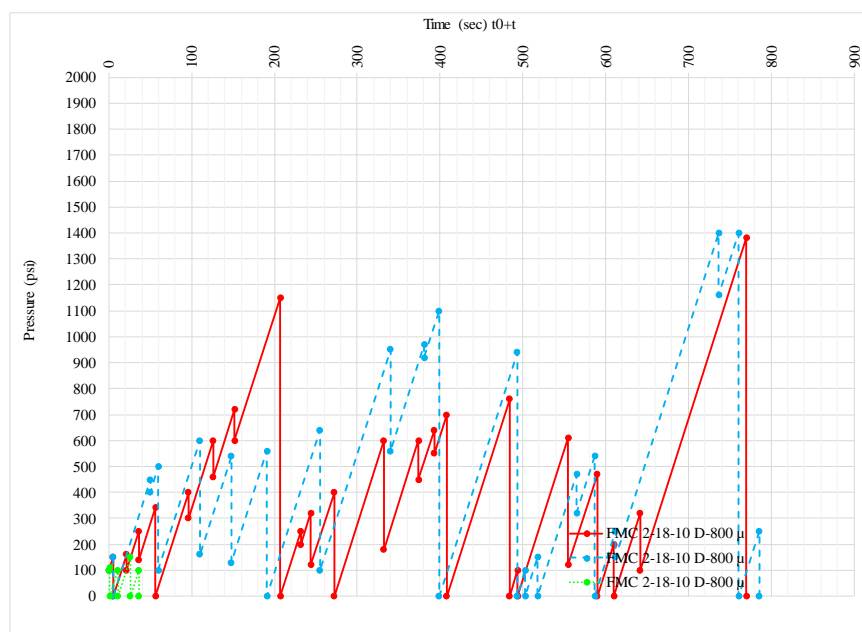


Figure H. 14: Pressure vs Time curve for FMC 2-18-10 on 800-micron fracture width

Table H. 14: Mud Loss & Total Sealing Time Values for FMC 2-18-10 on 800-micron fracture width

Code	Mud Loss (ml)				Total Sealing Time (sec)
	Stage I	Stage II	Stage III	Total	
FMC 02-18-10 D-800μ	15.4	*	*	>125	FAIL
FMC 02-18-10 D-800μ-R1	14	*	*	>125	FAIL
FMC 02-18-10 D-800μ-R2	73	*	*	>125	FAIL

H. I. 15. FMC 18-6-6

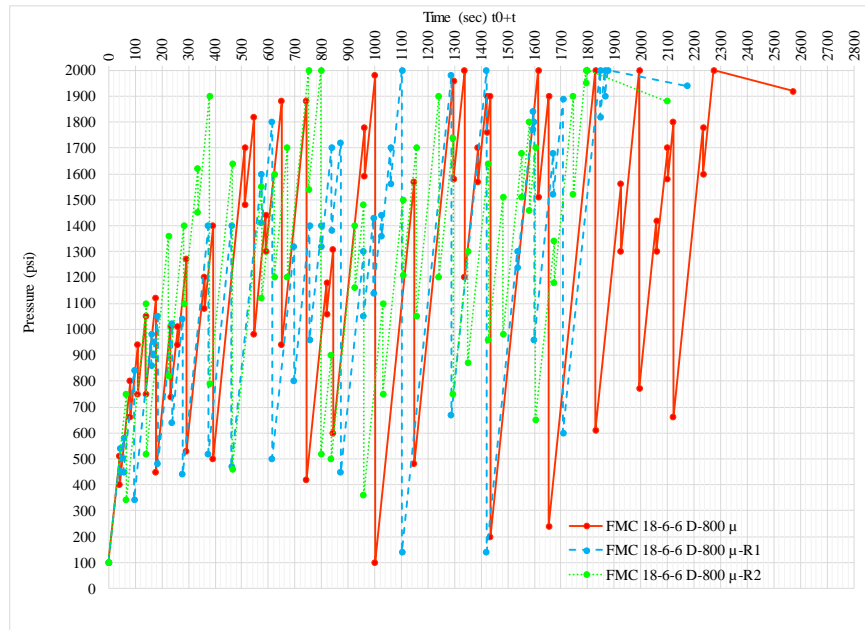


Figure H. 15: Pressure vs Time curve for FMC 18-6-6 on 800-micron fracture width

Table H. 15: Mud Loss & Total Sealing Time Values for FMC 18-6-6 on 800-micron fracture width

Code	Mud Loss (ml)				Total Sealing Time (sec)
	Stage I	Stage II	Stage III	Total	
FMC 18-6-6 D-800μ	12.4	60.6	1.2	74.2	2574
FMC 18-6-6 D-800μ-R1	14.2	54	0.1	68.3	2176
FMC 18-6-6 D-800μ-R2	12	47.2	0.6	59.8	2099
Mean	-	-	-	67.4	2283.0
Std Dev	-	-	-	7.2	254.9
Deviation range, min	-	-	-	60.2	2028.1
Deviation range, max	-	-	-	74.7	2537.9
Recommended Range, min	-	-	-	-	2054.7
Recommended Range, max	-	-	-	-	2511.3

H. I. 16. FMC 6-18-6

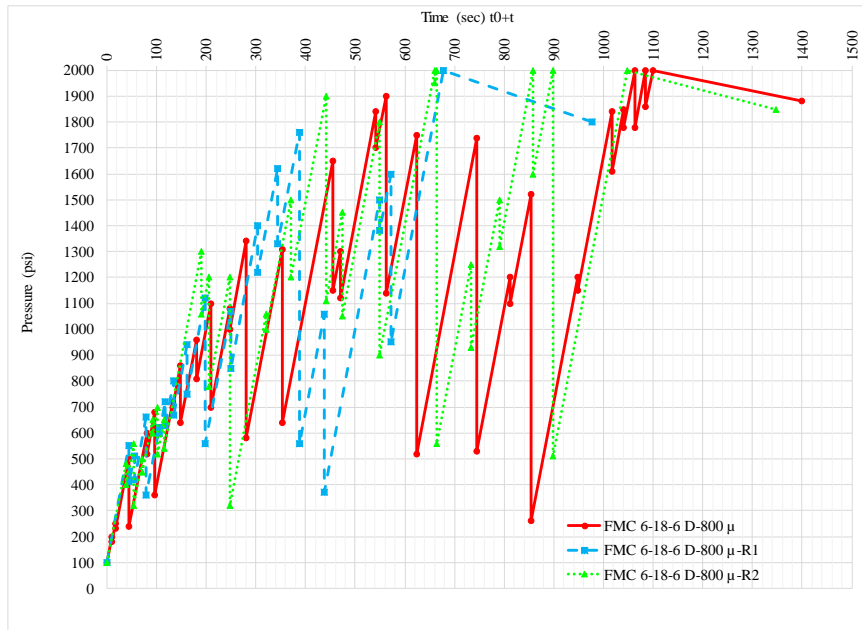


Figure H. 16: Pressure vs Time curve for FMC 6-18-6 on 800-micron fracture width

Table H. 16: Mud Loss & Total Sealing Time Values for FMC 6-18-6 on 800-micron fracture width

Code	Mud Loss (ml)				Total Sealing Time (sec)
	Stage I	Stage II	Stage III	Total	
FMC 06-18-06 D-800μ	10.2	27.8	1.2	39.2	1399
FMC 06-18-06 D-800μ-R1	12.6	15.4	0.8	28.8	977
FMC 06-18-06 D-800μ-R2	12	24	1	37	1348
Mean	-	-	-	35.0	1241.3
Std Dev	-	-	-	5.5	230.3
Deviation range, min	-	-	-	29.5	1011.0
Deviation range, max	-	-	-	40.5	1471.7
Recommended Range, min	-	-	-	-	1117.2
Recommended Range, max	-	-	-	-	1365.5

H. I. 17. FMC 6-6-18

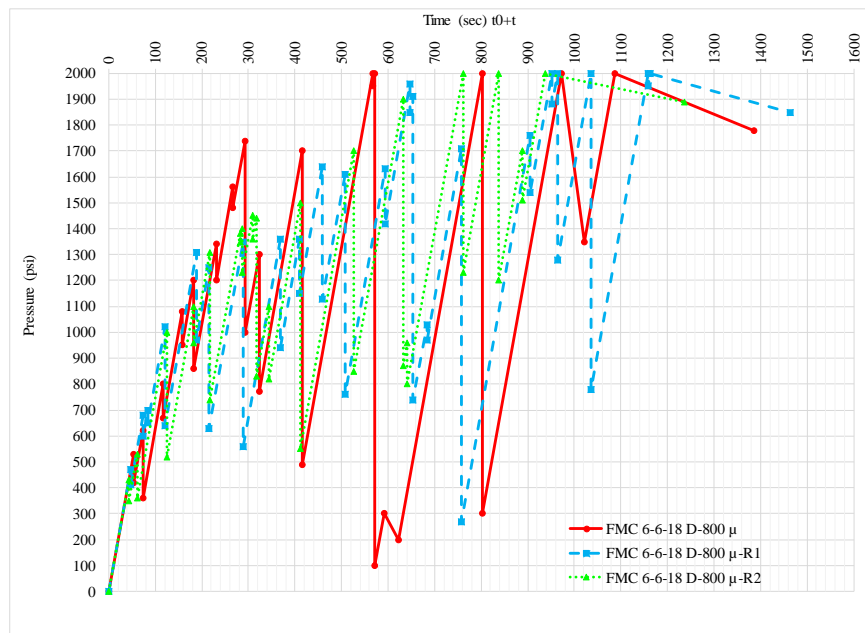


Figure H. 17: Pressure vs Time curve for FMC 6-6-18 on 800-micron fracture width

Table H. 17: Mud Loss & Total Sealing Time Values for FMC 6-6-18 on 800-micron fracture width

Code	Mud Loss (ml)				Total Sealing Time (sec)
	Stage I	Stage II	Stage III	Total	
FMC 06-06-18 D-800μ	9	27	1.4	37.4	1387
FMC 06-06-18 D-800μ-R1	9	28.2	1.4	38.6	1463
FMC 06-06-18 D-800μ-R2	8.6	20.4	0.6	29.6	1237
Mean	-	-	-	35.2	1362.3
Std Dev	-	-	-	4.9	115.0
Deviation range, min	-	-	-	30.3	1247.3
Deviation range, max	-	-	-	40.1	1477.3
Recommended Range, min	-	-	-	-	1226.1
Recommended Range, max	-	-	-	-	1498.6

H. II. Results Obtained for Total Concentration of 28 ppb for 800- μ m Slot

H. II. 1. FMC 8-10-10

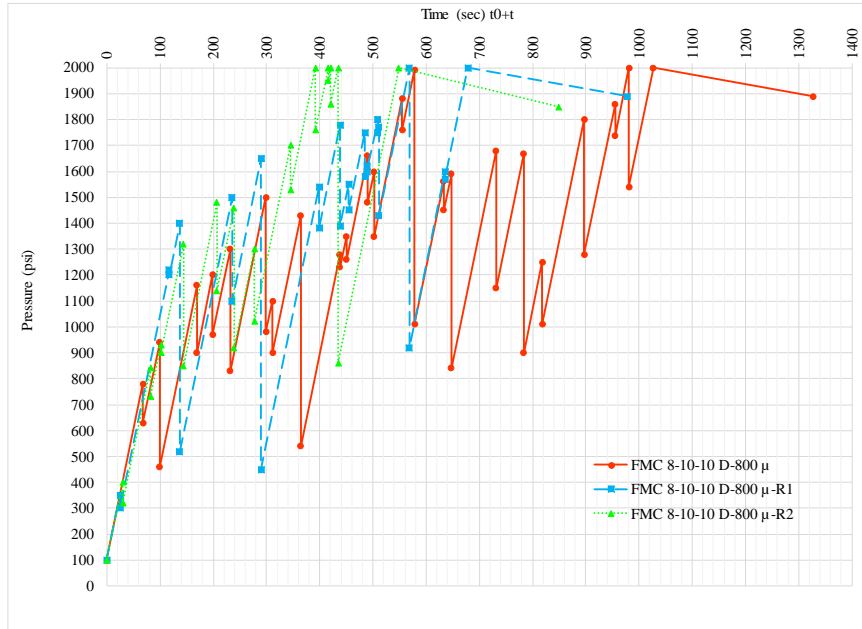


Figure H. 18: Pressure vs Time curve for FMC 8-10-10 on 800-micron fracture width

Table H. 18: Mud Loss & Total Sealing Time Values for FMC 8-10-10 on 800-micron fracture width

Code	Mud Loss (ml)				Total Sealing Time (sec)
	Stage I	Stage II	Stage III	Total	
FMC 8-10-10 D-800μ	9.2	23.3	0.5	33	1327
FMC 8-10-10 D-800 μ -R1	8	14.6	0.4	23	979
FMC 8-10-10 D-800μ-R2	10.2	12.2	0.6	23	849
Mean	-	-	-	26.3	1051.7
Std Dev	-	-	-	5.8	247.1
Deviation range, min	-	-	-	20.6	804.5
Deviation range, max	-	-	-	32.1	1298.8
Recommended Range, min	-	-	-	-	946.5
Recommended Range, max	-	-	-	-	1156.8

H. II. 2. FMC 10-8-10

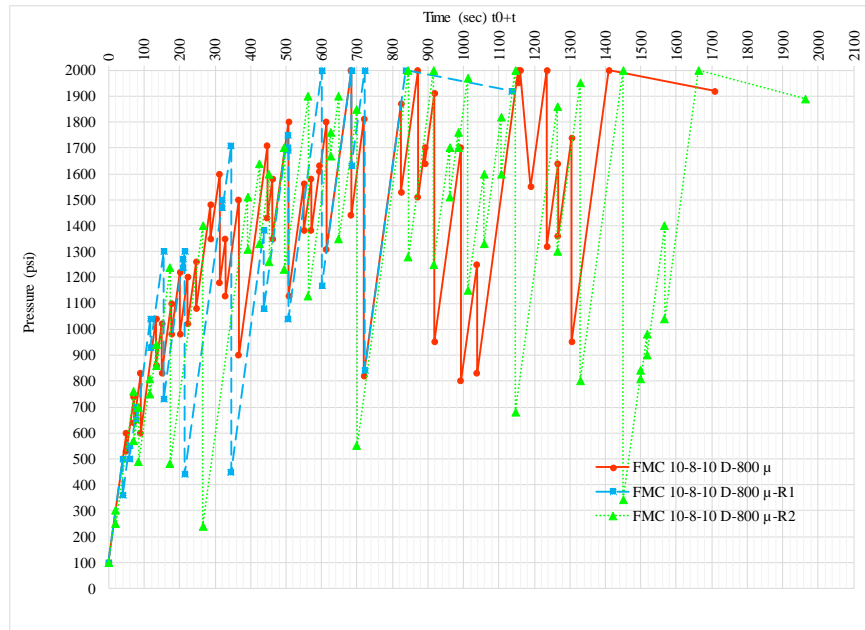


Figure H. 19: Pressure vs Time curve for FMC 10-8-10 on 800-micron fracture width

Table H. 19: Mud Loss & Total Sealing Time Values for FMC 10-8-10 on 800-micron fracture width

Code	Mud Loss (ml)				Total Sealing Time (sec)
	Stage I	Stage II	Stage III	Total	
FMC 10-8-10 D-800μ	7.8	31.2	1	40	1710
FMC 10-8-10 D-800μ-R1	9	17.8	0.4	27.2	1138
FMC 10-8-10 D-800μ-R2	10.1	38.9	0.6	49.6	1963
Mean	-	-	-	38.9	1603.7
Std Dev	-	-	-	11.2	422.7
Deviation range, min	-	-	-	27.7	1181.0
Deviation range, max	-	-	-	50.2	2026.3
Recommended Range, min	-	-	-	-	1443.3
Recommended Range, max	-	-	-	-	1764.0

H. II. 3. FMC 10-10-8

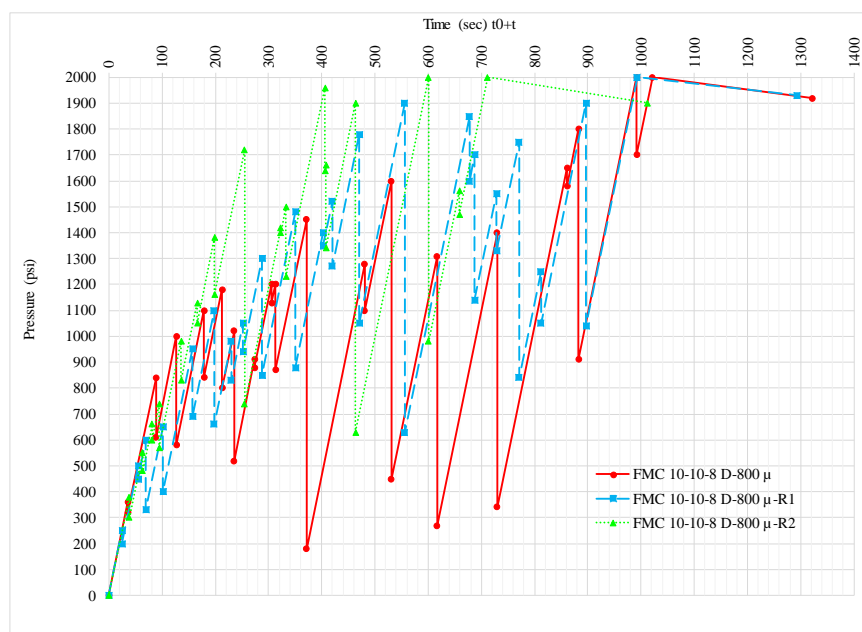


Figure H. 20: Pressure vs Time curve for FMC 10-10-8 on 800-micron fracture width

Table H. 20: Mud Loss & Total Sealing Time Values for FMC 10-10-8 on 800-micron fracture width

Code	Mud Loss (ml)				Total Sealing Time (sec)
	Stage I	Stage II	Stage III	Total	
FMC 10-10-8 D-800μ	9.8	21.7	0.5	32	1322
FMC 10-10-8 D-800μ-R1	8.5	22.5	0.6	31.6	1293
FMC 10-10-8 D-800μ-R2	7.2	15.4	0.2	22.8	1012
Mean	-	-	-	28.8	1209.0
Std Dev	-	-	-	5.2	171.2
Deviation range, min	-	-	-	23.6	1037.8
Deviation range, max	-	-	-	34.0	1380.2
Recommended Range, min	-	-	-	-	1088.1
Recommended Range, max	-	-	-	-	1329.9

H. III. Results Obtained for Total Concentration of 26 ppb for 800- μ m Slot

H. III. 1. FMC 6-10-10

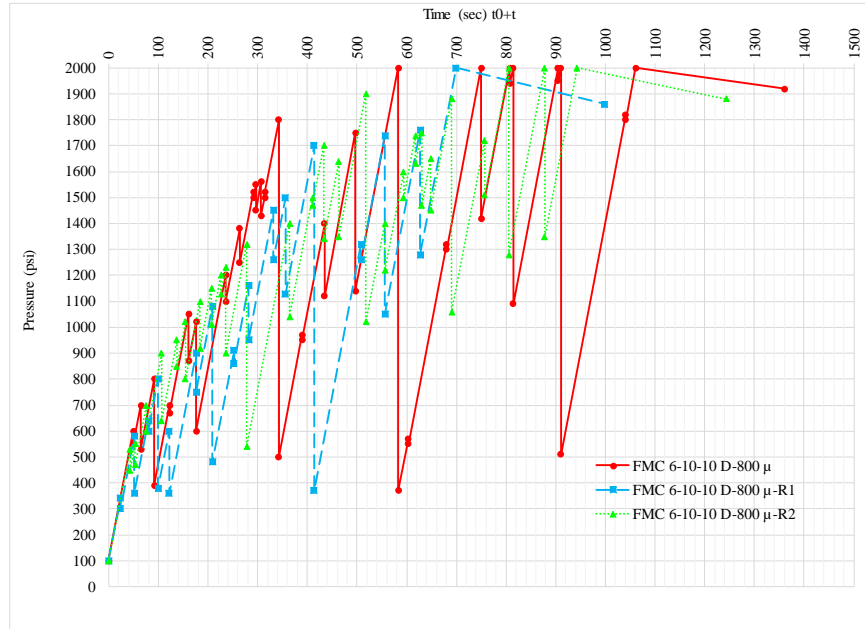


Figure H. 21: Pressure vs Time curve for FMC 6-10-10 on 800-micron fracture width

Table H. 21: Mud Loss & Total Sealing Time Values for FMC 6-10-10 on 800 micron fracture width

Code	Mud Loss (ml)				Total Sealing Time (sec)
	Stage I	Stage II	Stage III	Total	
FMC 6-10-10 D-800μ	10	23.2	0.2	33.4	1361
FMC 6-10-10 D-800μ-R1	10.1	14.9	0.4	25.4	999
FMC 6-10-10 D-800 μ -R2	9	19.8	0.4	29.2	1243
Mean	-	-	-	29.3	1201.0
Std Dev	-	-	-	4.0	184.6
Deviation range, min	-	-	-	25.3	1016.4
Deviation range, max	-	-	-	33.3	1385.6
Recommended Range, min	-	-	-	-	1080.9
Recommended Range, max	-	-	-	-	1321.1

H. III. 2. FMC 10-6-10

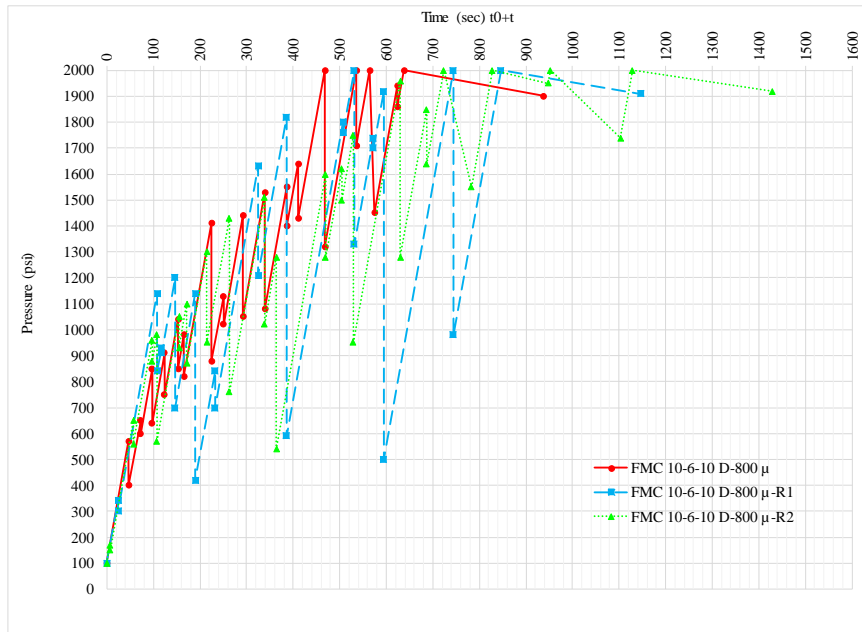


Figure H. 22: Pressure vs Time curve for FMC 10-6-10 on 800-micron fracture width

Table H. 22: Mud Loss & Total Sealing Time Values for FMC 10-6-10 on 800 micron fracture width

Code	Mud Loss (ml)				Total Sealing Time (sec)
	Stage I	Stage II	Stage III	Total	
FMC 10-6-10 D-800μ	7.8	12.8	0.4	21	938
FMC 10-6-10 D-800μ-R1	8	19.8	0.2	28	1146
FMC 10-6-10 D-800μ-R2	8.2	17.5	0.5	26.2	1429
Mean	-	-	-	25.1	1171.0
Std Dev	-	-	-	3.6	246.5
Deviation range, min	-	-	-	21.4	924.5
Deviation range, max	-	-	-	28.7	1417.5
Recommended Range, min	-	-	-	-	1053.9
Recommended Range, max	-	-	-	-	1288.1

H. III. 3. FMC 10-10-6

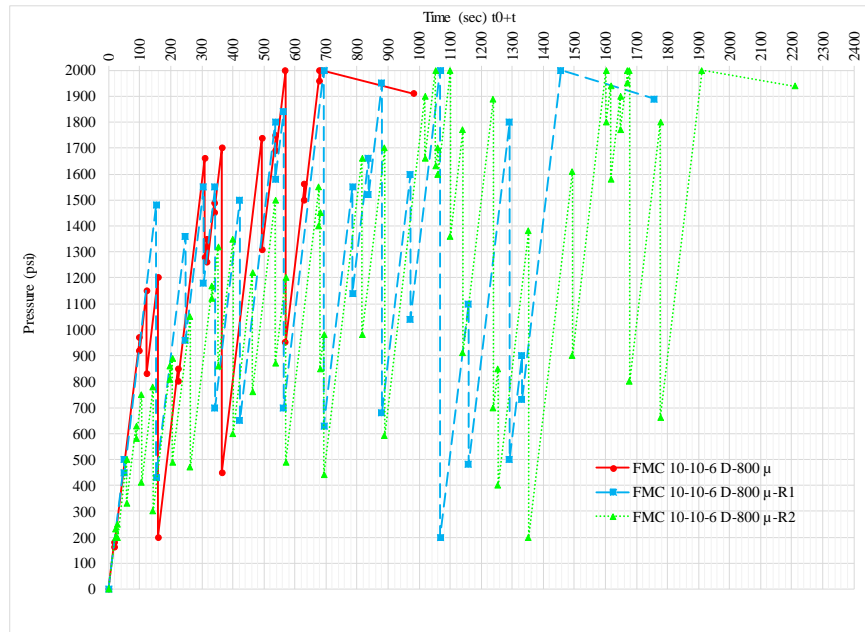


Figure H. 23: Pressure vs Time curve for FMC 10-10-6 on 800-micron fracture width

Table H. 23: Mud Loss & Total Sealing Time Values for FMC 10-10-6 on 800-micron fracture width

Code	Mud Loss (ml)				Total Sealing Time (sec)
	Stage I	Stage II	Stage III	Total	
FMC 10-10-6 D-800μ	10.2	14.8	0.6	25.6	984
FMC 10-10-6 D-800μ-R1	13.5	34	0.5	48	1757
FMC 10-10-6 D-800μ-R2	7	47	0.2	54.2	2211
Mean	-	-	-	42.6	1650.7
Std Dev	-	-	-	15.0	620.4
Deviation range, min	-	-	-	27.6	1030.3
Deviation range, max	-	-	-	57.6	2271.0
Recommended Range, min	-	-	-	-	1485.6
Recommended Range, max	-	-	-	-	1815.7

H. IV. Results Obtained for Total Concentration of 24 ppb for 800- μ m Slot

H. IV. 1. FMC 4-10-10

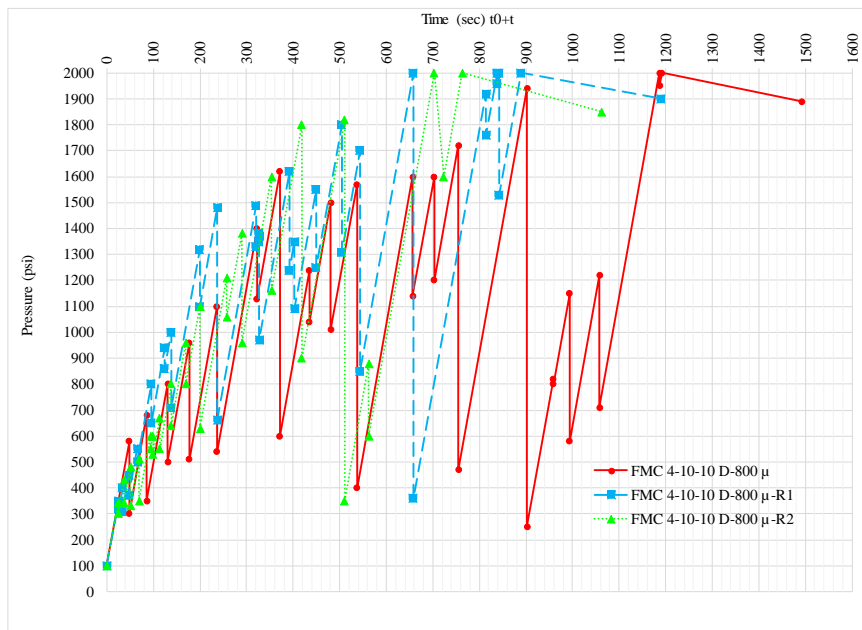


Figure H. 24: Pressure vs Time curve for FMC 4-10-10 on 800-micron fracture width

Table H. 24: Mud Loss & Total Sealing Time Values for FMC 4-10-10 on 800-micron fracture width

Code	Mud Loss (ml)				Total Sealing Time (sec)
	Stage I	Stage II	Stage III	Total	
FMC 4-10-10 D-800μ	12.5	28.7	0.9	42.1	1492
FMC 4-10-10 D-800 μ -R1	12	18.8	0.6	31.4	1189
FMC 4-10-10 D-800μ-R2	10.6	18	0.5	29.1	1063
Mean	-	-	-	34.2	1248.0
Std Dev	-	-	-	6.9	220.5
Deviation range, min	-	-	-	27.3	1027.5
Deviation range, max	-	-	-	41.1	1468.5
Recommended Range, min	-	-	-	-	1123.2
Recommended Range, max	-	-	-	-	1372.8

H. IV. 2. FMC 10-4-10

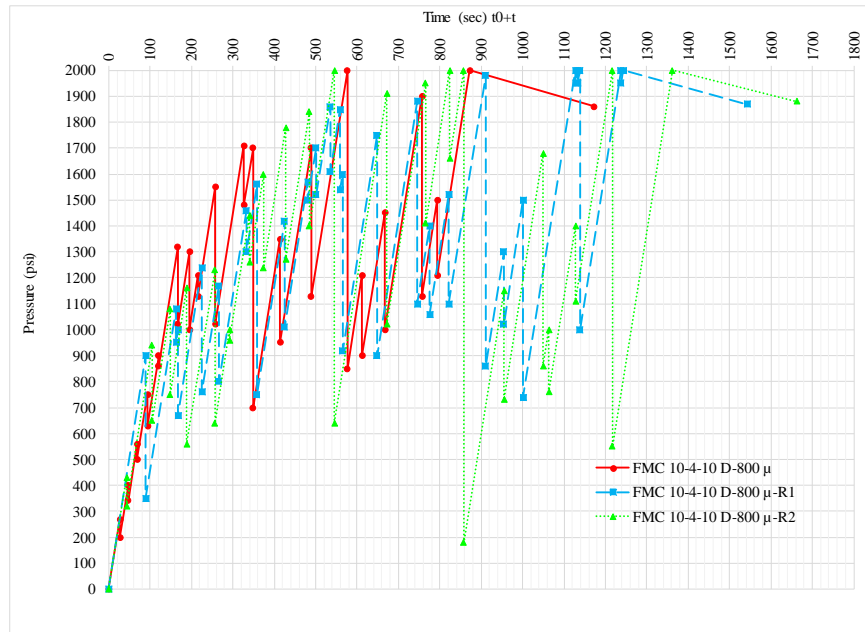


Figure H. 25: Pressure vs Time curve for FMC 10-4-10 on 800-micron fracture width

Table H. 25: Mud Loss & Total Sealing Time Values for FMC 10-4-10 on 800-micron fracture width

Code	Mud Loss (ml)				Total Sealing Time (sec)
	Stage I	Stage II	Stage III	Total	
FMC 10-4-10 D-800μ	10	19	0.6	29.6	1173
FMC 10-4-10 D-800 μ -R1	10.2	26.8	1	38	1543
FMC 10-4-10 D-800μ-R2	8.6	27.8	0.8	37.2	1662
Mean	-	-	-	34.9	1459.3
Std Dev	-	-	-	4.6	255.0
Deviation range, min	-	-	-	30.3	1204.3
Deviation range, max	-	-	-	39.6	1714.3
Recommended Range, min	-	-	-	-	1313.4
Recommended Range, max	-	-	-	-	1605.3

H. IV. 3. FMC 10-10-4

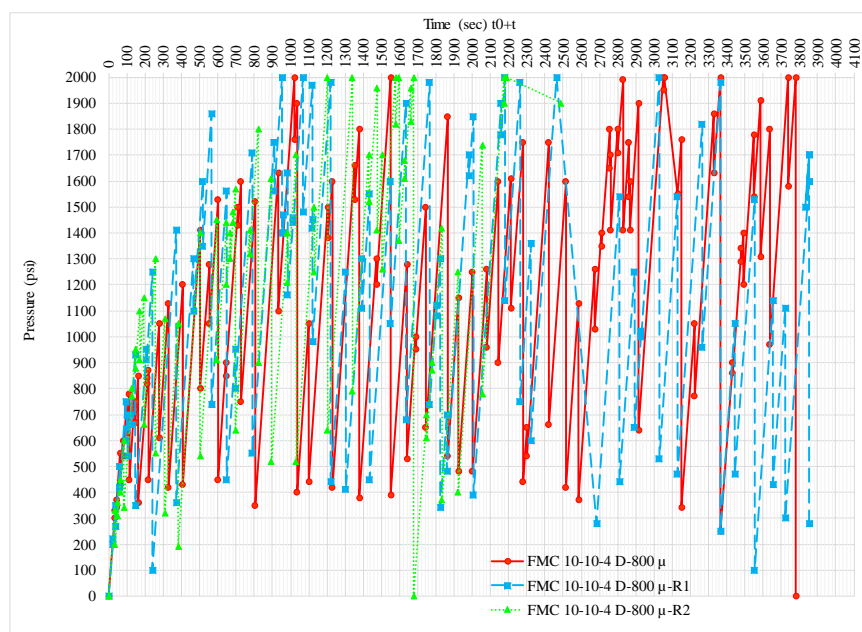


Figure H. 26: Pressure vs Time curve for FMC 10-10-4 on 800-micron fracture width

Table H. 26: Mud Loss & Total Sealing Time Values for FMC 10-10-4 on 800-micron fracture width

Code	Mud Loss (ml)				Total Sealing Time (sec)
	Stage I	Stage II	Stage III	Total	
FMC 10-10-4 D-800μ	13	*	*	>125	FAIL
FMC 10-10-4 D-800μ-R1	15	*	*	>125	FAIL
FMC 10-10-4 D-800μ-R2	15	59.4	2.2	76.6	2487

H. V. Results Obtained for Total Concentration of 22 ppb for 800- μ m Slot

H. V. 1. FMC 2-10-10

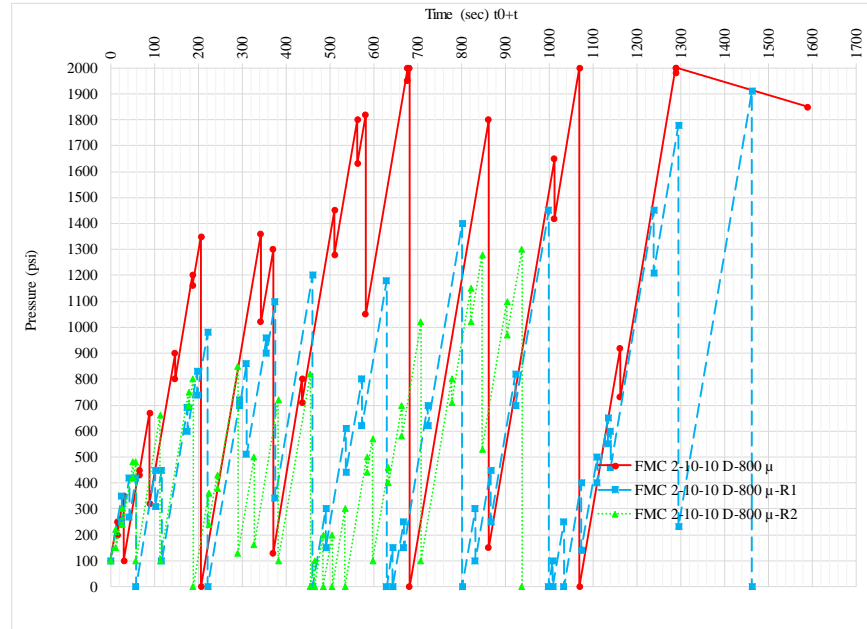


Figure H. 27: Pressure vs Time curve for FMC 10-10-10 on 800-micron fracture width

Table H. 27: Mud Loss & Total Sealing Time Values for FMC 2-10-10 on 800-micron fracture width

Code	Mud Loss (ml)				Total Sealing Time (sec)
	Stage I	Stage II	Stage III	Total	
FMC 2-10-10 D-800 μ	15	48	1	64	1591
FMC 2-10-10 D-800 μ -R1	14	*	*	>125	FAIL
FMC 2-10-10 D-800 μ -R2	14	*	*	>125	FAIL

H. V. 2. FMC 10-2-10

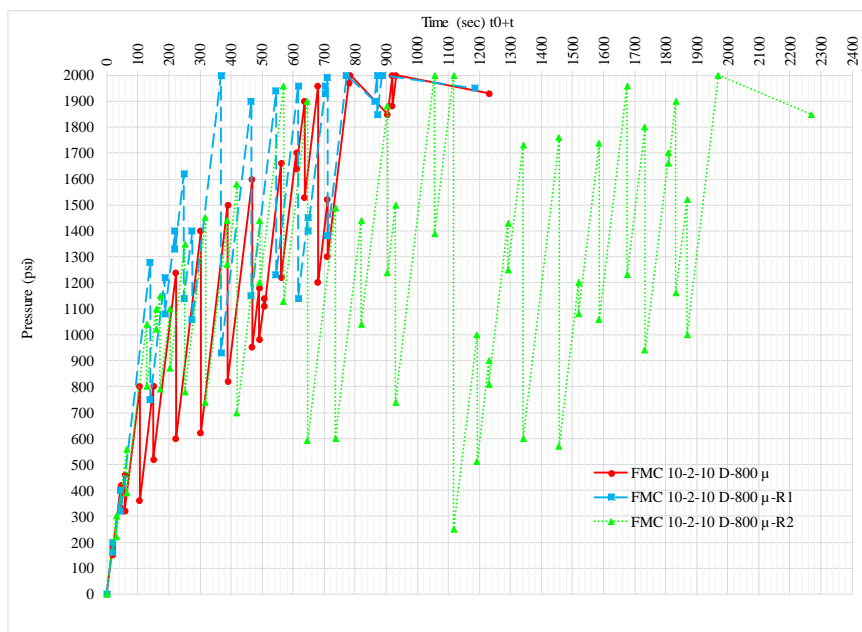


Figure H. 28: Pressure vs Time curve for FMC 10-2-10 on 800-micron fracture width

Table H. 28: Mud Loss & Total Sealing Time Values for FMC 10-2-10 on 800-micron fracture width

Code	Mud Loss (ml)				Total Sealing Time (sec)
	Stage I	Stage II	Stage III	Total	
FMC 10-2-10 D-800μ	9.2	19.2	0.5	28.9	1231
FMC 10-2-10 D-800μ-R1	9.6	15.6	0.2	25.4	1187
FMC 10-2-10 D-800μ-R2	9.6	44	0.2	53.8	2269
Mean	-	-	-	36.0	1562.3
Std Dev	-	-	-	15.5	612.4
Deviation range, min	-	-	-	20.5	949.9
Deviation range, max	-	-	-	51.5	2174.7
Recommended Range, min	-	-	-	-	1406.1
Recommended Range, max	-	-	-	-	1718.6

H. V. 3. FMC 10-10-2

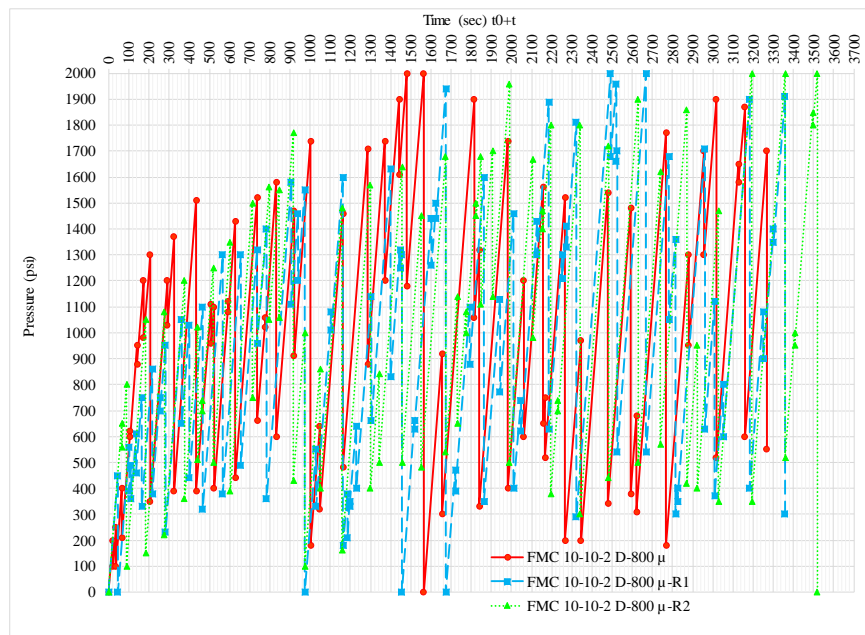


Figure H. 29: Pressure vs Time curve for FMC 10-10-2 on 800-micron fracture width

Table H. 29: Mud Loss & Total Sealing Time Values for FMC 10-10-2 on 800-micron fracture width

Code	Mud Loss (ml)				Total Sealing Time (sec)
	Stage I	Stage II	Stage III	Total	
FMC 10-10-2 D-800μ	17	*	*	>125	FAIL
FMC 10-10-2 D-800μ-R1	16.6	*	*	>125	FAIL
FMC 10-10-2 D-800μ-R2	14	*	*	>125	FAIL

H. VI. Results Obtained for Total Concentration of 20 ppb for 800- μ m Slot

H. VI. 1. FMC 0-10-10



Figure H. 30: Pressure vs Time curve for FMC 0-10-10 on 800-micron fracture width

Table H. 30: Mud Loss & Total Sealing Time Values for FMC 0-10-10 on 800-micron fracture width

Code	Mud Loss (ml)				Total Sealing Time (sec)
	Stage I	Stage II	Stage III	Total	
FMC 0-10-10 D-800 μ	*	*	*	>125	FAIL
FMC 0-10-10 D-800 μ -R1	*	*	*	>125	FAIL
FMC 0-10-10 D-800 μ -R2	*	*	*	>125	FAIL

H. VI. 2. FMC 10-0-10

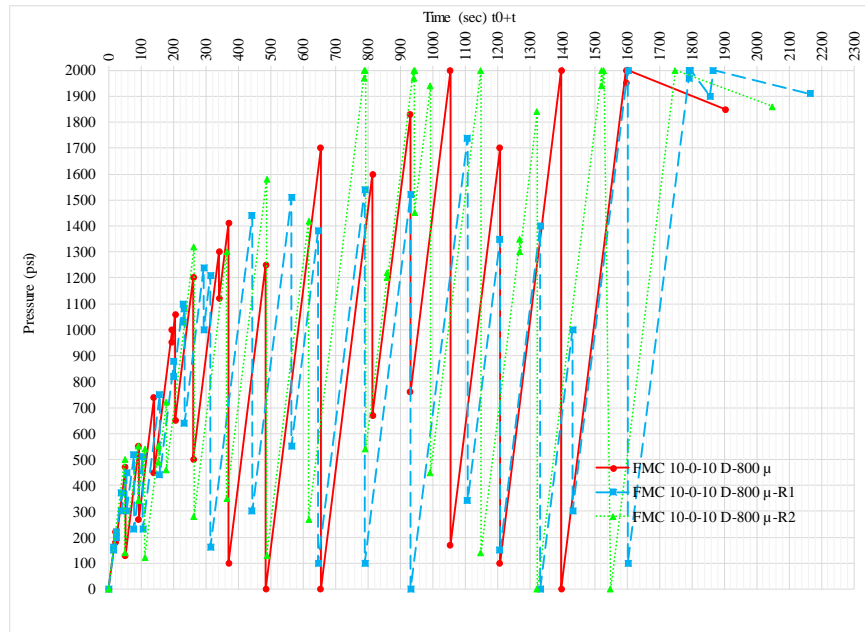


Figure H. 31: Pressure vs Time curve for FMC 10-0-10 on 800-micron fracture width

Table H. 31: Mud Loss & Total Sealing Time Values for FMC 10-0-10 on 800-micron fracture width

Code	Mud Loss (ml)				Total Sealing Time (sec)
	Stage I	Stage II	Stage III	Total	
FMC 10-0-10 D-800 μ	11.4	51.8	1	64.2	1903
FMC 10-0-10 D-800 μ -R1	13.5	55.9	1	70.4	2166
FMC 10-0-10 D-800 μ -R2	14	50.6	0.8	65.4	2049
Mean	-	-	-	66.7	2039.3
Std Dev	-	-	-	3.3	131.8
Deviation range, min	-	-	-	63.4	1907.6
Deviation range, max	-	-	-	70.0	2171.1
Recommended Range, min	-	-	-	-	1835.4
Recommended Range, max	-	-	-	-	2243.3

H. VI. 3. FMC 10-10-0

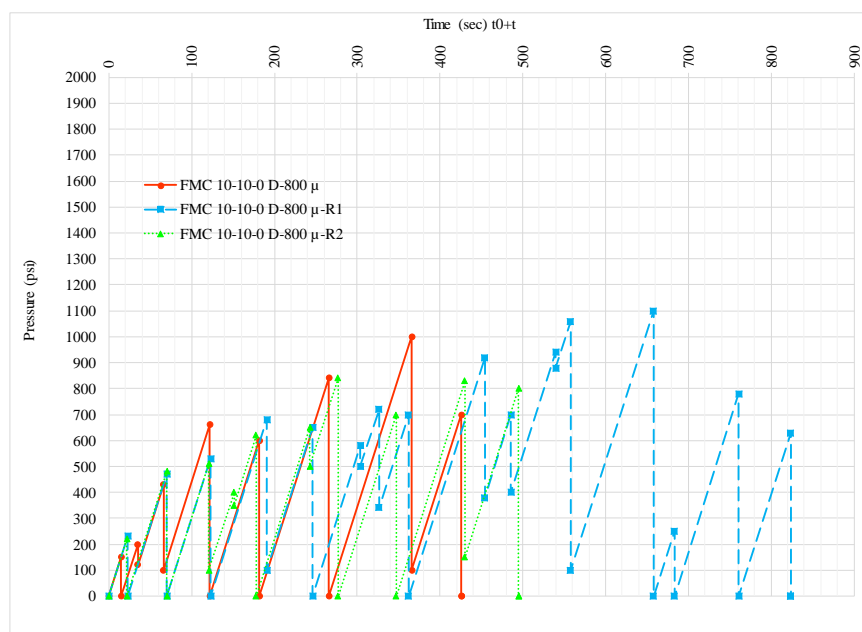


Figure H. 32: Pressure vs Time curve for FMC 10-10-0 on 800-micron fracture width

Table H. 32: Mud Loss & Total Sealing Time Values for FMC 4-10-10 on 800-micron fracture width

Code	Mud Loss (ml)				Total Sealing Time (sec)
	Stage I	Stage II	Stage III	Total	
FMC 10-10-0 D-800μ	70.6	*	*	>125	FAIL
FMC 10-10-0 D-800μ-R1	33	*	*	>125	FAIL
FMC 10-10-0 D-800μ-R2	69	*	*	>125	FAIL

H. VI. 4. FMC 6-6-8

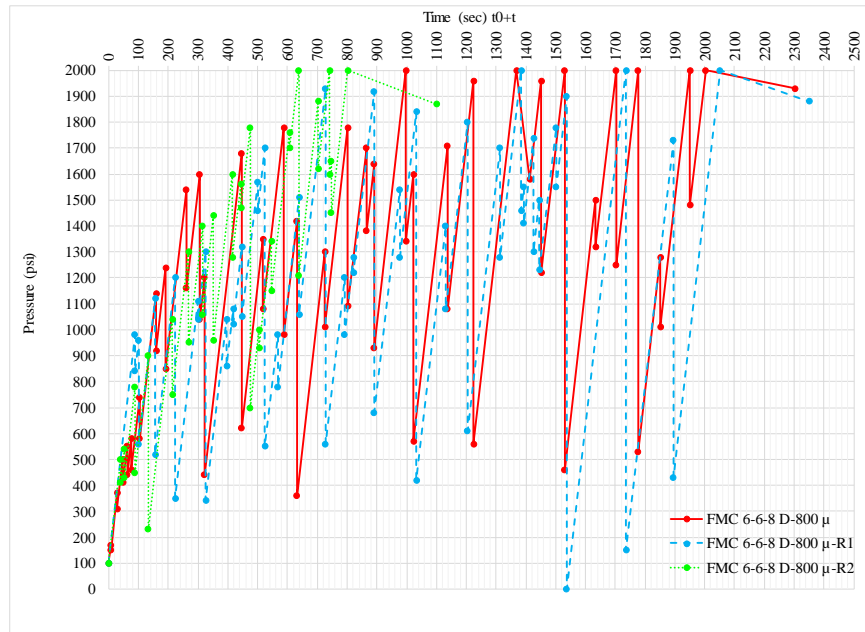


Figure H. 33: Pressure vs Time curve for FMC 6-6-8 on 800-micron fracture width

Table H. 33: Mud Loss & Total Sealing Time Values for FMC 6-6-8 on 800-micron fracture width

Code	Mud Loss (ml)				Total Sealing Time (sec)
	Stage I	Stage II	Stage III	Total	
FMC 6-6-8 D-800μ	14	52	1	67	2303
FMC 6-6-8 D-800μ-R1	9.8	55.6	0.7	66.1	2351
FMC 6-6-8 D-800μ-R2	9.2	20.8	1	31	1102
Mean	-	-	-	54.7	1918.7
Std Dev	-	-	-	20.5	707.7
Deviation range, min	-	-	-	34.2	1211.0
Deviation range, max	-	-	-	75.2	2626.3
Recommended Range, min	-	-	-	-	1726.8
Recommended Range, max	-	-	-	-	2110.5

I. Effect of Concentration of Ground Marble on Sealing 800- μ fracture

I. I. 1. FMC 15-15-15

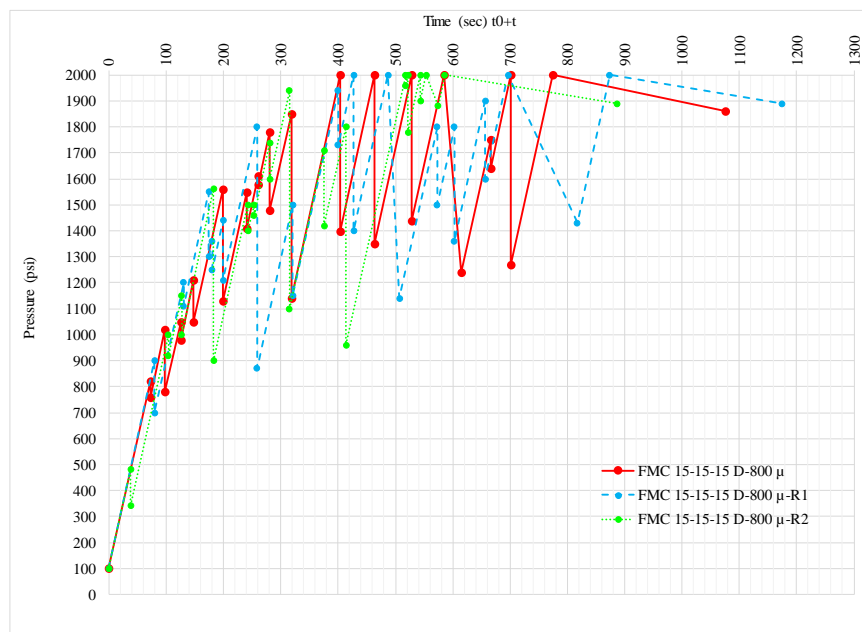


Figure I. 1: Pressure vs Time curve for FMC 15-15-15 on 800-micron fracture width

Table I. 1: Mud Loss & Total Sealing Time Values for FMC 15-15-15 on 800-micron fracture width

Code	Mud Loss (ml)				Total Sealing Time (sec)
	Stage I	Stage II	Stage III	Total	
FMC 15-15-15 D-800 μ	4	16.1	0.1	20.2	1085
FMC 15-15-15 D-800μ-R1	5.8	14.8	0.5	21.1	1184
FMC 15-15-15 D-800 μ -R2	6.4	11.2	0.2	17.8	886
Mean	-	-	-	19.7	1051.7
Std Dev	-	-	-	1.7	151.8
Deviation range, min	-	-	-	18.0	899.9
Deviation range, max	-	-	-	21.4	1203.4
Recommended Range, min	-	-	-	-	946.5
Recommended Range, max	-	-	-	-	1156.8

I. I. 2. FMC 20-20-20

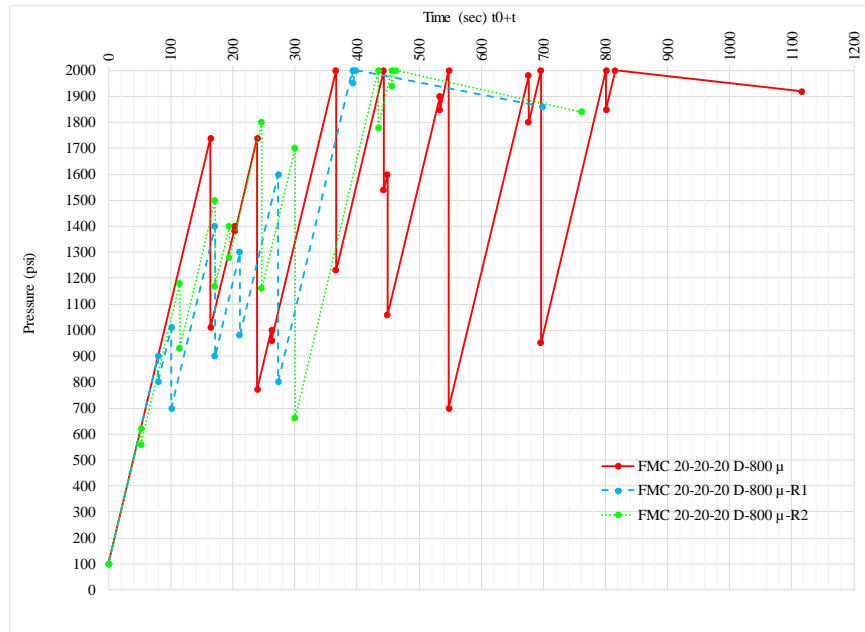


Figure I. 2: Pressure vs Time curve for FMC 20-20-20 on 800-micron fracture width

Table I. 2: Mud Loss & Total Sealing Time Values for FMC 20-20-20 on 800-micron fracture width

Code	Mud Loss (ml)				Total Sealing Time (sec)
	Stage I	Stage II	Stage III	Total	
FMC 20-20-20 D-800μ	4.1	16.6	0.4	21.1	1116
FMC 20-20-20 D-800μ-R1	3.2	6.6	0.2	10	698
FMC 20-20-20 D-800μ-R2	2.6	9.1	0.1	11.8	762
Mean	-	-	-	14.3	858.7
Std Dev	-	-	-	6.0	225.1
Deviation range, min	-	-	-	8.3	633.5
Deviation range, max	-	-	-	20.3	1083.8
Recommended Range, min	-	-	-	-	772.8
Recommended Range, max	-	-	-	-	944.5

I. I. 3. FMC 9-15-21

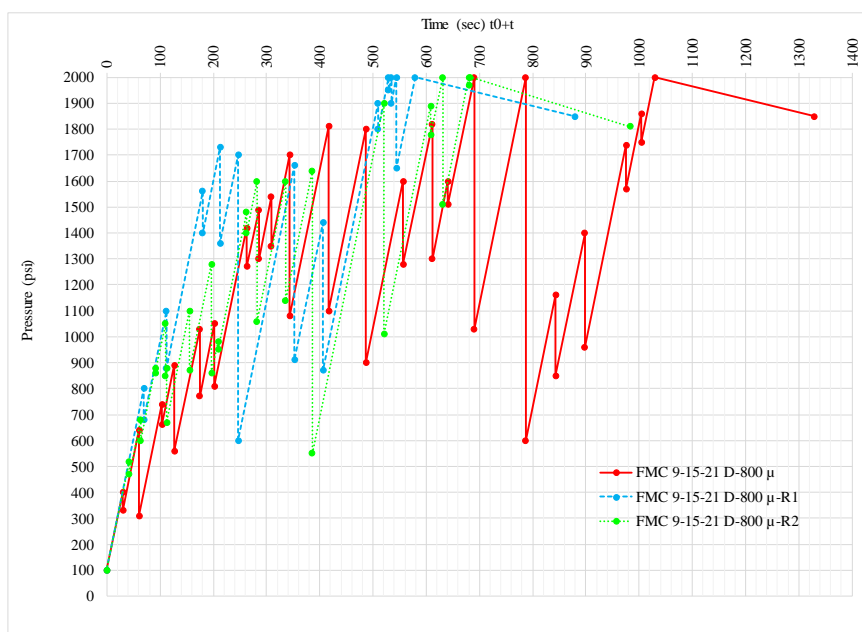


Figure I. 3: Pressure vs Time curve for FMC 9-15-21 on 800-micron fracture width

Table I. 3: Mud Loss & Total Sealing Time Values for FMC 9-15-21 on 800-micron fracture width

Code	Mud Loss (ml)				Total Sealing Time (sec)
	Stage I	Stage II	Stage III	Total	
FMC 9-15-21 D-800μ	5.9	19.5	4	29.4	1330
FMC 9-15-21 D-800μ-R1	4.8	11.6	0.2	16.6	879
FMC 9-15-21 D-800μ-R2	5.6	13.8	1.2	20.6	983
Mean	-	-	-	22.2	1064.0
Std Dev	-	-	-	6.5	236.2
Deviation range, min	-	-	-	15.7	827.8
Deviation range, max	-	-	-	28.7	1300.2
Recommended Range, min	-	-	-	-	957.6
Recommended Range, max	-	-	-	-	1170.4

I. I. 4. FMC 12-20-28

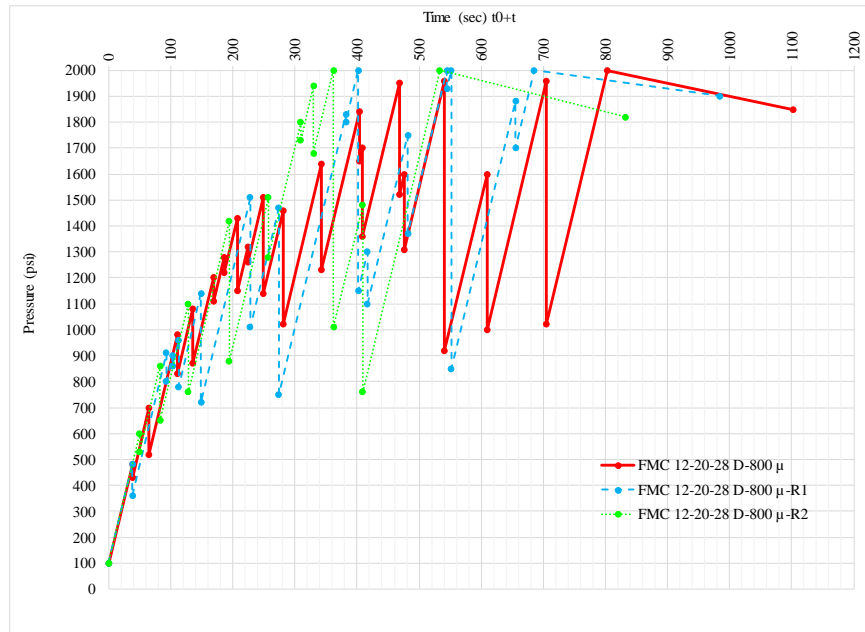


Figure I. 4: Pressure vs Time curve for FMC 12-20-28 on 800-micron fracture width

Table I. 4: Mud Loss & Total Sealing Time Values for FMC 12-20-28 on 800-micron fracture width

Code	Mud Loss (ml)				Total Sealing Time (sec)
	Stage I	Stage II	Stage III	Total	
FMC 12-20-28 D-800μ	4.2	17	0.4	21.6	1103
FMC 12-20-28 D-800μ-R1	4.8	15.5	0.2	20.5	985
FMC 12-20-28 D-800μ-R2	4.2	10	0.2	14.4	833
Mean	-	-	-	18.8	973.7
Std Dev	-	-	-	3.9	135.4
Deviation range, min	-	-	-	15.0	838.3
Deviation range, max	-	-	-	22.7	1109.0
Recommended Range, min	-	-	-	-	876.3
Recommended Range, max	-	-	-	-	1071.0

J. Effect of Particle Size Distribution of Ground Marble on Sealing 1200- μ Fracture Width

J. I. Results Obtained for Total Concentration of 30 ppb for 1200- μ Slot

J. I. 1. FMC 30-0-0, FMC 0-30-0 & FMC 0-0-30

Table J. 1: *Mud Loss & Total Sealing Time Values for each particle range individually on 1200-micron fracture width*

Code	Mud Loss (ml)				Total Sealing Time (sec)
	Stage I	Stage II	Stage III	Total	
FMC 30-0-0 D-1200 μ	*	*	*	>125	FAIL
FMC 0-30-0 D-1200 μ	*	*	*	>125	FAIL
FMC 0-0-30 D-1200 μ	*	*	*	>125	FAIL

J. I. 2. FMC 10-10-10

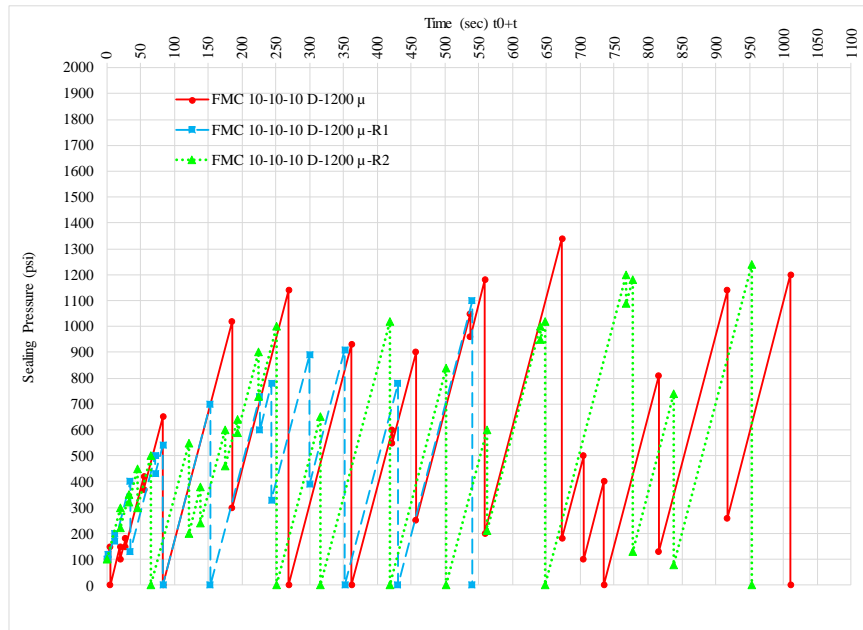


Figure J. 1: Pressure vs Time curve for FMC 10-10-10 on 1200-micron fracture width

Table J. 2: Mud Loss & Total Sealing Time Values for FMC 10-10-10 on 1200-micron fracture width

Code	Mud Loss (ml)				Total Sealing Time (sec)
	Stage I	Stage II	Stage III	Total	
FMC 10-10-10 D-1200μ	36.1	*	*	>125	FAIL
FMC 10-10-10 D-1200μ-R1	56.0	*	*	>125	FAIL
FMC 10-10-10 D-1200μ-R2	38.0	*	*	>125	FAIL

J. I. 3. FMC 10-6-14

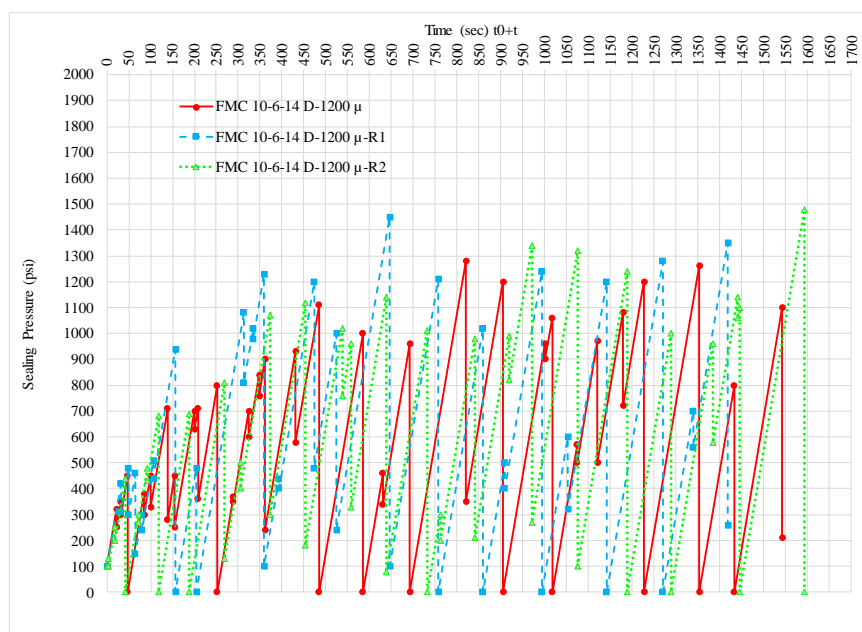


Figure J. 2: Pressure vs Time curve for FMC 10-6-14 on 1200-micron fracture width

Table J. 3: Mud Loss&Total Sealing Time Values for FMC 10-6-14 on 1200-micron fracture width

Code	Mud Loss (ml)				Total Sealing Time (sec)
	Stage I	Stage II	Stage III	Total	
FMC 10-6-14 D-1200μ	30.0	*	*	>125	FAIL
FMC 10-6-14 D-1200μ-R1	40.0	*	*	>125	FAIL
FMC 10-6-14 D-1200μ-R2	22.6	*	*	>125	FAIL

J. I. 4. FMC 10-2-18

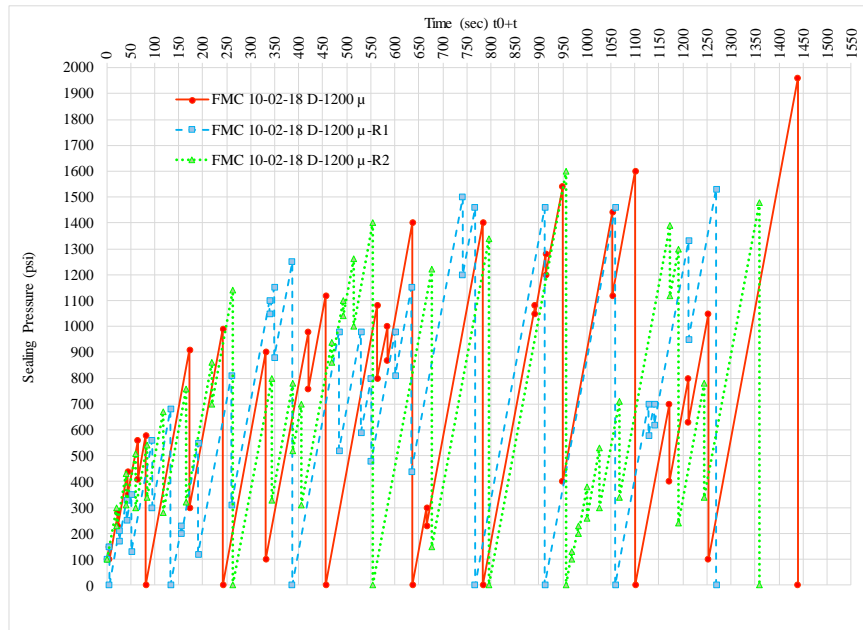


Figure J. 3: Pressure vs Time curve for FMC 10-2-18 on 1200-micron fracture width

Table J. 4: Mud Loss & Total Sealing Time Values for FMC 10-2-18 on 1200-micron fracture width

Code	Mud Loss (ml)				Total Sealing Time (sec)
	Stage I	Stage II	Stage III	Total	
FMC 10-2-18 D-1200μ	28.0	*	*	>125	FAIL
FMC 10-2-18 D-1200μ-R1	32.0	*	*	>125	FAIL
FMC 10-2-18 D-1200μ-R2	35.0	*	*	>125	FAIL

J. I. 5. FMC 10-18-2

Table J. 5: *Mud Loss&Total Sealing Time Values for FMC 10-18-2 on 1200-micron fracture width*

Code	Mud Loss (ml)				Total Sealing Time (sec)
	Stage I	Stage II	Stage III	Total	
FMC 10-18-2 D-1200 μ	*	*	*	>125	FAIL
FMC 10-18-2 D-1200 μ -R1	*	*	*	>125	FAIL
FMC 10-18-2 D-1200 μ -R2	*	*	*	>125	FAIL

J. I. 6. FMC 10-14-6

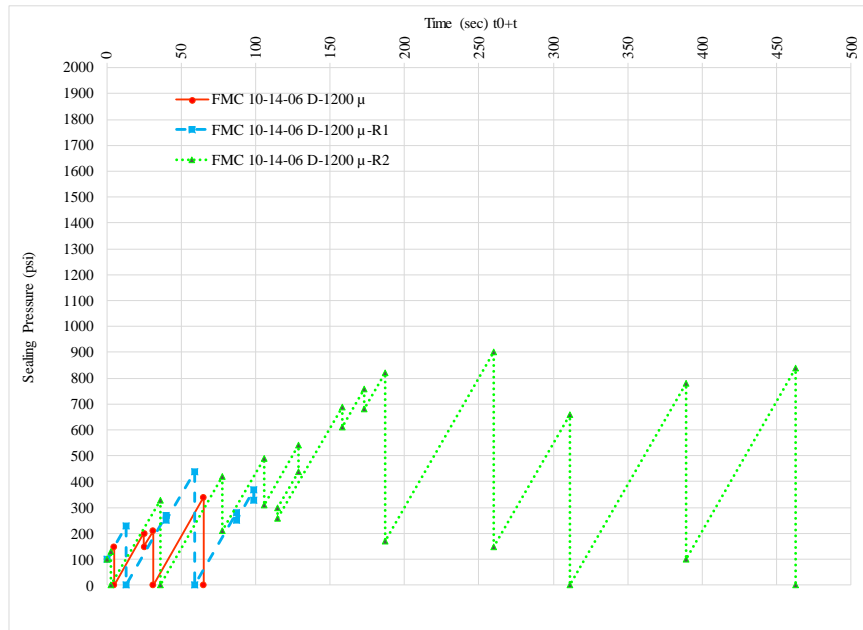


Figure J. 4: Pressure vs Time curve for FMC 10-14-6 on 1200-micron fracture width

Table J. 6: Mud Loss&Total Sealing Time Values for FMC 10-14-6 on 1200-micron fracture width

Code	Mud Loss (ml)				Total Sealing Time (sec)
	Stage I	Stage II	Stage III	Total	
FMC 10-14-6 D-1200μ	99.4	*	*	>125	FAIL
FMC 10-14-6 D-1200μ-R1	100.4	*	*	>125	FAIL
FMC 10-14-6 D-1200μ-R2	77.6	*	*	>125	FAIL

J. I. 7. FMC 6-10-14

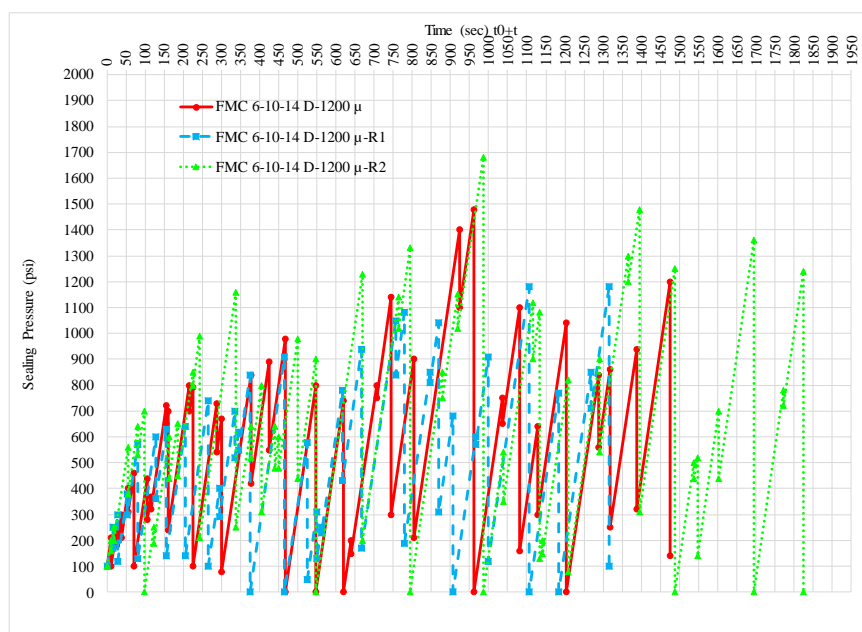


Figure J. 5: Pressure vs Time curve for FMC 6-10-14 on 1200-micron fracture width

Table J. 7: Mud Loss & Total Sealing Time Values for FMC 6-10-14 on 1200-micron fracture width

Code	Mud Loss (ml)				Total Sealing Time (sec)
	Stage I	Stage II	Stage III	Total	
FMC 6-10-14 D-1200μ	31.0	*	*	>125	FAIL
FMC 6-10-14 D-1200μ-R1	40.0	*	*	>125	FAIL
FMC 6-10-14 D-1200μ-R2	21.5	*	*	>125	FAIL

J. I. 8. FMC 2-10-18

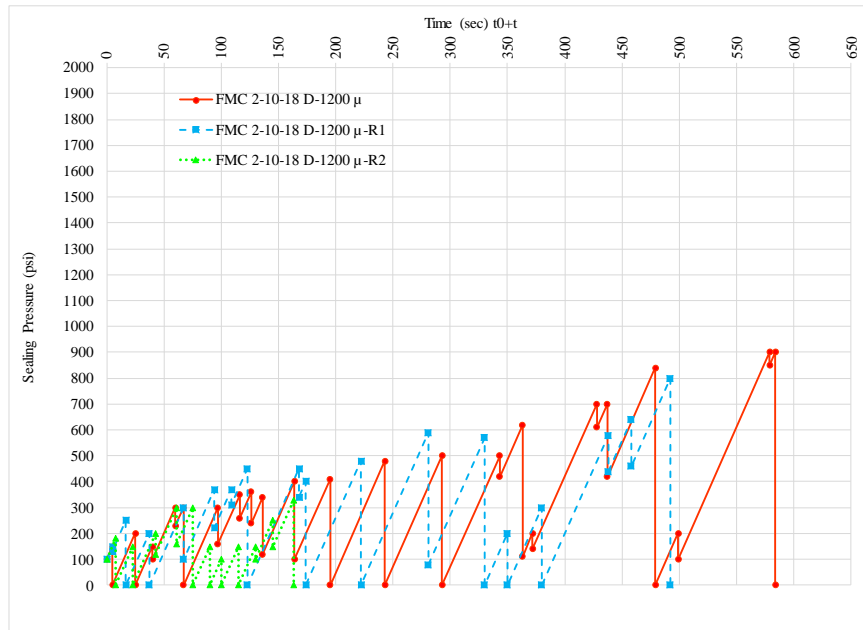


Figure J. 6: Pressure vs Time curve for FMC 2-10-18 on 1200-micron fracture width

Table J. 8: Mud Loss & Total Sealing Time Values for FMC 2-10-18 on 1200-micron fracture width

Code	Mud Loss (ml)				Total Sealing Time (sec)
	Stage I	Stage II	Stage III	Total	
FMC 2-10-18 D-1200μ	31.0	*	*	>125	FAIL
FMC 2-10-18 D-1200μ-R1	57.0	*	*	>125	FAIL
FMC 2-10-18 D-1200μ-R2	57.0	*	*	>125	FAIL

J. I. 9. FMC 18-10-2

Table J. 9: *Mud Loss & Total Sealing Time Values for FMC 18-10-2 on 1200-micron fracture width*

Code	Mud Loss (ml)				Total Sealing Time (sec)
	Stage I	Stage II	Stage III	Total	
FMC 18-10-2 D-1200 μ	*	*	*	>125	FAIL
FMC 18-10-2 D-1200 μ -R1	*	*	*	>125	FAIL
FMC 18-10-2 D-1200 μ -R2	*	*	*	>125	FAIL

J. I. 10. FMC 14-10-6

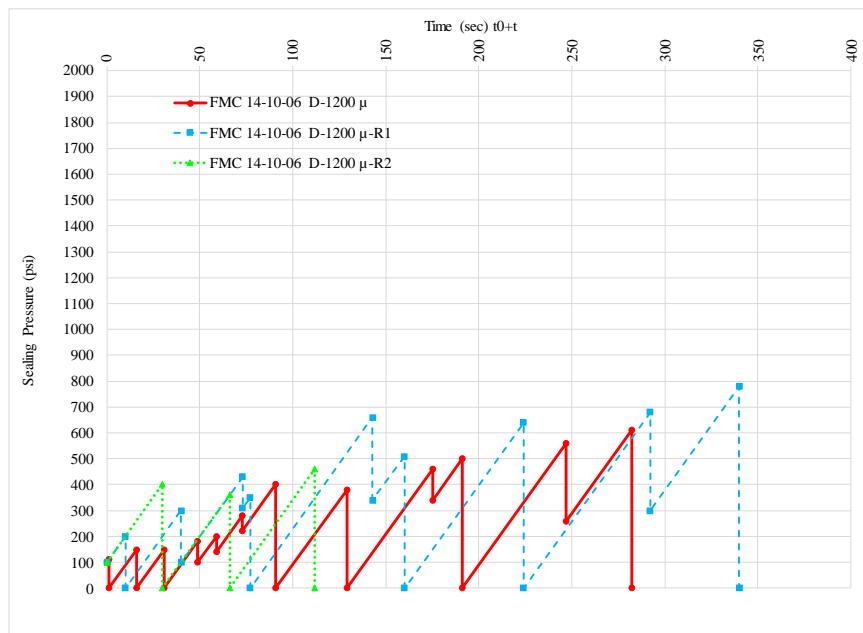


Figure J. 7: Pressure vs Time curve for FMC 14-10-6 on 1200-micron fracture width

Table J. 10: Mud Loss & Total Sealing Time Values for FMC 14-10-6 on 1200-micron fracture width

Code	Mud Loss (ml)				Total Sealing Time (sec)
	Stage I	Stage II	Stage III	Total	
FMC 14-10-6 D-1200μ	80.8	*	*	>125	FAIL
FMC 14-10-6 D-1200μ-R1	74.0	*	*	>125	FAIL
FMC 14-10-6 D-1200μ-R2	103.0	*	*	>125	FAIL

J. I. 11. FMC 6-14-10

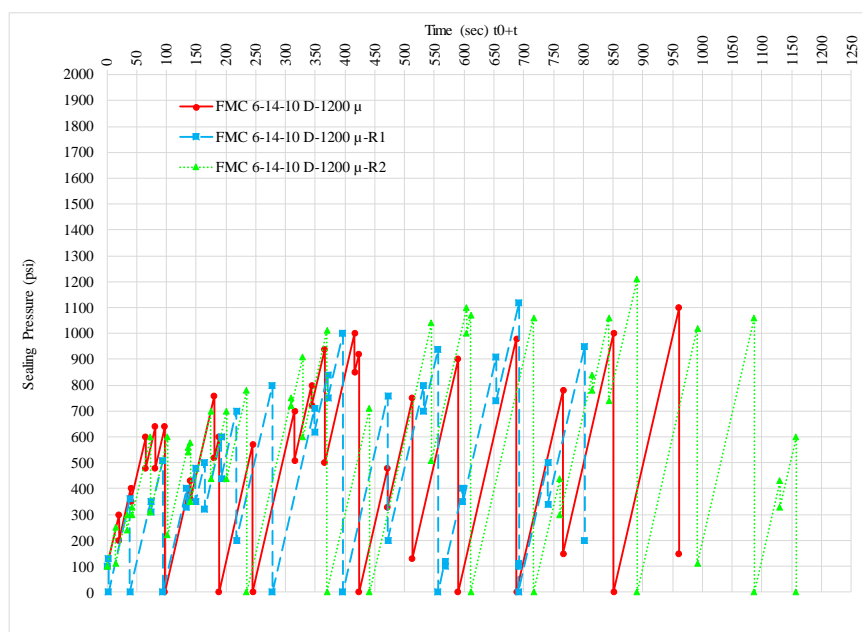


Figure J. 8: Pressure vs Time curve for FMC 6-14-10 on 1200-micron fracture width

Table J. 11: Mud Loss & Total Sealing Time Values for FMC 6-14-10 on 1200-micron fracture width

Code	Mud Loss (ml)				Total Sealing Time (sec)
	Stage I	Stage II	Stage III	Total	
FMC 6-14-10 D-1200μ	54.0	*	*	>125	FAIL
FMC 6-14-10 D-1200μ-R1	52.0	*	*	>125	FAIL
FMC 6-14-10 D-1200μ-R2	36.0	*	*	>125	FAIL

J. I. 12. FMC 2-18-10

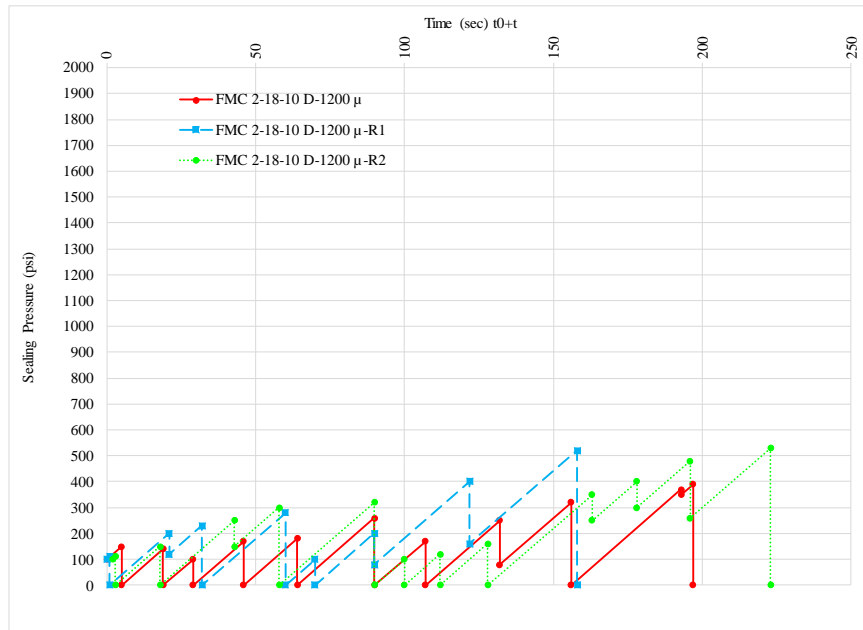


Figure J. 9: Pressure vs Time curve for FMC 2-18-10 on 1200-micron fracture width

Table J. 12: Mud Loss & Total Sealing Time Values for FMC 2-18-10 on 1200-micron fracture width

Code	Mud Loss (ml)				Total Sealing Time (sec)
	Stage I	Stage II	Stage III	Total	
FMC 2-18-10 D-1200μ	32.0	*	*	>125	FAIL
FMC 2-18-10 D-1200μ-R1	56.0	*	*	>125	FAIL
FMC 2-18-10 D-1200μ-R2	56.0	*	*	>125	FAIL

J. I. 13. FMC 18-2-10

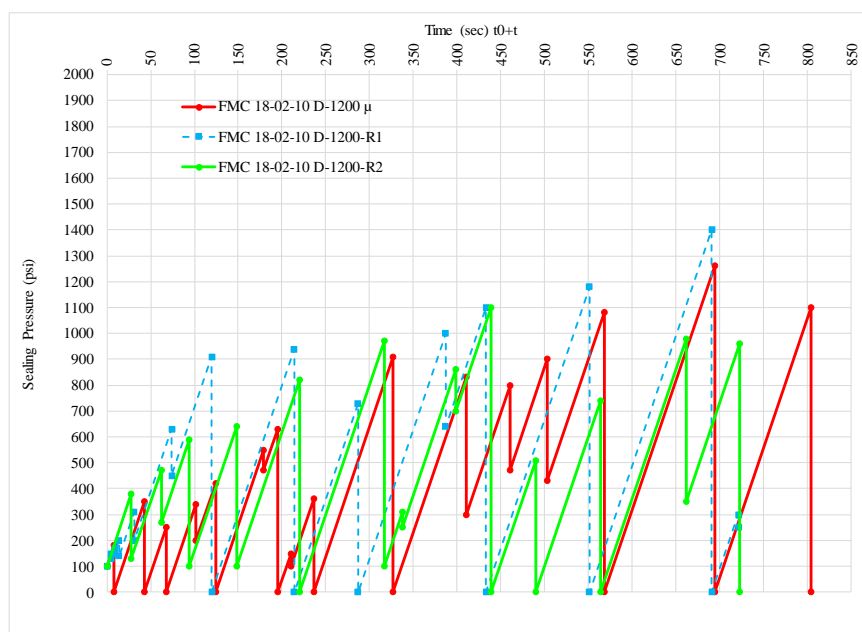


Figure J. 10: Pressure vs Time curve for FMC 18-2-10 on 1200-micron fracture width

Table J. 13: Mud Loss & Total Sealing Time Values for FMC 18-2-10 on 1200-micron fracture width

Code	Mud Loss (ml)				Total Sealing Time (sec)
	Stage I	Stage II	Stage III	Total	
FMC 18-2-10 D-1200 μ	51.0	*	*	>125	FAIL
FMC 18-2-10 D-1200 μ -R1	63.0	*	*	>125	FAIL
FMC 18-2-10 D-1200 μ -R2	61.2	*	*	>125	FAIL

J. I. 14. FMC 14-6-10

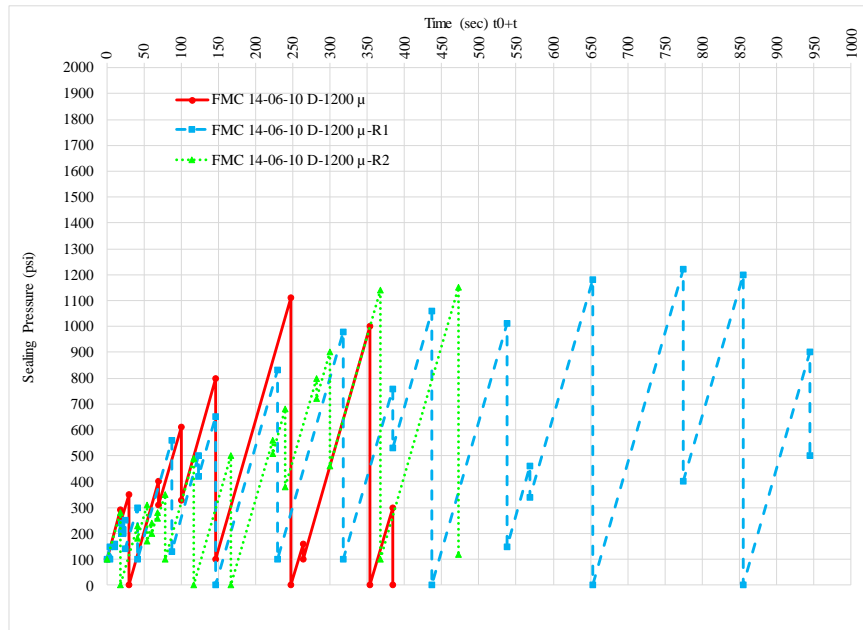


Figure J. 11: Pressure vs Time curve for FMC 14-6-10 on 1200-micron fracture width

Table J. 14: Mud Loss&Total Sealing Time Values for FMC 14-6-10 on 1200-micron fracture width

Code	Mud Loss (ml)				Total Sealing Time (sec)
	Stage I	Stage II	Stage III	Total	
FMC 14-6-10 D-1200μ	84.6	*	*	>125	FAIL
FMC 14-6-10 D-1200μ-R1	50.0	*	*	>125	FAIL
FMC 14-6-10 D-1200μ-R2	84.9	*	*	>125	FAIL

J. II. Results Obtained for Total Concentration of 60 ppb for 1200- μ Slot

J. II. 1. FMC 20-4-36

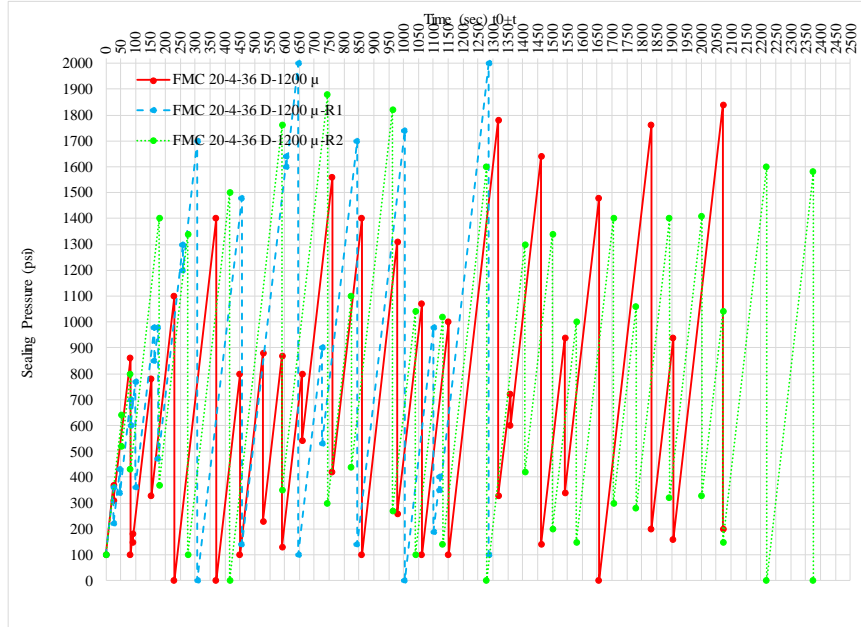


Figure J. 12: Pressure vs Time curve for FMC 20-4-36 on 1200-micron fracture width

Table J. 15: Mud Loss & Total Sealing Time Values for FMC 20-4-36 on 1200-micron fracture width

Code	Mud Loss (ml)				Total Sealing Time (sec)
	Stage I	Stage II	Stage III	Total	
FMC 20-4-36 D-1200 μ	20.2	*	*	>125	FAIL
FMC 20-4-36 D-1200 μ -R1	14.0	*	*	>125	FAIL
FMC 20-4-36 D-1200 μ -R2	13.0	*	*	>125	FAIL

J. II. 2. FMC 20-12-28

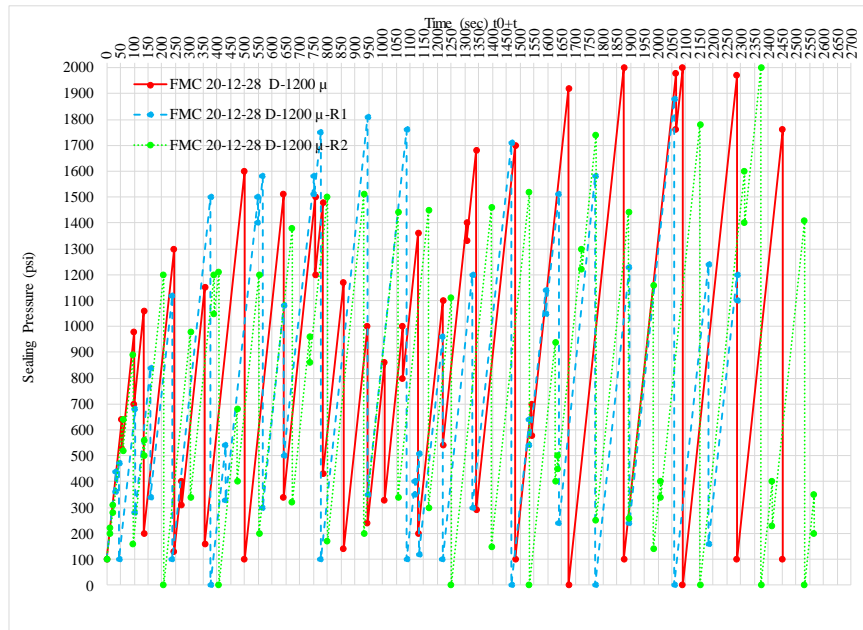


Figure J. 13: Pressure vs Time curve for FMC 20-12-28 on 1200-micron fracture width

Table J. 16: Mud Loss & Total Sealing Time Values for FMC 20-12-28 on 1200-micron fracture width

Code	Mud Loss (ml)				Total Sealing Time (sec)
	Stage I	Stage II	Stage III	Total	
FMC 20-12-28 D-1200μ	16.0	*	*	>125	FAIL
FMC 20-12-28 D-1200μ-R1	12.0	*	*	>125	FAIL
FMC 20-12-28 D-1200μ-R2	14.0	*	*	>125	FAIL

J. II. 3. FMC 15-15-30

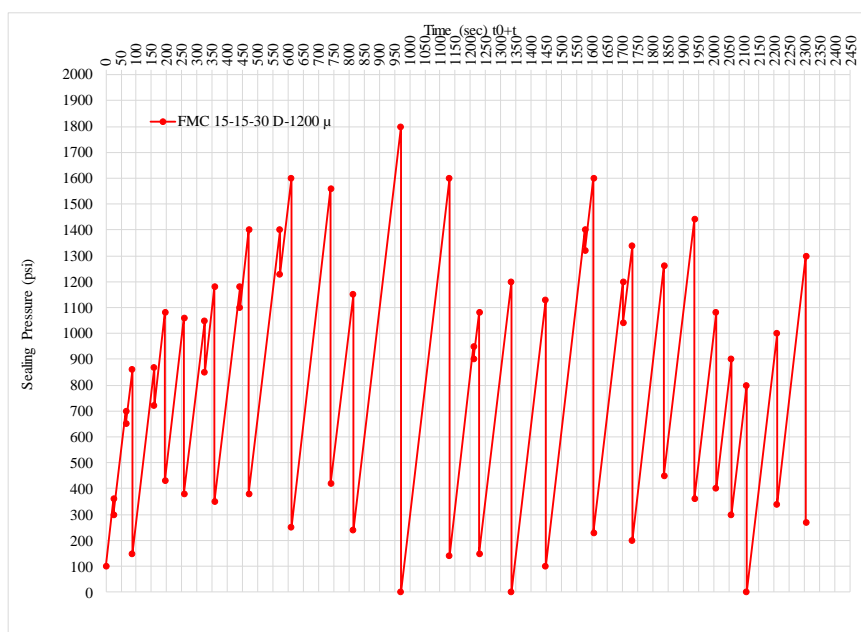


Figure J. 14: Pressure vs Time curve for FMC 15-15-30 on 1200-micron fracture width

Table J. 17: Mud Loss & Total Sealing Time Values for FMC 15-15-30 on 1200-micron fracture width

Code	Mud Loss (ml)				Total Sealing Time (sec)
	Stage I	Stage II	Stage III	Total	
FMC 15-15-30 D-1200 μ	15.6	*	*	>125	FAIL

J. II. 4. FMC 10-10-40

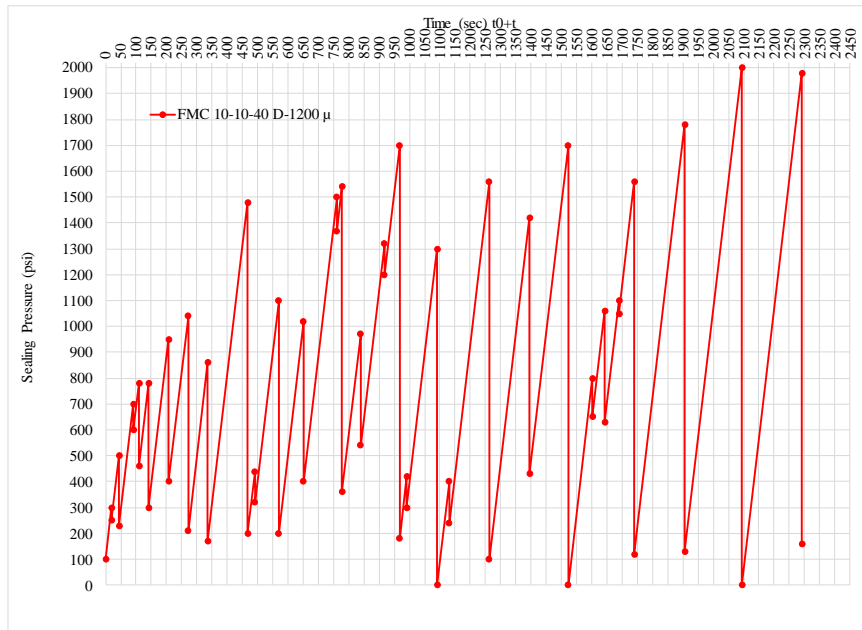


Figure J. 15: Pressure vs Time curve for FMC 10-10-40 on 1200-micron fracture width

Table J. 18: Mud Loss & Total Sealing Time Values for FMC 10-10-40 on 1200-micron fracture width

Code	Mud Loss (ml)				Total Sealing Time (sec)
	Stage I	Stage II	Stage III	Total	
FMC 10-10-40 D-1200μ	13.0	*	*	>125	FAIL

J. II. 5. FMC 25-5-30

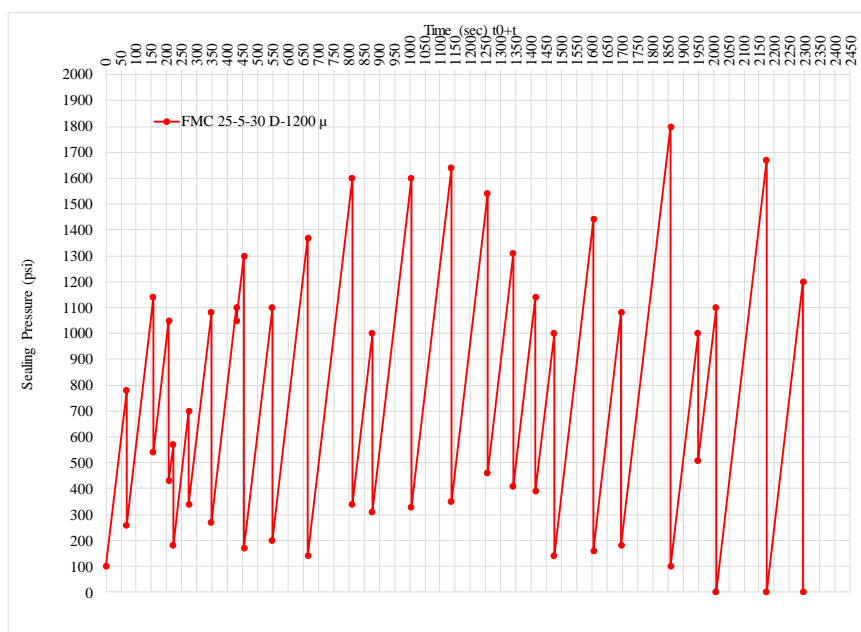


Figure J. 16: Pressure vs Time curve for FMC 25-5-30 on 1200-micron fracture width

Table J. 19: Mud Loss & Total Sealing Time Values for FMC 25-5-30 on 1200-micron fracture width

Code	Mud Loss (ml)				Total Sealing Time (sec)
	Stage I	Stage II	Stage III	Total	
FMC 25-5-30 D-1200μ	10.8	*	*	>125	FAIL

LCP Applications

J. III. Results Obtained for Total Concentration of 90 ppb for 1200- μ Slot

J. III. 1. FMC 15-30-45

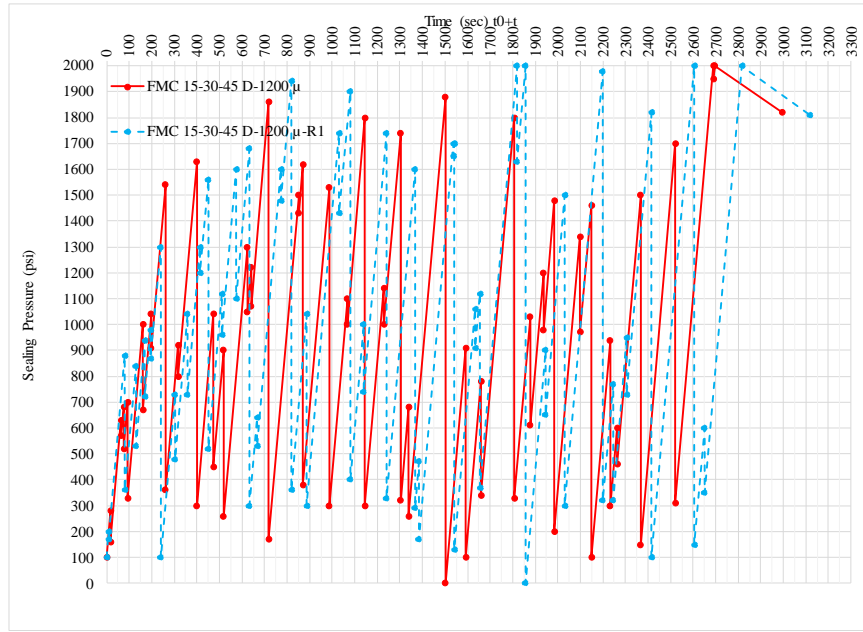


Figure J. 17: Pressure vs Time curve for FMC 15-30-45 on 800-micron fracture width

Table J. 20: Mud Loss & Total Sealing Time Values for FMC 15-30-45 on 1200-micron fracture width

Code	Mud Loss (ml)				Total Sealing Time (sec)
	Stage I	Stage II	Stage III	Total	
FMC 15-30-45 D-1200 μ	14.0	103.2	1.2	118.4	2996.0
FMC 15-30-45 D-1200 μ -R1	11.3	101.7	1.2	114.2	3116.0

J. IV. Results Obtained for Total Concentration of 120 ppb for 1200- μ Slot

J. IV. 1. FMC 20-40-60

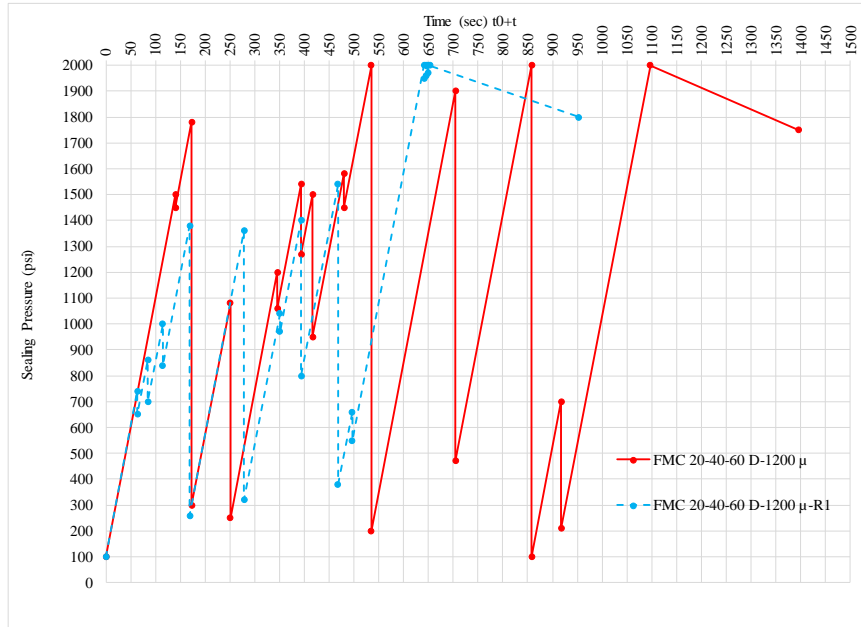


Figure J. 18: Pressure vs Time curve for FMC 20-40-60 on 1200-micron fracture width

Table J. 21: Mud Loss & Total Sealing Time Values for FMC 20-40-60 on 1200-micron fracture width

Code	Mud Loss (ml)				Total Sealing Time (sec)
	Stage I	Stage II	Stage III	Total	
FMC 20-40-60 D-1200 μ	6.4	30.6	1.0	38.0	1397.0
FMC 20-40-60 D-1200 μ -R1	9.6	18.2	0.4	28.2	953.0

J. V. Results Obtained for Total Concentration of 150 ppb for 1200- μ Slot

J. V. 1. FMC 25-50-75

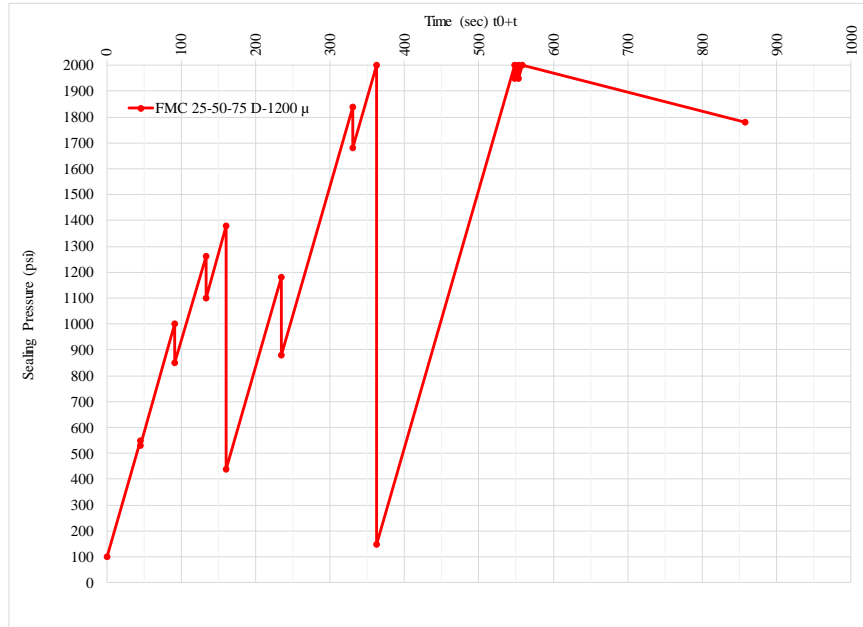


Figure J. 19: Pressure vs Time curve for FMC 25-50-75 on 800-micron fracture width

Table J. 22: Mud Loss & Total Sealing Time Values for FMC 25-50-75 on 1200-micron fracture width

Code	Mud Loss (ml)				Total Sealing Time (sec)
	Stage I	Stage II	Stage III	Total	
FMC 25-50-75 D-1200 μ	4.2	14.8	0.8	19.8	858.0

K. Effect of Concentration of Ground Marble on Sealing 1200- μ Fracture

K. I. 1. FMC 16-16-16

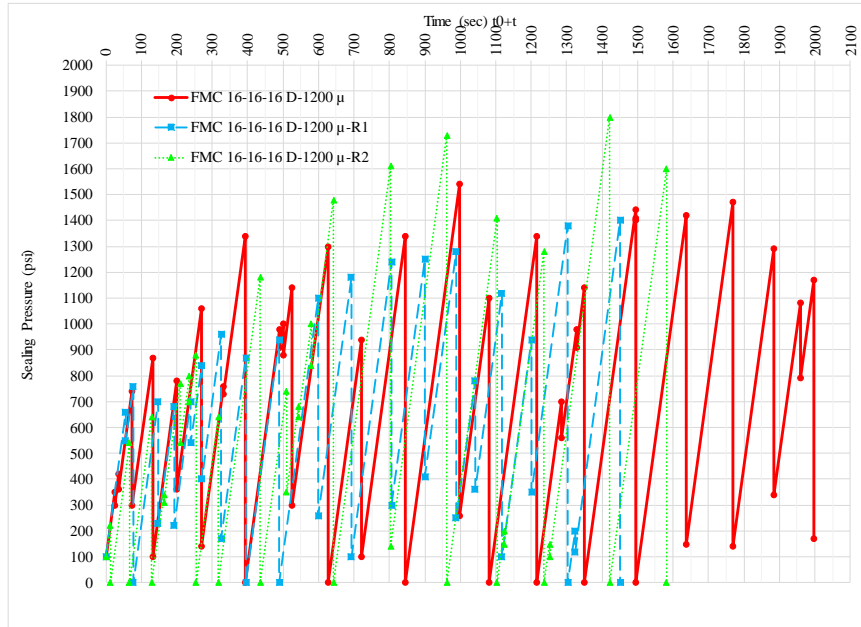


Figure K. 1: Pressure vs Time curve for FMC 16-16-16 on 1200-micron fracture width

Table K. 1: Mud Loss & Total Sealing Time Values for FMC 16-16-16 on 1200-micron fracture width

Code	Mud Loss (ml)				Total Sealing Time (sec)
	Stage I	Stage II	Stage III	Total	
FMC 16-16-16 D-1200 μ	20.6	*	*	>125	FAIL
FMC 16-16-16 D-1200 μ -R1	29.1	*	*	>125	FAIL
FMC 16-16-16 D-1200 μ -R2	21.0	*	*	>125	FAIL

K. I. 2. FMC 20-20-20

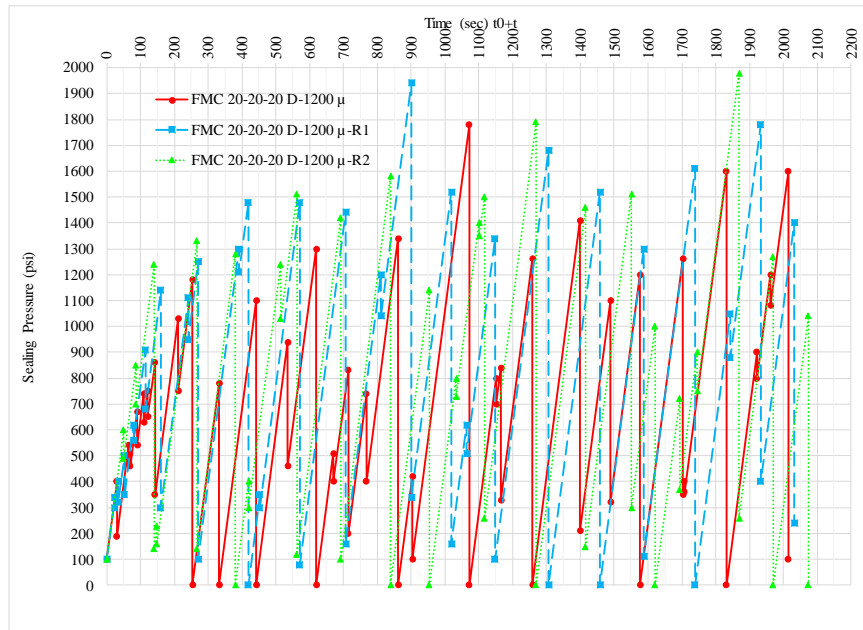


Figure K. 2: Pressure vs Time curve for FMC 20-20-20 on 1200-micron fracture width

Table K. 2: Mud Loss & Total Sealing Time Values for FMC 20-20-20 on 1200-micron fracture width

Code	Mud Loss (ml)				Total Sealing Time (sec)
	Stage I	Stage II	Stage III	Total	
FMC 20-20-20 D-1200μ	16.0	*	*	>125	FAIL
FMC 20-20-20 D-1200μ-R1	28.0	*	*	>125	FAIL
FMC 20-20-20 D-1200μ-R2	14.0	*	*	>125	FAIL